

CRANFIELD UNIVERSITY

ATHANASIOS IOANNIS KOLIOS

A MULTI-CONFIGURATION APPROACH TO RELIABILITY BASED
STRUCTURAL INTEGRITY ASSESSMENT FOR ULTIMATE
STRENGTH

SCHOOL OF ENGINEERING
Department Of Offshore, Process & Energy Engineering

Thesis Submitted for the Degree of Doctor of Philosophy
Academic Year: 2010

Supervisor: Professor Feargal Brennan
November 2010

CRANFIELD UNIVERSITY

SCHOOL OF ENGINEERING
Department Of Offshore, Process & Energy Engineering
Thesis Submitted for the Degree of Doctor of Philosophy

Academic Year 2010

ATHANASIOS IOANNIS KOLIOS

Thesis Submitted for the Degree of Doctor of Philosophy

Supervisor: Professor Feargal Brennan

November 2010

© Cranfield University 2010. All rights reserved. No part of this publication may be reproduced without the written permission of the copyright owner.

ABSTRACT

Structural Reliability treats uncertainties in structural design systematically, evaluating the levels of safety and serviceability of structures. During the past decades, it has been established as a valuable design tool for the description of the performance of structures, and lately stands as a basis in the background of the most of the modern design standards, aiming to achieve a uniform behaviour within a class of structures. Several methods have been proposed for the estimation of structural reliability, both deterministic (FORM and SORM) and stochastic (Monte Carlo Simulation etc) in nature.

Offshore structures should resist complicated and, in most cases, combined environmental phenomena of greatly uncertain magnitude (eg. wind, wave, current, operational loads etc). Failure mechanisms of structural systems and components are expressed through limit state functions, which distinguish a failure and a safe region of operation. For a jacket offshore structure, which comprises of multiple tubular members interconnected in a three dimensional truss configuration, the limit state function should link the actual load or load combination acting on it locally, to the response of each structural member.

The response of a structure under specific loading conditions can be determined through Finite Element Analysis Methods. Based on that, advanced methods (intrusive and non-intrusive) have been developed, such as the Spectral Stochastic Finite Element Method and the Stochastic Response Surface method. This Thesis presents a methodology for the structural reliability assessment of an offshore jacket structure, which has been selected as a reference application, based on a generalized Stochastic Response Surface Method. According to the methodology that is proposed, simulation results obtained by FEA Modelling are combined with numerical reliability procedures, through multivariate (quadratic) polynomial regression (MPR), in order to calculate the reliability indices of members. This procedure is particularly useful as it enables efficient analysis of members under a stochastic perspective, incorporating design uncertainties. By effectively dividing the analysis into

different independent 'blocks' in an open sequence, the required number of Finite Element simulations is greatly reduced. This implies that depending on the requirements of the structure, different resolutions and tools can be used in each of those blocks. The reduced resource requirements of this method can later allow optimization of a complex structure in a closed design procedure. The novelty of this methodology is in its simplicity and the ability to analyze a wide range of structures, and further intricate reliability problems, under complicated load combinations in a more efficient way.

Consideration of appropriate limit state functions is an essential decision for accurate prediction of the reliability index. For the reference structure, analytical limit states have been introduced following fundamental failure criteria for ultimate strength and buckling resistance of ductile members. Hence, after appropriate modelling of stochastic variables, and based on the derived limit states, the reliability level is calculated in both a local and a system level. A sensitivity analysis of the design parameters (surface roughness, variables' modelling, corrosion deterioration etc) illustrates their effect on the derived values. On a parallel study, deriving limit states based on the design requirements of the most widely used design standards for offshore steel structures (API RP-2A, ISO 19902) but also generic standards for steel structures (EN 1993, AISC/ANSI), the minimum reliability indices of members are derived and later compared to the ones obtained by the analytical limit states. Using the same calculation procedure for the estimation of reliability, such a comparison can be realistically executed and useful conclusions can be drawn for the performance of different design standards

The methodology that is derived and presented in this Thesis, can be extended to the probabilistic assessment of different engineering problems, including problems of solid mechanics and heat transfer, where detailed analysis is required for the derivation of the response of the structure. Further, this methodology can stand as a generic document that can be applied in conjunction to design standards towards a robust reliability based design.

Keywords:

Offshore Structures, Reliability Assessment, Stochastic Response Surface Method, Structural Integrity, Design Standards, API RP-2A, ISO 19902, EN 1993, AISC/ANSI

Dedicated to John, Irene, Helen and Michael...

“Της δικαιοσύνης ήλιε νοητέ
και μυρσίνη συ δοξαστική
μη παρακαλώ σας μη
λησμονάτε τη χώρα μου...”

Οδυσσέας Ελύτης, (Το Άξιον Εστί, 1959)
Νόμπελ Λογοτεχνίας, 1979

“Notional sun of justice
and you myrtle of glory
don't, please don't
forget my country...”

Odysseas Elytis, (To Axion Esti, 1959)
Nobel Prize in Literature, 1979

ACKNOWLEDGEMENTS

First of all I would like to thank my supervisor, Professor Feargal Brennan, for his confident supervision and generous support throughout the three years of this PhD. His advice has mentored my future academic endeavors.

I should express my greatest gratitude to my friend and colleague Dr. Amir Chahardehi (Cranfield University), not only for proof reading my Thesis but also for the hours of long discussions we have spent related to fundamental aspects of Engineering, that have enlightened different perspectives for research.

I would like to thank Professor Iberahin Jusoh, who honors me with his friendship, from the Technical University of Malaysia for his valuable experience and advice on the design of offshore structures and his support in my research.

Professor Dimitrios Papantonis (National Technical University of Athens) and Dr. Pavlos Aleiferis (University College London) have trusted me with their references; I hope that the contribution of this PhD meets their expectations.

I own appreciation to everyone that has supported this endeavor, especially my dear friends Mr. Dimitros Katsaros, Mr. Antonios Antoniadis, Mr. George Kosmidis, and my colleagues in Cranfield University. A special thank to Dr. Anastasia Athanasoulia.

Finally, I would like to grant the deepest gratitude to my parents, for the principles they inspired me, and their constant support to all of my dreams.

TABLE OF CONTENTS

ABSTRACT	i
ACKNOWLEDGEMENTS.....	iii
LIST OF FIGURES.....	ix
LIST OF TABLES	xi
NOMENCLATURE	xiii
Symbols.....	xiii
Abbreviations.....	xxi
1 INTRODUCTION – CONTEXT OF STRUCTURAL SAFETY.....	1
1.1 Introduction	1
1.2 Structural Reliability.....	5
1.3 Overview of Reliability Analysis of Offshore Structures.....	9
1.4 Design of Offshore Structures	11
1.4.1 Permissible stresses.....	11
1.4.2 Global Safety Factor	12
1.4.3 Partial Safety factor	12
1.4.4 Probabilistic Methods.....	13
1.4.5 Comments on design methods	13
1.5 Limit State Design	14
1.5.1 Serviceability Limit State.....	15
1.5.2 Ultimate Limit State.....	16
1.5.3 Fatigue Limit State.....	18
1.5.4 Accidental Limit State	18
1.6 Design Standards for Steel Structures	19
1.6.1 General.....	19
1.6.2 Categorization of Design Standards	20
1.6.3 Standards for Offshore Structures	20
1.7 Target – Acceptable Reliability	24
1.8 Summary.....	27
2 RELIABILITY ANALYSIS OF OFFSHORE STRUCTURES	31
2.1 Basic formulation of the Problem	31
2.2 Background and motivation.....	34
2.2.1 Development of Structural Reliability Applications.....	34
2.2.2 Development of offshore industry	35
2.2.3 Application of Reliability Analysis in the offshore industry	36
2.3 Response Analysis.....	38
2.3.1 Static Analysis	38
2.3.2 Dynamic Analysis	39
2.3.3 Deterministic and Stochastic Processes.....	40
2.3.4 Selection of type of analysis	40
2.3.5 System Response.....	42
2.3.6 Practical Methods of Analysis.....	45
2.3.7 Modelling of Post-Failure Behaviour	46
2.3.8 Methods in Computing System Reliability.....	47
2.4 Review of Stochastic Methods	51
2.4.1 Stochastic Expansions.....	51

2.4.2	Spectral Stochastic Finite Elements	53
2.5	Summary.....	58
3	NUMERICAL METHODS FOR STRUCTURAL RELIABILITY ANALYSIS	59
3.1	Introduction	59
3.2	Numerical Methods	59
3.2.1	Deterministic Methods	59
3.2.2	Simulation Methods	76
3.3	Stochastic Response Surface Method	87
3.3.1	General Concept.....	87
3.3.2	Review and Notation.....	90
3.3.3	Adaptive Response Surface Method	92
3.3.4	Algorithms of the Stochastic Response Surface Method	94
3.4	Regression methods	95
3.4.1	Linear Regression.....	95
3.4.2	Multivariate Regression	97
3.4.3	Alternative Regression Methods	98
3.5	Numerical model Developed	99
3.5.1	Description.....	99
3.5.2	Verification Process	102
3.5.3	Validation of the FORM/SORM code	108
3.5.4	Codes Included.....	112
3.6	Summary.....	112
4	STOCHASTIC MODELING OF ENVIRONMENTAL LOADING AND LOAD CAPACITY OF OFFSHORE STRUCTURES	115
4.1	Introduction	115
4.2	Classification of Loads	115
4.3	Environmental Loading.....	117
4.3.1	Design Environmental Conditions.....	118
4.3.2	Environmental Loads	119
4.3.3	Wave Modelling	124
4.3.4	Joint Probability of Environmental Parameters	132
4.3.5	Estimation of Extreme and Design Values.....	136
4.3.6	Fluid Loading on Offshore Structures	140
4.3.7	Response of Structure under Environmental Loading	143
4.4	Capacity of Offshore Structures	144
4.4.1	Resistance Model	144
4.4.2	Material Data	145
4.4.3	Geometry Data	147
4.4.4	Capacity of Members and Joints.....	148
4.4.5	Geotechnical Data	149
4.4.6	Fatigue Data	153
4.4.7	Corrosion Modelling.....	154
4.5	Summary.....	163
5	APPLICATION OF THE RESPONSE SURFACE METHOD IN A TYPICAL JACKET STRUCTURE	165
5.1	Introduction	165
5.2	Limit State Formulation	165
5.2.1	Maximum shear stress (MSS) – Tresca or Guest Theory.....	168

5.2.2	Distortion energy (DE) – von Mises Stress Theory	170
5.2.3	Ductile Coulomb-Mohr (DCM).....	172
5.2.4	Comments on Failure Criteria	174
5.2.5	Buckling Limit state	176
5.3	Application of Joint Probability Distribution.....	179
5.4	Reference Structure	187
5.5	Component Structural Reliability Assessment.....	191
5.5.1	Base case.....	191
5.5.2	Sensitivity analysis of design parameters	196
5.5.3	System Reliability Integration	206
5.6	A Note on the dynamic loading of structures.....	213
5.7	Summary.....	215
6	COMPARISON OF THE ULTIMATE STRENGTH RELIABILITY PERFORMANCE OF RELEVANT DESIGN PROCEDURES.....	217
6.1	Introduction	217
6.2	API RP-2A: Recommended practice for planning, designing and constructing fixed offshore platforms LRFD	218
6.2.1	Design Provisions	218
6.2.2	Numerical Results.....	224
6.3	ISO 19902:2002: Petroleum and natural gas industries-general requirements for offshore structures	229
6.3.1	Design Provisions	229
6.3.2	Numerical Results.....	236
6.4	BS EN 1993-1-1:2005 Eurocode 3: Design of Steel Structures	241
6.4.1	Design Provisions	242
6.4.2	Numerical Results.....	250
6.5	ANSI/AISC 360-05: Specification for structural steel buildings.....	254
6.5.1	Design Provisions	255
6.5.2	Numerical Application	259
6.6	Discussion.....	262
6.7	Summary.....	267
7	CONCLUSIONS AND RECCOMENTATIONS	269
7.1	Summary.....	269
7.2	Contribution of this PhD	271
7.3	Future recommendations:	277
	REFERENCES.....	281
	APPENDICES	313
	APPENDIX A.....	313
	APPENDIX B.....	322
	APPENDIX C.....	327
	APPENDIX D.....	329

LIST OF FIGURES

Figure 1: Response Surface Method Flow Chart.....	3
Figure 2: Structural Design Consideration of the ULS.....	17
Figure 3: Iterative procedure for Risk Assessment [48].....	29
Figure 4: Relationship between β and Probability of failure.....	33
Figure 5: Definition of Reliability Index	33
Figure 6: Scatter of response (Max Base Shear-MN) by different Analysis Methods [75]	41
Figure 7: Classification of methods for system reliability assessment [76].....	43
Figure 8: Models of Post-Failure Behaviour	46
Figure 9: Intrusive and non-intrusive formulation [93].....	53
Figure 10: First and Second order approximations.....	60
Figure 11: Transformation to the U-space [93].....	61
Figure 12: Algorithm of HL Reliability Index Calculation.....	68
Figure 13: Normalized Tail Approximation [116].....	70
Figure 14: Area calculation with Monte Carlo Simulation (500 and 5000 sampling points).....	77
Figure 15: Inverse transformation method.....	78
Figure 16: Latin Hypercube Method	79
Figure 17: Monte Carlo Simulation Method	80
Figure 18: Design Point Simulation	83
Figure 19: Directional Simulation.....	85
Figure 20: Axis-Orthogonal Simulation.....	87
Figure 21: Regression vs. Order of Polynomial.....	89
Figure 22: Different Sampling Approaches [160].....	89
Figure 23: Calculation of reliability based on Direct Simulation.....	100
Figure 24: Calculation of reliability based on Normal Response Surface Method	100
Figure 25: Calculation of reliability based on Adaptive Response Surface Method	101
Figure 26: Reference structure.....	105
Figure 27: ABAQUS and Matlab code deformed model.....	106
Figure 28: FEA model in DNV Genie software	109
Figure 29: Methods for combining current and wave [186].....	121
Figure 30: Ranges of appropriate wave theories [1].....	124
Figure 31: Ranges of appropriate wave theories [193].....	125
Figure 32: Coordinate system of wave propagation [194]	126
Figure 33: Applicability regions of wave theories based on the relative error on the fit of the two nonlinear free surface boundary conditions [195]	127
Figure 34: CD-KC number for different values of Re and $\beta=Re/KC$ [199]	130
Figure 35: CM-KC number for different values of Re and $\beta=Re/KC$ [199].....	130
Figure 36: Frequency domain analysis [232].....	142
Figure 37: Static and Dynamic analysis response curve	144
Figure 38: Continuous load process and potential exceedance of the deteriorating structural Resistance [268].....	156
Figure 39: Strength Deterioration Structural Reliability Problem [269].....	156

Figure 40: Corrosion depth as a function of sea water temperature [269].....	157
Figure 41: Effect of water velocity on early loss corrosion [268].....	157
Figure 42: Different corrosion mechanism as a function of time [269].....	159
Figure 43: Thickness of corrosion wastage as a function of time [275]	161
Figure 44: Model for maximum pit depth as a function of exposure period [276]	162
Figure 45: The MSS theory for plane stress problems (two nonzero principal stresses).....	169
Figure 46: Distortion Energy Theory for plane stress problems.....	172
Figure 47: Mohr Cycles and Coulomb-Mohr Failure criterion	173
Figure 48: Coulomb-Mohr Failure criterion for Plane Stress problems.....	174
Figure 49: Linear Plot of real data (Hs (m), Tp (s)).....	180
Figure 50: Logarithmic Plot of real data (Hs (m), Tp (s))	180
Figure 51: Linear Plot of regenerated data (Hs (m), Tp (s))	181
Figure 52: Logarithmic plot of LogN bivariate joint distribution (smoothened) (Hs (m), Tp (s))	183
Figure 53: Logarithmic plot of Weibull bivariate joint distribution (smoothened) (Hs (m), Tp (s)).....	183
Figure 54: Logarithmic plot of LogN-Weibull bivariate joint distribution (smoothened) (Hs (m), Tp (s)).....	184
Figure 55: Comparison of best fit on the tail region of the CDF for Hs (m).....	185
Figure 56: The Reyleigh distribution of wave heights	187
Figure 57: FEA model of a jacket structure developed in DNV GeniE software	190
Figure 58: Thickness deterioration as a function of time	203
Figure 59: Reliability index deterioration of critical members (b454, b458)	204
Figure 60: Reliability index deterioration of members (b403-b103)	205
Figure 61: Post failure behaviour.....	208
Figure 62: Critical Failure paths.....	208
Figure 63: Displacement vs overturning moment (intact structure)	209
Figure 64: Displacement vs load factor (intact structure)	209
Figure 65: Displacement vs overturning moment (one member removed).....	211
Figure 66: Displacement vs overturning moment (two members removed) ...	211
Figure 67: Displacement vs load factor (one member removed).....	212
Figure 68: Displacement vs load factor (two members removed).....	212
Figure 69: Buckling curves	247
Figure 70: Stress distribution.....	275
Figure 71: Reliability distribution.....	275
Figure 72: Reliability Based Optimization	279
Figure 73: Corrosion Cell	326
Figure 74: Numbering of the structural members	327

LIST OF TABLES

Table 1: Examples of Limit States according to DNV	16
Table 2: Reliability Index and Reliability Classes [7]	28
Table 3: Values of acceptable annual probabilities of failure (PF) [14].....	28
Table 4: Comparative estimates of target Pf [35]	29
Table 5: Reliability Index and Probability of Failure vs. Sampling Number.....	92
Table 6: Stochastic Loads Consideration	105
Table 7: Verification of FEA code: results (kPa).....	106
Table 8: Sensitivity Analysis of MCS Probability of failure results	107
Table 9: MCS vs ARSM Probability of failure results.....	107
Table 10: Stochastic loads on verification model.....	109
Table 11: Results of comparative analysis of test case structure	111
Table 12: Values of hydrodynamic coefficient for circular cylinders [202]	131
Table 13: Yield Strength Properties [235].....	146
Table 14: Young's modulus and Poisson's ratio.....	146
Table 15: Variation in thickness of steel plates [239].....	147
Table 16: Probability Density Function for Soil Characteristics [254]	151
Table 17: Typical annual corrosion rates [270], [271].....	158
Table 18: Phases in pitting corrosion and calibrated functions for model parameters [276]	162
Table 19: MSS Failure Criterion for Plane stress problems.....	170
Table 20: CM Failure Criterion for Plane stress problems.....	173
Table 21: Limit states for different Failure Criteria.....	176
Table 22: Distribution coefficients.....	182
Table 23: Wave Height Statistical Correlations [286]	186
Table 24: Design load input parameters for dimensioning of the structure.....	190
Table 25: Properties of stochastic variables	191
Table 26: Reliability Index of Horizontal Members	192
Table 27: Reliability Index of Vertical Members.....	192
Table 28: Reliability Index of Legs Members.....	193
Table 29: Minimum Reliability index of members, incorporating 8 different directions.....	195
Table 30: Reliability indices for buckling limit states (10 critical members)	196
Table 31: Reliability index of smooth and rough cylinders (30 critical members)	197
Table 32: Reliability index for different wave theories (20 members with critical effect)	198
Table 33: Parameters of equivalent normal distributions.....	199
Table 34: Reliability indices for equivalent normal distributions.....	200
Table 35: Reliability indices for cases of 25% reduced loads	201
Table 36: Reliability indices for S355 and S275 steels.....	202
Table 37: Reliability indices for 20 years for different corrosion models	204
Table 38: Bounds of System Reliability	213
Table 39: Effective length and bending reduction factors.....	224
Table 40: Limit States according to API-LRFD	225
Table 41: Reliability indices for Leg Members	225

Table 42: Reliability indices for Horizontal Brace Members	226
Table 43: Reliability indices for Vertical Brace Members.....	227
Table 44: Effective length and moment reduction factors for member strength checking.....	236
Table 45: Limit States according to ISO 19902	237
Table 46: Reliability indices for Leg Members	237
Table 47: Reliability indices for Horizontal Brace Members	238
Table 48: Reliability indices for Vertical Brace Members.....	239
Table 49: Classification of members	242
Table 50: Imperfection factors for buckling curves	246
Table 51: Limit States according to EN 1993	250
Table 52: Reliability indices for Leg Members	251
Table 53: Reliability indices for Horizontal Brace Members	251
Table 54: Reliability indices for Vertical Brace Members.....	252
Table 55: Limit States according to ANSI/AISC 360-05	260
Table 56: Reliability indices for Leg Members	260
Table 57: Reliability indices for Horizontal Brace Members	260
Table 58: Reliability indices for Vertical Brace Members.....	261
Table 59: Minimum Reliability indices for Leg Members	265
Table 60: Minimum Reliability indices for Horizontal Brace Members.....	266
Table 61: Minimum Reliability indices for Vertical Brace Members	266
Table 62: Reduction factors of different standards	266
Table 63: Critical Members.....	276
Table 64: Shallow and deep water approximation to linear wave theory [194]	315
Table 65: Φ_n' and η_n' the coefficients [194].....	317
Table 66: Stokes fifth-order wave theory [194].....	318
Table 67: The coefficients for Stokes fifth-order wave theory [311].....	319
Table 68: Typical coating systems used for offshore structures.....	323
Table 69: Requirements of Galvanic and an Impressed-Current Corrosion Protection System	326
Table 70: Dimension of group of members	328

NOMENCLATURE

Symbols

A	Coefficient of Reyleigh Parameter
A	Cross Sectional Area
A	Transformation matrix
A_I, A_D	Characteristic Areas
A_e	Effective net area, calculated as the product of the net area A_n and the shear lag factor U specified for different connections of tension members.
A_g	Gross area of section based on design wall thickness
A_g	Gross area of member
B	Matrix Relating Strains to Displacements
C	Global Damping Matrix
C	Buckling Parameter
C	Multiplication Correction
C	Torsional constant
C	Total Loss of Material Function
$C(x, \theta)$	Randomness Matrix
C_D	Drag Coefficient
C_M	Inertia Coefficient
C_S	Shape Coefficient
$C_{m,y}, C_{m,z}$	Moment Reduction Factors
C_{my}, C_{mz}	Reduction factors
C_x	Elastic Critical Buckling Coefficient D Outside diameter
D	Diameter of Cylindrical Members
D	Elasticity Matrix
D	Spatial Domain
D_k	Relative Distance Between Sampling Points and Current Design Point
E	Load Effect
E	Modulus of Elasticity
E	Vector of Environmental Conditions
E	Young's Modulus of Elasticity
$E(u)$	Expected Value of Response
$\bar{E}(x)$	Mean value of stochastic process
E_p	Probability of Excedance during L_f
E_d	Design Value of Load Effect
E_k	Characteristic Value of Load Effect
$F_{x_i}(x_i)$	Marginal Cumulative Distribution Function
F_{hc}	Nominal critical hoop buckling strength
F_{bn}	Nominal Bending Strength
F_{cn}	Nominal Axial Compressive Strength
F_{cn}	Nominal Axial Compressive Strength

F_{cr}	The greatest of (without exceeding $0.6F_y$)
F_d	Design Value of variables
F_e	Elastic critical buckling
F_{ey}, F_{ez}	Euler buckling strengths
F_{int}	Internal reaction force vector
F_u	Specified minimum tensile stress
F_{vn}	Nominal Shear strength
F_{vtn}	Nominal torsional strength
F_{xc}	Nominal Inelastic Local Buckling Strength
F_{xe}	Nominal Elastic Local Buckling Strength
F_y	Nominal Yield Strength
F_y	Specified minimum yield stress
G	Shear Modulus
$G(t, z)$	Gust Factor
G_{CM}	Failure Limit State for CM failure criterion
G_{DE}	Failure Limit State for DE failure criterion
G_{MSS}	Failure Limit State for MSS failure criterion
G_{eq}	Equivalent Limit State
H	Wave Height
H	Transformed Orthogonal Matrix
$H_{1/10}$	1/10 Highest Wave Height
H_{max}	Maximum Design Wave Height
H_o	Average Wave Height
$H_s, H_{1/3}$	Significant Wave Height
H_w	Wave Height
I	Moment of inertia
$I(z)$	Turbulence Intensity
$I(x)$	Indicator Function
I_p	Polar moment of inertia
I_p	Polar Moment of Inertia
J	Polar Moment of inertia
K	Effective length factor in plane of bending, equals 1 unless different analysis indicates a smaller value
K	Effective Length Factor
K	Effective Length Factor
K	Global Stiffness Matrix
K	Covariance Matrix
KC	Kuelegan-Carpenter Number
K_{IC}	Stress Intensity Factors
K_y, K_z	Effective length factors
L	Laterally un-braced length of member
L	Length of Member
L	Load
L	Un-braced Length
L	Wave Length
L_{er}	Buckling length in the buckling plane

L_f	Service Life
L_v	Distance from maximum to zero shear force
L_y, L_z	Un-braced lengths
M	Applied Bending moment
M	Bending Moment
M	Global Mass Matrix
M_{Ed}	Design value of the moment
M_{Ed}	Bending moment
$M_{N,Rd}$	Design plastic moment resistance reduced due to axial force
$M_{b,Rd}$	Design buckling resistance moment
M_c	Available flexural strength
M_{cr}	Elastic critical moment for lateral-torsional buckling
M_r	Required flexural strength
M_r	Required flexural strength
M_u	Regression Design Matrix
$M_{v,t}$	Torsional Moment due to Factored Actions
M_{vt}	Torsional moment
M_c	Design flexural strength
N	Total Realizations
N_{Ed}	Design value of the compression force
N_{Ed}	Design value of the compression force
$N_{Ed}, M_{y,Ed}, M_{z,Ed}$	Design values of the action at point of consideration
$N_{Rd}, M_{y,Rd}, M_{z,Rd}$	Design Values of the Resistance depending on the cross sectional classification and including any reduction that may be caused by shear effects
$N_{b,Rd}$	Design buckling resistance of the compression member
N_{cr}	Elastic critical force for the relevant buckling mode
N_f	Successful Realizations
N_{xx}	Axial Force
P	Orthogonal Eigenvector Matrix
P	Tensile Force
P	Vector of Parameters for the CPS
P_A	True Probability of Event
P_E	Estimated Probability in LHC
P_L	Probability of linear zed domain
P_c	Available axial compressive strength
P_c	Available axial tensile strength
P_c	Design tensile or compressive strength
P_{cr}	Critical Load for Unstable Bending
P_d	Design Value of Probability of Failure
P_f	Probability of Failure
P_r	Required axial strength
P_r	Required axial compressive (tensile) strength
\hat{P}_E	Estimated Probability of an Event
Q	Bernoulli's constant
Q	Probability of Excedance

R	Nodal Load Vector
R	Structural Resistance
R	Time-dependent Load
Re	Reynolds Number
\hat{R}, \hat{S}	Standard Normalized Random Variables
R^2	Coefficient of Determination
R_U	Ultimate Lateral Load Capacity
R_d	Design Value of Resistance
R_k	Characteristic Value of Resistance
R_n	Nominal strength, as specified for each case of loading
R_u	Required strength
S	Elastic section modulus
S	Elastic Section Modulus
S	First moment of area
$S_F(\omega)$	Wave Force Transfer Function
S_R	Reference Lateral Loading
$S_W(\omega)$	Sea Surface Spectrum Function
S_t	Material Tensile Strength
S_{uc}	Material Ultimate Compressive Stress
S_{ut}	Material Ultimate Tensile Stress
S_y	Material Yield Strength
T	Correlated Random Vector
T	Wave Period
T_C	Design torsional strength
T_{Ed}	Design value of the torsional moment
T_P	Spectral Peak Period
T_P	Peak spectral period
T_R	Return Period
T_{Rd}	Design torsional resistance of the cross section.
T_r	Required torsional strength
U	Vector of Standardized Independent Variables
$U_G(z)$	Gust Wind Speed at z m above SWL
U_{TS}	Speed of Current
U_{TZ}	Speed of Current at z -level
$U_w(1m, z)$	1-minute Mean Sustained Wind Speed at 10 m above Sea Water Level
V	Beam Shear
V	Member Shear
V_{Ed}	Design value of the shear force
V_{Ed}	Shear force
$V_{c,Rd}$	Design shear resistance
V_n	Design shear strength
V_r	Required shear strength
W_G	Weight Matrix
$W_{el,min}, W_{eff,min}$	Maximum elastic stress
X	Matrix of Dependent Variables
X	Stochastic Variables vector

X	Uncorrelated Random Variables
Y	Matrix of Independent Variables
Y	Transformed Matrix
\bar{Y}	Estimated Values
Z	Plastic section modulus about the axis of bending
Z	Plastic Section Modulus
Z_e	Elastic Section Modulus
Z	Safety Margin, Limit state equation
b_i	First Order Regression Coefficients
b_i	Polynomial Coefficients
c	Celerity
c_i	Linear Coefficients
c_i	Second Order Regression Coefficients
d	Still water depth
d	Total Water Depth
$d(t)$	Corrosion Wastage Thickness
d_∞	Long term thickness corrosion wastage
d_{ij}	Mixed Term Regression Coefficients
e	Regression Error
f	Identification Coefficient
f	Total Hydrodynamic Wave Force
$f(x, y)$	Bivariate Distribution Function
$f_{x_i}(x_i)$	Probability Density Function
f_h	Hoop stress due to factored hydrostatic pressure
$f_{b,h}$	Representative Bending Strength in the presence of external hydrostatic pressure
f_b	Bending Stress
f_b	Representative Bending Strength
f_{by}, f_{bz}	Bending stresses about y and z- axis
$f_{c,h}$	Representative Axial Compressive Strength in the presence of external hydrostatic pressure
f_c	Axial Compressive Stress
f_c	Representative Axial Compressive Strength
$f_{e,y}, f_{e,z}$	Euler Buckling Strengths
f_e	Euler Buckling Strength
$f_{t,h}$	Representative Axial Tensile Strength in the presence of external hydrostatic pressure
f_t	Representative Axial Tensile Strength
f_t	Axial Tensile Stress
f_{vt}	Torsional shear stress
$f_x(x)$	Initial Distribution Function
f_{xe}	Representative Elastic Local Buckling Strength
f_y	Representative Yield Strength
f_{yc}	Representative Local Buckling Strength

f_{yc}	Representative Load Buckling Strength
f_v	Representative Shear Strength
$g(t)$	Gust Factor Component
$g(x)$	Indicator function
$g(U)$	Transformed Limit State Surface
$\tilde{g}(x)$	Approximate Limit State Function
i	Radius of gyration about the relevant axis
k	Area of gyration
k	Safety Factor
k	Wave Number
$k(\theta)$	Global Stiffness Matrix
$k_{yy}, k_{yz}, k_{zy}, k_{zz}$	Interaction factors (App. A and B of standard)
m	Number of Segments in LHC
n	Limit State Safety Factor
p	Hydrostatic Pressure
$p_x(x)$	Sampling Distribution
$p_m(x_n)$	Regression Polynomials
r	Governing radius of gyration
r	Correlation coefficient
r	Element Stiffness Matrix
r	Radius of Gyration
r	Radius of Gyration
$r(t)$	Displacement Vector
s	Global Safety Factor
s_0	Target Global Safety Factor
t	Time Parameter
t	Time Variables
u	Coefficient vector
u	Poisson's Ratio
u	Strain Energy
$u(\theta)$	Gaussian Random Response
u_i	Transformed x_i into their Standardized Forms
u_i^*	Transformed Intermediate Coordinates
v	Poisson's Ratio
u_{max}	Maximum Effect in Response
u_{static}	Static Effect in Response
w	Sea water density
w_{Dk}	Weight Factor
w_{Gk}	Weight Factor
x_i^*	Intermediate Coordinates
x	Subscript relating symbol to strong axis bending
y	Subscript relating symbol to weak axis bending
\hat{y}_{best}	Best Design Value
z	Depth below still water surface
z	Distance above the Seabed

Γ_n	n-th order polynomial of variables
Γ_p	Hermite Polynomials
$\Delta M_{y,Ed}, \Delta M_{z,Ed}$	Moments due to the shift of the centroidal axis
Λ	Eigen-value Matrix
Φ	Cumulative Distribution Function
Φ, Ψ	Stream Function (velocity potential)
$\Phi_U^{-1}()$	Inverse Standardized Normal Distribution Function
α	Imperfection factor
$\alpha, \beta, \gamma, \lambda$	Coefficients of Weibull Bivariate Distribution
α_{LT}	Imperfection factor
\bar{a}	Coefficients Matrix
a_d	Material's Uncertainties
a_i	Indicator Variables
a_i	Sensitivity Factors
a_k	Characteristic Value of Material's Uncertainties
β	Reliability index
β_{HL}	Hasofer-Lind reliability index
β_d	Design Value of Reliability index
γ	Partial Factor
γ_D	Hydrostatic pressure load factor
γ_{M0}	Resistance partial factor of cross section applicable to all classes
γ_{M1}	Resistance of members to instability
γ_{M1}	Resistance of members to instability
γ_{M2}	Resistance of cross section in tension to fracture
$\gamma_{R,b}$	Partial Resistance Factor for Bending Strength
$\gamma_{R,c}$	Partial Resistance Factor for Axial Compressive Strength
$\gamma_{R,t}$	Partial Resistance Factor for Axial Tensile Strength
$\gamma_{R,v}$	Partial Resistance Factor for Shear Strength
γ_m	Material Reduction Factor
γ_o	Partial safety factor
δ_{ij}	Delta Function
ε	Perturbation Parameter
ε	Residual
ε	Strain
ε	Zero Mean Error Function
ε_f	Maximum Strain (Elongation) before Failure
η	Free Surface Profile
θ	Random Process
θ	Wave Phase Angle
θ_d	Model's Uncertainties
θ_k	Characteristic Value of Model's Uncertainties
λ	Column Slenderness Parameter
λ	Eigen-values
λ_y, λ_z	Column slenderness parameters
$\mu(x)$	Mean Value

$\mu_d(t)$	Mean Value of Deterioration Model
μ_X	Vector of Mean Values
(ξ_1, ξ_2)	Gaussian variables
ρ	Air Density
ρ	Correlation coefficient
ρ_{RS}	Correlation Coefficient between R and S
σ	Stress
$\sigma_{\tilde{g}}$	Standard Deviation of the Approximate Limit-State Function
σ'	von Mises stress
$\sigma_1, \sigma_2, \sigma_3$	Principle Stresses
σ_h	Hoop Stress due to forces from factored hydrostatic pressure
σ_A, σ_B	Principle Stresses for plane stress problems
$\sigma_{a,xx}$	Axial Stress
σ_{av}	Hydrostatic Stress
$\sigma_{b,xy}, \sigma_{b,xz}$	Bending Stress
$\sigma_{b,y}, \sigma_{b,z}$	Bending Stress about the member y and z-axis
σ_b	Bending Stress
σ_c	Axial Compressive Stress
σ_{crit}	Critical Stress
$\sigma_d(t)$	Standard Deviation of Deterioration Model
σ_{max}	Maximum Stress
σ_{per}	Allowable Stress)
σ_q	Compressive Axial Strength due to capped end hydrostatic action
σ_t	Axial Tensile Stress
$\sigma_{x,Ed}$	Design Value of the Longitudinal Stress at the point of consideration
$\sigma_{x,Ed}$	Design value of the longitudinal stress due to moment and axial force
σ_x	Standard Deviation
$\sigma_{z,Ed}$	Design Value of the Transverse Stress at the point of consideration
τ_{Ed}	Design Value of the Shear Stress at the point of consideration
τ_b	Maximum Beam Shear Stress
τ_c	Coating Life
τ_{max}	Maximum Shear Stress
τ_t	Torsional Shear Stress
φ	Resistance factor, as specified for each case of loading
φ_C	Resistance factor for compression
φ_b	Resistance Factor for Bending Strength
φ_b	Resistance factor for flexure
φ_b	Resistance factor for hoop buckling strength
φ_c	Resistance Factor for Axial Compressive Strength
$\varphi_i(x)$	Base Functions
φ_t	Resistance factor for tension (as described above)
φ_t	Resistance Factor for Axial Tensile strength
φ_v	Resistance Factor for Member Shear Strength

$\varphi_x(x)$	Joint Probability Density Function
χ	Reduction factor for the relevant buckling mode
χ_{LT}	Reduction factor for lateral-torsional buckling.
ψ	Eigen-functions
ψ	Reduction Factor
ψ	Reduction Factor
ω	Angular Frequency

Abbreviations

<i>AISC</i>	American Institute of Steel Construction
<i>ALS</i>	Accidental Limit State
<i>ANSI</i>	American National Standards Institute
<i>API</i>	American Petroleum Institute
<i>ARESA</i>	Adaptive Reliability Estimation Response Surface Algorithm
<i>BCM</i>	Brittle Coulomb-Mohr
<i>COV</i>	Coefficient of Variation
<i>CPS</i>	Corrosion Protection System
<i>CTOD</i>	Crack Tip Opening Displacement
<i>DCM</i>	Ductile Coulomb-Mohr
<i>DE</i>	Distortion Energy
<i>DNV</i>	Det Norske Veritas
<i>DTR</i>	Damage Tolerance Ratio
<i>EDF</i>	Empirical Distribution Function
<i>EN</i>	Euro Norm
<i>FEA/FEM</i>	Finite Element Analysis/Methods
<i>FLS</i>	Fatigue Limit State
<i>FORM</i>	First Order Reliability Method
<i>HLRF</i>	Hasofer Lind – Rackwitz Fiessler
<i>ISO</i>	International Standardization Organization
<i>LHS</i>	Latin Hypercube Simulation
<i>LRFD</i>	Load Resistance Factor Design
<i>LSM</i>	Least Square Method
<i>MCS</i>	Monte Carlo Simulation
<i>MM</i>	Modified Mohr
<i>MNS</i>	Maximum Normal Stress
<i>MPP</i>	Most Probable failure Point
<i>MSS</i>	Maximum Shear Stress
<i>MVFOSM</i>	Mean Value First Order Second Moment
<i>NACA</i>	National Association of Corrosion Engineers
<i>ORA</i>	Organizational Reliability Analysis
<i>PCE</i>	Polynomial Chaos Expansion
<i>QRA</i>	Quantitative Risk Analysis
<i>RIF</i>	Residual Resistance Factor
<i>RSEAD</i>	Response Surface with Adaptive Experimental Design

<i>RSR</i>	Reserve Strength Ratio
<i>SLS</i>	Servicability Limit State
<i>SORM</i>	Second Order Reliability Method
<i>SRA</i>	Structural Reliability Analysis
<i>SRSM</i>	Stochastic Response Surface Method
<i>SSE</i>	Error Sum of Squares
<i>SSFEM</i>	Spectral Stochastic Finite Element Method
<i>SSR</i>	Regression Sum of Squares
<i>SST</i>	Total Sum of Squares
<i>SWL</i>	Still Water Level
<i>TANA(2)</i>	Two point Adaptive Nonlinear Approximations
<i>TLP</i>	Tension Leg Platform
<i>ULS</i>	Ultimate Limit State
<i>WSD</i>	Working Stress Design

1 INTRODUCTION – CONTEXT OF STRUCTURAL SAFETY

1.1 Introduction

Current evolution in engineering practices has allowed more critical and complicated structures to be designed with greater confidence than in the past. In addition, the constantly increasing cost of construction materials, due to higher demand over the last years, indicates that design optimization can provide competitive structures, compromising performance characteristics for more cost effective designs. Structural Reliability has been established as a valuable design tool for the description of the performance of structures; therefore and towards this purpose, it can serve as a design restriction that will ensure derivation of preferable structures which comply to minimum safety requirements. The requirements set above, indicate the demand of a more systematic assessment of the uncertainties of the basic design variables; the functional and environmental loads, geometrical and model parameters, as well as material properties.

Cases with limited levels of randomness can be treated deterministically, applying a magnification factor on the loading or a reduction on the capacity modelling, to account cumulatively for the effect of uncertainties. This simplification in the design process produces most of the times oversized designs without providing accurate information on the service life performance of the structure, or ensuring adequate levels of structural safety. In contrast, when the level of uncertainty is high, a stochastic approach of the design variables seems essential. Following this approach, statistical representation of the design parameters will provide the response of the structural member or system in a stochastic way, allowing a better understanding of its service life performance.

This contribution will focus on the reliability assessment of offshore structures, and particularly frame-type jacket structures due to the important environmental

phenomena they have to withstand throughout their service life and the complicated failure mechanisms that they form. This Thesis will report the development of the Stochastic Response Surface Method (SRSM) that allows reliability assessment of a structure, in the form of individual design blocks. This methodology, contrary to complicated Stochastic Finite Element Analysis Methods that demand deep knowledge of the mathematical background in order to express explicitly uncertainty within the analysis, treats the simulation procedure as a 'black box', extracting the response of the structure and later processing it, within an individual reliability assessment routine.

The methodology that is proposed allows reliability assessment of structural components through a sequence of individual steps that permit calculation of reliability, based on easy to program procedures. After execution of a finite series of simulations, the response of each member can be identified and a quadratic polynomial response surface can be formulated based on the values of the limit states that are examined through data regression analysis. Later, a separate routine can account for the estimation of the reliability index based on one of the available numerical techniques. Those discrete steps, which may employ different tools and procedures for each task, can handle several problems that are difficult to be modelled in one unified simulation code. For the problem of the design of offshore structures that has been studied, reliability analysis took place using the specialized software DNV SESAM for a confident representation of the response of structural members through appropriate modelling of the environmental loads acting on the structure. Following this methodology, specialized commercial tools for different applications may be employed for the probabilistic assessment of several engineering problems. Figure 1, initially presents this procedure, which will be developed in the next chapters.

The First Chapter of this Thesis presents the background of structural reliability and the context of structural safety. Evolution of design methods and design standards is discussed. Target reliability requirements are included, based on

requirements of regulatory bodies and classification societies, in order to set the general requirements of a structural reliability assessment.

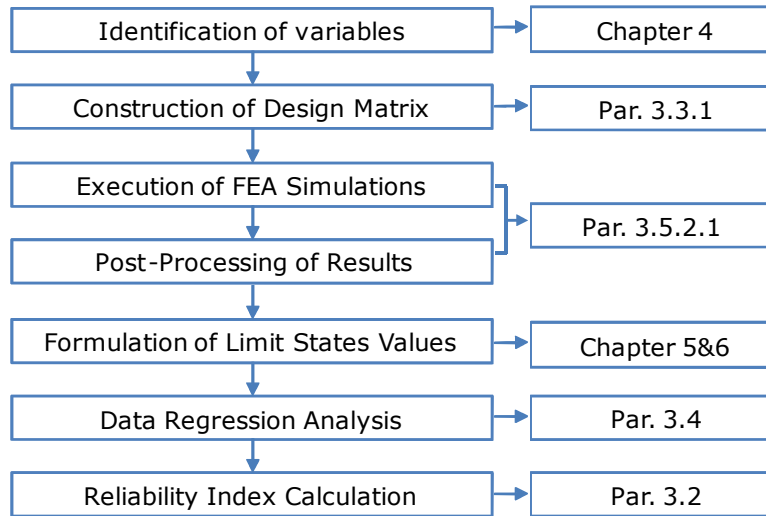


Figure 1: Response Surface Method Flow Chart

The Second Chapter presents a review of reliability assessment of steel and offshore structures. Selection of the appropriate type of response analysis and consideration of the integration from component to system reliability is discussed. Finally, a comprehensive review of the Stochastic Methods for reliability assessment will provide the background for the development of the methodology that will be applied later in this contribution.

The Third Chapter includes the numerical procedures for the computation of structural reliability. Deterministic methods, First and Second Order Reliability Method (FORM/SORM), as well as Simulation Methods will be presented and the background to the codes that have been written for the scope of this Thesis will be set. A review of the Stochastic Response Surface Method (SRSM) and the methodology that is introduced and will be applied in the later chapters are analytically discussed. Finally Regression techniques are included as fundamentals of the (weighted) regression analysis that is applied in the SRSM, and a variation of the conventional least square method (LSM) will be proposed for more accurate regression and prevention form ill conditioned systems of

equations. Verification of the mathematical tools that are developed is included, providing confidence on their later application.

In the Fourth Chapter, the environmental loading and capacity modelling of Offshore Structures will be analytically presented. Modelling of wave loads according to different wave theories and the correlation between significant wave height and peak spectral period based on joint distribution of statistical distributions is presented. Wind and current modelling, are also covered. An extensive review of literature data for material properties and methodologies for the consideration of corrosion is included. Geotechnical data regarding piling properties are also presented.

Once the stochastic variables and a reference structure have been identified, in the Fifth Chapter the reliability of structural tubular members of a typical offshore structure is assessed for ultimate strength under different combinations of stochastic and deterministic loads. Limit states are formulated based on fundamental failure criteria of ductile structural members, in order to comprehensively represent multiple load actions that they are subjected to. A sensitivity analysis of the design parameters (surface roughness, variables' modelling, corrosion deterioration etc) is also included. System reliability integration, based on the reliability performance of the structural members and the failure mechanism of the structure, is also discussed.

The Sixth Chapter introduces the most widely used standards for the design of offshore structures API RP 2A [1], [2], and ISO 19902 [3]. Further, ANSI/AISC 360-05 [4], and EUROCODE 3 [5], are included as generic codes of the design of steel structures with strong probabilistic background. For the same reference case structure, limit state functions will be examined based on their individual design requirements and the minimum reliability indices of members are derived and later compared to the ones obtained by the analytical limit states, using the same calculation procedure.

The final chapter of this Thesis, Chapter Seven, gathers the conclusions of this endeavour and proposes some future work towards a completely robust design of steel structures.

1.2 Structural Reliability

In [6], the most complete definition of reliability, which has been adopted with minor alterations from most current design standards, summarizes that “reliability is the ability of a structure to comply with given requirements under specific conditions during the intended life for which it was designed”. In this definition, the important elements of design requirements, service life period, and design conditions are included. A more practical, direct approach defines reliability of a structure as the opposite of its probability to fail.

Reliability is the entity that will compromise the two requirements of design; structural integrity and economy. In [7], a fundamental requirement for design states that “a structure should be designed and executed in such a way that it will, during its intended life time with appropriate degrees of reliability and in an economic way sustain all actions and influences likely to occur during execution and use and remain fit for the use for which it is required”. Structures can be designed to have nearly zero probability to fail. Absolute no failure is an oversimplification and can never be achieved because every forthcoming event cannot be realistically predicted. Therefore, failures are accepted up to a level that all parties involved in the design and operation of the structure will agree.

Structural reliability works on the prediction of the probability of exceedance of the structural restrictions imposed by the design requirements at any stage of its service life. The probability of occurrence of such an event is directly correlated to its reliability, and once this is derived, design alterations can be identified, in order to either improve structural reliability, or optimize already adequate designs. Techniques of structural reliability, following computational resources and numerical methods evolution, can be applied in wider multidisciplinary

design environments, considering the joint effect of multiple uncertain variables. Practice can verify that structures that have been designed deterministically, neglecting analytical modelling of uncertainty in variables, can have a greater probability of failure compared to less expensive structures of similar service that have been designed following a stochastic approach.

Within different application fields, different methods for reliability assessment can be distinguished including Quantitative Risk Analysis (QRA), Structural Reliability Analysis (SRA) and Organizational Reliability Analysis (ORA), which is not applicable in the case of structural design. In order to better understand the use of Structural Reliability Analysis, it is important to consider its interaction with other disciplines.

Structural Reliability Analysis is related to the estimation of the probability of failure of a structure or a structural member for given loading conditions. Numerical implementation should be based on the most up-to-date modelling techniques. Combination of fundamentals of structural reliability and modelling techniques can allow calibration of design standards as will be discussed in a later section. Quantitative Risk Assessment relates to the evaluation of the overall risk of potential failure to humans, safety, environment and assets. The main steps should include the following, according to [8]:

- Identification of hazards
- Assessments of frequency of initiating events
- Accident development
- Consequence Assessment
- Calculation of risks

A classification between probability concepts, distinguishes frequentistic to Bayesian Probability. The first refers to the statistical interpretation of the outcomes of stochastic experiments and its approach to probability can be adequately predicted when the number of experimental iterations is increased respectively. Bayesian probability, proposed by Bayes [9], is considered subjective as it is based on the knowledge of each individual decision maker

rather than in the outcome of a repeated experiment and it is considered as an expression of a “degree of belief” [10], [11]. Although in literature [12] the two concepts are considered fundamentally different, both of them satisfy the mathematical theory of probability. Structural Reliability Assessment follows the Bayesian approach for the definition of probability since, although it uses data from experiments or experience of existing structures, the basic scope is to mathematically estimate the value of reliability. Presence of uncertainty in materials, fabrication defects, effects of loading etc, constitutes each structure as a unique outcome of the ‘design experiment’.

Statistical modelling of uncertainties is analytically studied in [13], while in [14] a classification of uncertainty in structural design distinguishes the following types of uncertainty:

- Physical (intrinsic or inherent) uncertainty describes the natural randomness of a quantity. Typical examples of this type are the yield stress affected by production variability (manufacturing defects) or the variability in the wave and wind loading.
- Measurement uncertainty which is caused by errors in instruments or instrumental configurations and sample disturbance due to external factors (eg. ‘noise’ in experimental measurements).
- Statistical uncertainty which occurs due to inadequate data or information such as a limited number of samples.
- Model uncertainty due to imperfections and idealizations made in the physical model, formulations for load and resistance variables as well as the allocation of statistic distribution to the main variables.

Structural Reliability Methods are classified according to their Level, Moment and Order:

- Level, refers to the extent of information that the reliability problem incorporates.
- Moment, refers to the order of statistical moments applied to better represent the stochastic nature of an uncertain variable.

- Order, refers to the polynomial order used for the approximation of the limit state surface.

From the above attributes, that of Level describes the development of reliability methods [14]:

- Level I methods are deterministic reliability methods that only use one characteristic value to describe each uncertain variable. Common design standard formats, load-resistance and allowable stress, belong to this category. Those methods correspond to standard deterministic design methods. They can be combined with more advanced, higher level methods in the case of partial safety factors calibration, which can optimize the application of those methods.
- Level II methods use two values for the representation of each uncertain variable (eg. the mean and the variance) and a supplementary measure of the correlation between the variables (eg. covariance). Reliability determined following such methods can be geometrically interpreted as a relative distance from the mean value.
- Level III methods introduce the joint probability distribution of the sum of the uncertain variables, calculating directly the probability of failure for a limit state function. Advanced mathematical techniques such as numerical integration, approximate analytical methods, including the First and Second Order Reliability Methods, and simulation methods, such as the Monte Carlo Simulation and the Directional Sampling methods, belong to this category.
- Level IV reliability methods, are the most advanced, introducing the element of target cost to the principles of engineering in order to derive a technically feasible and at the same time economically optimized solution. These methods can set an acceptable target reliability level for the application of Level III methods.

1.3 Overview of Reliability Analysis of Offshore Structures

Offshore structural reliability analysis becomes of particular importance recently considering numerous changes within offshore industry. Introduction of the Load Resistance Factor Design format in standards has significantly contributed to a more systematic design of offshore structures. Further, the introduction of a 'goal setting regime' [15] which stands as a requirement as well as a target restriction in the structural design, allows more flexibility in the procedure of the design of offshore structures. This has resulted to the establishment of basic guidelines for a thorough reliability based design.

The above changes combined with the increasing need for a better understanding of the performance of structures throughout their service life in aspects of inspection, maintenance and reliability have created a wider acceptance framework for reliability assessment methods. More accurate modeling techniques and tools together with a higher available computational capacity, allow for analytical assessment of the reliability evaluation of structures in different stages and under different loading and capacity conditions.

Structural reliability analysis can provide significant benefit to the potential safety and cost; however the level of confidence of a reliability assessment strongly depends on the uncertainty consideration, accuracy of modeling and simplifying assumptions made as it has already been mentioned in Chapter One. Structural problems, and even more extensively in offshore environments, are in most cases non-deterministic, with limited information and knowledge in both the conceptual and the design phase. Therefore, risk quantification yields for stochastic (random) variables to be considered.

From the variables considered, the main concern is the environmental loads due to its great randomness. In Chapter Four, a probabilistic consideration of the joint environmental load will be presented. Extensive literature is available for the meteocean conditions mainly for the Gulf of Mexico and the North Sea sites, since those areas serve as a baseline for the development of design

standards. Application of those data in different regions might provide inaccurate results, and calibration of the statistical properties of variables to specific areas is essential. Stochastic modeling of capacity of structures and structural members is less significant, as shown in [16], affecting the reliability results in a lower scale. This phenomenon is also illustrated by design standards consideration for partial safety factors, where those that account for loads are significantly higher than those for material properties.

During the last decades, momentous developments have occurred in the methodology as well as the tools for calculation of structural reliability. In a component level, methods such as the First and Second order reliability methods (FORM/SORM) have been widely used, proposing modifications to account for complicated formulations of limit state functions and transformation of complicated statistical distributions to a normalized u -space. Further, simulation techniques, such as the widely known Monte Carlo Simulation, have been introduced overcoming limitations of the deterministic techniques. Chapter Three that follows presents the theory and the solution algorithms of those methods. In a structural system reliability analysis level, different methods are used from a component-based approach to a fully probabilistic analysis where advanced mathematical and computational effort is required. In [17], the well-known theory for system reliability assessment of the “branch and bound” method is described.

Based on the context presented so far the research problems that will be covered within this Thesis are summarized as follows:

- I. Development of a methodology for the reliability assessment of a complex frame type structure, using sequential steps of high capabilities tools and widely used numerical techniques.
- II. Provide analytical guidelines for the modeling of stochastic variables for environmental loading and capacity of offshore jacket structures.
- III. For a reference structure, identify critical members and failure paths that will result to global failure of the structure and examine the sensitivity of the derived values of reliability to significant design parameters.

- IV. For the same reference structure, evaluate the reliability performance of different design standards.

1.4 Design of Offshore Structures

Development of our knowledge of structures and their behaviour, and the tools that are available, have advanced design procedures and methodologies applied on the design of structures. In this section, a classification of design methods will be presented, based on the way uncertainties are treated, and with a view for classification of design standards to follow.

1.4.1 Permissible stresses

This is the first widely accepted approach to systematic design, also noted as “allowable (working) stress method”. It is in line with the linear elastic theory. The condition that the design should satisfy is:

$$\sigma_{max} < \sigma_{per} \text{ or } \sigma_{max} < \frac{\sigma_{crit}}{k} \quad (1-1)$$

The coefficient k , also noted SF by safety factor, is the only explicit measure considered to account for all types of uncertainties. The maximum acting stress on the structure should not exceed the critical value of the materials divided by the coefficient k . The expressions above refer to a local effect on the structure and therefore the comparison should be applied at its most exposed locations (maximum stress). The basic principle of this method does not allow any treatment of non linearity, stress distribution, ductility of materials and structural members [18].

The inability of the method to consider analytically all the imposed uncertainties of variables and models, the strict consideration of linear performance as well as the fact that it does not consider combinations of loads, impose a great factor of conservativeness in the design outcome. Different actions that should be examined as well as use of different materials can produce different and unreliable results.

1.4.2 Global Safety Factor

The method of global safety factors is based on the relation between the mean values of the structural resistance R and the load effects E . The ratio of the two specifies the quantity of the global safety factor.

$$s = \frac{R}{E} > s_0 \quad (1-2)$$

The value of s_0 should be defined and is the target that the designer should aim to meet. Contrary to the permissible stresses method, this method takes into account the structural behaviour of members and their cross sections, geometric non linearity, stress distribution and ductility in the individual calculation of R and S .

The disadvantage of the method is that although R and S are calculated in a more scientific method, the only explicit value is that of the global safety factor s . In addition, no special consideration of uncertainties of modeling is made and therefore the results are forced to become conservative to account for any unpredicted and unfavorable events. Combinations of loads and use of different materials still cannot be handled.

1.4.3 Partial Safety factor

The method of Partial Safety Factors is the most up-to-date used method to the establishment of design methodologies. It is also called 'Limit State Method' because it is applied in parallel with the concepts of limit states design for different design conditions. The method is advanced considering that it gives potential for mathematical optimization in several aspects. It can be summarized as follows:

$$E_d(F_d, f_d, a_d, \theta_d) < R_d(F_d, f_d, a_d, \theta_d) \quad (1-3)$$

Where: E_d and R_d represent the design values of actions effects and resistance respectively, $F_d = \psi \cdot \gamma_F \cdot F_k$ design values of variables describing the actions, $f_d = \frac{f_k}{\gamma_m}$ describes the material properties, a_d describes the geometrical

uncertainties, and θ_d the model uncertainties. The design values derive from the corresponding characteristic values of the variables $(F_k, f_k, a_k, \theta_k)$, applying the required partial factors γ , reduction factors ψ and any other specified factor, which are the control values of the reliability of the design. It is obvious that this method compared to the previous ones is the most analytical one, making the fewest simplifying assumptions. Use of the method, allows handling of load combinations as well as multiple different materials.

1.4.4 Probabilistic Methods

The Probabilistic Design Methods are the most advanced that have been proposed. Their basic requirement is that during the service life of a structure the probability of failure does not exceed an acceptable design value. This can be expressed as:

$$P_f \leq P_d \text{ or } \beta > \beta_d \quad (1-4)$$

The above two expressions are equivalent. The design values that should be fulfilled can be determined by the specifications of the structure. Those methods are not widely used yet and undergo some controversy due to their increased complexity. However, they can achieve optimized results leading to lighter and more economically efficient structures.

In addition to the Partial Safety Factor method, concepts of probabilistic analysis can be used to optimize the values of the partial safety factors. This procedure is noted as calibration and can be found on the Annexes or guiding material of the recently introduced modern structural codes [19]. Probabilistic design methods are very important for the design of special cases or novel structures where previous experience does not exist and application of accepted methodologies is not applicable.

1.4.5 Comments on design methods

The design methods as presented above, starting from the permissible loads method and heading to the fully or partially probabilistic methods become more

complicated, demanding greater engineering and mathematical skills. However towards the same direction, the level of conservativeness and therefore the over sizing of the structures is reduced leading to more efficient structures with a better understanding of their service life performance.

Modern Standards and Codes follow the Partial Safety factor methods, giving the engineer the ability for further optimization. This trend has been countersigned by the fact that the most widely used standard for offshore platforms API RP-2A – WSD (Working Stress Design) [1], has been also published from 1993 in a Partial Factor format API RP-2A – LRFD (Load Resistance Factor Design) [2].

1.5 Limit State Design

Since the common trend in modern design is the design according to limit states, this will be presented more analytically in the following sections. The general design requirement is to provide structures with adequate safety margins in order to account for all types of uncertainties affecting its integrity (load and capacity variability, modelling idealizations etc). A simplistic definition of limit state design indicates that the demand (load) of a structural system should under no conditions exceed its capacity (resistance). Considering a case of multiple loading, the safe region criterion should be expressed as:

$$D_d = \gamma_o \sum_i D_{ki}(F_{ki}, \gamma_{ki}) < C_d = C_k / \gamma_M \quad (1-5)$$

In the above expression, index k represents the characteristic value of a load or resistance variable while index d the design values that incorporates the required magnification or reduction to account for consideration of uncertainties. Load variables are magnified with load factors γ_{ki} in order to account for unforeseen events, while the capacity is diminished with the material factor γ_M in order to account for capacity uncertainties (material properties, quality of construction, corrosion etc). A further partial safety factor γ_o is added to

consider the seriousness of the examined limit state to the integrity of the structure.

The characteristic (nominal) value of a variable is defined by its statistical properties. For a capacity variable, it can be based on the lower bound or 95% exceedance value, while for a load variable, the characteristic value on an upper bound or a 5% exceedance value. Derivation of partial safety factors is based on either previous experience or through a rigorous procedure that provide acceptable levels of safety and performance. In the previous methodology of allowable (or working) stress design the basic concept was to make sure that the response of the structure due to loads acting on it will remain below specific levels throughout the service life of the structure. The limit state design approach systematically examines the response of the structure under various conditions it might have to withstand, as a combination of loads and capacity.

For offshore and marine structures, several limit states are proposed by regulatory bodies and classification societies that should be examined within a comprehensive design. Table 1, adopted by [20], presents some common limit states for the four main types of limit states that should be considered:

- Serviceability limit state (SLS)
- Ultimate limit state (ULS)
- Fatigue limit state (FLS)
- Accidental limit state (ALS)

1.5.1 Serviceability Limit State

This type of limit states, refers to conditions where, due to extensive deformation, vibration or noise, the structure's functionality is influenced. The factors mentioned are in many cases correlated. Criteria that have been established based on practice experience of the functionality of the structure are expressed in the form of maximum allowable deflection [5], or similar restrictions that should be fulfilled in order for the structure to operate without requirements of maintenance or further intervention. Buckling phenomena are

often incorporated in order to control the behaviour of the structure and prevent cases of extensive deflection.

Ultimate limit states (ULS)	Loss of structural resistance (excessive yielding and buckling)
	Failure of components due to brittle fracture
	Loss of static equilibrium of the structure, or of a part of the structure, considered as a rigid body, e.g. overturning or capsizing
	Failure of critical components of the structure caused by exceeding the ultimate resistance (in some cases reduced by repeated loads) or the ultimate deformation of the components
	Transformation of the structure into a mechanism (collapse or excessive deformation).
Fatigue limit states (FLS)	Cumulative damage due to repeated loads.
Accidental limit states (ALS)	Structural damage caused by accidental loads
	Ultimate resistance of damaged structures
	Maintain structural integrity after local damage or flooding
	Loss of station keeping (free drifting).
Serviceability limit states (SLS)	Deflections that may alter the effect of the acting forces
	Deformations that may change the distribution of loads between supported rigid objects and the supporting structure
	Excessive vibrations producing discomfort or affecting non-structural components
	Motion that exceed the limitation of equipment
	Temperature induced deformations

Table 1: Examples of Limit States according to DNV

1.5.2 Ultimate Limit State

In many cases, this is the most important limit state that should be considered since it checks the ability of the structure to resist plastic collapse or reach to ultimate strength. For an analytical description of a structural member, its post buckling behaviour should be considered in order to avoid additional conservatism on the strength of the element. Figure 2, illustrates this approach

(point B) compared to a more traditional approach (point A) where the point of elastic buckling determines the strength of the element.

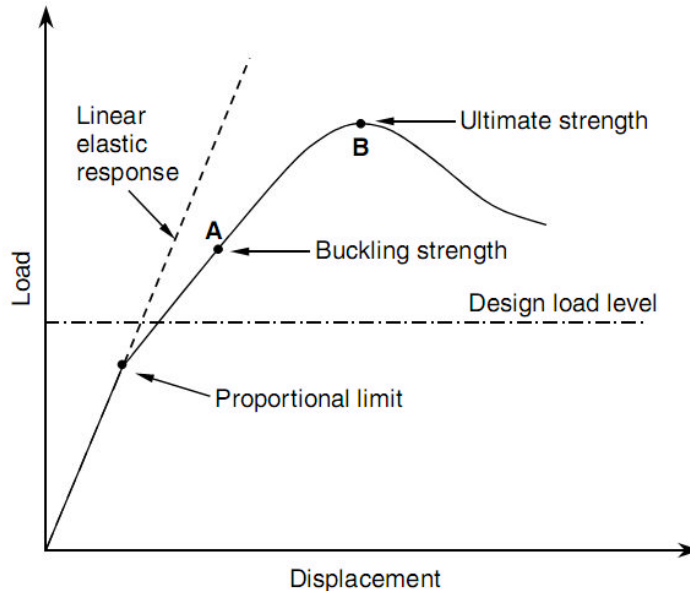


Figure 2: Structural Design Consideration of the ULS

The safety margin of such members cannot be directly evaluated. However, the practice trend is to design structures for ultimate strength. In cases of structures that have suffered any type of damage, a new ultimate strength should be calculated, based on the deterioration of their capacity. Structural design should also take into account the response of the structure in the case of a potential failure. The structure should be designed to fail in a ductile rather than brittle manner in order to allow progressive collapse, by redistribution of stresses in alternative load paths, rather than failing suddenly without providing any warning and therefore potential of intervention. Ductility in a design can be facilitated by design techniques such as avoidance of high stress concentrations, weld defects, allowing some level of plastic deformations etc.

The design problems that are studied in this Thesis mostly deal with ultimate limit states, so in the later sections, several issues as well as design standards provisions will be discussed in greater depth.

1.5.3 Fatigue Limit State

Fatigue Limit State is particularly important in structures that undergo significant cyclic phenomena. Large offshore structures, such as wind turbines are designed for their fatigue life in addition to ultimate strength. Offshore structures have a long service period that might exceed 20 or even 40 years. This, in conjunction with the inspection intervals, affects the reliability requirements of the structural design. The effect of fatigue is preliminarily a local effect, concerning welded joints and areas of stress concentrations.

The Fatigue Limit State criteria are based on a cumulative fatigue damage of a structure under repeated fluctuation of loading. The fatigue damage at a crack initiation is affected by many factors such as the stress ranges experienced during load cycles, local stress concentration characteristics and the number of stress range cycles.

1.5.4 Accidental Limit State

This category of limit states aims to limit the consequences in a case of a failure, such as avoidance of loss of life and assets, environmental pollution and financial losses. The criteria that should be satisfied are based on accidental scenarios and associated performance that should be decided upon analytical risk assessment. Progressive collapse in case of failure, impact, excessive loads due to human error or machinery failure, explosions etc are some of the scenarios that should be addressed. In order to have an economically efficient design, a trade off should be made between ultimate safety and prevention costs, setting realistic survivability consequences.

For Accidental limit state design, the integrity of the structure should be assessed initially in a global level (accident events) and later in a post-accident assessment to account for the real impact on the structure. In the case of an impact on a jacket structure for example the major requirement is to sustain its stability avoiding total collapse. Once this has been evaluated, the remaining

capacity of the structure should be assessed in order to ensure that it will remain functional after such instance.

1.6 Design Standards for Steel Structures

1.6.1 General

Historical development has provided design methods with empirical, experimental and theoretical knowledge of mechanics and probabilistic concepts. The systematic recording of this knowledge under a sound scientific foundation can derive a methodology that will allow design of specific structures in a way that defined levels of reliability may be obtained. The analytical documentation of this methodology can help in the composition of structural standards and design codes. In the following section, after a brief classification, standards applied in the design of offshore structures will be introduced.

In [21], the background principles of modern offshore standards and guidelines are summarized as follows:

- i. Design criteria are formulated in terms of limit states
- ii. Semi-Probabilistic Methods for ultimate limit strength design, have been calibrated by reliability or risk analysis methodologies
- iii. Fatigue design checks depending on consequences of failure and access for inspection
- iv. Explicit accidental collapse design criteria to achieve damage tolerance for the system
- v. Consideration of loads that include payload; wave, current and wind loads, ice, earthquake loads as well as accidental loads (fires, explosions, ship impacts)
- vi. Global and local structural analysis by finite element methods for ultimate strength and fatigue design checks
- vii. Nonlinear analyses to demonstrate damage tolerance in view of inspection planning and progressive failure due to accidental damage

The elements referred above, are followed in order to set safety requirements to avoid ultimate consequences such as fatalities, environmental or property damages. The corresponding regulatory regimes set different acceptance criteria for these consequences as it will be discussed later.

1.6.2 Categorization of Design Standards

Following the categorization of the design methods that have been presented so far, the available structural Codes and Standards are distinguished as either allowable (working) stress or limit state design.

The allowable stress codes, consider that the stress under the maximum loading conditions should not exceed the material yield or ultimate strength divided by an appropriate safety factor. Typical values for the safety factor can be in order of magnitude of 1.5 for yield strength or 2.5-3.0 for the ultimate strength [22]. As already discussed, the explicit calculation of the safety factor is a very demanding task in order to incorporate all sources of uncertainty that can impose a considerable degree of conservativeness in the resultant design.

In the limit state design, the structure is designed to resist specific loading conditions described in each corresponding limit state. Commonly, the loads are multiplied by partial safety factors, the resistance divided by safety factors and combinations of loads are considered. Application of those standards can be more complicated involving several aspects of decision making from the engineer but will generally produce more favourable results.

1.6.3 Standards for Offshore Structures

1.6.3.1 API RP-2A: Recommended practice for planning, designing and constructing fixed offshore platforms WSD/LRFD

This recommended practice was introduced by the American Petroleum Industry in 1969. It is based on sound engineering principles, extensive testing and field application experience. In its initial publication it followed the working design stress format. In 1989, a draft was issue in a Load Resistance Factor

Design format that was publicly released in 1993, based on the fact that two decades of application of the WSD edition of the standard had provided structures with sufficient reliability performance [7]. This standard is based on data for the Gulf of Mexico environmental conditions; however complementary documentation is available for different regions [23].

1.6.3.2 ISO 19902:2002: Petroleum and natural gas industries-general requirements for offshore structures

The publication of the ISO 19902 [3] offshore structure standard for Fixed Steel structures represents the culmination of significant efforts over many years. Providing guidance and procedures for the design and fabrication of offshore fixed steel structures, the Standard has been developed based on established standards for fixed offshore steel structures and through direct input from many of the countries actively engaged in the development of the offshore, including the United States, United Kingdom, France, Norway, Canada etc. ISO Standards are been adopted by several countries as National Standards, introducing them as legal requirements that allow certification of structures from world widely recognized certification bodies.

As for API, significant work has been carried for the applicability of the ISO standard in different regions around the world [24]. This consideration, proposes methodologies for custom derivation of load factors that lead to optimization of resulting designs.

1.6.3.3 BS EN 1993-1-1:2005 Eurocode 3: Design of Steel Structures

EUROCODEs is a set of standards produced by the European Commission in order to “establish a set of common technical rules for the design of buildings and civil engineering works which will ultimate replace the differing rules in the various Member States” [25]. EUROCODEs embody National experience and research, presenting a world class standard for structural design. The standard was formally released in 2007 and was subjected to a three years period until conflicting National Standards were withdrawn. The verification procedure is

based on the limit state concept. One of the most important aspects of those standards is that they allow for design based on probabilistic methods [26], giving the opportunity for further design optimization.

EN 1993:2005 [5] refers to the design of Steel structures. Although it is not yet used for the design of offshore structures, its highly scientific, probabilistic background provides a systematic design methodology that, if used in conjunction with established standards for this class of structures, may provide more efficient, optimized designs.

1.6.3.4 ANSI/AISC 360-05: Specification for structural steel buildings

This Specification provides the generally applicable requirements for the design and construction of structural steel buildings and other structures. The American Institute of Steel Construction incorporates in a single document both allowable stress design (ASD) and load and resistance factor design (LRFD) methods, allowing design according to provisions of either method. Based on previous experience and up-to-date technical knowledge, it aims to provide design guidelines for commonly used steel-framed buildings and other, similar structures.

1.6.3.5 Other Standards for Offshore Structures

Petroleum industry involved with offshore oil gas platforms and marine/naval engineering have assisted crucially the process of systematic design of offshore structures, due to their high demands on reliability and safety. Apart from the standards that have been referred to so far, Lloyd's published the "LRS Code for Offshore Platforms" [27] in 1988 and recently in 2007, Germanischer Lloyd, published the "Guideline IV – Industrial Services: Offshore Technology" [28]. Det Norske Veritas published "DnV: Rules for the classification of Offshore Installations" [29] in 1989, and recently in 2008 the "Offshore Standard OS-C101: Design of offshore steel structures, General – LRFD Method" [30]. Finally, the Norwegian petroleum industry has introduced the NORSOK standards, which refer to ISO, EN 1993 and is currently on its 5th edition [31].

1.6.3.6 Limitations of Structural Standards

Although in general use of standards results in design of structures with acceptable reliability, limitations arise for their application on novel and special structures, due to the fact that they primarily refer to specific structures and are presented in a high level that generally provides limited detail information and guidance on the background of the methodology they follow [32]. In this aspect the concept of reliability based design method can provide adequate results for the design of novel structures.

Adopting the target reliability requirements from relevant standards, partial safety factors can be calculated independently, avoiding unwanted conservativeness imposed. Further, in areas of high uncertainty, design details are approached in such a way that the consequences of failure can be reduced (eg. structural redundancy, etc). The former can be realized by combination of different standards where appropriate, resulting in solutions that provide a reliable design that meets the specifications set.

During fabrication and service of the structure, safety elements can be introduced such as quality control, alignment control, visual inspection, instrumented monitoring and proof loading. Those practices provide information about the structure, additional to those available at the design stage, reducing the overall uncertainty. Once the manufacturing process is completed, a structural integrity monitoring system can compare real data to ones initially calculated, verifying the conditions of the structure. Data obtained, can provide, throughout its service life, all the necessary information having good confidence levels for life-cycle fitness-for-service assessments including cases following unforeseen events such as local collision or component failure. Therefore, current reliability can be calculated, identifying the actual condition of the structure and indicating the actions that should be taken for any required intervention as well as the ability of the structure to work above the initially considered service life. Finally, the database that has been created, can provide substantial information for relevant optimized future structures and systems.

1.7 Target – Acceptable Reliability

Structural design aims to develop structures that are able to perform adequately, compromising cost and safety. The consequence of failure is an important parameter that should be assessed in order to specify the potential of injury or life loss, economic losses (direct and indirect), environmental pollution etc. Quantification of consequences is a very difficult task affecting the outcome of a reliability assessment [33]. Previous experience for a class of structures is an essential guide for the determination of target reliability levels for similar structures.

On the other hand, innovative structures cannot follow provisions of existing standards that refer to different structures since loading behaviour and consequences of failure strongly depend on their service, even if more conservative loading factors are adopted. This practice would drive the cost of the design without ensuring sufficient levels of reliability. One typical example of this problem, refers to the design of offshore wind turbines with jacket type foundation; although the general layout of the structure is similar to that of an offshore oil and gas platform, the loads added due to the rotor, the fact that the structures are unmanned and the large scale of production, constitute standards that refer to the latter application unable to ensure sufficient levels of reliability. For such cases, a robust reliability based design should be adopted [34] that would allow from basis derivation of load factors applicable to each case.

In the determination of the target reliability of structures the following fundamental parameters should be assessed. This is particularly important for cases when different structures or concepts are compared:

- Interpretation of calculated reliability. This identifies derived reliability not as a property of the structure, but as the level of our knowledge of its performance. This means that the level of uncertainty modelling (quantity and quality of information) will influence the results of the reliability assessment.

- Reference Period. The reliability of a structure should be measured for a specific period of time. This period is usually one year or its specified service life. This is a very important parameter for the inspection and maintenance requirements of the structure as well as for its reassessment in cases when the initially planned service life is to be exceeded and requalification assessment is required. Table 2, presents an example of target reliability for different structures and different reference periods.
- Scale of Reliability. Values of target reliability may be provided either in a local-component level or on a global-structural system level. Limit states may refer to the response of a member, but exceedance of this limit state in the failure region might not lead to structural failure. Typical example of this parameter is a local failure of a brace of a frame structure with structural redundancy. In such a case, load paths should be identified in a way that all possible failure mechanisms are identified and through integration to system reliability the total reliability of the structure may be derived.
- Structural modelling. The tools and techniques used for calculation of reliability, both in estimating the response of the structure as well as in the reliability calculation methods might affect the accuracy of the results.
- Stochastic modelling. This parameter refers to the statistical representation of the stochastic variables. The more accurate the statistical model the better uncertainties in modelling are considered.

Design according to standards can achieve minimum levels of target reliability. Some standards clearly state the target reliability they aim for, such as the EUROCODEs, while others rely on producing sufficient structures when the provisions of the code are followed as close as possible. Obtaining a better understanding of structures, may be update the reliability performance of standards.

As it has been already mentioned, marine and offshore engineering has provided valuable experience on the establishment of agreed target reliability

levels for different classes of structures. In [35], an analytical assessment on the development of target reliability for offshore structures can be found. Evaluation of the performance of ABS (American Bureau of Shipping) 'Rules for ship structures' that was carried out in [36] predicts the reliability index achieved is between 3.15-3.65. In a study [37] of API recommended practices for Offshore Jacket structures (LRFD edition) estimates an annual average estimated probability of failure in the order of 4×10^{-4} ($\beta \sim 3.35$). DNV [14] suggests calibration of target reliabilities based on existing cases with previous experience; however a very comprehensive table is proposed and adopted by the DNV group of standards, distinguishing classes of consequence and redundancy of a structure. Table 3 presents those recommended values of acceptable annual probabilities of failure. ISO proposes a model that incorporates the possibility of injury or fatality in the case of a collapse with a mathematical correlation that accounts for the number of people at risk. A lower boundary of 10^{-6} Probability (annual death per failure) is set, corresponding to a $\beta \sim 4.75$). Evaluation of AISC, in studies performed in [38] and [39] for structural members of a bridge, predict target reliability in the ultimate limit state ($\beta \sim 3.5$). Finally, EUROCODEs, prescribe a target probability of failure of about $P_f = 10^{-4}$ [25]. From the figures that were summarized here, it can be observed that in the more general standards, a more conservative approach of reliability is observed. This fact is reasonable since they should account for different types of uncertainty for application in different structures.

Evaluation of risk is a dynamic task based on information update and experience gained from similar cases. Serious accidents such as the Piper Alpha offshore platform accident [40], is an example of events that initiated assessment of rules and codes for the avoidance of similar phenomena through a knowledge-based approach. Some analytical methods have been proposed for a systematic determination of risk and reliability [35]:

- A risk based approach, focuses in the quantification of consequences in an absolute measuring unit, such as loss of lives per accident or cost of

failure in economic units [41], [42]. This method involves great subjectivity on the valuation of human life loss.

- Life cycle cost analysis, is a method applicable especially in cases of structures that can operate well with regular maintenance interventions. It is based on the maximization of a cost function with the restriction of minimized reliability [43], [44].
- Social tolerable risk for failure and fatalities. This method incorporates the different reaction of societies to hazards and risks' providing more strict safety requirements in general, since the element of cost efficiency becomes secondary [45]. In [46] and [47] mathematical expressions are proposed for the calibration of the safety requirements according to the social impact factor and the level of warning before failure. .

Generic standards, such as [14], [6] propose analytical methodologies for the reliability assessment of structures. In [48] a procedure is described for this purpose and has been adopted by many of the existing standards as a way to achieve calibration of target reliability levels. Figure 3, illustrates in an iterative block diagram format this risk assessment procedure. Further, Table 4 summarizes some target probabilities of failure for offshore applications based on what has been discussed so far [35].

1.8 Summary

In this Chapter, the context of structural reliability has been set, incorporating different sources of uncertainty in structural design. Classification of available methods has been presented, based on the extent of information that the problem treats, and the accuracy in the representation of the design variables. Evolution of design methods from permissible (allowable) stresses to limit states formats was also included, with a view for classification of design standards, and a reference to the consideration of appropriate limit states for the latter class. Finally, after identification of the most important available standards for the design of offshore and steel structures, and some comments on the

limitations they involve, an investigation of the target reliability levels that are documented from widely accepted certification bodies have been presented.

Reliability Classes	Consequences for loss of human life, economical, social and environmental consequences	Reliability index β		Examples of building and civil engineering works
		β_a for $T_a=1$ year	β_d for $T_d=50$ year	
3-high	High	5.2	4.3	Bridges, Public Buildings
2-normal	Medium	4.7	3.8	Residential and office buildings
1-low	Low	4.2	3.3	Agricultural buildings, greenhouses

Table 2: Reliability Index and Reliability Classes [7]

Class of failure	Consequence of failure	
	Less serious	Serious
I - Redundant structure	$P_F=10^{-3}$ ($\beta_t=3.09$)	$P_F=10^{-4}$ ($\beta_t=3.71$)
II - Significant warning before the occurrence of failure in a non-redundant structure	$P_F=10^{-4}$ ($\beta_t=3.71$)	$P_F=10^{-5}$ ($\beta_t=4.26$)
III - No warning before the occurrence of failure in a non-redundant structure	$P_F=10^{-5}$ ($\beta_t=4.26$)	$P_F=10^{-6}$ ($\beta_t=4.75$)

Table 3: Values of acceptable annual probabilities of failure (PF) [14]

Source	Allowable system failure probability
Risk Analysis (analytical Assessment)	$10^{-6}/\text{yr}$
CSA	$10^{-5}/\text{yr}$
DNV	$10^{-6}-10^{-5}/\text{yr}$
ISO-1000 people	$10^{-7}/\text{yr}$
Professional recommendations	10^{-5} life time
Social Criteria	$10^{-7}-10^{-5}/\text{yr}$
Existing Structures	$10^{-7}-10^{-5}/\text{yr}$

Table 4: Comparative estimates of target Pf [35]

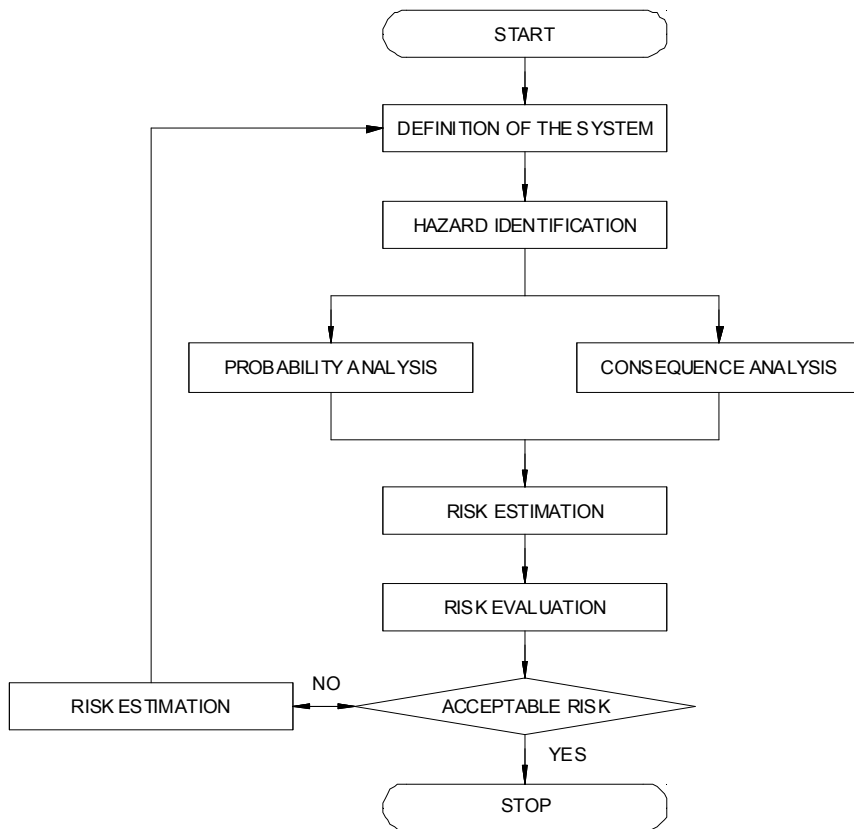


Figure 3: Iterative procedure for Risk Assessment [48]

2 RELIABILITY ANALYSIS OF OFFSHORE STRUCTURES

2.1 Basic formulation of the Problem

Following an initial, general approach, the behaviour of a structure can be determined by the values of loads (actions) or load effects L acting on it and its load bearing capacity (resistance) R . The following correlation between the two variables can form the acceptance criterion of the structure for a specific failure mode – limit state:

$$R - L > 0 \text{ or } \frac{R}{L} > 1 \quad (2-1)$$

The safety margin, of the structure can be expressed as:

$$Z = R - L \quad (2-2)$$

In practice, both resistance as well as loading effects, involve a number of variables or material properties, subject to several sources of uncertainty. In the critical case where the resistance and load values are equal, limit state equations can be formed as:

$$Z(X) = 0 \quad (2-3)$$

In the case when $Z(X) \geq 0$ the structure operates in the safe region while when $Z(X) < 0$, it is considered in the failure region. For each limit state, the probability of failure can be expressed as:

$$P_f = P\{Z(X) < 0\} \quad (2-4)$$

Alternatively, considering probabilistic models for the assessment of the variables $X = [X_1, X_2, \dots, X_n]$ and simplifying that they are described by time independent joint probability density function $\varphi_x(x)$, the expression of the probability of failure can be described with the integral:

$$P_f = \int_{Z(x) < 0} \varphi_x(x) dx \quad (2-5)$$

The expression above can be extended to become applicable to some cases of time dependent quantities which can be transformed into time independent ones [18]. For cases where this is not feasible, the process of calculating the probability of failure becomes much more complicated and in practice should be assisted by different numerical methods and software products [6].

Instead of using the term of “probability of failure”, the equivalent term of reliability index ‘ β ’ is usually referred to in the design standards and relevant documentation. This is the negative value of the standardized normal variable, corresponding to the probability of failure:

$$\beta = -\Phi_U^{-1}(P_f) \quad (2-6)$$

Where, $\Phi_U^{-1}(P_f)$, is the inverse standardized normal distribution function. The benefit of using this notation is that β can provide results for several types of statistical distributions based on deterministic methods as it will be discussed in Chapter Three. Figure 4, illustrates the correlation between the reliability index and the probability of failure. Considering a simple case of a single load acting on a member and its resistance, both distributed normally, the correlation of their means, standard deviations and β can be shown in Figure 5.

A quantitative definition of risk derives it as the product between the probability of occurrence of an adverse event and its consequences [22]. The first is influenced by the reliability of the structure while the latter of its function and specifications. This implies that different values of risk can exist for different combinations of these parameters. Unmanned offshore structures for example can experience failures that halt the operation/production but without fatalities and therefore the measured consequences can be considered lower; the same risk can be achieved with designs of increased probability of failure but lower consequences in the case of potential failure. Taking this into account, the calculated reliability levels can be interpreted.

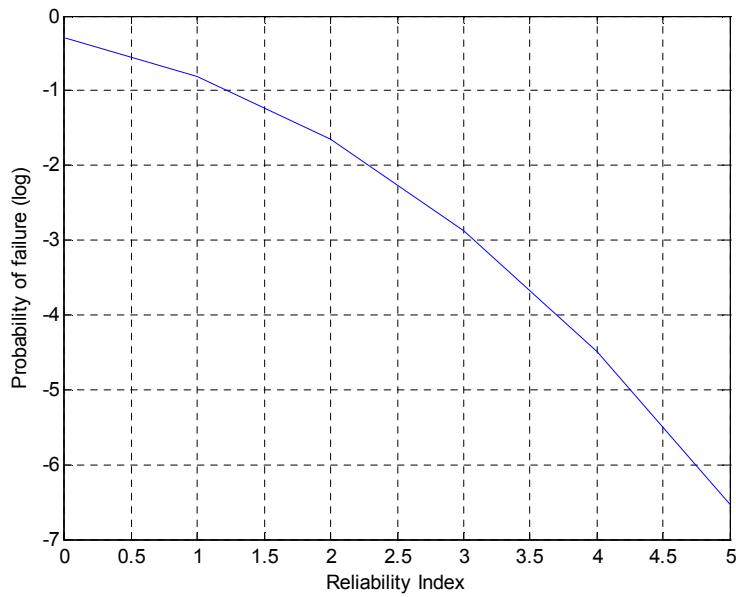


Figure 4: Relationship between β and Probability of failure

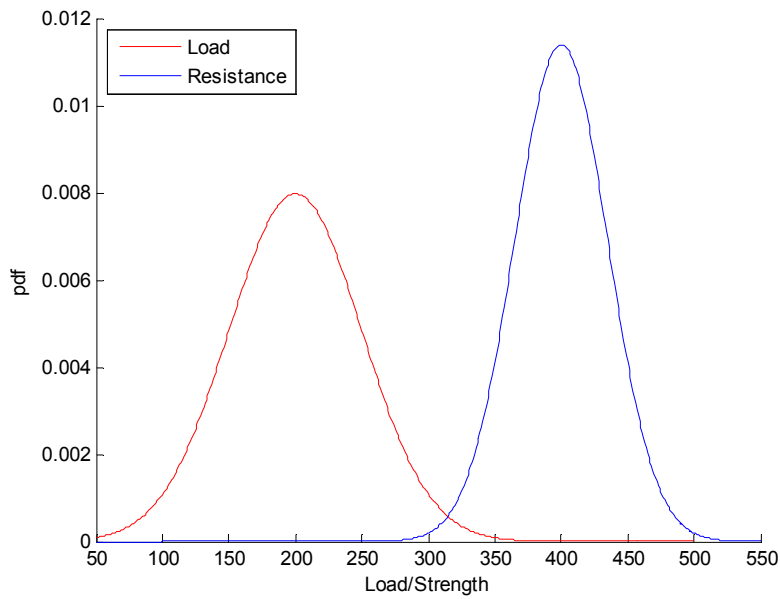


Figure 5: Definition of Reliability Index

An interesting parameter of the reliability index which represents the relative positions of the Load and Resistance distributions is its performance throughout the operational life-cycle. The load effects may increase with time due to crack growth etc, moving the corresponding curve to the right while the resistance might decrease due to deterioration of fracture toughness or other age related

mechanisms. This fact leads to a decrease in the relative difference between mean values, which reflects to a decrease in the reliability index and therefore an increase in the probability of failure. The importance of this characteristic is significant for the design process and the engineer should incorporate this time dependent component into the design model in order to avoid unwanted residual uncertainties in the calculations.

2.2 Background and motivation

2.2.1 Development of Structural Reliability Applications

Conventional deterministic structural design has been established successfully during the past years in the design, construction, maintenance and inspection of structures. Although, in general, it provides structures of sufficient performance, uncertainties are considered in a generalized way incorporating a significant degree of conservatism. Further, requalification of structures that have exceeded their predetermined service life demands reassessment on a basis that will ensure safety in further operation. Both of the above facts introduce reliability analysis, providing the framework for effective decision making in cases where uncertainties cannot be incorporated following a deterministic approach.

An initially application of structural reliability, as it is presented in [49], can be found back in 1926 by Mayer, in an attempt to quantify the safety of a structure, treating uncertain variables by using the mean and standard deviation. Initial applications of reliability theory are focused in the field of aerospace, electronics and nuclear industry. Interest in structural reliability begins in 1947 when in a study of Columbia University [50], safety margins and safety factors are analyzed in a way that allows their systematic derivation. Evolution in computation of reliability is traced in 1969 where the Mean Value First Order Second Moment method (MVFOSM) was proposed [51]. This is an initial approach to the derivation of the reliability index based on mean values of load

and resistance variables. The fact that this method was not taking into account different formulations of limit state functions, initiated the Hasofer and Lind [52] reliability index methodology to be formulated which was the first method to geometrically approach the reliability index calculation as the minimum distance of the failure surface from the origin of the normalized space. Methods for handling non-normal random variables have been introduced and will be discussed later in this Thesis. Following the development of FORM, SORM managed to deal with more complicated limit state functions with multiple minimization points and cases of non linear curves. In a very important review paper [53], summarizing the general belief of the 1990 decade, has illustrated that the development of deterministic methods had been completed. In addition, competent simulation techniques have evolved, able to produce accurate results at the expense of greater numerical effort.

Development of structural reliability is now moving towards structural optimization schemes with reliability to stand as the basic design restriction. As this is a relatively new practice, important issues of time performance should be included, constituting this as a time-variant analysis [54]. Apart from this, another very important issue is the transformation of the state-of-the-art into state-of-practice methods in order to allow application in more essential engineering problems.

2.2.2 Development of offshore industry

The first offshore drilling activities started in 1947, when the first platform was built in Louisiana in the Gulf of Mexico. This was a very short structure of 5.1 m height. During the last decades, deployment of offshore structures is moving in deeper waters. Cognac platform [55] has been installed in a depth of 338 m, followed by Shell's Bullwinkle platform [56] standing in 415 m of water. An economic sensitivity analysis, had set 300 m to be the restriction for fixed offshore platforms however this number has been revised to 615 m.

Evolution of technology has come up with new configurations of offshore structures in order to accommodate the harsh conditions of deeper waters. In

mid 1990s, Shell has installed a tension leg platform (Auger TLP) in depth of 872 m [57] setting the up-to-date record for any installed offshore structure. In [58], a review of installed offshore platforms refers to a total of 5238 platforms, 15% of which are very heavy structures (more than 5000 tn). Due to the depleting resources in the oil reserves, the fluctuation in prices of oil and the world's constantly increasing demand in resources, the challenge of exploration in harsher environments is now active. For 2005, an estimate on deployed structures considered approximately 1100 active rigs [59].

Design of oil and gas platforms, has stood as the basis for significant developments in offshore wind industry. Deployment of wind turbines offshore goes back to 1930, however it was only in 1990 when the first offshore unit (220 kW, 38 m hub height, 7 m water depth) was deployed in the North Sea. Similar structures were deployed in Denmark at the same time, accommodating wind turbines rated up to 500 kW each at depths of up to 6 m. Several projects were completed up to 2000, increasing the capacities of the wind turbines supported, the depths of deployment, and the distance from shore considering harsher environmental conditions. 2000 can be considered a breakthrough for wind industry, initiating England's involvement in the field, deploying units of 2 MW on the Blyth wind park (800 m from shore, up to 11 meters water depth). Water depths of 20 m have been reached by 2002 in Denmark, moving even further offshore (3.5 km). The state-of-the-art installed support structure so far, refers to the Beatrice wind farm, built in 2007, consisting of 2x5 MW wind turbines in a site 22 km from the Scottish coast, and 45 m of water depth [60]. The constant demand of clean energy constitutes efficient design of deep water foundations an essential task, considering that, contrary to oil and gas platforms, wind turbine support structures are aimed to be built in massive production.

2.2.3 Application of Reliability Analysis in the offshore industry

Application of Reliability Methods appears to provide particular benefits in the marine environment, due to the randomness and the restricted knowledge of the phenomena structures resist. Proper modeling of the structures' capacity

and loads encountered can predict its probability of failure through reliability analysis. This analysis, for offshore structures, includes component and system reliability analysis, specific design assessment and various forms of cost-benefit optimization and maintenance planning. For a fixed offshore unit, the benefits reliability analysis can provide can be summarized as follows [61]:

- I. Achieve uniformity in the reliability at a component level
- II. More efficient utilization of material properties, compared to over-sizing followed by deterministic procedures
- III. Account directly for randomness and uncertainties in engineering parameters

Reliability assessment was introduced in the field of offshore structures in 1980s, following the 'goal setting' philosophy in the safety and economic consideration [62]. Application of reliability methods for offshore structures was initiated and motivated for ship hulls [63], [64] and was later applied in the reliability of offshore structures. Important work is carried out in [65] and [66] applying reliability analysis theory for the safety assessment of existing structures, allowing efficient maintenance planning based on risk involved under certain conditions of a deteriorating structure.

Reliability Analysis is also applicable in the optimization of structural design. Setting a target level of reliability, structures can be designed compromising risk and cost. In [67], a reliability-based design format for jacket platforms under wave loads is presented by resizing members until the target reliability is sufficiently approached. Reliability based design as well as design optimization is in its infancy since several restrictions should be set for realistic designs to be derived. However, moving towards more economic structures, this topic should be investigated further.

The demands of reliability methods in mathematics skills, have led to the development of reliability calculation software. PROBAN, developed by DNV, is a general purpose reliability program able to analyze different failure modes simultaneously, determine conditional probabilities, and derive partial safety

factors [68]. Further, STRUREL/COMREL [69] and RASOS are some common software packages used for the reliability of offshore structures. Apart from those standalone general application programs, incorporation of reliability calculation procedures is attempted by well established FEA software (ANSYS, SOFISTIK etc) in order to provide users with a friendly interface that demand minimum knowledge of the background theory of reliability analysis.

2.3 Response Analysis

A fundamental decision to be made before the analysis is the identification of the type that is required. Several analytical methods are available and may be categorized as static or dynamic, linear or non-linear, deterministic or stochastic. Combinations of the above categories can identify the analysis method to be employed, depending on the properties of the structure under consideration. The type of response of a structure may require different types of analysis. In [70], an analytical block diagram for global response analysis of marine structures is presented, guiding selection of the most appropriate method.

2.3.1 Static Analysis

The general equilibrium equation for static analysis can be expressed as follows:

$$K\mathbf{r} = \mathbf{R} \quad (2-7)$$

Where: K is the global stiffness matrix formed from the combination of the element stiffness matrices; \mathbf{r} , is the vector of unknown nodal displacements and \mathbf{R} is the nodal load vector. The typical finite element analysis based on the above equilibrium equation should follow the steps as described in [71]:

- Discretization, where the actual structure is approximated by an assembly of finite interconnected elements

- Element Analysis, where the stiffness properties of each individual element is determined and any loading is transformed into equivalent nodal forces
- System Analysis, where the individual elements of the structure are merged to form the elements stiffness matrix K and load vector R . The above equation, will then determine the nodal displacement vector r .
- Post-processing of the results, will derive the stresses from translational and rotational displacements in each of the structural members.

Non-linear problems can generally be solved with both analytical (e.g., the Ritz method) and numerical methods. The numerical methods seem to be the most prominent, based upon the principle of stepwise integration of the problem such that any non-linear structural problem can be transformed into a series of linear problems. Reduction of an analytical non-linear structural system, can diminish the problem to finding the displacement vector $r(t)$ that produces an internal reaction force vector $F_{int}(t)$ that balances the applied forces $R(t)$. The expression of the equilibrium equation is formulated as follows and can be solved incrementally with corrective iteration:

$$F_{int}(t)r(t) = R(t) \quad (2-8)$$

2.3.2 Dynamic Analysis

Following the same consideration, dynamic analysis includes time dependency, damping and inertia as local and system effects:

$$M\ddot{r} + C\dot{r} + Kr = R(t, \dot{r}, \ddot{r}) \quad (2-9)$$

Where: $R()$ is the time-dependent load, $r(t)$ the displacement, M the global matrix, C is the global damping matrix, and K the global stiffness matrix. Mass and damping properties of the system, can be derived as the assembly of the properties of each element. The internal reaction forces for any element can then be computed by use of virtual work equations. The above equation is applicable both for linear and non-linear systems.

2.3.3 Deterministic and Stochastic Processes

Deterministic process is a process for which it is possible to describe the exact magnitude of the load at any given time. A deterministic analysis involves an initial consideration of the statistical data for environmental loading. For extreme response analysis, for example, a suitable event could be defined as the wave which is expected to cause the most severe response. This requires that the structural model is exposed to a unidirectional, periodic wave. The loading is calculated in the time domain at given points in time during a wave cycle.

Contrary to deterministic processes, a stochastic process is described by the use of probabilities. Therefore, a stochastic load or response may not be fully described by exact magnitude at a given time, but rather by the probability (statistical distribution) by which it will exceed some specified value. Further discussion of modelling of environmental and capacity variables will be presented in Chapter Four of this Thesis.

2.3.4 Selection of type of analysis

Literature can provide a range of methods for the selection of the most appropriate analysis, considering that all relevant global and local effects, dynamic as well as non-linear, are satisfactorily accounted for in the analysis [72], [73]. In [74], a study based on different types of analysis for a reference structure and for the same loading conditions was executed, including combinations of linear and non-linear analysis, with regular and random wave loads. Figure 6, adopted by [75], illustrate the results comparing the maximum base shear that was derived.

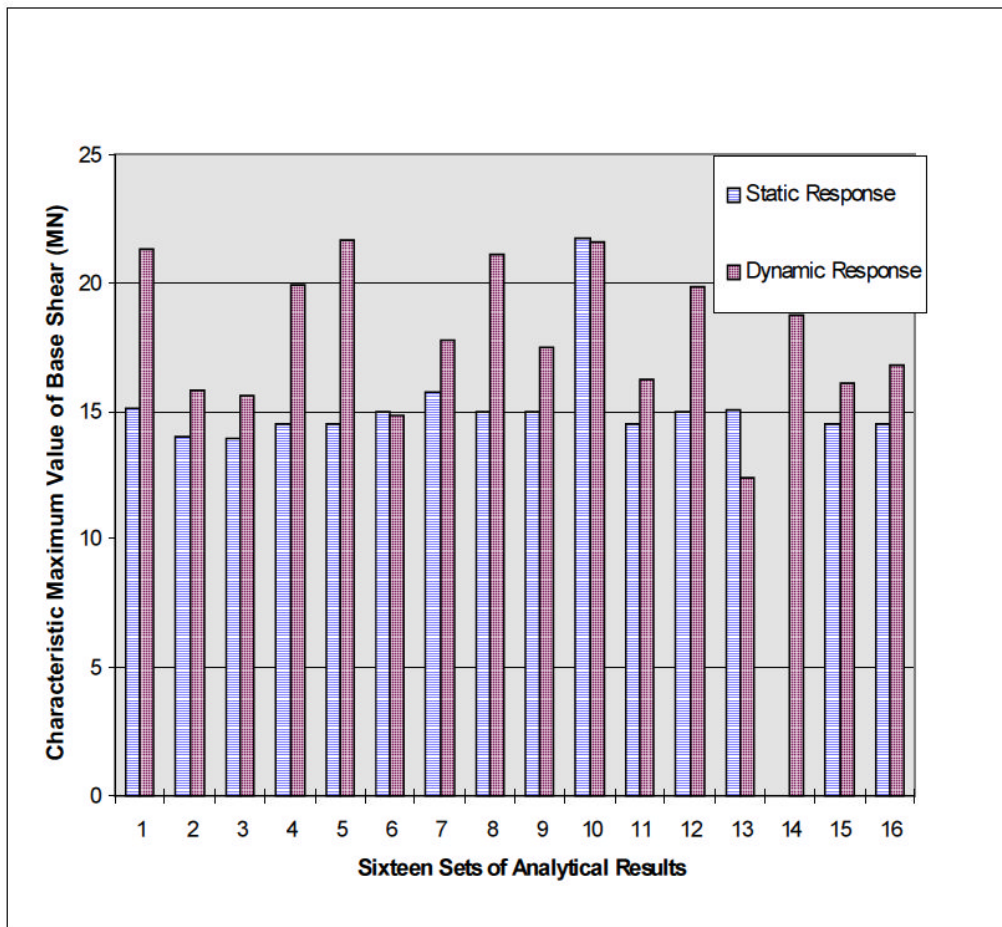


Figure 6: Scatter of response (Max Base Shear-MN) by different Analysis Methods [75]

Different approaches can be considered to account for dynamic effects, either directly by dynamic analysis, or by applying ‘correction factors’ to the results of a static analysis, such that the analysis may be referred to as ‘quasi-static’. For the choice between a static and a dynamic analysis approach the following recommendations may be considered [70]:

- For typical fixed offshore structures (e.g., jacket type structures) the effects of dynamics, for extreme global response analysis, should be included when the global natural period of the structure is greater than three seconds.

- For floating structures, including compliant structures, a dynamic analysis should always be undertaken to identify contribution of extreme response dynamic effects.
- A dynamic analysis should be executed in order to establish structural response when impulse or resonant effects may be governing.
- Model and/or prototype measurements should be considered for structures or effects not amenable to analytical calculations.

2.3.5 System Response

Significant developments have been identified in the latest decades in the area of system reliability assessment. A structural system with multiple failure paths can be represented by a series of parallel sub-systems, with each subsystem representing a failure mode. Starting from a component reliability level, the combined structures reliability of the system can be then calculated. In the case of complex structures such as offshore platforms, there is a number of potential failure paths and structural components which makes this approach not practical. Thus efforts have concentrated in developing more accurate system reliability methods for these structures. Figure 7, presents some of the methods for system reliability assessment [76].

The increased available computational resources for a system reliability analysis of an offshore platform has given motivation for the development of a number of “search algorithms”, in order to identify the most dominant failure paths and calculate the combined system probability of failure [76]. For the case of large structures, such as offshore platforms, the search algorithms technique such as the ‘branch and bound method’ [77] can provide sufficient results. Alternative methods towards identification of dominant failure paths are the selective enumeration techniques [78] and the marginal probability and leading probability methods [79]. Among methods, the ‘branch and bound method’ has the drawback of computational cost while the enumeration techniques cannot guarantee identification of every potential failure path.

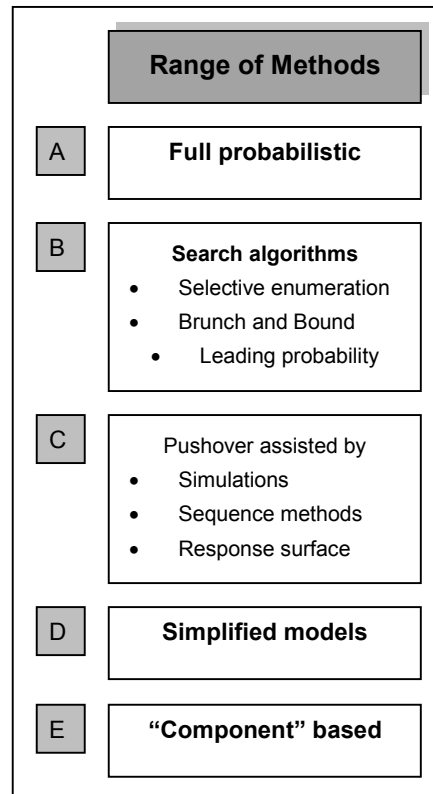


Figure 7: Classification of methods for system reliability assessment [76]

Identification of the most dominant failure path can be also performed by the so called 'pushover analysis'. This analysis will identify deterministically the most critical members but will not take into account the effect of possible residual strength after failure which may redistribute loads and result in different sequences of failure and different combination of members. However, in [80], for cases under extreme loading conditions, it is found that the reliability index of the failure path identified through a deterministic pushover analysis closely identifies the one obtained after extensive searches or simulations.

From all of the approaches that have been proposed, the component based approach is the simplest. In this approach the whole structure is treated as one component, with either deterministic resistance or an associated coefficient of variation (COV) suitable to quantify the probability of system collapse of a fixed platform [81], [82]. Based on this approach it is proposed that with accurate representation of the resistance, a good non-linear model and a competent

analyst it is possible to reduce significantly the modeling uncertainties associated with the resistance.

Another, simplified, system reliability method, that can be applied as a preliminary design tool for configuration of new platforms, has been based on a series system where the components in series are the deck, each platform bay and the foundations [83]. This method, considers within each component parallel elements including deck, legs, braces, joints and piles. For each component to fail, failure of all parallel elements should happen. The use of simplified analytical procedures to estimate reference storm lateral loadings and the ultimate capacities of platforms are comparably well in agreement to those derived from more complex analysis.

The selection on the various methods discussed depends on the application. Classification in Figure 7, distinguish the methods closer to “A” associated in general with higher level of complexity which is more suitable as research tools, while methods towards the other end of the scale (towards “E”) would be more appropriate for practical assessment [76]. However, the choice of the methods would also be influenced by other factors such as the availability of computational and analytical tools, significance of local effects such as foundation uncertainties in the overall system reliability and the expertise of the analyst.

In the application that is presented in Chapter Five, the pushover analysis approach was selected in combination with simulation method in order to address the possible variations and their effect. The difficulty associated with this approach was the limiting number of simulations which can be performed given the size of the problem and the high computational demands. Simple approaches found in literature [81], [84] can provide useful conclusions in the implementation of the above combination.

2.3.6 Practical Methods of Analysis

Among the various methods available in literature, this section will present a practical procedure for the assessment of structural system reliability. The main assumption indicates that failure will occur at one instant, for example when the lateral wave load reaches a maximum value, implying that failure will occur over a short period of time, during which the load is applied proportionally. This assumption makes the reliability calculation problem time-independent.

Local failure on a structural member will alter the structural stiffness of the structure, redistributing stresses in alternative load paths. Residual strength is modelled by applying appropriate forces at the nodes of the failed members, or by changing the properties of the failed members. Once the system has been redefined, a new stress calculation should be performed, initiating an iterative process, which after a sufficient number of successive member failures has occurred, the structure will be considered to have failed when the structural failure criterion (collapse or large displacement) is met. Therefore, this procedure can identify a potential load path. In real structures, due to their complexity, a large number of possible failure paths exist. For this reason a search technique should be used in order to identify the important paths. Pushover analysis is a method that can be followed for this purpose until the platform collapses.

This manual search of failure paths, usually expressed in the form of failure trees, can provide sufficient information for a system reliability assessment [85]. The failure tree is a representation of all possible failure paths in the structure. Nodes represent damaged states of the structure and the branches represent member failures in the corresponding damaged structure. The number in the node is the element number. In the failure tree, each path represents a failure mode, which can be modeled as a parallel system since the structure can only fail when all its members reach their limit state. A redundant system might have several failure modes. In such case, each of the failure modes can be modeled

as a parallel system and all modes, in turn, can be modeled as a series system to find the reliability of the complete system.

2.3.7 Modelling of Post-Failure Behaviour

Reliability of a structural member will strongly depend on whether it behaves on a brittle or a ductile way. This does not mainly refer to the material of the structure but in the behaviour of the potential members to fail. The response of the component's post-failure behaviour is one of the key factors that determine the effective redundancy of a structure. The two extreme types of failure are the perfect brittle and the perfect ductile failure performance. The first type becomes completely ineffective after failure, eliminating completely its load-bearing capacity. If a failure element maintains its load-bearing capacity after failure it is categorized as ductile. Real materials, in most of cases lay between the two extreme categories. One model which can be incorporated in the probabilistic analysis is the bi-linear, two state model. In the non-failure condition, the component is linear elastic, while in the failed condition the component still behaves linearly but with a modified stiffness matrix. Figure 8, illustrates this behaviour.

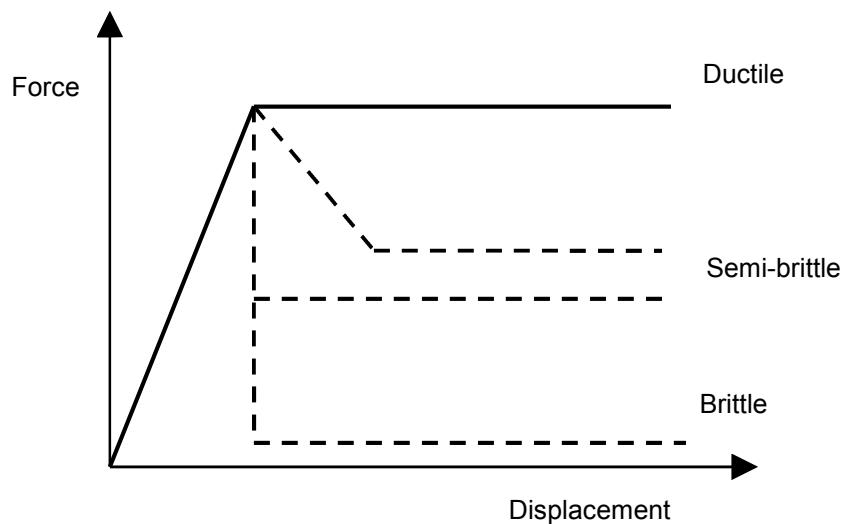


Figure 8: Models of Post-Failure Behaviour

With this type of models, various component behaviours, ranging from brittle to perfect plastic, can be described. In the semi-brittle model, the member force increases elastically to the member capacity or resistance. After failure, if the axial deformation in the element is increased beyond its failure value, the element force abruptly drops to a fraction, φ , of its non-failure capacity. Based in literature [86] a deterministic value of $\varphi = 0.4$ can be adopted for members failing in compression and $\varphi = 1.0$ for tension failure. This assumes ductile tension failure behaviour, maintaining the failure load and an abrupt drop by 40% capacity when failing in compression.

2.3.8 Methods in Computing System Reliability

Accurate estimation of reliability can be hindered by the multiple failure paths existing and any potential correlation between the failures. The latter, should be primarily identified since this correlation will affect the final results of the calculations. Generally there are two approaches; the Hohenbichler approximation [87] and the bounding method [88].

Hohenbichler approximation computes the probability of failure from the multi-normal distribution function, providing a very accurate prediction of the probability of failure of the structure. However, for complex structures, the method becomes complicated from a computational point of view [79]. For such structures, use of bounding techniques for the calculation of the probability of failure, which is the simple bound and Ditlevsen bounds [89], are proven to be more efficient methods. The Ditlevsen bound is a narrower bound compared to the simple bound, providing a smaller range between the upper and the lower bound. The computation of the Ditlevsen bound is calculated through numerical methods in order to calculate the joint probabilities.

The simple bound method can be also applied for the computation of structural reliability however the results derived lack in accuracy compared to the Hohenbichler approximation and the Ditlevsen bound. On the other hand, the limited requirements in computational demands constitute the simple bound method widely used. The simple bound is a range between the maximum and

minimum value of the probability of failure; however this range can be significantly wide and it can only serve as a rough indication of the system reliability. Before proceeding with the calculation of the simple bound method, the types of system has to be identified, as series system, parallel system or combination of both.

2.3.8.1 Classification

A series system, or as is called the weakest link system, is the system where failure corresponds to failure of the weakest element in the system. In describing the status of each member, each element is assumed to be either in a functioning or in a failed state. This consideration can be expressed by introducing a binary state indicator variables a_i ($=1$ for functioning members, and $=0$ for failed members), considering n number of elements in the structure. The simple bound for the derivation of the probability of failure for series system [79], is defined as:

$$\max_{i=1} P(a_i = 0) \leq P_{fs} \leq 1 - \prod_{i=1}^n (1 - P(a_i = 0)) \quad (2-10)$$

The lower bound in the above equation is equal to the exact value of P_{fs} if there is full dependence between all elements and the upper bound correspond to no dependence between any pair of elements. When the probability of failure of one element is predominant in relation to the other failure elements, the probability of failure of series system is approximately equal to the predominant probability of failure and the gap between the upper bound and lower bound is narrow. In the opposite case, when the probabilities of failure are in the same order, the simple bounds are wide.

For a parallel system, it is considered to be in a functioning state if at least one element is functioning. Simple bounds for the probability of failure for parallel system are defined as:

$$\prod_{i=1}^n P(a_i = 0) \leq P_{fs} \leq \min_{i=1} P(a_i = 0) \quad (2-11)$$

Following a parallel concept as for the series systems, the lower bound in the above equation is equal to the exact value of P_{fp} if there is no dependence between any pair of members and the upper bound corresponds to full dependence between all elements.

2.3.8.2 System effects

System effects in fixed offshore platforms can distinguish deterministic effects which relate to the redundancy of the system and probabilistic effects which relate to the randomness of the member capacities under stochastic loading. Deterministic system effects relate to the redundancy incorporated into the structure, which allows load redistribution after the first member failure and results in a higher ultimate load capacity. Due to this, it can result to lower requirements of reliability for individual members.

For perfectly balanced structures, the system effects for overload capacity beyond first member failure are due to the randomness in the member capacities. A balanced structure in this sense refers to a structure where, in a linear analysis, the first member to fail has the same probability as for all other members. For a more realistic unbalanced structure, system effects are from both deterministic and probabilistic effects. Deterministic effects are due to the fact that the remaining members in the structure can still carry the load after one or several members have failed, while the probabilistic effects are due to the randomness in the member capacities [90]. Structural behavior beyond first member-failure depends on the degree of static indeterminacy, ability of structure to redistribute the load and ductility of individual members, as well as by aspects such as wave-in-deck loading, the behavior of the joints and the behavior of the foundation. In order to assess system effects, there are a number of factors, such as reserve strength and residual strength that can be derived from the analysis of a structural model.

The failure of only one part of a system may not limit the capacity of the structure as a whole; instead, a sequence of component failures may occur before the ultimate strength is reached. The reserve strength ratio (RSR) is generally defined as:

$$RSR = \frac{\textit{ultimate platform resistance}}{\textit{design load}} \quad (2-12)$$

RSR can be quoted in terms of ratios of platform base shear or overturning moment. For every platform, a different value of RSR will be obtained for every different load case. Apart from that, in order to make comparisons between different RSR values, one should note that the definition which is used to quantify this value is the same. In [83] and [91], an extensive study on the definition and the use of RSR value was undertaken developing a four-tier system for the assessment of structures. An alternative definition of RSR may be defined is:

$$RSR = \frac{R_U}{S_R} \quad (2-13)$$

Where: R_u is ultimate lateral load capacity of the platform and S_R is a reference lateral loading. The primary objective in the four-tier system is to allow a simple assessment and re-qualification of platforms. The more complicated levels in this system would be used for more complex platforms including intense analyses for re-qualification. Another definition of RSR value, used by Shell [82], is given as:

$$RSR = \frac{\textit{environmental load at collapse}}{\textit{original design environmental load}} \quad (2-14)$$

Considering an undamaged structure, some residual capacity may exist, the magnitude of which can be described by its degree of in-determinacy. The effect of a certain damage scenario can be assessed by the concept of residual strength. This can be an important indicator of structural behavior, and can be defined by the residual resistance factor (RIF), generally defined as follows [92]:

$$RIF = \frac{\text{damaged structure's environmental load at collapse}}{\text{intact structure's environmental load at collapse}} \quad (2-15)$$

The ratio of the ultimate capacity of the damaged structure, when compared to the ultimate capacity of the intact structure, can also give a useful indication of platform behavior [92]. This can be defined as the damage tolerance ratio (DTR), which can be expressed as follows:

$$DTR = \frac{\text{damaged structure's ultimate capacity}}{\text{intact structure's ultimate capacity}} \quad (2-16)$$

The value of DTR characterizes the weakening of the structure caused by the damage. For example, a DTR of 0.9 would indicate a 10% loss in the reserve strength.

The damage tolerance ratio has been calculated in order to investigate the residual strength in the application of Chapter Five. Push over analysis was carried out in 8 wave directions of the platform; 45 degrees apart as indicated from standards for orthogonal (4 legs) cross section, to derive the DTR for each direction. The most critical member, i.e. the member that has the highest probability of failure was removed for each direction. After analyzing the first damage, the second critical member was removed iteratively, in order to study the effect of multiple damages.

2.4 Review of Stochastic Methods

2.4.1 Stochastic Expansions

Extensive use of Finite Elements in various fields of engineering has evolved using stochastic field theory in structural engineering. The critical issue towards this scope is the discrete representation of stochastic variables and the corresponding interpretation of stochastic responses [93]. Stochastic expansion is an efficient tool for reliability analysis. The purpose of stochastic expansions is to consider uncertainties through a series of polynomials in order to investigate the reliability of a system. Karhunen-Loeve expansion (K-L) and

Polynomial Chaos Expansion (PCE) can serve the above purpose. Combination of the above two techniques together with principles of the Finite Element Analysis Methods provide a useful tool, the Spectral Stochastic Finite Element Method (SSFEM), towards an analytical assessment of the reliability of structural systems [94].

Applied in the Spectral Stochastic Finite Element Method (SSFEM) [95], Polynomial Chaos Expansion (PCE) has been successfully used to represent uncertainty in a variety of applications, including structural response. This method uses orthogonal polynomials of random variables. Most commonly, the random variables are standard-normal, and Hermite polynomials are used in SSFEM. Efficiency of this method has found multiple applications in various engineering problems such as two dimensional elasticity [95], soil mechanics [96], heat conduction [97] and composite materials [98].

In [99] the probabilistic collocation method is introduced; according to this the responses of stochastic systems are projected onto the PCE. In [100] the limitation of the probabilistic collocation method for large-scale models was indicated and a different approach was suggested, using a stochastic response surface method that uses the partial derivatives of model outputs with respect to model inputs. In [101] combination of PCE with MCS was applied while in [102] extended PCE were used to represent different distribution functions by using the Askey scheme.

Stochastic Expansions could be classified in two categories: the non-intrusive and intrusive formulation procedures, as shown in Figure 9 [93]. An intrusive formulation is the one in which the representation of uncertainty is expressed explicitly within the analysis of the system. Practically this refers to methods that use PCE and KL expansions to directly modify the stiffness matrix of a finite element analysis procedure. SSFEM [103] and the stochastic Galerkin FEM [104] are both intrusive formulations. On the other hand, non intrusive formulations, represents uncertainties in a non explicit way, treating the analysis code as a “black box” without requiring access to the analysis code. This

method is called Stochastic Response Surface Method, and will be studied in depth in the following sections.

Although this Thesis does not deal with the Spectral Stochastic Finite Element Method, for reasons of completeness, it will be briefly presented in the following sections, as the combination of stochastic expansions and Finite Element Methods. The Stochastic Response Surface Method will be presented in the next chapter in greater detail since it will be used in the numerical part of this Thesis.

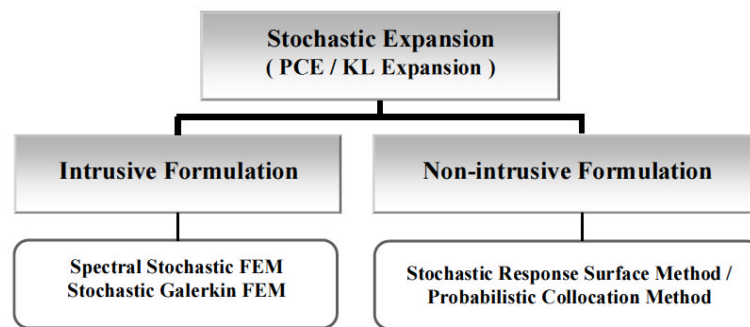


Figure 9: Intrusive and non-intrusive formulation [93]

2.4.2 Spectral Stochastic Finite Elements

The key aspect of SSFEM, is the appropriate transformation of a complicated random quantity, to a set of simpler random quantities, easier to assess. Towards this scope, two different stages can be distinguished:

- One involving representation of the random processes used to model the corresponding random properties.
- One involving the solution process.

The properties mentioned in the first stage, are assumed to be represented through their second-order statistics, varying continuously over space. Each of those processes is considered as an uncountable set of random variables which should be replaced by a finite set, able to be truncated at a prescribed level that represents sufficient accuracy. Karhunen-Loeve expansion, or different

expansions eigensolutions of self-adjoint operators [105], can be employed towards this scope.

As far as the solution process is concerned, it consists of a vectorial random process whose members represent the random solution at the nodes of the finite element discretization. For the description of the solution in a formulation independent to the unknown properties, Polynomial Chaos Expansion should be employed, degrading the problem to the calculation of deterministic coefficients representing the solution process with respect to this expansion. In [106] and [107], expansions that refer to non-Gaussian processes can be found, as a variation of the conventional Polynomial Chaos expansion.

2.4.2.1 Karhunen-Loeve (KL) Transform

Stochastic analysis faces the challenge of appropriate representation of uncertainty in a computationally feasible way. The concept of random fields can adequately represent space and time varying variables such as distributed loads and material properties. Large numbers of variables often cause problems to uncertainty analysis, affecting the accuracy of analysis and therefore the predicted reliability. This fact, especially for cases with highly correlated variables, yields a demand for compromising reduction in dimensionality and at the same time ensuring accuracy for the uncertainty analysis.

Karhunen and Loeve, have represented the continuous-time random process in terms of ortho-normal coordinate functions derived from the covariance function while in [108] principle components were used to analyze the correlation among different variables. Further, various methodologies have been presented in order to achieve reduction of the variables and their correlation. In [109], rank correlation is used to generate the resultant dependent random variables and in [110] a modification of this approach was proposed using ranks of the sample elements. In [111], [112], [113] a complete non-intrusive procedure combined K-L transform, PCE and LHS to account uncertainties in properties in structural reliability assessment. Finally, orthogonal decomposition is often used to generate correlated random variables.

K-L transform is a more advanced tool than the orthogonal transform method and will be briefly analyzed in this section in order to later derive the methodology of the SSFEM. It is an important tool in computational application since it can reduce the dimensionality of the problem generating correlated random variables [114].

Considering the stochastic process $E(\chi, \theta)$, the corresponding K-L expansion will be based on the spectral expansion of its covariance function $C_{EE}(x, y)$, where x and y denote spatial coordinates and θ indicates the random quantity. Common properties of the covariance function are symmetry and positive definition, with mutually orthogonal eigen-functions. The expansion can be formulated as:

$$E(\chi, \theta) = \bar{E}(x) + \sum_{i=1}^x \sqrt{\lambda_i} \xi_i(\theta) \psi_i(x) \quad (2-17)$$

Where: $\bar{E}(x)$ denotes the mean of the stochastic process, $\{\xi_i(\theta)\}$ a set of orthogonal random variables, $\{\psi_i(x)\}$ are the eigen-functions and $\{\lambda_i\}$ are the eigenvalues, that can be evaluated as the solution to the following equation:

$$\int_{\mathcal{D}} C_{EE}(x, y) \psi_i(y) dy = \lambda_i \psi_i(x) \quad (2-18)$$

Where: \mathcal{D} denotes the spatial domain over which the process $E(\chi, \theta,)$ is defined.

The expression of (2-18) denotes that the random fluctuations have been decomposed into a set of deterministic functions in the spatial variables by combination of random coefficients that are independent of these variables. The vector of the random variables $\{\xi_i\}$ will follow the properties of $E(\chi, \theta)$.

2.4.2.2 Polynomial Chaos expansion

Polynomial Chaos Expansions is a stochastic method used for the representation of the correlation between the basic design variables and the response of the structure or the structural members. Considering that the

solution process is a function of the material properties, the nodal response vector \hat{u} can be formed stochastically by a set of non linear functions $\{\xi_i(\theta)\}$. This functional dependence can be expanded in terms of polynomials in Gaussian random variables, referred to as Polynomial Chaos [115], as follows:

$$u(\theta) = a_0\Gamma_0 + \sum_{i_1=1}^x a_{i_1}\Gamma_1(\xi_{i_1}(\theta)) + \sum_{i_1=1}^x \sum_{i_2=1}^{i_1} a_{i_1 i_2}\Gamma_2(\xi_{i_1}(\theta), \xi_{i_2}(\theta)) + \dots \quad (2-19)$$

Where: $\Gamma_n(\xi_{i_1}, \dots, \xi_{i_n})$ denotes the n -th order Polynomial Chaos of the variables $(\xi_{i_1}, \dots, \xi_{i_n})$. $\{\gamma_i(\theta)\}$, being a one-to-one mapping to a set with ordered indices and truncating the Polynomial Chaos expansion the above can be reduced to:

$$u(\theta) = \sum_{j=0}^P u_j \gamma_j(\theta) \quad (2-20)$$

In those polynomials, the inner product $\langle \gamma_i \gamma_k \rangle$, which is defined as the statistical average of their product, is equal to zero for $j \neq k$. Once u_j are calculated, the process $u(\theta)$ can be assessed. Increasing the amount of random variables or the order of PCE polynomials can refine those series. Further, PCE can be used to represent non-Gaussian processes (variables). Combination of Karhunen-Loeve expansion and the Polynomial Chaos expansion will be presented in the next section in order to formulate a Spectral Stochastic Finite Element Method procedure.

2.4.2.3 Formulation of Spectral Stochastic Finite Element Method

The formulation of the global stiffness matrix for uncertain stiffness can be expressed as:

$$\mathbf{K}(\theta) = \int_{\Omega} \mathbf{B}^T \mathbf{C}(x, \theta) \mathbf{B} d\Omega \quad (2-21)$$

Where: \mathbf{B} is the matrix relating strains to nodal displacements and $\mathbf{C}(x, \theta)$ is the randomness matrix. Introducing the K-L expansion for $\mathbf{C}(x, \theta)$, (2-21) can be transformed as:

$$\mathbf{K}(\theta) = \bar{\mathbf{K}} + \sum_{i=1}^x \xi_i(\theta) \int_{\Omega} \mathbf{B}^T \mathbf{C}_1(x) \mathbf{B} d\Omega \quad (2-22)$$

Redefining, $\xi_0 = 1$ and $\mathbf{K}_0 = \bar{\mathbf{K}}$, the above can be expressed as:

$$\mathbf{K}(\theta) = \sum_{i=1}^x \xi_i(\theta) \int_{\Omega} \mathbf{B}^T \mathbf{C}_1(x) \mathbf{B} d\Omega \quad (2-23)$$

While, truncating the K-L expansion, the final matrix equation for the finite element model is transformed to:

$$\left(\sum_{i=0}^M \xi_i(\theta) \mathbf{K}_i \right) u(\theta) = f \quad (2-24)$$

Combining PCE with K-L expansions through (2-20) and (2-24), the nodal response values can be obtained as:

$$\left(\sum_{j=0}^P \sum_{i=0}^M \xi_i(\theta) \gamma_i(\theta) \mathbf{K}_i \right) u_j = f \quad (2-25)$$

Enforcing orthogonality to the above equation, a system of linear equations can be obtained as:

$$K \hat{u} = f \quad (2-26)$$

Where: $\mathbf{K}_{ik} = \sum_{i=0}^M \mathbf{K}_i \langle \xi_i(\theta) \gamma_i(\theta) \gamma_k(\theta) \rangle$, $j, k = 0, \dots, p$, and \hat{u} is an extended solution vector containing u_j as its sub-vectors. Solution of the system for the coefficient vector \hat{u} , provides the statistical properties of the nodal response values.

2.5 Summary

This chapter has dealt with fundamental aspects of the reliability analysis of offshore and steel structures. After basic mathematical formulation of the reliability estimation problem, the motivation of a reliability framework and the evolution in its application on the assessment of structures was presented. Selection of the appropriate type of analysis was also discussed in conjunction with methods for integration from a local to a global level of reliability calculation, distinguishing a practical method for the deterministic assessment of the non linear performance of structures to failure. Finally, a review of stochastic expansions was included, followed by a brief formulation of the Spectral Stochastic Finite Elements Method, in order to set the background for the development of the Stochastic Response Surface Method, which will be analytically discussed in the next chapter.

3 NUMERICAL METHODS FOR STRUCTURAL RELIABILITY ANALYSIS

3.1 Introduction

In this Chapter the numerical procedures for the computation of reliability will be presented. Solution of the integral of the joint probability distribution function imposes difficulties in the calculation of the probability of failure equation. Therefore, use of limit state function approximations can be employed in order to overcome this problem. Appropriate selection of the proper technique, can handle many engineering problems of great importance. In the following sections, Level III reliability analysis methods will be presented analytically, as they will be applied later in this Thesis. Both deterministic and probabilistic formulations will be discussed. The Stochastic Response Surface Method (SRSM) will be presented and after a literature review of this method and multivariate regression techniques, the methodology that will be used in this Thesis will be derived.

3.2 Numerical Methods

3.2.1 Deterministic Methods

The methods and algorithms that will be discussed in this section refer to deterministic handling of the limit state functions through geometrical approximation of the stochastic variables. Random variables are characterized by their moments. Initially the First-order Second Moment Reliability Method (FOSM) will be presented that will stand as a basis for the First-order and later the Second-order Reliability Methods (FORM/SORM). Analytical description of those methods can be found in [116].

The multiple variables participating in the probability of failure calculation have yielded several methods that would simplify this procedure. Employment of first

and second order Taylor series expansion is a common practice applied to linearize the limit state equation. This practice refers respectively to the First and Second Order Moment methods. FOSM is referred to as mean value first order second moment method (MVFOSM) and is a simplistic method that cannot provide results of sufficient accuracy for very low probabilities of failure or non linear limit state functions [117]. Addition of the second term, in SOSM methods cannot sufficiently handle this problem.

In order to overcome the above difficulties, a geometrical solution, the safety index approach, transforms the problem to a mathematical optimisation problem of finding the point of the limit state surface with the minimum distance to the origin of the standard normal space. In [52], the Hasofer and Lind (HL) algorithm is introduced transforming the vector of the design stochastic variables X into a vector of standardized independent variables U . The design point in the U -space represents the point of greatest probability density and is called the Most Probable failure Point (MPP). The transformed limit state surface $g(U) = 0$ can be approached with first or second order approximations and therefore account for First and Second Order Reliability Methods (FORM/SORM).

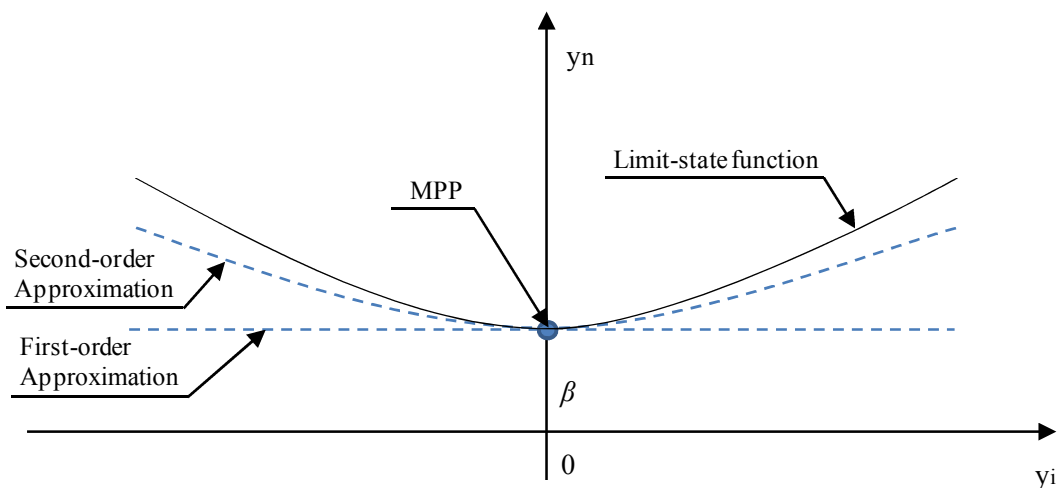


Figure 10: First and Second order approximations

The interpretation of the above approach is that in FORM, the limit state surface is approximated by a tangent plane at the MPP while for SORM the MPP is

approximated by a curve as it can be seen in Figure 10. FORM gives inaccurate results in cases of highly non linear limit state surfaces and large curvatures.

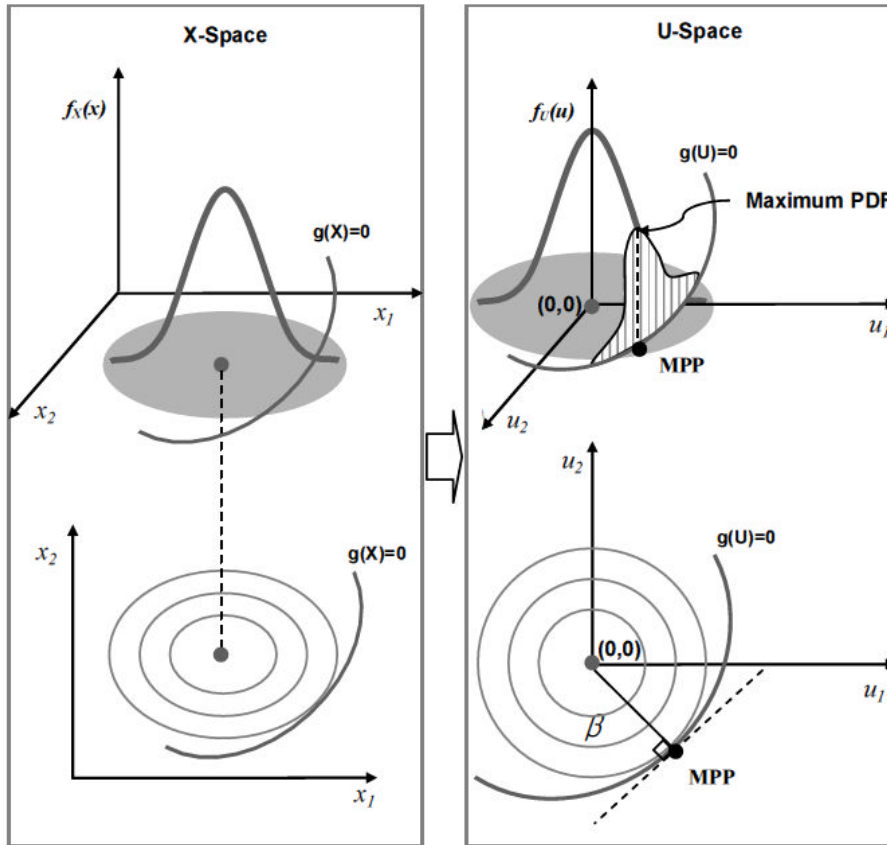


Figure 11: Transformation to the U-space [93]

3.2.1.1 First Order Reliability Methods

3.2.1.1.1 The Mean Value FOSM (MVFOSM)

The Mean Value FOSM (MVFOSM) simplifies the calculation procedure of the probability of failure of a limit state function. The characterization “first-order” derives from the employment of first order expansions for the linearization of the initial function, expressing inputs and outputs as the corresponding mean and standard deviation. This simplifying approximation, neglects higher moments, and therefore increases the subsequent model uncertainty. According to this method, the limit-state function is approximated by the first-order Taylor series expansion at the mean value point. Considering X to be the vector of statistically

independent variables, the approximate limit-state function at the mean can be expressed as:

$$\tilde{g}(X) \approx g(\mu_X) + \nabla g(\mu_X)^T \cdot (X_i - \mu_{x_i}) \quad (3-1)$$

Where: the vector of mean values is $\mu_X = \{\mu_{x_1}, \mu_{x_2}, \dots, \mu_{x_n}\}^T$, and the gradient of g evaluated at μ_X as:

$$\nabla g(\mu_X) = \left\{ \frac{\partial g(\mu_X)}{\partial x_1}, \frac{\partial g(\mu_X)}{\partial x_2}, \dots, \frac{\partial g(\mu_X)}{\partial x_n} \right\}^T \quad (3-2)$$

The mean (expected) value of the approximated limit-state function $\tilde{g}(X)$ is:

$$\mu_{\tilde{g}} \approx E[g(\mu_X)] = g(\mu_X) \quad (3-3)$$

Following some fundamental statistics transformations, the standard deviation of the approximate limit-state function is calculated as:

$$\begin{aligned} \sigma_{\tilde{g}} &= \sqrt{\text{Var}[\tilde{g}(X)]} = \sqrt{[\nabla g(\mu_X)^T]^2 \cdot \text{Var}(X)} \\ &= \left[\sum_{i=1}^n \left(\frac{\partial g(\mu_X)}{\partial x_i} \right)^2 \cdot \sigma_{x_i}^2 \right]^{\frac{1}{2}} \end{aligned} \quad (3-4)$$

The reliability index β is then calculated as:

$$\beta = \frac{\mu_{\tilde{g}}}{\sigma_{\tilde{g}}} \approx \frac{g(\mu_X)}{\left[\sum_{i=1}^n \left(\frac{\partial g(\mu_X)}{\partial x_i} \right)^2 \cdot \sigma_{x_i}^2 \right]^{\frac{1}{2}}} \quad (3-5)$$

For cases of linear limit state functions, the above expression of the reliability index can be analytically derived by expressing the safety margin between a resistance R and a loading S of a system with normal variables as:

$$g(X) = R(X) - S(X) \quad (3-6)$$

The resulting mean value μ_g and standard deviation σ_g are respectively:

$$\mu_g = \mu_R - \mu_S \quad (3-7)$$

$$\sigma_g = \sqrt{\sigma_R^2 + \sigma_S^2 - 2 \cdot \rho_{RS} \cdot \sigma_R \cdot \sigma_S} \quad (3-8)$$

Where: ρ_{RS} is the correlation coefficient between R and S , and $\mu_R, \mu_S, \sigma_R, \sigma_S$ the mean values and standard deviations of the R and S variables. The reliability index β is calculated as:

$$\beta = \frac{\mu_g}{\sigma_g} = \frac{\mu_R - \mu_S}{\sqrt{\sigma_R^2 + \sigma_S^2 - 2 \cdot \rho_{RS} \cdot \sigma_R \cdot \sigma_S}} \quad (3-9)$$

And for the case of uncorrelated variables, where: $\rho_{RS} = 0$:

$$\beta = \frac{\mu_g}{\sigma_g} = \frac{\mu_R - \mu_S}{\sqrt{\sigma_R^2 + \sigma_S^2}} \quad (3-10)$$

In cases of nonlinear limit-state functions, the approximate limit-state surface can be derived by linearization of the initial limit-state function at the mean value point. In the generalized case with multiple independent variables, the failure surface is represented by a hyper plane that is defined as a linear-failure function:

$$\tilde{g}(X) = c_0 + \sum_{i=1}^n c_i \cdot x_i \quad (3-11)$$

$$\mu_{\tilde{g}} = c_0 + c_1 \mu_{x_1} + c_2 \mu_{x_2} + \dots + c_n \mu_{x_n} \quad (3-12)$$

$$\sigma_{\tilde{g}} = \sqrt{\sum_{i=1}^n c_i^2 \cdot \sigma_{x_i}^2} \quad (3-13)$$

The MVFOSM method is a simplistic method for the calculation of reliability indices, using minimum representation of basic variables. This fact diminishes the range of applicability of the method due to the following reasons:

- Non linearity or large variations cannot be efficiently handled by that method, since linearization of the limit-state function about the mean values can lead to inaccurate results.

- The MVFOSM method is dependent on different - mathematically equivalent - formulations of a same problem; both for linear and non linear expressions of the limit state function.

3.2.1.1.2 Hasofer and Lind

The reliability index can be interpreted as the geometrical distance defined from the origin of a u -dimensional space to the Most Probable failure Point (MPP) on the failure surface. The Hasofer and Lind reliability index method transforms the expansion point from the mean value point to the MPP improving the approach of the MVFOSM. To expand this practice for problems with multiple variables, Hasofer and Lind [52] proposed a linear transformation of the basic variables x_i into a set of normalized and independent variables u_i .

For the basic case with two independent, normally distributed variables of strength R , and stress, S , Hasofer and Lind transformed the initial variables to standard normalized ones, following:

$$\hat{R} = \frac{R - \mu_R}{\sigma_R}, \quad \hat{S} = \frac{S - \mu_S}{\sigma_S} \quad (3-14)$$

Where: μ_R and μ_S are the mean values and σ_R and σ_S are the standard deviations of R and S , respectively. Following, the limit-state surface $g(R, S) = R - S = 0$ should be transformed from the original (R, S) coordinate system into the limit-state surface, in the standard normalized (\hat{R}, \hat{S}) coordinate system as:

$$g(R(\hat{R}), S(\hat{S})) = \hat{g}(\hat{R}, \hat{S}) = \hat{R} \cdot \sigma_R - \hat{S} \cdot \sigma_S + (\mu_R - \mu_S) = 0 \quad (3-15)$$

The distance from the origin in the (\hat{R}, \hat{S}) coordinate system to the failure surface $\hat{g}(\hat{R}, \hat{S}) = 0$ is equal to the safety-index:

$$\beta = \widehat{OP}^* = \frac{(\mu_R - \mu_S)}{\sqrt{\sigma_R^2 + \sigma_S^2}} \quad (3-16)$$

The point $P^*(\hat{R}^*, \hat{S}^*)$ on $\hat{g}(\hat{R}, \hat{S}) = 0$, is the Most Possible failure Point (MPP), and corresponds to this shortest distance. In the general case with n normally

distributed and independent variables, the failure surface is described by a nonlinear function:

$$g(X) = g(\{x_1, x_2, \dots, x_n\}^T) = 0 \quad (3-17)$$

Transformation of the variables into their standardized forms should follow:

$$u_i = \frac{x_i - \mu_{x_i}}{\sigma_{x_i}} \quad (3-18)$$

Where: μ_{x_i} and σ_{x_i} represent the mean and the standard deviation of x_i , respectively. The mean and standard deviation of the standard normally distributed variable u_i are zero and unity, respectively.

The failure surface $g(X) = 0$ in X -space is mapped into the corresponding failure surface $g(U) = 0$ in U -space. Due to the rotational symmetry of the second-moment representation of U , the geometrical distance from the origin in U -space to any point on $g(U) = 0$ refers to the number of standard deviations from the mean value point in X -space to the corresponding point on $g(X) = 0$. The safety-index β is the shortest distance from the origin to the failure surface $g(U) = 0$, as:

$$\beta = \min_{U \in g(U)=0} (U^T \cdot U)^{1/2} \quad (3-19)$$

This value of β is called the 'Hasofer and Lind (HL) safety-index' β_{HL} . The point $U^*(u_1^*, u_2^*, \dots, u_n^*)$ on $g(U) = 0$ is the design point, which can provide the corresponding vector point in the X -space.

Based on the above theoretical presentation of the method, the problem of the calculation of the reliability index β can be derived as the solution of a constrained optimization problem in the standard normal U -space.

$$\text{minimize: } \beta(U) = (U^T \cdot U)^{1/2} \text{ with } g(U) = 0 \quad (3-20)$$

Several algorithms are available that can solve this problem, such as mathematical optimization schemes or other iteration algorithms. In [118],

several constrained optimization methods were used in order to solve this optimization problem, including primal methods (feasible directions, gradient, projection, and reduced gradient), penalty methods, dual methods, and Lagrange multiplier methods [116]. Each method's applicability depends on the nature of the problem that is investigated. Following, the HL and HL-RF methods are presented, as the most commonly used algorithms.

The HL algorithm was proposed by Hasofer and Lind, allowing consideration of normally distributed random variables. Rackwitz and Fiessler extended the HL method in order to handle non-Gaussian statistical distributions, forming the extended HL-RF method. Assuming that the (linear or non linear) limit state surface with n normally distributed and independent random variables X can be expressed as:

$$g(X) = g(\{x_1, x_2, \dots, x_n\}^T) = 0 \quad (3-21)$$

Based on the transformation the limit-state function becomes:

$$g(U) = g(\{\sigma_{x_1}u_1 + \mu_{x_1}, \sigma_{x_2}u_2 + \mu_{x_2}, \dots, \sigma_{x_n}u_n + \mu_{x_n}\}^T) = 0 \quad (3-22)$$

The normal vector from the origin \hat{O} to the limit-state surface $g(U)$ generates an intersection point P^* . The distance from the origin to the MPP is the safety-index β . The first-order Taylor series expansion of $g(U)$ at the MPP P^* is:

$$\tilde{g}(U) \approx g(U^*) + \sum_{i=1}^n \frac{\partial g(U^*)}{\partial U_i} \cdot (u_i - u_i^*) \quad (3-23)$$

From the transformation:

$$\frac{\partial \hat{g}(U)}{\partial U_i} = \frac{\partial g(X)}{\partial x_i} \cdot \sigma_{x_i} \quad (3-24)$$

The minimum distance from \hat{O} to the $\tilde{g}(U)$ surface may be given as:

$$\hat{O}P^* = \beta = \frac{g(U^*) - \sum_{i=1}^n \frac{\partial g(U^*)}{\partial x_i} \cdot \sigma_{x_i} \cdot u_i^*}{\sqrt{\sum_{i=1}^n \left(\frac{\partial g(U^*)}{\partial x_i} \cdot \sigma_{x_i} \right)^2}} \quad (3-25)$$

The direction cosine of each of the transformed variables, often called sensitivity factor, is given as follows, expressing the relative effect of the corresponding random variable on the total variation.

$$a_i = \cos \theta_{x_1} = \cos \theta_{u_1} = -\frac{\frac{\partial g(U^*)}{\partial u_i}}{|\nabla g(U^*)|} = \frac{\frac{\partial g(X^*)}{\partial x_i} \cdot \sigma_{x_i}}{\left[\sum_{i=1}^n \left(\frac{\partial g(X^*)}{\partial x_i} \cdot \sigma_{x_i} \right)^2 \right]^{1/2}} \quad (3-26)$$

The coordinates of the point P^* are computed as:

$$u_i^* = \frac{x_i^* - \mu_{x_i}}{\sigma_{x_i}} = \hat{O}P^* \cos \theta_{x_1} = \beta \cos \theta_{x_1} \quad (3-27)$$

And, transforming them into the original space X :

$$x_i^* = \mu_{x_i} + \beta \sigma_{x_i} \cos \theta_{x_1}, \quad (i = 1, 2, \dots, n) \quad (3-28)$$

Since P^* is a point on the limit-state surface, it should satisfy:

$$g(\{x_1^*, x_2^*, \dots, x_n^*\}^T) = 0 \quad (3-29)$$

In cases where the failure surface may contain several points corresponding to stationary values of the reliability-index function (multiple MPP problem), it may be necessary to use several starting points in order to find all the values $\{\beta_1, \beta_2, \dots, \beta_m\}$, deriving the HL safety-index as:

$$\beta_{HL} = \min\{\beta_1, \beta_2, \dots, \beta_m\} \quad (3-30)$$

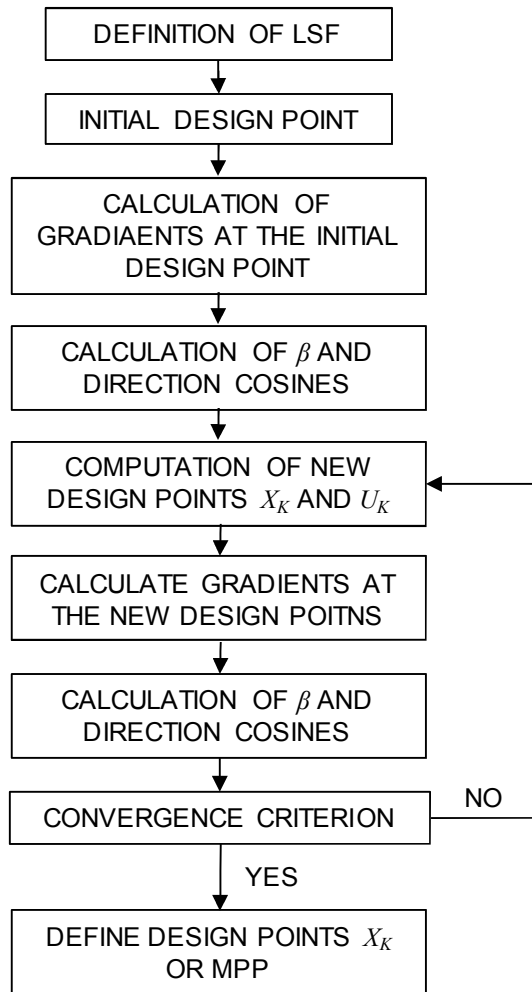


Figure 12: Algorithm of HL Reliability Index Calculation

The difference between the MVFOSM method and the HL method is that the HL method approximates the limit-state function using the first-order Taylor expansion at the design point $X^{(k)}$ or $U^{(k)}$ instead of the mean value point μ_X [116]. Further, the MVFOSM method is a straight forward procedure, while the HL method needs several iterations to converge, especially for nonlinear problems. The HL method usually provides better results than the mean-value method for nonlinear problems. The quality of the linearized limit-state function, $\tilde{g}(U) = 0$ will determine the accuracy of the calculation of the probability of failure P_f .

3.2.1.1.3 Hasofer Lind - Rackwitz Fiessler (HL-RF) Method

In the Hasofer-Lind reliability index method, the random variables X are assumed to be normally distributed. In cases of non-Gaussian variables, the reliability calculation procedures as presented so far are inefficient. Many structural reliability problems involve non-Gaussian random variables; therefore it is necessary to find a way to treat such problems. There are many methods available for conducting transformations to the normalized space, such as those found in [119], and [120]. A simple, approximate transformation called ‘the equivalent normal distribution’, or ‘the normal tail approximation’, is presented in this section. The main advantages of this transformation are:

- i. Avoidance of the multi-dimensional integration of the main integral for the probability of failure.
- ii. Transformation of non-Gaussian variables into equivalent normal variables is accomplished prior to the solution of the final equations avoiding overcomplicated procedures.
- iii. Results often agree with the exact solution of the multi-dimensional integral of the fundamental probability integral.

Considering, mutually independent variables, the transformation is given as:

$$u_i = \Phi^{-1}[F_{x_i}(x_i)] \quad (3-31)$$

Where: $\Phi^{-1}[\cdot]$ is the inverse of $\Phi[\cdot]$.

Employment of Taylor series expansion of the transformation at the MPP X^* , neglecting nonlinear terms [121], can provide the equivalent normal distribution as:

$$u_i = \Phi^{-1}[F_{x_i}(x_i^*)] + \frac{\partial}{\partial x_i}([\Phi^{-1}F_{x_i}(x_i)])|_{x_i^*} \cdot (x_i - x_i^*) \quad (3-32)$$

Where:

$$\frac{\partial}{\partial x_i} \Phi^{-1}[F_{x_i}(x_i)] = \frac{f_{x_i}(x_i)}{\varphi(\Phi^{-1}[F_{x_i}(x_i^*)])} \quad (3-33)$$

After substitution of the above and rearrangement of terms:

$$u_i = \frac{x_i - [x_i^* - \Phi^{-1}[F_{x_i}(x_i^*)]]\varphi(\Phi^{-1}[F_{x_i}(x_i^*)])/f_{x_i}(x_i^*)}{\varphi(\Phi^{-1}[F_{x_i}(x_i^*)])/f_{x_i}(x_i^*)} = \frac{x_i - \mu_{x_i'}}{\sigma_{x_i'}} \quad (3-34)$$

Where: $F_{x_i}(x_i)$ is the marginal cumulative distribution function $f_{x_i}(x_i)$, is the probability density function, and $\mu_{x_i'}$ and $\sigma_{x_i'}$ are the equivalent means and standard deviations of the approximate normal distributions, which are given as:

$$\sigma_{x_i'} = \frac{\varphi(\Phi^{-1}[F_{x_i}(x_i^*)])}{f_{x_i}(x_i^*)} \quad (3-35)$$

$$\mu_{x_i'} = x_i - \Phi^{-1}[F_{x_i}(x_i^*)] \cdot \sigma_{x_i'} \quad (3-36)$$

Another way to get equivalent normal distributions is to match the cumulative distribution functions and probability density function of the original, non-normal random variable distribution, and the approximate or equivalent normal random variable distributions at the MPP [119].

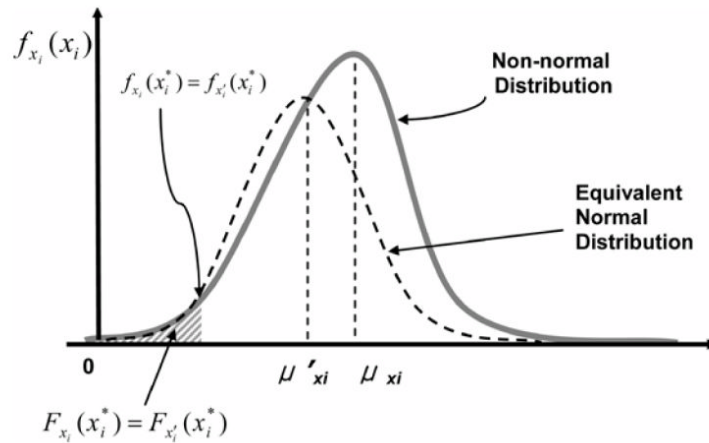


Figure 13: Normalized Tail Approximation [116]

This normalized-tail approximation is shown in Figure 13. Using the above procedure, the transformation of the random variables from the X -space to the U -space can be easily achieved, and the performance function $g(U)$ in U -space is approximately obtained.

The RF method is also called the HL-RF method, since the iteration algorithm was originally proposed by Hasofer and Lind and later extended by Rackwitz and Fiessler to include random variable distribution information. For the extended RF algorithm, the same steps as shown in Figure 12 should be followed considering one extra block for the transformation of variables before the definition of the initial design point.

The HL and HL-RF algorithm, approximates the limit-state function, $g(U)$, by the first-order Taylor expansion at the MPP. For nonlinear problems, this approach cannot adequately approximate β , requiring several iterations until convergence, especially for poorly linearization of nonlinear functions $g(U)$. Different approximation could be used alternatively, such as the Two-point Adaptive Nonlinear Approximations (TANA) [122], including TANA and TANA2. This set of approximations uses Taylor series expansion in terms of adaptive intervening variables, overcoming non-linearity problems by using updated information through the iteration process. TANA2 further includes a correction term for second-order terms.

3.2.1.2 Second Order Reliability Methods

FORM approximation provides adequate results when the limit-state surface has only one minimal distance point and the function is nearly linear close to the design point. For cases where the failure surface has large or irregular curvatures (high nonlinearity), the failure probability estimated by FORM, using the safety-index β , may give unreliable and inaccurate results [121]. Introducing second-order Taylor series expansions (or other polynomials) may overcome this problem.

Various nonlinear approximate methods have been proposed in the literature. In [123], [124], [125], [126], [127], and [128] SORM have been developed using the second order approximation to simplify the original surfaces. In [129] and [130] second-order approximations are used, forming approximate curvatures in order to avoid exact second-order derivatives calculations of the limit state surface.

3.2.1.2.1 Orthogonal Transformations

Transformation of the U -space to a rotated new standard normal Y -space would simplify the integration of the limit state function. This can be achieved by introducing an orthogonal transformation matrix H . Formulation of this is initiated by defining an initial matrix as:

$$\begin{pmatrix} \frac{-\partial g(U^*)/\partial U_1}{|\nabla g(U^*)|} & \frac{-\partial g(U^*)/\partial U_2}{|\nabla g(U^*)|} & \cdots & \frac{-\partial g(U^*)/\partial U_n}{|\nabla g(U^*)|} \\ 0 & 1 & \cdots & 0 \\ 0 & 0 & \cdots & 0 \\ \cdots & \cdots & \cdots & \cdots \\ 0 & 0 & \cdots & 1 \end{pmatrix} \quad (3-37)$$

The above matrix can be orthogonalized to obtain H , using several algorithm such as the Gram-Schmidt algorithm [131]. Denoting f_1, f_2, \dots, f_n for the i -th row vector of the above matrix, respectively:

$$f_1 = \left\{ \frac{-\partial g(U^*)/\partial U_1}{|\nabla g(U^*)|}, \frac{-\partial g(U^*)/\partial U_2}{|\nabla g(U^*)|}, \dots, \frac{-\partial g(U^*)/\partial U_n}{|\nabla g(U^*)|} \right\}^T, \quad (3-38)$$

$$f_2 = \{0, 1, 0, \dots, 0\}^T, \dots,$$

$$f_n = \{0, 0, 0, \dots, 1\}^T$$

Setting:

$$D_1 = (f_1, f_1)^{\frac{1}{2}}, e_{11} = \frac{1}{D_1}, \gamma_1 = e_{11} \cdot f_1,$$

$$D_2 = [(f_2, f_2) - |(f_2, \gamma_1)|^2]^{\frac{1}{2}}, \quad (3-39)$$

$$e_{12} = -\frac{(f_2, \gamma_1)}{D_2}, e_{22} = \frac{1}{D_2}, \gamma_2 = e_{12} \cdot \gamma_1 + e_{22} \cdot f_2$$

And in a general form:

$$D_k = [(f_k, f_k) - |(f_k, \gamma_1)|^2 - |(f_k, \gamma_2)|^2 - \dots - |(f_k, \gamma_{k-1})|^2]^{\frac{1}{2}} \quad (3-40)$$

$$e_{1k} = -\frac{(f_k, \gamma_1)}{D_k}, e_{2k} = -\frac{(f_k, \gamma_2)}{D_k}, \dots, e_{k-1,k} = -\frac{(f_k, \gamma_{k-1})}{D_k}, \quad (3-41)$$

Where: (f, f) and (f, γ) represent the scalar (element by element) product of two vectors. The generated orthogonal matrix H_0 is therefore:

$$H_0^T = \{\gamma_1^T, \gamma_2^T, \dots, \gamma_n^T\} \quad (3-42)$$

The final orthogonal matrix H is derived by moving the first row of the orthogonal matrix H_0 to the last row as:

$$H^T = \{\gamma_2^T, \gamma_3^T, \dots, \gamma_n^T, \gamma_1^T\} \quad (3-43)$$

3.2.1.2.2 First-order Approximation

Parallel to what has been discussed in the presentation of the FORM, assuming the most probable failure point (MPP) in U -space to be $U^* = \{u_1^*, u_2^*, \dots, u_n^*\}^T$, the linear approximation of the response surface $g(U) = 0$ is given by the first-order Taylor Series expansion at the MPP:

$$\tilde{g}(U) \approx g(U^*) + \nabla g(U^*) \cdot (U - U^*) = 0 \quad (3-44)$$

Considering: $g(U^*) = 0$, on the response surface, and dividing by $|\nabla g(U^*)|$:

$$\tilde{g}(U) \approx \frac{\nabla g(U^*)}{|\nabla g(U^*)|} \cdot (U - U^*) \quad (3-45)$$

And therefore, as in (3-26), we obtain:

$$\frac{\nabla g(U^*) \cdot U^*}{|\nabla g(U^*)|} = -\beta \quad (3-46)$$

Back substituting this equation into the expanded first-order Taylor Series expression:

$$\tilde{g}(U) \approx \frac{\nabla g(U^*) \cdot U^*}{|\nabla g(U^*)|} \cdot U + \beta = 0 \quad (3-47)$$

Applying the transformation H into a set of mutually independent standard normal random variables:

$$Y = H \cdot U \quad (3-48)$$

And (3-46) becomes:

$$\tilde{g}(U) \approx -y_n + \beta = 0 \text{ or, } y_n = \beta \quad (3-49)$$

The above equation represents the first-order approximation of the response surface in the Y -space. As in the comparison between FORM and SORM, for linear or close to linear cases this first order approximation can provide adequate results. In different cases, second order approximations might be employed.

3.2.1.2.3 Second-order Approximation

Applying the second-order Taylor series expansion at the MPP for the response surface $g(U) = 0$ we obtain:

$$\begin{aligned} \tilde{g}(U) \approx g(U^*) + \nabla g(U^*)^T (U - U^*) \\ + \frac{1}{2} (U - U^*)^T \nabla^2 g(U^*) (U - U^*) = 0 \end{aligned} \quad (3-50)$$

Where:

$$\nabla^2 g(U^*)_{ij} = \frac{\partial^2 g(U^*)}{\partial u_i \cdot \partial u_j} \quad (3-51)$$

Considering: $g(U^*) = 0$, on the response surface, and dividing by $|\nabla g(U^*)|$:

$$\tilde{g}(U) \approx \left(\frac{\nabla g(U^*)}{|\nabla g(U^*)|} \right)^T \cdot (U - U^*) + \frac{1}{2} (U - U^*)^T \left(\frac{\nabla^2 g(U^*)}{|\nabla g(U^*)|} \right) \cdot (U - U^*) \quad (3-52)$$

Denoting:

$$B = \left(\frac{\nabla^2 g(U^*)}{|\nabla g(U^*)|} \right) \quad (3-53)$$

Transformation from U to Y -space, the second order approximated limit state functions may be written as:

$$\tilde{g}(Y) \approx -y_n + \beta + \frac{1}{2} \cdot (H^{-1}Y - H^{-1}Y^*) \cdot B \cdot (H^{-1}Y - H^{-1}Y^*) \quad (3-54)$$

Where: $Y^* = \{0, 0, \dots, \beta\}^T$ corresponding to the U -space MPP U^* . Due to the transformation in the Y -space, the y_n axis is in coincidence with the β vector geometrically approaching the calculation problem. Applying the orthogonality properties of H , $H^{-1} = H^T$ and substituting:

$$\tilde{g}(Y) \approx -y_n + \beta + \frac{1}{2} \cdot (Y - Y^*)^T \cdot H \cdot B \cdot H^T \cdot (Y - Y^*) \quad (3-55)$$

Where: $(Y - Y^*)^T = (y_1, y_2, \dots, y_n - \beta)^T$

By a series of orthogonal transformations, H_1, H_2, \dots, H_m for the first $(n-1)$ variables, $\bar{Y} = \{y_1, y_2, \dots, y_{n-1}\}^T$:

$$\bar{Y}' = H_1 H_2 \dots H_m \bar{Y} \quad (3-56)$$

The resultant $\bar{H}\bar{B}\bar{H}^T$ matrix may be written as:

$$\bar{H}\bar{B}\bar{H}^T = \begin{pmatrix} k_1 & 0 & \dots & 0 \\ 0 & k_2 & \dots & 0 \\ 0 & 0 & \dots & 0 \\ \dots & \dots & \dots & \dots \\ 0 & 0 & \dots & k_{n-1} \end{pmatrix} \quad (3-57)$$

Where:

$$k_{ij} = (\bar{H}\bar{B}\bar{H}^T)_{ij}, (i, j = 1, 2, \dots, n-1) \quad (3-58)$$

Having obtained the $\bar{H}\bar{B}\bar{H}^T$ matrix, and using Breitung's formulation [132], the revised value of the P_f , can be estimated as a correction of the value obtained by FORM:

$$P_f \approx \Phi(-\beta) \prod_{j=1}^{n-1} (1 + k_j \beta)^{-1/2} \quad (3-59)$$

Based on the same logic, for the calculation of P_f different formulations can be used, such as Tvedt's formulation, applying two further corrective terms for the calculation of P_f , providing:

$$\begin{aligned}
P_f \approx & \Phi(-\beta) \prod_{j=1}^{n-1} (1 + k_j \beta)^{-\frac{1}{2}} + \\
& + [\Phi(-\beta) - \varphi(\beta)] \left\{ \prod_{j=1}^{n-1} (1 + k_j \beta)^{-\frac{1}{2}} - \prod_{j=1}^{n-1} (1 + k_j (\beta + 1))^{-\frac{1}{2}} \right\} + \\
& + (\beta + 1) [\Phi(-\beta) - \varphi(\beta)] \left\{ \prod_{j=1}^{n-1} (1 + k_j \beta)^{-1/2} \right\} - Re \left\{ \prod_{j=1}^{n-1} (1 + k_j (\beta + 1))^{-1/2} \right\}
\end{aligned} \tag{3-60}$$

Although the second order approximation can in general provide more accurate results for a wider range of limit state functions it involves a considerable computational cost in the computation of the derivatives of B . Especially for problems with a high number of variables where the size of matrices increases, this problem becomes even more extensive, yielding for appropriate selection of calculation method or scheme.

3.2.2 Simulation Methods

Simulation methods have been proposed in literature both for the representation of statistical distributions, but also for the solution of the complicated integral of the probability of failure using directly the results from multiple computational experiments. In the following sections, Monte Carlo Simulation, including importance sampling, and Latin Hypercube Simulation will be presented as sampling methods and Design Point, Monte Carlo Simulation, Directional and Axis-orthogonal Simulation as simulation methods that will be used in later sections. Presentation of simulation methods will be based on [133], since PROBAN software will be used for the verification of the codes developed.

3.2.2.1 Sampling Methods

3.2.2.1.1 Monte Carlo Simulation

Monte Carlo Simulation is based on the work of Neumann and Ulam [134]. It refers to a simple random sampling method that generates random sampling sets for several types of uncertain variables. During the last decades, this tool has been developed significantly allowing approximation of the probability of an

event that is the output of a stochastic process. Once a distribution type has been selected, a sampling set is generated that will later serve as input in the simulations.

The basic concept of the method can be described by a simple problem of calculation of the area of a specific polygon, as it is shown in Figure 14. The area can be approximately calculated by the ratio of the number of points that fall inside the specified area, over the total number of the sample, normalized to the total area of sampling. The area can also be calculated geometrically, and a simple sensitivity analysis can show that the greater the sampling number the more accurate the results. Therefore the reference area is represented by the probability of falling inside the area for a given number of trials.

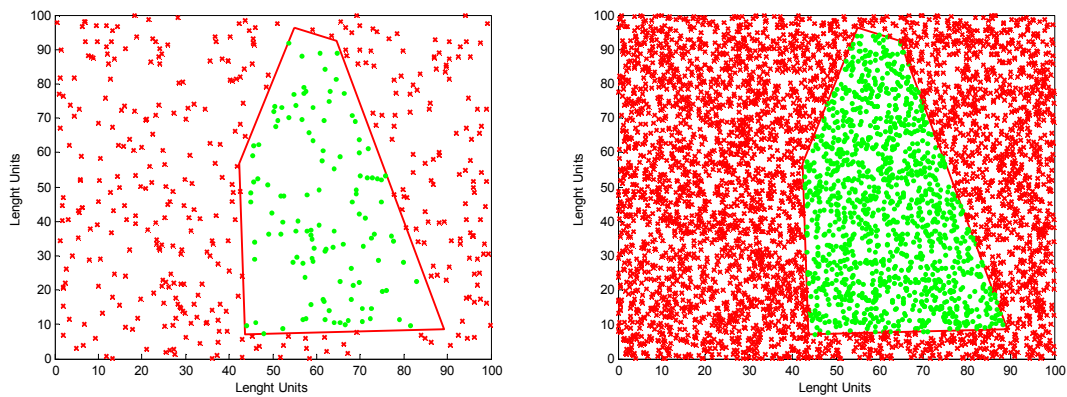


Figure 14: Area calculation with Monte Carlo Simulation (500 and 5000 sampling points)

In problems of structural reliability, once the stochastic variables have been identified, sampling sets are generated according to the corresponding probability density functions. Following, simulations are executed using the generated sampling sets in order to obtain the response of the structure. In the area calculation example, the limit state function is represented by the boundaries of the area to be calculated. For N trials, the probability of failure is given as:

$$P_f = \frac{N_f}{N} \quad (3-61)$$

Generation of random variables of a stochastic distribution can be realized based on the inverse transform method. Considering F_x to be the cumulative distribution function of the random variable x_i with values in the range $[0,1]$. Assuming v_i to be a generated random variable that follows a uniform distribution, this method connects x_i and v_i as follows:

$$F_x(x_i) = v_i \rightarrow x_i = F_x^{-1}(v_i) \quad (3-62)$$

Figure 15, illustrates the basic concept of the inverse transform method.

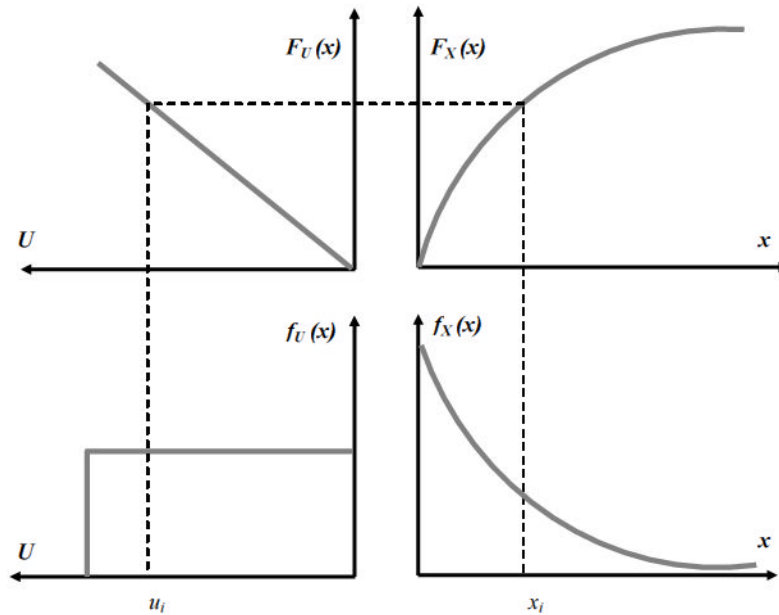


Figure 15: Inverse transformation method

3.2.2.1.2 Latin Hypercube Method

The Latin Hypercube Method, initially proposed in [135], is a method that can represent multiple variables avoiding over-lapping data sets. Application of the method initiates by dividing the distribution of each stochastic variable in n non-overlapping intervals with equal probability. For each of the variables, one value should be randomly selected from each interval and the analysis point obtained from each dataset is then associated. The homogeneous allocation of intervals

on the probability distribution function results in relatively small variance in the response, compared to the conventional Monte Carlo sampling. At the same time, the analysis is much less computationally demanding to generate. Figure 16, presents the case of a two variable sampling problem.

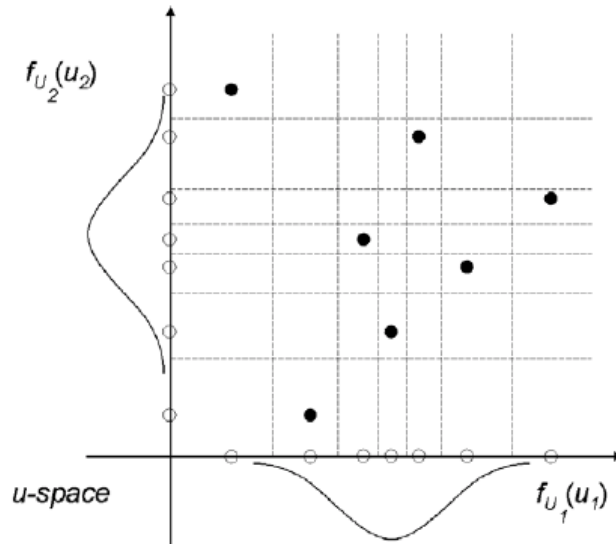


Figure 16: Latin Hypercube Method

3.2.2.2 Simulation on Reliability Analysis

3.2.2.2.1 Monte Carlo Simulation Method

The basic formulation of the Monte Carlo Simulation for the calculation of the probability of success of an event, introduces the indicator function $I(x)$, in the x_i -space as follows:

$$I(x) = \begin{cases} 1 & \text{if } G(x) \leq 0 \\ 0 & \text{if } G(x) > 0 \end{cases} \quad (3-63)$$

The probability of success of an event is then estimated as the fraction of the successful realizations of the iterations over the number of samples:

$$\hat{P}_E = \frac{1}{N} \sum_{i=1}^N I(x_i) \quad (3-64)$$

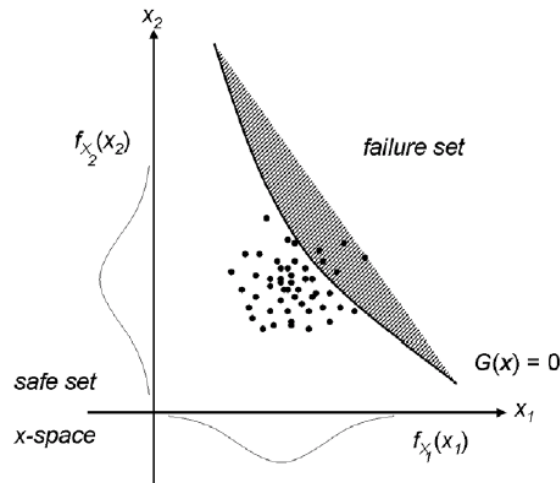


Figure 17: Monte Carlo Simulation Method

For cases with a large number of random variables or with a very low probability of failure, a large number of sampling sets is required, hence increasing highly the computational time and effort. For example, the probability of failure could be as small as 10^{-9} ; this implies that at least a billion simulation repetitions are required to predict this behaviour. Several techniques may be employed in order to avoid the inefficiency of direct MCS: importance sampling, subset simulation, line sampling, etc. Further, variance reduction techniques have been developed for a dual purpose: to reduce the computational cost and increase accuracy using the same number of runs [136].

The importance sampling method is a modification of Monte Carlo simulation in which the simulation is biased for greater efficiency; the sampling is done primarily in the tail of the distribution to ensure that sufficient simulation failures occur [137]. Starting from the basic definition of Monte Carlo Simulation for uncorrelated variables, the mathematical formulation of the method for the expected value of the probability of failure is described as [138]:

$$E(g(X)) = \sum_{x \in \mathcal{X}} g(x) f_X(x) \quad (3-65)$$

Where: $g(x)$ is the indicator function, and $f_X(x)$ the initial statistical distribution. The Importance Sampling introduces another distribution $p_X(x)$ called 'the sampling distribution' from which samples will be drawn instead of $f_X(x)$.

$$E(g(X)) = \sum_{x \in \mathcal{X}} g(x) f_X(x) = \sum_{x \in \mathcal{X}} g(x) \frac{f_X(x)}{p_X(x)} p_X(x) \quad (3-66)$$

Thus,

$$\tilde{E}(g(X)) = \frac{1}{n} \sum_{i=1}^n g(x_i) \frac{f_X(x_i)}{p_X(x_i)} = \frac{1}{n} \sum_{i=1}^n g(x_i) b(x_i) \quad (3-67)$$

Where:

$$b(x) = \frac{f_X(x)}{p_X(x)} \quad (3-68)$$

The basic idea of importance sampling is to draw from a similar distribution and then modify the result to correct the bias introduced by sampling the wrong distribution. For the normal distribution, using a density function with a higher standard deviation in Monte Carlo analysis leads in more samples being drawn from the extremes of the distribution [139].

This importance sampling density function satisfies the four following properties [137]:

- $p_X(x) > 0$ whenever $f_X(x) \neq 0$
- $p_X(x)$ should be close to being proportional to $|f_X(x)|$
- It should be easy to simulate values from $p_X(x)$
- It should be easy to compute the density $p_X(x)$ for any value x

Another variance reduction technique is that of the subset sampling. The main concept behind this is to express the failure event as a sequence of partial failure events (subsets) [140]:

$$F_1 \supset F_2 \supset \dots \supset F_m = F \quad (3-69)$$

Then:

$$\bigcap_{i=1}^k F_i = F_k \quad \forall k \leq m \quad (3-70)$$

Hence the probability of failure is a product of conditional probabilities:

$$\begin{aligned} P_f = P(F_m) &= P\left(\bigcap_{i=1}^m F_i\right) = P\left(F_m \mid \bigcap_{i=1}^{m-1} F_i\right) P\left(\bigcap_{i=1}^{m-1} F_i\right) \\ &= P(F_m | F_{m-1}) P\left(\bigcap_{i=1}^{m-1} F_i\right) \end{aligned} \quad (3-71)$$

And finally:

$$P_f = P(F_m) = P(F_1) \prod_{i=1}^{m-1} P(F_{i+1} | F_i) \quad (3-72)$$

The determination of a small probability of failure using Monte Carlo simulation requires high computational effort. The division into subsets allows transferring the simulation of rare events to a set of simulations of more frequent events where the probabilities of failure are easier to calculate in terms on computational effort. The probabilities $P(F_1)$ and $P(F_{i+1}|F_i)$ can be made sufficiently large so that their estimation can be performed efficiently by direct Monte Carlo Simulation [141].

3.2.2.2.2 Design Point Simulation

This method was introduced in [142] and it refers to application of MC sampling around the design point. After initial approximation of the MPP in the u -dimensional space, Monte-Carlo simulation is executed around this point instead of running simulations in the wider range of each distribution. As for the Monte Carlo Simulation, a weighted indicator function for each simulation is introduced in the sampled u -space point $u_i = d + v_i$ where d is the design point u^* or optionally a point shifted from the design point, and v_i the normal independent variables from which the Monte-Carlo simulation method samples from. The indicator function $I(u)$ for each simulation is:

$$I(\mathbf{u}) = \begin{cases} 1 & \text{if } g(\mathbf{u}) \leq 0 \\ 0 & \text{if } g(\mathbf{u}) > 0 \end{cases} \quad (3-73)$$

The probability of success of an event is then estimated as:

$$\hat{P}_E = \frac{1}{N} \sum_{i=1}^N I(u_i) \left(\prod_{j=1}^n \sigma_j \right) \frac{\exp(\sum_{j=1}^n u_{i,j}^2)}{\exp\left(-\sum_{j=1}^n \left(\frac{u_{i,j} - d_{i,j}}{\sigma_j}\right)^2\right)} \quad (3-74)$$

Where: d_i is the design point coordinate, and σ_i is the standard deviation of the sampling density. Back substituting $v = u - d$, the probability of success of an event is:

$$\hat{P}_E = \varphi(d) \frac{(2\pi)^{n/2}}{N} \sum_{i=1}^N I(u_i) \left(\prod_{j=1}^n \sigma_j \right) \exp\left(-d^T v_i - \sum_{j=1}^n v_{i,j}^2 \left(1 - \frac{1}{\sigma_j^2}\right)\right) \quad (3-75)$$

Considering standard deviation to be equal to 1 for standardized variables and d is the design point:

$$\hat{P}_E = \varphi(u^*) \frac{(2\pi)^{n/2}}{N} \sum_{i=1}^N I(u_i) \exp(-(u^*)^T v_i) \quad (3-76)$$

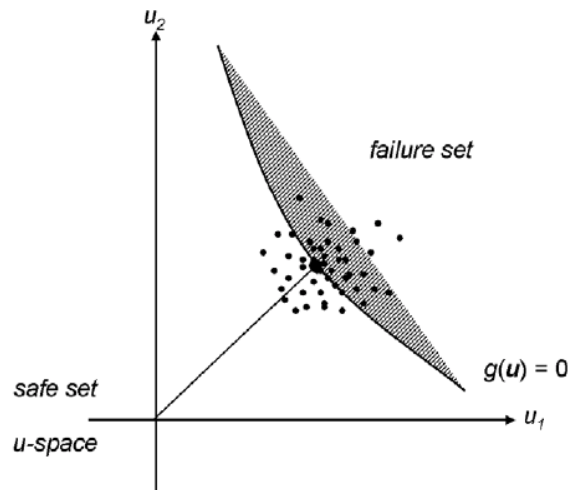


Figure 18: Design Point Simulation

3.2.2.2.3 Directional Simulation

The Directional Simulation method, introduced in [143], samples different directions, uniformly distributed on the n -dimensional surface at the origin of the u -space. Different variance reduction methods have been proposed in order to increase efficiency of the method. The method allows unbiased and efficient sampling of small probabilities, provided that the number of variables is not large. The probability of success of an event is expressed as:

$$P_E = \int_{g(\mathbf{u}\mathbf{a}) \leq 0} f_{x_n^2}(v) dv d\Omega \quad (3-77)$$

Where: v is a x_n^2 -distributed random variable, a is a unit vector and $d\Omega$ is the surface element of the n -dimensional unit sphere. Each unit direction a_i is sampled and the function x_n^2 conditioned on a is integrated. This is done by finding the upper bound $v_{u,i}$ and the lower bound $v_{l,i}$ of the intervals where $g(\mathbf{u}\mathbf{a}) \leq 0$ and by adding these contributions to the integral.

$$P(\mathbf{a}_i) = \sum_{i=1}^m (x_n^2(v_{u,i}) - x_n^2(v_{l,i})) \quad (3-78)$$

The estimated probability of occurrence of the event sampled in N total directions is:

$$\hat{P}_E = \frac{1}{N} \sum_{i=1}^N P(\mathbf{a}_i) \quad (3-79)$$

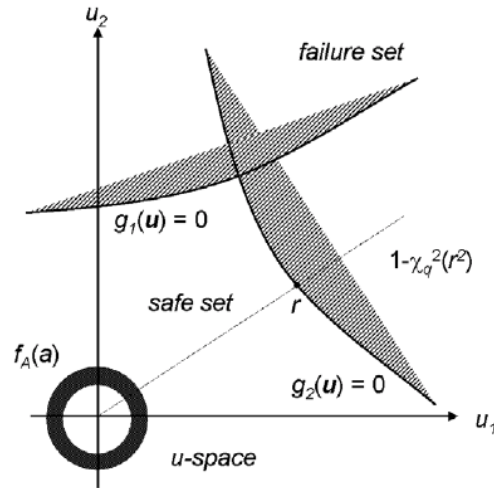


Figure 19: Directional Simulation

3.2.2.2.4 Axis-Orthogonal Simulation

The method, proposed in [144] and [145] defines an axis for a small intersection domain, and a sampling density in a plane orthogonal to this axis. The method approximates the boundaries of an event by a set of linear surfaces obtained by using the FORM linearization of small intersection domains. The probability of the linearized domain is obtained by methods available for the multi-normal distribution. The axis-orthogonal simulation method estimates an approximation of the true probability; the quality of this approximation follows that of the quality of the multi-normal integral. A method for correction of the approximate results is described in [146].

Considering: a_a , to be the averaged gradient of a set of normalized gradients a_i for the single events, pointing into the interior of at the design point as:

$$a_a = - \frac{\sum_{i=1}^n a_i}{|\sum_{i=1}^n a_i|} \quad (3-80)$$

A new axis is defined rotating the initial coordinates as:

$$a_u = \tilde{u}_0 + u_n e_n \quad (3-81)$$

Where: \tilde{u}_0 is the design point in the new coordinates and e_n is the unit vector in direction of u_n . The probability of the event E is calculated as follows:

$$P_E = P_L \int_{g(u) \leq 0} \frac{P_A(\tilde{u})}{\Phi(-u_n(\tilde{u}))} H_M(\tilde{u}) d\tilde{u} = P_L C \quad (3-82)$$

Where: P_L is the probability of the linearized domain, C is the multiplicative correction, $u_n(\tilde{u})$ is the intersection of the linearized domain and

$$I(u_n) = \tilde{u} + u_n e_n \quad (3-83)$$

$P_A(\tilde{u})$ is the true probability of the event conditioned on the line defined by $I(u_n)$.

The estimator for C is:

$$\hat{C} = \frac{1}{N} \sum_{i=1}^N \frac{P_A(\tilde{u}_i)}{\Phi(-u_n(\tilde{u}_i))} \quad (3-84)$$

The integral estimator is implemented:

$$P_A(\tilde{u}) = \int_{g(\tilde{u}, u_n) \leq 0} \Phi(u_n) du_n \quad (3-85)$$

The integral is evaluated through a search for the points $u_n(I_i)$ and $u_n(u_i)$ denoting the lower and upper bounds of the intervals where is less than zero, and then to sum up for m intervals as:

$$P_A(\tilde{u}) = \sum_{i=1}^m \left(\Phi(u_n(u_i)) - \Phi(u_n(l_i)) \right) \quad (3-86)$$

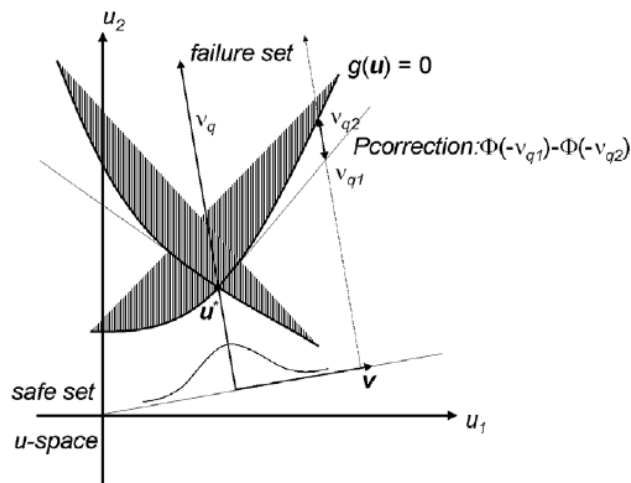


Figure 20: Axis-Orthogonal Simulation

3.3 Stochastic Response Surface Method

3.3.1 General Concept

In complex three-dimensional structures, such as a jacket structure, A mathematical relationship between the actual loading acting on the whole structure (eg. wave or wind loads) and the actions that each member is subjected to (eg. axial force and bending moments) is difficult to be explicitly expressed. For such cases of complicated failure processes, simulation techniques can deal with the complexity of the problem; however, they are often inefficient for the calculation of small values of probability of failure, since a great number of iterations is required until sufficient results are derived. In [147] an analytical procedure from Rubinstein is presented. Alternative procedures for the calculation of the optimum sampling number can also be found in [148], [149], but comprehensive presentation is beyond the scope of this Thesis.

For such cases, where simulation techniques are computationally intensive, the stochastic response surface method (SRFM) [150], [151], can provide an accurate estimation of structural reliability, regardless of the complexity of the system under consideration. The concept of this method is the approximation of the actual limit state function, which in some cases can be unknown, using

simple and explicit mathematical functions of the random (stochastic) variables affecting the response of the structural member or system. Those functions can be simple polynomials (eg. second or of higher order) with coefficients that can be calculated by fitting the response surface function to a number of sample points from calculation of the response of the member. In this explicit expression of the limit state function First and Second Order Reliability Methods can be applied for the estimation of the reliability index and therefore the probability of failure. Further, although the number of variables is the same in the response surface function and the initial limit state function, simulation techniques are more computationally efficient since this expression is less complicated than matrix manipulation.

Limitations of the Stochastic Response Surface Method arise in cases where the initial limit state includes non linearities or in cases where very low probabilities of failure should be accurately calculated. The above comments are highlighted in [152] and [153], and are caused due to the improper representation of the response surface based on arbitrary sample points that might be relatively far from the MPP. In order to overcome these restrictions, several methods have been proposed based on the adaptation of the response surface function to the location close to the design point, as this will be indicated by the FORM, are included in [154], [155], [156], [157], [158], and will be presented later in this chapter. In [159], the accuracy of a highly non-linear limit state depends on the initial selection of sampling points.

In most cases, the order of polynomials that is selected for the approximation of the response surface function is 2 (quadratic terms) since it demands few sample points - $(2n + 1)$ - for the approximation of the coefficients of the function. In [159], the use of higher order polynomials is investigated in depth. The disadvantage of this practice is that it needs more sampling points, requirement that is not always feasible, due to difficulty in the computational process and the fact that ill conditioned matrices are structured for the derivation of the coefficients of the polynomials through regression [160], [161]. The latter problem can be overcome through use of Chebyshev polynomials

and statistical analysis of the high-order response surface [160]. In Figure 21, a chart representing the regression coefficient based on the Least Square Method (LSM) and the R^2 criterion is presented for the estimation of the stress (v. Mises) response of a structural member under combined loading, modelled with three stochastic variables and using 25 sampling points from the original limit state function. The oscillation of the regression coefficient due to the quality of the regression design matrix can be observed.

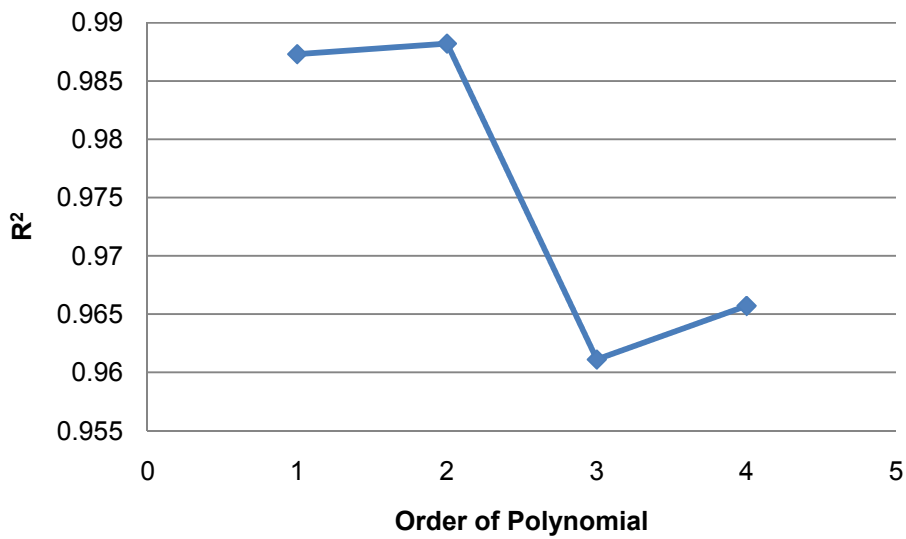


Figure 21: Regression vs. Order of Polynomial

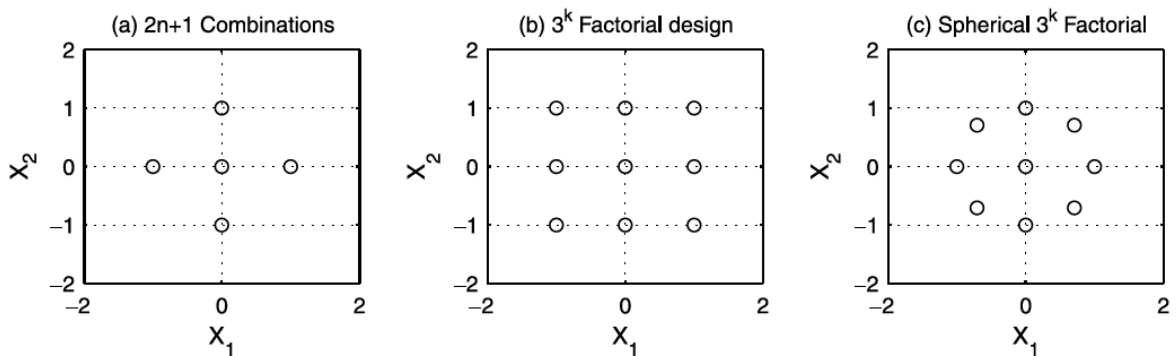


Figure 22: Different Sampling Approaches [160]

In [162], an algorithm is presented that uses quadratic response surface obtained from central composite designs (ARERSA - Adaptive Reliability Estimation Response Surface Algorithm). After a global search and once the

most likely failure point domain is identified, an updated response surface is fitted locally, in order to apply the reliability calculation routines. Complementary checks for valid solutions might be executed in order to ensure validity of the results. In [163], an algorithm is proposed (RSAED - Response Surface with Adaptive Experimental Design) which approximates the response surface in the standardized u -space. This algorithm uses previous results and calculations and reduced numerical procedures. In cases of highly non linear target limit state surfaces, the 'gradient projected technique' [164] would approximate the actual limit state surface with a linear one. Further to this work, a 'cumulative response surface method' has been proposed [165] according to which a design point is calculated based on FORM and an initial linear response surface. Second order terms are then employed to more accurately approximate the limit state function and SORM should be used to find the new design points. Further refinement of the response surface is done in the area around the current design point.

Most of the methods and algorithms that are available in literature, concentrate of the use of polynomials with quadratic terms due to the simplicity of the linear systems and the limited sample points required. In [166], a method is proposed that aims to reduce the number of samples based on statistical properties of polynomials to account for the dependence of the stochastic variables with the response of the system.

3.3.2 Review and Notation

Considering a vector $X = [x_1, x_2, \dots, x_n]$ to be the vector containing n stochastic variables of a system, and $g(x)$ to be the limit state function that represents the critical failure surface, the probability of failure of the system is described as $P_f = P[g(x) < 0]$. The approach of the response surface method, introduces a new polynomial function $\tilde{g}(x)$, of k -th order, that will use adequate sample points to determine the coefficients of the polynomial. The most common notation of the function, as it has been initially proposed [150] uses second order – quadratic – polynomials:

$$\tilde{g}(x) = a + \sum_{i=1}^n b_i X_i + \sum_{i=1}^n c_i X_i^2 \quad (3-87)$$

In order to calculate the $(2n+1)$, a , b_i and c_i coefficients, an equal or a greater number of sample points is required. Determination of sampling points can be done in a way that the measured response is mapped in a better way. According to different methods, the number of samples can be from $(2n+1)$ to 3^n , commonly combining μ_i and $\mu_i \pm f\sigma_i$ where μ_i and σ_i are the mean value and standard deviation of stochastic variable X_i , and f is a coefficient (typical value is 3). Figure 22, presents different patterns of samples combinations for a two variables problem [160].

In cases of linear limit states, selection of parameter f is less significant than for those with a non linear performance. In the later cases, selection of sampling points is significant for the approximation of the initial limit state functions. Another expression of the generic polynomial approximation of quadratic limit states is presented in [167], and includes mixed terms of the stochastic variables. Although this expression increases the complexity of the design matrix for the calculation of the polynomial coefficients, it may capture non-linearity of a limit state. The required number of sample points among the n -dimensional space is between $\left(\frac{n(n-1)}{2} + 2n + 1\right)$ and (3^k) , and the corresponding mathematical formulation:

$$\tilde{g}(x) = a + \sum_{i=1}^n b_i X_i + \sum_{i=1}^n c_i X_i^2 + \sum_{i=1}^{n-1} \sum_{j=i+1}^n d_{ij} X_i X_j \quad (3-88)$$

Table 5, presents an example of approximation of a quadratic limit state function of 3 stochastic variables, approached by $(2n+1)=7$ and $3^n=27$ neglecting mixed terms since, for the problem considered (response of a member), linear performance was expected. Reliability index was calculated with FORM and SORM Methods. From those results it can be observed that the smaller sample can approximate the limit state for reliability index calculation introducing an error in estimation.

N	β		Pf	
	FORM	SORM	FORM	SORM
3^n	4.6661	4.6488	1.54E-06	1.67E-06
$3n+1$	4.2853	4.2853	9.13E-06	9.13E-06

Table 5: Reliability Index and Probability of Failure vs. Sampling Number

3.3.3 Adaptive Response Surface Method

In [168], a procedure of weighted regression is been presented and in [169] examples are examined in order to illustrate the benefits of the method. An initial sample, as it was been described in Figure 22, ‘maps’ the whole range of each variable, and the sample points contribute equally in the formation of the design matrix for the calculation of the regression coefficients. Conventional formulation of the least square method, as it can be found in [170] or other regression analysis handbooks, denotes that for quadratic approximation and p sampling points, the design matrix M_u of the independent variables and the vector \bar{g} with values of the response (dependent variables) as:

$$M_u = \begin{bmatrix} 1 & u_{11} & \cdot & u_{n1} & u_{11}^2 & \cdot & u_{n1}^2 & u_{11} \cdot u_{j1} \\ \cdot & \cdot \\ 1 & u_{1p} & \cdot & u_{np} & u_{1p}^2 & \cdot & u_{np}^2 & u_{ip} \cdot u_{jp} \end{bmatrix} \quad (3-89)$$

$$\bar{g} = [g_1 \quad \cdot \quad g_p]^T$$

Calculation of coefficients vector \bar{a} , based on normal regression, is obtained by solving the following linear system:

$$\bar{a} = (M_U^T M_U)^{-1} M_U^T \bar{g} \quad (3-90)$$

The weighted regression introduces a diagonal weighted matrix W_G that gives greater weights in the points closer to the limit state function. Therefore, the equation in a matrix form, that includes the weighted regression would become:

$$\bar{a} = (M_U^T W_G M_U)^{-1} M_U^T W_G \bar{g} \quad (3-91)$$

According to [168], for the construction of W_G , after an initial set of simulations, a limit state function is obtained and the best design value \hat{y}_{best} (or g_{min}) is selected as the one that minimizes the initial response surface:

$$\hat{y}_{best} = \min |g'_x| \quad (3-92)$$

The w_i element in the diagonal weight matrix W , would be obtained as:

$$w_i = \exp\left(-\frac{g'(x)_i - \hat{y}_{best}}{\hat{y}_{best}}\right) \quad (3-93)$$

Based on this weight matrix, weighted regression formulas can be executed, correcting the initial approximation. This formulation of the weight coefficients has the drawback that if one of the sample points lies on or very close to the limit state function, $\hat{y}_{best} \approx 0$ and therefore the regression system becomes ill conditioned, providing inconsistent results. In order to overcome this problem, two different expressions for the weight coefficients are proposed in [169]. Initially, a different reference point is selected rather than \hat{y}_{best} . This is the value of the limit state function at the origin of the standardized space $g(u_0)$, which for commonly measured probabilities of failure is different than zero. Therefore:

$$w_{Gk} = \exp\left(-\frac{g'(x)_i - g(u_0)}{g(u_0)}\right) \quad (3-94)$$

Further optimization of the procedure, based on CQ2RS (Complete Quadratic Response Surface with Resampling) Method [171], imports an additional 'penalty factor'. For each iteration of the reliability calculation procedure, the relative distance D_k between the sampling points and the current design point P is used to form the weight factors as:

$$w_{Dk} = \exp\left(-\frac{D_k^2}{2}\right) \quad (3-95)$$

The resulting weight matrix for the linear regression system is:

$$W_G = w_{Gk} \cdot w_{Dk} \quad (3-96)$$

3.3.4 Algorithms of the Stochastic Response Surface Method

Based on the work that has been carried out so far, algorithms that combine FORM/SORM with linear and quadratic response surfaces approximation are developed. The normal Response Surface Method is initiated by formulation of combinations of different sets of variables, as presented in Figure 22. From the responses that are obtained, quadratic regression can be executed and the limit state surface can be formulated. This algorithm provides sufficient results for cases where the response of the system under investigation behaves linearly as a function of the basic stochastic variables. Especially for cases such as the complex jacket structure that will be investigated in the next chapters, where simulations are obtained by an external software package, this method provides efficient results both in accuracy and in computational effort considering that the number of simulations can be obtained by $(2n + 1)$ combinations Figure 22 (a).

In cases where the simulation procedure can be programmed to automatically execute new simulations, the adaptive Response Surface Method can be formed, which can perform better in cases of non-linear limit state functions and accurate calculation of small probabilities. The first step of application of the method suggests characterization of main variables as either favourable (resistance variable) or unfavourable (load variables). In order to achieve this, a reference value $g(\bar{X})$ should be obtained by calculating the value of the limit state function for the mean values of the stochastic variables \bar{X} . For each of the variables a value of $x_i = \bar{x}_i - f\sigma_i$ (value for f can be selected as 3 in order to represent a point at the tail of the distribution) is calculated, and the comparison $|g(X)| < |g(\bar{X})|$ will mark for the variable an indicator -1 else wise +1. The above procedure will provide $(n+1)$ points that will allow linear regression to be executed.

Having obtained an initial, linear response surface function based on samples that lie within the whole range of each variable, a first iteration of FORM will run, based on the mean values of the stochastic variables. An initial value for β and a new design point can then be obtained as:

$$\begin{aligned}
x_1 &= \bar{x}_i + \beta \sigma_{x_i} a_i \\
&= \bar{x}_i + \frac{g(U^*) - \sum_{i=1}^n \frac{\partial g(U^*)}{\partial x_i} \cdot \sigma_{x_i} \cdot u_i^*}{\sqrt{\sum_{i=1}^n \left(\frac{\partial g(U^*)}{\partial x_i} \cdot \sigma_{x_i} \right)^2}} \sigma_{x_i} \frac{\frac{\partial g(X^*)}{\partial x_i} \cdot \sigma_{x_i}}{\left[\sum_{i=1}^n \left(\frac{\partial g(X^*)}{\partial x_i} \cdot \sigma_{x_i} \right)^2 \right]^{1/2}} \quad (3-97)
\end{aligned}$$

Based on this new series of n points combined with the mean value point and including the previous $(n+1)$ points, quadratic regression can be executed. A weight matrix will account for the contribution of each of the sample points to the actual response surface giving a higher weight to the points closer to the design point.

$$w_{Gk} = \exp\left(-\frac{g'(x)_i - g(x_1)}{g(x_1)}\right) \quad (3-98)$$

Following this procedure of a dynamically constructed response surfaces and considering that linear limit state functions converge after only a few iterations, this procedure can provide adequate results in the calculation of FORM/SORM reliability index.

3.4 Regression methods

3.4.1 Linear Regression

In the problem where two (or more) variables are required to be expressed as a function, linear regression is the fundamental concept to follow. In an experimental procedure this can represent the problem of correlating measurements to properties. Linear regression refers to approaching the dependent variable as a linear function of some parameters (independent variables); otherwise regression should be characterized non-linear. Graphically, this approach assumes that the plotted sets of dependent and independent variables can be represented efficiently with one straight line. The earlier method proposed by Gauss and Legendere is referred to as the Least Squares Method (LSM), and provides a solution by minimizing the absolute

distance between the data provided and the potential function (residuals) to find the optimum fit. Following a mathematical notation it can be expressed as:

$$y(x) = a_0 + a_1 \cdot f_1(x) + a_2 \cdot f_2(x) + \dots + a_v \cdot f_v(x) + e \quad (3-99)$$

Where, a_i $i = 1, 2, \dots, v$ is the regression coefficient vector and e the error of the model equation. Forming the above equation in a matrix form:

$$Y = X \cdot a + e \quad (3-100)$$

Where,

$$Y = \begin{bmatrix} y_1 \\ y_2 \\ \vdots \\ y_n \end{bmatrix}, X = \begin{bmatrix} 1 & f_1(x_1) & f_2(x_1) & \dots & f_m(x_1) \\ 1 & f_1(x_2) & f_2(x_2) & \dots & f_m(x_2) \\ \vdots & \vdots & \vdots & \vdots & \vdots \\ 1 & f_1(x_n) & f_2(x_n) & \dots & f_m(x_n) \end{bmatrix}, a = \begin{bmatrix} a_1 \\ a_2 \\ \vdots \\ a_n \end{bmatrix}, e = \begin{bmatrix} e_1 \\ e_2 \\ \vdots \\ e_n \end{bmatrix}$$

The least squared method, expressed in a matrix form, is expressed as follows in order to derive the regression coefficients vector a :

$$a = (X^T \cdot X)^{-1} \cdot X^T \cdot Y \quad (3-101)$$

Having calculated the regression coefficients, the values of the dependent variables for the sampled dependent ones and the error for each of them is:

$$\bar{Y} = X \cdot a \text{ and } e = Y - \bar{Y} \quad (3-102)$$

The total sum of squares SST , regression sum of squares SSR and error sum of squares SSE are calculated as:

$$SST = Y^T \cdot Y$$

$$SSR = \bar{Y}^T \cdot \bar{Y} = a^T \cdot X^T \cdot Y \quad (3-103)$$

$$SSE = SST - SSR$$

In order to evaluate the level of accuracy of the modelled equation, a coefficient of determination (R^2) can be calculated as follows. The practical meaning of this equation, implies that when the regression sum of errors equals zero, and

therefore $R^2 = 1$ the modelled function satisfies all of the sets of (y, x_i) and therefore absolute regression has been achieved.

$$R^2 = 1 - \frac{SSE}{SST} \quad (3-104)$$

3.4.2 Multivariate Regression

For the case where more than one independent or dependent variables are present, the fundamental equation can be solved providing adequate sets of (y, x_i) . The general problem can be described as:

$$y(x) = \sum_i \mathbf{a}_i \cdot p_i(x_1, x_2, \dots, x_n) + e \quad (3-105)$$

Considering monomials, this can also be described as:

$$y(x) = \sum_i \mathbf{a}_i \cdot x_1^{\alpha_i} \cdot x_2^{\beta_i} \dots x_n^{\omega_i} + e \quad (3-106)$$

Where: \mathbf{a}_i are the regression coefficients and $\alpha_i, \beta_i, \dots, \omega_i$ are the power coefficients for the independent variables.

For a case where the maximum monomial degree is 2, with 2 independent variables, the expression can be rewritten as:

$$y(x) = a_0 + a_1 \cdot x_1 + a_2 \cdot x_2 + a_3 \cdot x_1^2 + a_4 \cdot x_2^2 + a_5 \cdot x_1 \cdot x_2 + e \quad (3-107)$$

Considering Y to be a $(n \times q)$ data matrix containing the dependent variables, X to be a $(n \times p)$ data matrix containing the independent variables, A a $(p \times q)$ data matrix with the regression coefficients and E is $(n \times q)$ matrix with the error terms. It forms the above equation in a matrix form:

$$Y = \tilde{X} \cdot A + E \quad (3-108)$$

Where \tilde{X} denotes a matrix formed from X , containing the different powered values of X .

The above dimensions of the participating matrices imply that in order for the system to have a solution, $(p \times q)$ sets of data should be available. An important observation that can ensure accuracy in the regression coefficients results is the level of how well conditioned the matrix $X^T \cdot X$ is.

3.4.3 Alternative Regression Methods

For a higher quality of response surface, schemes such as the central composite design method [172] might be employed allowing redundancy in some of the data sets. Drawback of this scheme is that it requires a large number of data ($N=2^n+2n+1$) in order to approach the exact limit state function with a quadratic equation by regression. Increase in the number of variables exponentially increases the required computational effort. A different approach, suitable for asymptotic behaviour of the structural behaviour is the selection of inverse polynomials as interpolating functions [173] providing good regression results but increasing the complexity of the problem.

A different method for regression analysis is 'kriging', which is a procedure for constructing a minimum error variance linear estimate at a location where the true value is unknown. Initially used for geological applications its use has been extended to a wide variety of different applications including aerodynamics, structures, and multi objective problems [174]. Extensive background theory of the method can be found in [175] and [176] while an initial application in the response surface method is presented in [177] for the solution of the problem of the reliability analysis of damaged steel structures using finite element analysis. Corresponding to the common regression expressions, the predicted results from the kriging model may be obtained from:

$$\hat{y} = \hat{\beta} + r^T(x)R^{-1}(y - f\hat{\beta}) \quad (3-109)$$

Where 'y' is predicted response value at x, 'x' are the sample points, 'β' is the constant underlying global portion of the kriging model, 'r' is the correlation vector of length n, 'R' is an $n \times n$ symmetric matrix with ones along the diagonal

and ' f ' is column vector of length n . The method can in general approach complicated surfaces with multiple variables.

3.5 Numerical model Developed

3.5.1 Description

The algorithm that has been implemented for the reliability calculation in the application sections of this Thesis is based on the methodology that has been presented in paragraph 3.3 and 3.4. MATLAB was selected as the proper programming language for this scope due to its simplicity and the wide range of tools that are available in order to simplify and optimize the programming procedure.

In the case when a methodology is proposed and a new code is conducted, verification is a very important step towards establishing its accuracy and efficiency. In the next sections, the algorithm that has been proposed using a normal and an adaptive response surface and FORM/SORM reliability methods, will be compared to results obtained by direct simulation for the problem of a simple 3-dimensional truss under stochastic loading. For this to be achieved an FEA code will be initially conducted and the corresponding sequence of steps will be followed. The Matlab FEA code has been verified for a deterministic case using the commercial software ABAQUS (and DNV SESAM Genie), while the reliability estimation routine has been verified according to DNV SESAM PROBAN software for different cases of estimation of the probability of failure within different range of values and using different numerical techniques. In all cases the algorithms and the codes have been found to provide adequately good results. Figure 23 to Figure 25 present in a block diagram form the reliability analysis procedure based on direct simulation as well as the normal and adaptive Response Surface Method.

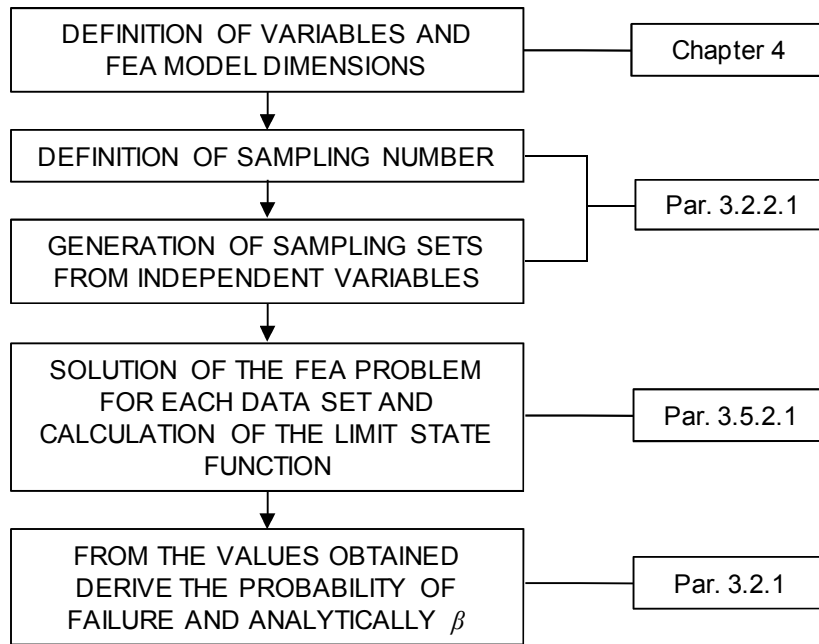


Figure 23: Calculation of reliability based on Direct Simulation

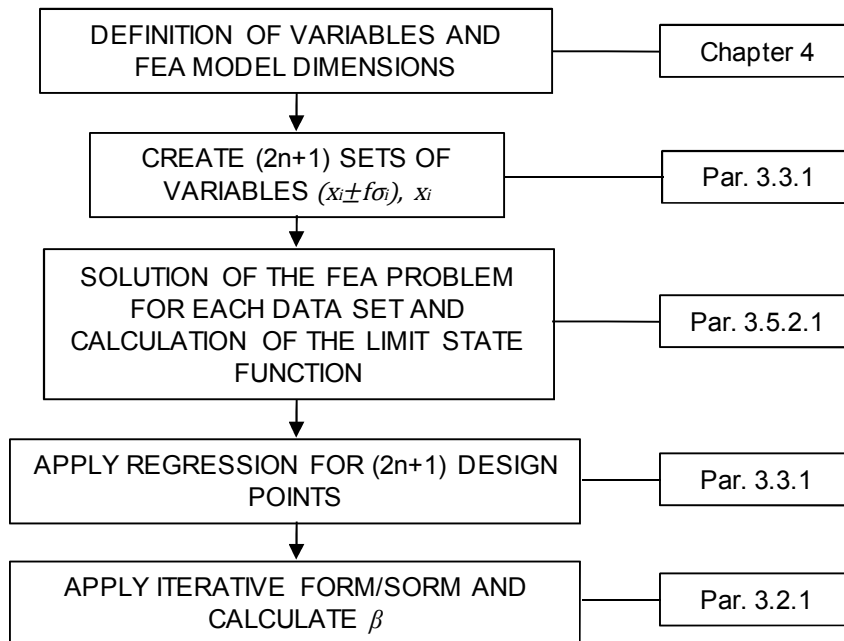


Figure 24: Calculation of reliability based on Normal Response Surface Method

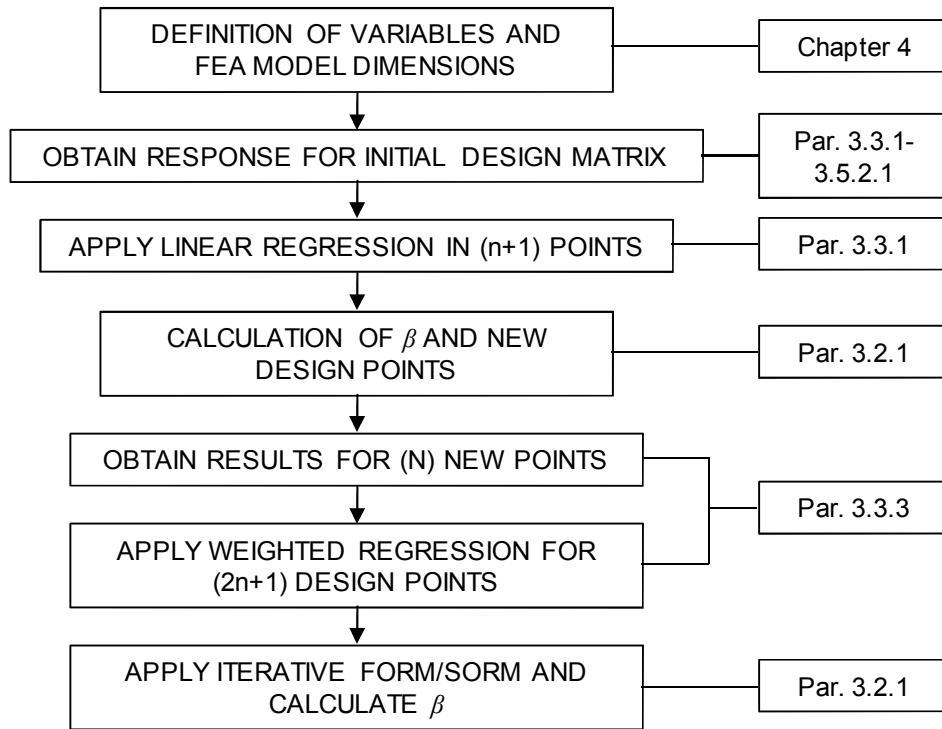


Figure 25: Calculation of reliability based on Adaptive Response Surface Method

3.5.2 Verification Process

3.5.2.1 FEA Code

3.5.2.1.1 Basic Theory of FEA

The FEA code that is conducted is based on the fundamental idea of the Finite Element Analysis method to numerically find approximate solutions of the partial differential equations (or integral equations) that model the system. Basic literature can be found in [178], [179] and [180]. Here the case of a 3 dimensional frame structure will be considered. Based on linear interpolation and matrix calculations, programming of this method is feasible and obtaining of a solution with a low computational cost. The most significant operation in computational effort is the derivation of the inverse of a square matrix. The background theory modelled is mainly based on [181].

For a 3D frame two-node element, each node has 6 global degrees of freedom: 3 in translation, 3 in rotation. A vector of displacements in the local coordinates system can be formulated as:

$$\mathbf{u}^T = [u_{ix} \quad u_{iy} \quad u_{iz} \quad \theta_{ix} \quad \theta_{iy} \quad \theta_{iz} \quad u_{jx} \quad u_{jy} \quad u_{jz} \quad \theta_{jx} \quad \theta_{jy} \quad \theta_{jz}] \quad (3-110)$$

Following an analytical method starting from single beams, moving to 2D frames and extending to 3D frames, the derived stiffness matrix is defined in local coordinates as:

$$\mathbf{K} = \begin{bmatrix} \frac{EA}{L} & 0 & 0 & 0 & 0 & 0 & -\frac{EA}{L} & 0 & 0 & 0 & 0 & 0 \\ 12\frac{EI_z}{L^3} & 0 & 0 & 0 & 6\frac{EI_z}{L^2} & 0 & -12\frac{EI_z}{L^3} & 0 & 0 & 0 & 6\frac{EI_z}{L^2} \\ 12\frac{EI_y}{L^3} & 0 & -6\frac{EI_y}{L^2} & 0 & 0 & 0 & -12\frac{EI_y}{L^3} & 0 & -6\frac{EI_y}{L^2} & 0 & 0 \\ \frac{GJ}{L} & 0 & 0 & 0 & 0 & 0 & 0 & -\frac{GJ}{L} & 0 & 0 & 0 \\ 4\frac{EI_y}{L} & 0 & 0 & 0 & 6\frac{EI_y}{L^2} & 0 & 0 & 0 & 2\frac{EI_y}{L} & 0 & 0 \\ 4\frac{EI_z}{L} & 0 & -6\frac{EI_z}{L^2} & 0 & 0 & 0 & 0 & 0 & 0 & 2\frac{EI_z}{L} & 0 \\ \frac{EA}{L} & 0 & 0 & 0 & 0 & 0 & \frac{EA}{L} & 0 & 0 & 0 & 0 \\ 12\frac{EI_z}{L^3} & 0 & 0 & 0 & -6\frac{EI_z}{L^2} & 0 & 12\frac{EI_z}{L^3} & 0 & 0 & 0 & -6\frac{EI_z}{L^2} \\ 12\frac{EI_y}{L^3} & 0 & 6\frac{EI_y}{L^2} & 0 & 0 & 0 & 12\frac{EI_y}{L^3} & 0 & 6\frac{EI_y}{L^2} & 0 & 0 \\ \frac{GJ}{L} & 0 & 0 & 0 & 0 & 0 & \frac{GJ}{L} & 0 & 0 & 0 & 0 \\ 4\frac{EI_y}{L} & 0 & 0 & 0 & 0 & 0 & 4\frac{EI_y}{L} & 0 & 0 & 0 & 0 \\ 4\frac{EI_z}{L} & 0 & 0 & 0 & 0 & 0 & 4\frac{EI_z}{L} & 0 & 0 & 0 & 0 \end{bmatrix} \quad (3-111)$$

symmetry

Where: G is the shear modulus and J the polar moment of inertia. Adapting the above to the global coordinates system, the following basis for transformation may be used:

$$\mathbf{u}_{local} = \mathbf{M} \mathbf{u}_{global} \quad (3-112)$$

$$\mathbf{M} = \begin{bmatrix} m & 0 & 0 & 0 \\ 0 & m & 0 & 0 \\ 0 & 0 & m & 0 \\ 0 & 0 & 0 & m \end{bmatrix} \quad (3-113)$$

$$m = \begin{bmatrix} C_{Xx} & C_{Yx} & C_{Zx} \\ C_{Xy} & C_{Yy} & C_{Zy} \\ C_{Xz} & C_{Yz} & C_{Zz} \end{bmatrix} \quad (3-114)$$

$$C_{Xx} = \cos(\theta_{Xx})$$

Where: angles θ_{Xx} , θ_{Yx} and θ_{Zx} are measured from global axis X , Y and Z with respect to the local axis x , respectively. Hence the stiffness matrix in global coordinates system is defined by:

$$\mathbf{K}_{global} = \mathbf{M}^T \mathbf{K}_{local} \mathbf{M} \quad (3-115)$$

For a system composed of bars and beams, once the stiffness matrix K is derived, the vector of nodal forces f to statically represent the system is:

$$K \mathbf{u} = \mathbf{f} \quad (3-116)$$

where \mathbf{u} is the displacement vector.

This system can be solved to obtain the displacement vector \mathbf{u} :

$$\mathbf{u} = K^{-1}\mathbf{f} \quad (3-117)$$

Many processes can be used to solve easily and quickly this system: Cholesky resolution, QR or LU decomposition.

Further post processing can transform displacements and rotations to axial forces and bending moments, following a procedure that can be widely found in literature.

3.5.2.1.2 Verification Results

Figure 26 presents the hypothetical truss structure that has been considered for the verification process. This is a 3D structure, fixed at the bottom, with lateral (e.g. wind forces) and vertical forces (e.g. weight loads). Here the structure is considered only in tension-compression. Table 6, presents the four stochastic variables, normally distributed, considered in this application; $\mathcal{N}(\mu, \sigma)$ represents a normal distribution of mean μ and standard deviation σ .

The first step is to verify the 'core' of the whole procedure: the Finite Element Analysis. The code has been verified using the software ABAQUS on this simplified structure. The purpose was to compare the axial stresses obtained with both methods for the mean (deterministic) values of the stochastic variables. The stresses are listed in Table 7 to compare the results between ABAQUS and the MATLAB code, while Figure 27 illustrates the relative deformations of the two cases.

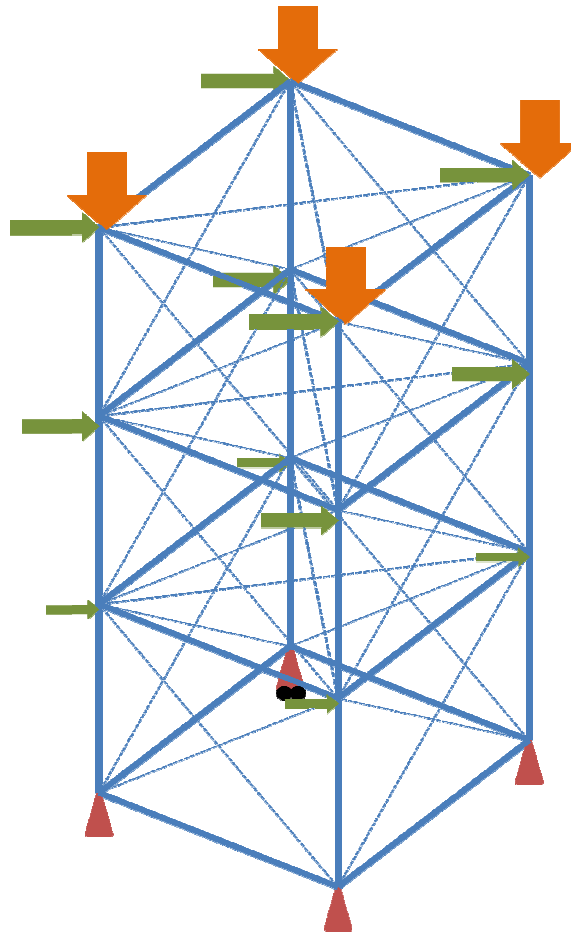


Figure 26: Reference structure

<i>Parameters</i>	<i>Probability's law</i>
Loads	$F \times N(1, 0.2)$
Elasticity	$N(21 \times 10^{10}, 1 \times 10^{10})$
Area	$A \times N(1, 0.01)$
Allowable stresses	$N(100000, 10000)$

Table 6: Stochastic Loads Consideration

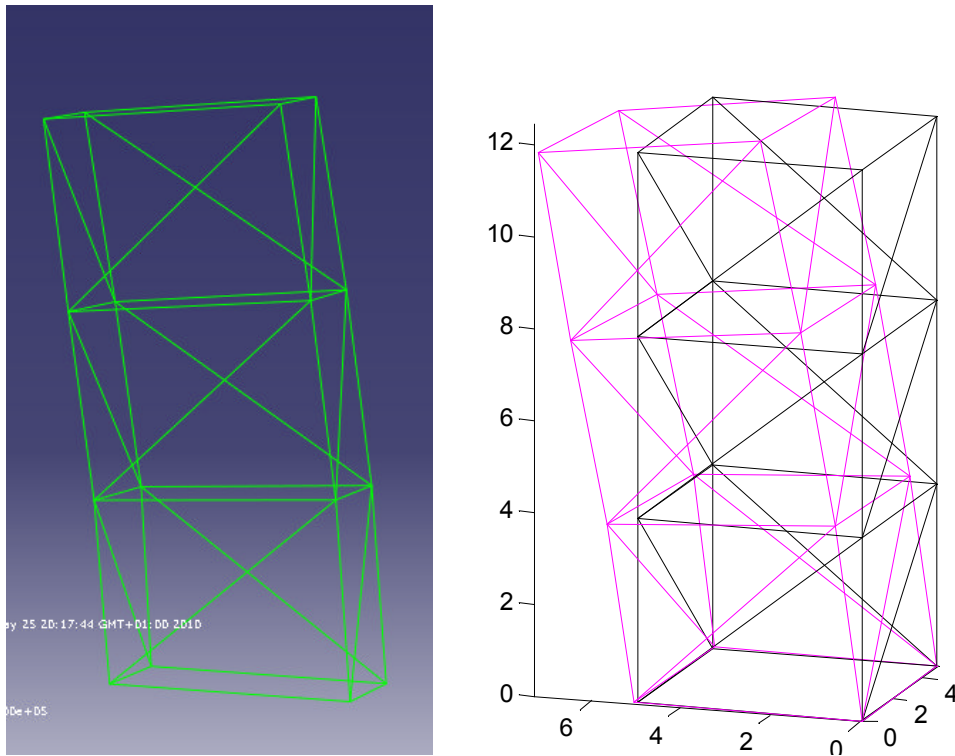


Figure 27: ABAQUS and Matlab code deformed model

<i>Element</i>	<i>Matlab</i>	<i>Abaqus</i>	<i>Element</i>	<i>Matlab</i>	<i>Abaqus</i>
1	0	-1.6676E-11	21	0	1.1117E-11
2	0	2.2235E-11	22	64031.2	64031.2
3	40000	40000	23	1E-10	-2.7793E-11
4	40000	40000	24	64031.2	64031.2
5	0	4.4469E-12	25	0	1.6676E-11
6	-64031.2	-64031.2	26	-50000	-50000
7	-64031.2	-64031.2	27	-40000	-40000
8	80000	80000	28	-64031.2	-64031.2
9	0	2.2235E-11	29	-120000	-120000
10	-50000	-50000	30	0	0
11	-3E-10	0	31	50000	50000
12	50000	50000	32	-80000	-80000
13	-80000	-80000	33	0	2.2235E-11
14	0	1.4369E-37	34	0	1.6676E-11
15	-50000	-50000	35	-40000	-40000
16	64031.2	64031.2	36	0	-4.4469E-11
17	0	-2.2235E-11	37	0	-2.2235E-11
18	80000	80000	38	0	0
19	0	2.7793E-11	39	120000	120000
20	0	-5.5587E-12	40	50000	50000

Table 7: Verification of FEA code: results (kPa)

From the above data, the coincidence obtained for the results of the two different methods provide adequate verification of the code.

3.5.2.2 Reliability calculation codes

After execution of Direct Simulation as well as the normal and the Adaptive FORM/SORM procedure, focus is been concentrated on the members of the reference structure that have a probability of failure different from 0 in every procedure. This is due to the fact that, as it has been described so far, Direct Simulations cannot describe low probabilities of failure, while FORM/SORM methods do. Table 8, presents a sensitivity analysis of Direct Simulations with different sampling numbers.

<i>(sample size)</i>	10000		100000		10000000	
<i>Elapsed time</i>	20s		4min		4h	
ELEMENT	PF	Beta	PF	Beta	PF	Beta
18	0,001500	2.97	0,001720	2.93	0,001790	2.91
21	0.00E+00	Inf	0	Inf	5.70E-03	4.39
22	0,021900	2.02	0,020580	2.04	0,020568	2.04
23	0.00E+00	Inf	0	Inf	5.70E-03	4.39
25	0,003700	2.68	0,004480	2.61	0,004489	2.61
26	0,025400	1.95	0,023980	1.98	0,024213	1.97
27	0,003700	2.68	0,004480	2.61	0,004489	2.61
28	0,000300	3.43	0,000270	3.46	0,000351	3.39

Table 8: Sensitivity Analysis of MCS Probability of failure results

<i>(sample size)</i>	DS (10000000)		Normal-RSM		ARSM	
<i>Elapsed time</i>	4h		18s		12m	
ELEMENT	PF	Beta	PF	Beta	PF	Beta
18	0.001790	2.91	0.000860	3.13	0.000692	3.19
21	5.70E-03	4.39	8.03E-08	5.24	3.850E-08	5.37
22	0.020568	2.04	0.018430	2.09	0.016752	2.12
23	5.70E-03	4.39	8.03E-08	5.24	3.850E-08	5.37
25	0.004489	2.61	0.002897	2.76	0.002454	2.81
26	0.024213	1.97	0.022259	2.01	0.020378	2.04
27	0.004489	2.61	0.002897	2.76	0.002454	2.81
28	0.000351	3.39	0.000084	3.76	0.000060	3.84

Table 9: MCS vs ARSM Probability of failure results

In Table 9, comparative results between the direct Simulation and the application of the normal and the adaptive Response Surface Method (ARSM) are presented for the meaningful members as before. It can be concluded that the difference between the deterministic and the simulation methods are acceptable for the validation of the method selected for the numerical application of this Thesis. Especially for the members with greater probability of failure (lower reliability index), such as members 22 and 26, the results appear to coincide significantly. Among the normal and the adaptive Response Surface Methods, the latter seems to provide a correction to the results; however due to the fact that the normal method is more conservative and the small difference in the results is small in the expense of computational cost, the normal SRSM seems to perform adequately and can be applied in the application section. However, in different cases with non-linear performance, the adaptive Stochastic Response Surface Method is expected to produce significantly more accurate results than the normal Response Surface Method.

3.5.3 Validation of the FORM/SORM code

For a typical jacket structure, where multiple members exist and their reliability should be assessed initially in a local level, a MATLAB code was conducted based on the theory that has been developed earlier in this Chapter. MATLAB has been selected as the most appropriate programming language due to the convenience in handling partial derivatives, a fact that minimizes the required computational time. This code, that was conducted and has been verified using the PROBAN commercial software provided by DNV, will allow combination with FEA codes and facilitate the procedure of multiple iterations required due to the large number of element comprising the structure. A simple case of a complex structure has been considered with four variables stochastically modelled. Figure 28, illustrates the FEA model created in DNV SESAM Genie software from which corresponding von Mises stresses were exported in order to formulate the limit state function that was later solved with both the MATLAB code and the commercial software. Table 10, presents the stochastic loads considered.

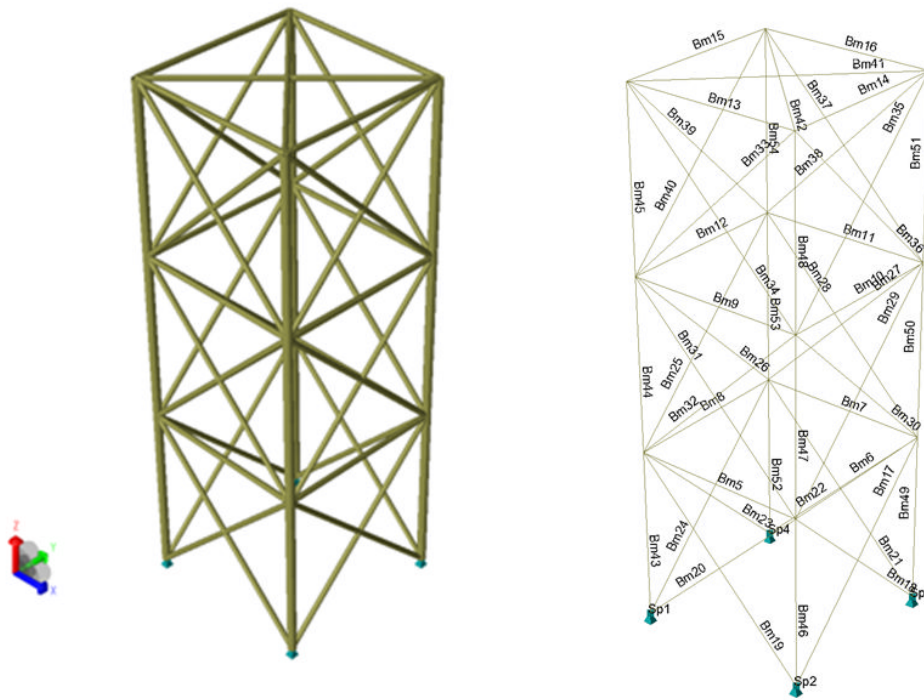


Figure 28: FEA model in DNV Genie software

Load	Description	Distribution	Characteristics	Unit
1	Force on top of the structure acting on x direction	Weibull	$a = 2129, b = 7.1867$	(kN)
2	Force on top of the structure acting on y direction	Normal	$\mu = 2200, \sigma = 200$	(kN)
3	Modulus of Elasticity	Normal	$\mu = 210, \sigma = 10$	(GPa)
4	Material Yield	Log-Normal	$\mu = 275, \sigma = 25$	(MPa)

Table 10: Stochastic loads on verification model

The MATLAB code that was conducted, applies the First and Second Order Reliability Methods (FORM/SORM), with the ability to handle different types of limit state functions (with some small alterations). Input to the code is a set of stresses obtained from a series of simulations in the DNV Genie FEA software

that are automatically converted in utilization ratios that will be used to derive the limit state functions, and a matrix of basic variables corresponding to the variable combinations of the cases that were executed. A separate function for multivariate data regression will return the regression coefficients for the quadratic variables of the linearized limit state function. This function has been verified with corresponding functions included in Microsoft Excel and was found to provide sufficient results. The scaling that is included in the code, prevents from ill conditioned results in cases where data with significant difference in order of magnitude exists. Those intermediate results from the code will be used both in the MATLAB reliability estimation routine and in the DNV PROBAN software. DNV PROBAN software can solve limit state integrals using both deterministic and probabilistic methods. From the later, the Axis Orthogonal simulation, the Directional simulation and the Design Point simulation will be applied in conjunction to FORM and SORM results and will be compared to the results obtained from the MATLAB code. Comparison of the results obtained is listed in Table 11. The test structure has been designed in a way that a wide range of reliability indices can be obtained, in order to better verify the validity of the comparison results.

From the results that have been obtained, it can be observed that for almost all cases, the results of the two methods used coincide with excellent accuracy. Therefore the Matlab code that is derived can be used with confidence for the analytical part of this Thesis. Among First and Second order deterministic methods, the results coincide significantly, which should be expected due to the high linearity of the limit state function. Between the three simulation techniques, the Axis Orthogonal simulation was found to be the most accurate one for the input parameters examined (50 simulations, standard normal density). Sufficient results, were also provided by the other two methods, with the Design Point simulation (1000 simulations) providing better results than the Directional simulation (100 simulations, 0.5 step, probability limit: $1.0e-080$) which presents some small variation for the cases of large values of beta.

		MATLAB		PROBAN				
		FROM	SORM	FROM	SORM	AXIS ORT.	DIRECT	DES.P.
1	Bm46	13.18	13.15	13.17	13.13	13.13	13.12	13.15
2	Bm49	N/A	N/A	N/A	N/A	N/A	N/A	N/A
3	Bm50	0.40	0.40	0.39	0.39	0.39	0.38	0.42
4	Bm51	9.22	9.22	9.24	9.24	9.24	9.26	9.25
5	Bm53	22.24	22.21	22.22	22.19	22.19	N/A	22.20
6	Bm54	26.75	26.83	26.72	26.81	26.72	N/A	26.71
7	Bm5	9.33	9.33	9.36	9.36	9.36	9.43	9.36
8	Bm6	8.22	8.22	8.17	8.17	8.17	8.15	8.18
9	Bm7	8.06	8.06	8.09	8.09	8.09	8.09	8.10
10	Bm8	9.51	9.51	9.46	9.46	9.46	9.45	9.44
11	Bm9	14.32	14.32	14.32	14.32	14.32	14.89	14.36
12	Bm10	13.62	13.55	13.63	13.56	13.63	13.93	13.65
13	Bm11	13.56	13.56	13.56	13.56	13.56	13.56	13.56
14	Bm12	14.41	14.41	14.40	14.40	14.40	14.67	14.40
15	Bm16	5.48	5.48	5.49	5.49	5.49	5.44	5.47
16	Bm13	6.30	6.30	6.32	6.32	6.33	6.31	6.31
17	Bm48	25.24	25.22	25.24	25.21	25.21	N/A	25.16
18	Bm14	5.58	5.58	5.55	5.55	5.55	5.55	5.55
19	Bm15	6.39	6.39	6.40	6.40	6.40	6.49	6.43
20	Bm17	13.41	13.41	13.41	13.41	13.41	13.45	13.40
21	Bm18	1.80	1.80	1.76	1.76	1.75	1.76	1.76
22	Bm19	16.77	16.77	16.76	16.76	16.76	16.75	16.78
23	Bm20	2.55	2.55	2.52	2.52	2.52	2.50	2.49
24	Bm21	1.84	1.84	1.81	1.81	1.81	1.83	1.78
25	Bm22	14.32	14.32	14.32	14.32	14.32	14.33	14.34
26	Bm23	15.66	15.66	15.65	15.65	15.65	15.67	15.68
27	Bm27	10.44	10.44	10.44	10.44	10.44	10.43	10.46
28	Bm24	2.50	2.50	2.46	2.46	2.46	2.47	2.46
29	Bm25	4.72	4.72	4.68	4.67	4.67	4.70	4.66
30	Bm26	11.08	11.08	11.08	11.08	11.08	11.18	11.08
31	Bm29	9.99	9.99	9.99	9.99	9.99	10.28	10.00
32	Bm28	4.57	4.57	4.53	4.53	4.53	4.62	4.54
33	Bm30	4.47	4.47	4.51	4.51	4.51	4.48	4.48
34	Bm31	11.51	11.51	11.51	11.51	11.51	11.44	11.51
35	Bm32	4.82	4.82	4.80	4.80	4.80	4.74	4.79
36	Bm33	6.86	6.86	6.88	6.88	6.88	6.89	6.89
37	Bm34	8.92	8.92	8.91	8.91	8.91	8.89	8.91
38	Bm35	8.95	8.95	8.90	8.90	8.90	9.00	8.90
39	Bm36	6.45	6.45	6.42	6.42	6.42	6.48	6.41
40	Bm37	6.65	6.65	6.65	6.65	6.65	6.70	6.66
41	Bm38	9.29	9.29	9.33	9.33	9.32	9.42	9.32
42	Bm39	8.60	8.60	8.61	8.61	8.61	8.58	8.60
43	Bm40	6.67	6.67	6.63	6.63	6.63	6.73	6.62
44	Bm41	N/A	N/A	N/A	N/A	N/A	N/A	N/A
45	Bm42	12.63	12.61	12.58	12.51	12.49	12.58	12.51
46	Bm43	N/A	N/A	N/A	N/A	N/A	N/A	N/A
47	Bm44	1.24	1.24	1.28	1.28	1.28	1.28	1.29
48	Bm45	10.57	10.57	10.57	10.57	10.57	10.56	10.60
49	Bm47	16.12	16.11	16.12	16.10	16.10	16.16	16.13
50	Bm52	15.88	15.87	15.88	15.87	15.87	15.91	15.87

Table 11: Results of comparative analysis of test case structure

The conclusions of this verification analysis is that for this type of linear limit state function derived by linear elastic analysis, deterministic methods provide sufficient results compared to the more complicated simulation methods. This can reduce required computational effort significantly allowing more simulations to be executed and more parameters to be examined. Between the MATLAB code and the DNV PROBAN code, both provide results that coincide, allowing the first to be used in the analysis that will be presented later in this Thesis. For the simple test case, the computational time required for the regression analysis and the computational of the reliability index with the FORM and SORM is less than 30 sec, while the manual input of coefficients in the less user friendly commercial software required more than 15 minutes; considering that this is a reduced time that has been achieved through an intermediate code conducted in Visual Basic.

3.5.4 Codes Included

In Appendix D of this Thesis the following codes are included:

- Response Surface Method code for FEA
- Adaptive Response Surface Method code for FEA
- Standalone code for FORM/SORM (limited to 4 variables)
- Multivariate Regression Analysis code with scaling

All the above codes have been modelled in MATLAB 2010a version, and use the MATLAB Statistics and Symbolic Math Toolboxes.

3.6 Summary

In this Chapter, the numerical methods for structural reliability assessment have been discussed. Deterministic Methods, including First and Second order reliability methods have been presented according to the procedure that has

been followed for the formulation of codes that have been developed. Simulation methods were also briefly discussed. The Stochastic Response Surface Method (SRSM) has been extensively presented, and the procedures for the normal and the adaptive SRSM were derived. Polynomial Regression analysis was also included as it is required for the transformation of the simulation output to a multivariate quadratic limit state surface. The Chapter closes with an extensive verification of the MATLAB codes that were derived, based on established tools/techniques, in order to obtain confidence for their application in the later chapters.

4 STOCHASTIC MODELING OF ENVIRONMENTAL LOADING AND LOAD CAPACITY OF OFFSHORE STRUCTURES

4.1 Introduction

In this Chapter, the issue of appropriate stochastic modelling of environmental loads as well as the load bearing capacity variables will be discussed. Treatment of variables is a very important decision that should be based on well informed data and experienced engineering judgement, as it should account for the extreme conditions the structure may suffer from throughout its service life.

As far as the environmental loads are concerned wave is the most important due to its volatile magnitude. Complementary to this, current wind and operational loads form a combination of loads that should be considered for the design of offshore structures. On the other hand, the load capacity of the structure should consider variables such as the material properties of members (yield strength, Young's Modulus and Poisson's Ratio, etc), geometrical properties and geotechnical conditions. Deterioration of capacity is also a significant issue to be considered due to its increasing effect throughout the service life of the structure. Incorporation of the above in the design will be discussed in the next sections.

4.2 Classification of Loads

In reliability analysis, appropriate consideration of loading is one of the most critical issues. During its operation, an offshore structure is subjected to several different types of loading depending on its service and the environmental conditions in the location of deployment. Those loads may be categorized as: dead loads, live loads, environmental loads, construction loads, removal and reinstallation loads, and dynamic loads [2].

Dead loads are the weight of the entire structure and any permanent equipment mounted on the platform which does not change with the mode of operation. Dead loads should include the hydrostatic forces acting on the structure below the waterline, including external pressure and buoyancy.

Live loads are the loads imposed on the structure during its operation. They include the weight of any drilling and production equipment, the weight of living quarters, heliport and other life support equipment, life saving equipment, diving equipment and utilities equipment, the weight of consumable supplies and liquids in storage tanks, the forces exerted on the structure from operations and the forces exerted on the structure from deck crane usage. Live loads are usually idealized as uniform distributed loads [182].

Environmental loads are loads imposed on the platform by the natural phenomena including wind, current, wave, earthquake, snow, ice and earth movement. Environmental loads also include the variation in hydrostatic pressure and buoyancy on members caused by changes in the water level due to waves and tides. Those loads are random in nature and can be accurately quantified combining sufficient meteocean data with probabilistic properties.

Construction loads are loads resulting from fabrication, load out, transportation and installation. Removal and reinstallation loads are those arising from removal, on loading, transportation, upgrading and reinstallation particularly for platforms which are to be relocated to new sites.

Dynamic loads are the loads imposed on the platform due to response to any excitation of cyclic nature caused by waves, wind, earthquake or machinery; or due to reaction to impact. Impact may be caused by a barge or boat approaching the platform or by drilling operations.

From the above loads, the environmental loads are the most important in the design of offshore structures due to their high level of randomness; therefore in this chapter they will be presented analytically. Especially for offshore

structures, wave is found to dominate the total loading of the structure [183], therefore different methods for wave modelling will be presented extensively.

4.3 Environmental Loading

Hydrodynamic forces play the most significant role in the design of offshore structures that are subjected to both steady and time dependent forces due to the action of winds, currents and waves. Parts of the structure that exceed the sea water level suffer from both steady wind forces but also from significant gusts which induce high unsteady local forces on structural components. In the part of the structure that stands below the sea surface, steady forces in conjunction with localized forces of vortex shedding induce substantial unsteady forces on structural members. For both wind and current loads a steady or unsteady flow will exert a correspondingly steady or unsteady (line) force parallel to the incident flow direction; however, the localized interaction between flows corresponding to a structural member will also cause flow irregularities and will induce unsteady transverse forces perpendicular to the incident flow direction.

Although several models are proposed for the modelling of wind and current loads, waves are found to induce the largest force on most offshore structures. For efficient structural design, it is essential to establish and appropriately select methods for the transformation of environmental loads into the resultant steady and time dependent forces acting on the structure. In this chapter the most important of those methods will be presented. This procedure of moving from a global level-environment to a structural level could categorize the following three steps [184]:

- Definition of design environmental conditions, i.e. design parameters to define waves, currents and winds

- Evaluation of water particle motions (kinematics) resulting from the waves and currents, assuming that the structure does not affect the gross kinematics
- Derivation of external forces on the individual members of the structure resulting from the water particle motions and wind velocity

4.3.1 Design Environmental Conditions

As discussed earlier in the definition of the parameters that should be considered in a reliability assessment, the reference return period should be set in order to relate the environmental conditions which are exceeded on average of N years. For offshore structures, a reference return period of 100-years is proposed by API in [2]. Different organizations, such as the UK Department of Energy, propose a different reference return period of 50-years. Use of widely applied statistical techniques can expand observations of a limited time period, 1-5 year time scale, to project the probability of failure of the 50 or 100 years that should be considered by standards.

Since the contribution of different environmental loads to the response of the structure cannot be defined, each of those loads is supposed to act at the same time and towards the same direction to account for the worst case scenario. Although this assumption is conservative, it can provide realistic results for the design against structural failure; however it cannot consider fatigue damage on the design. While in the North Sea sites, design values for the reference period of 100-years are assumed to act simultaneously on the structure, for the sites of the Gulf of Mexico, current is neglected completely or accounted in a smaller scale.

The most important load parameters for the evaluation of the extreme environmental loading are: significant wave height, mean zero-crossing period, wind speed averaged over a suitable time interval, and current speed and profile. Those parameters will be presented extensively in the following sections.

4.3.2 Environmental Loads

4.3.2.1 Sea State Condition

The sea state conditions for a selected site can be effectively described by the wave and current parameters. As it has already been mentioned, the design wave is the most important element in the determination of the forces acting on the structure. Design wave heights are expressed in terms of wave heights that have a low probability of occurrence within the prescribed reference design period (50 or 100 years) and achieve adequate safety considering the shorter life period of offshore structures (usually 20 years).

4.3.2.1.1 Wave Load

Prediction of wave conditions is based on collections of observed data and interpolation to the reference (return) period of investigation. Correlation between significant wave height and wave period should be based on joint probability distribution models, as it will be later described in greater detail. Different directions of wave loads should be considered for the offshore structure since in several cases different directions yield for different load distributions on the structure; therefore the dominant direction should be identified. In some cases, different combination of wave heights and corresponding periods should be also investigated, in order to determine the critical wave loading on a structure.

4.3.2.1.2 Current Load

Current refers to the motion of water due to reasons different than surface waves. Depending on the deployment sites, this load can contribute significantly to the total force applied in the submerged part of the structure. Common categories of currents are: tidal currents, circulation currents and storm-generated currents. The vector sum of these three currents is the total current, and the speed and direction specified elevations constitute the current profile. Appropriate consideration of the current properties is an important aspect in the design of the structure as it might affect the location and orientation of

deployment as well as that of boats approaching the structure. Forces due to currents are added in those due to the wave, therefore magnitude and relative direction of the two should be specified in a way that realistically represents the current's profile from sea water level to seabed.

Determination of the force induced by current is based on the maximum design velocity. Selection of this value should be based on actual measurements and/or suitable data tables. For cases of shallow waters, where not sufficient data are available, the vertical distribution of current velocity can be described as [185]:

$$U_{TZ} = U_{TS} \left(\frac{z}{d} \right)^{\frac{1}{7}} \quad (4-1)$$

Where: U_{TS} is the speed of current in the sea water surface, z is the distance above the seabed and d is the total water depth.

For the case of deep waters that in general correspond to more slender structures, wave and current interaction should be taken into account. In such cases the drag loading is proportional to the square of the wave and current velocity, therefore the response of the structure will be significantly affected by any change in the current velocity. The simplest model for the consideration of this interaction is the superposition of current and wave velocity. In [186], three methods to account for the combination of wave and current are described:

- Current profile stretching to the instantaneous surface
- Mass continuity with profile stretching
- Cut off in through, uniform current addition in crest

The above methods are pictorially illustrated in Figure 29. Reviewing the above methods, the first one seems the most appropriate since it represents the convection of water particles in a wave considering its horizontal velocity with an added component to account for the presence of the current [187].

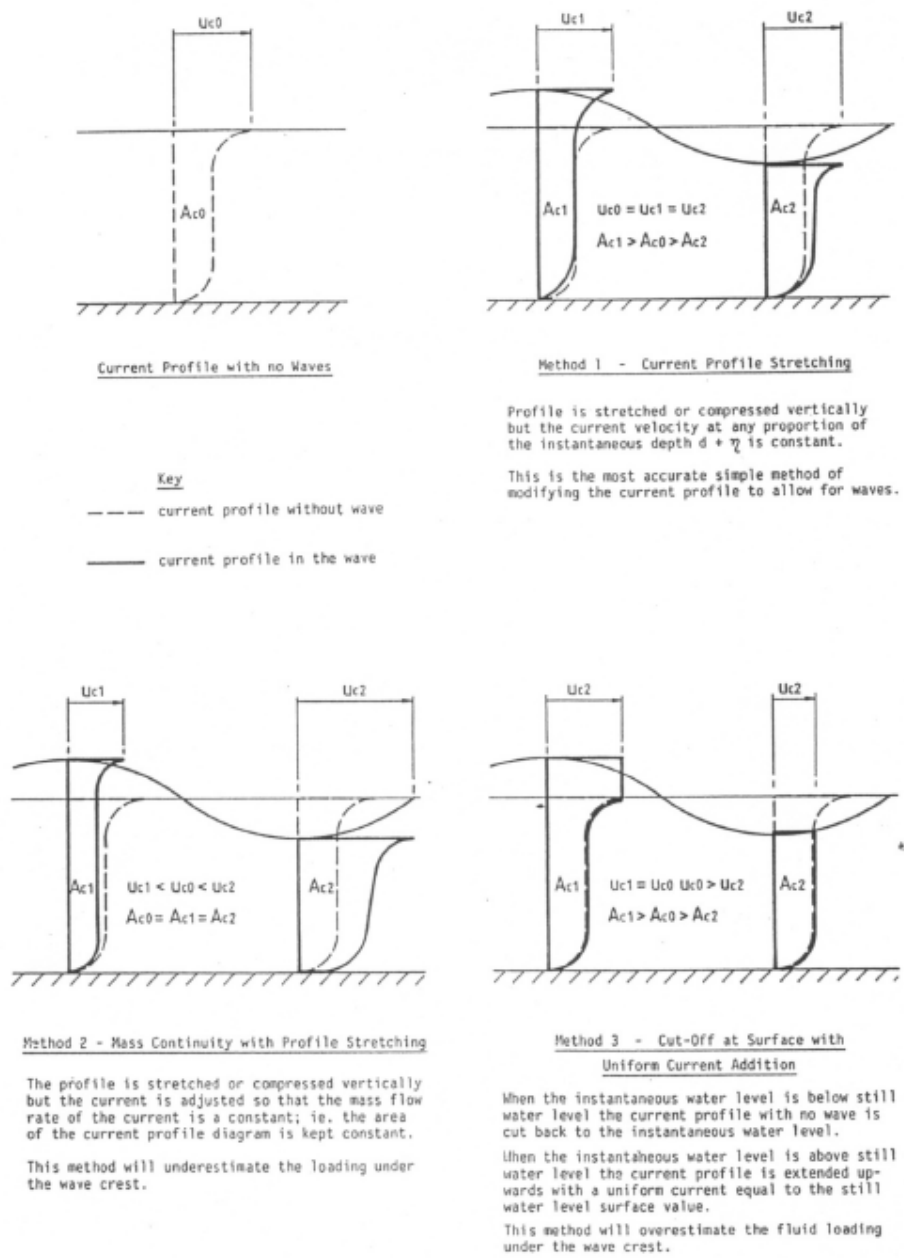


Figure 29: Methods for combining current and wave [186]

In cases where the wave ‘rides’ upon current, a current in the wave direction tends to stretch the wave length, while an opposing current shortens it [188]. Therefore, the frequency of the wave varies along the wave. This phenomenon is called “Doppler Effect” on wave frequency; a detailed mathematical explanation of this can be found in [189].

Further theoretical models on the description of wave-current interaction may be found [190], where two wave models are developed (the linear and bilinear shear current models) for the representation of symmetric finite amplitude water waves of arbitrary order, propagating on currents with velocity profiles which are described by two or three straight lines.

4.3.2.2 Wind Load

Wind load on the structure refers to the forces induced in the part that exerts above the sea water level and contains equipment, decks and irregularities that cause drag from the air particles motion. Wind speed is classified as either sustained or gust wind speed with direction varying in time and space. Data for values of wind speed should refer to specific elevation and duration of measurements.

The sustained wind speed is defined as the average wind speed over a time interval of 1 minute measured at an elevation of 10 m above still water level (SWL). The wind velocity varies significantly with height due to the boundary layer induced by viscosity. The speed at a height z above sea water level could be estimated by the following semi-empirical relationship [191]:

$$U_w(1m, z) = U_w(1m, 10) \cdot \left(\frac{z}{10}\right)^{0,113} \quad (4-2)$$

Where: $U_w(1 m, 10)$ is the 1 minute mean sustained wind speed at 10 m above sea water level. A similar expression, proposed in [2], connects the 1 hour mean speed to different elevations as:

$$U(1hr, z) = U_w(hr, z_R) \cdot \left(\frac{z}{z_R}\right)^{0,125} \quad (4-3)$$

The gust wind speed is defined as the average wind speed over a time interval of 3 seconds measured at an elevation of 10 meters above SWL. Following the same description adjustments for elevation are given by the following equation [191]:

$$U_G(z) = U_G(10) \cdot \left(\frac{z}{10}\right)^{0,100} \quad (4-4)$$

Where: $U_G(10)$ is the gust wind speed at 10m above SWL.

The gust factor is defined as:

$$G(t, z) = 1 + g(t) \cdot I(z) \quad (4-5)$$

Where: $I(z)$ is the turbulence intensity and t is the gust duration in seconds and can be estimated as follows:

$$I(z) = \begin{cases} 0.15 \cdot (z/z_s)^{-0.125}, & z \leq z_s \\ 0.15 \cdot (z/z_s)^{-0.275}, & z > z_s \end{cases} \quad (4-6)$$

Where: z_s is measured in elevation of 20 m. The factor $g(t)$ is calculated as:

$$g(t) = 3.0 + \ln[(3/t)^{0.6}] \quad (4-7)$$

The wind force acting on a structure is the sum of the wind forces acting on individual members. Loads from wind and waves are assumed to act simultaneously in the structure, since in most cases in the presence of high winds, severe wave phenomena are observed. The equation for the drag force of an object within a flow is applied in the case of a member exposed to a wind of uniform velocity U :

$$F = \frac{1}{2} C_S \rho U^2 A \quad (4-8)$$

Where: ρ is the air density, A is the characteristic area of the body facing the wind and depends on the shape of the exposed member and C_S is a shape coefficient. The values of this parameter will be extensively discussed in a later section, however typical values are provided by design standards.

4.3.3 Wave Modelling

4.3.3.1 Fundamentals of Wave Modelling

In [192], the most probable maximum wave height is approached by a Reyleigh distribution, based on the significant wave height, the mean zero-crossing period and the reference storm duration. This wave can be efficiently approached by a deterministic two dimensional wave with an associated period in order to be considered in the evaluation of water particle kinematics. A current profile is combined with the wave consideration to produce the total water particle motion. Several wave theories have been proposed for the combination of waves and currents.

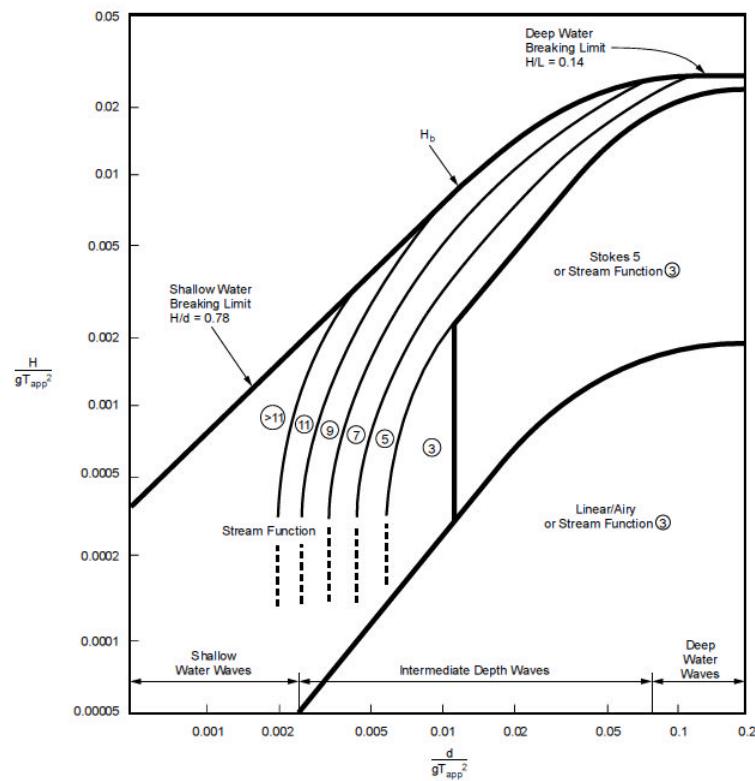


Figure 30: Ranges of appropriate wave theories [1]

Among different environments, different wave theories are applicable, based on different environmental parameters such as, water depth, wave height and wave period. Figure 30 [1] and Figure 31 [193], present the different areas of applicability of the different wave theories based on the above parameters.

The coordinate system employed in wave theories is a three dimensional (x, y, z) with x following the direction of wave propagation, and z is measured in the vertical depth direction. Those two dimensions are sufficient to describe a normal wave as it is described in Figure 32. Waves are assumed to be periodic, with a period T , and uniform with a height H . Further, fluid is assumed to be incompressible, the flow to be irrotational, and that the free surface uncontaminated [194].

For a periodic wave, the speed of a given crest or trough is called celerity. This parameter links the length and period of the wave as:

$$c = \frac{L}{T} \quad (4-9)$$

Alternative applicable definitions are that of the angular frequency, $\omega = 2\pi/T$ and the wave number, $k = 2\pi/L$.

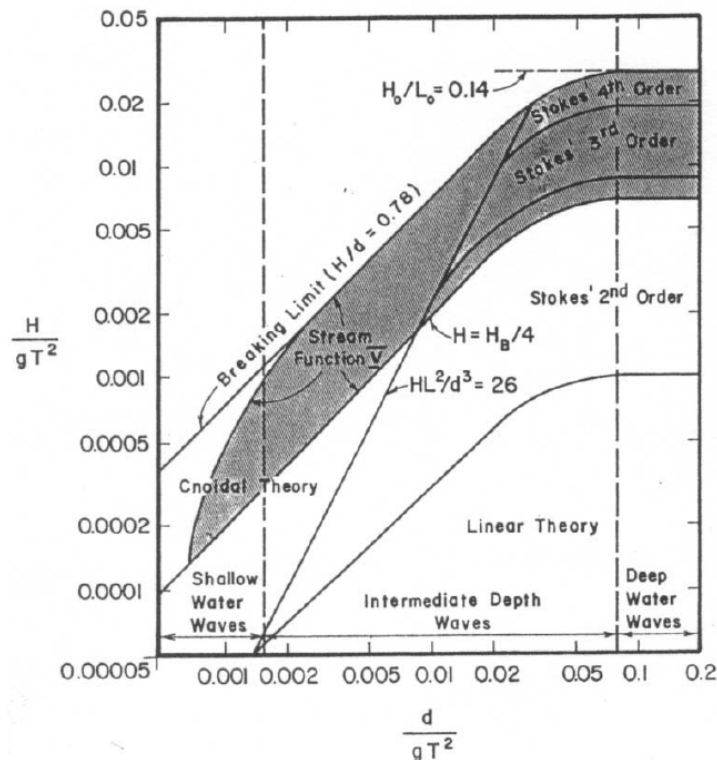


Figure 31: Ranges of appropriate wave theories [193]

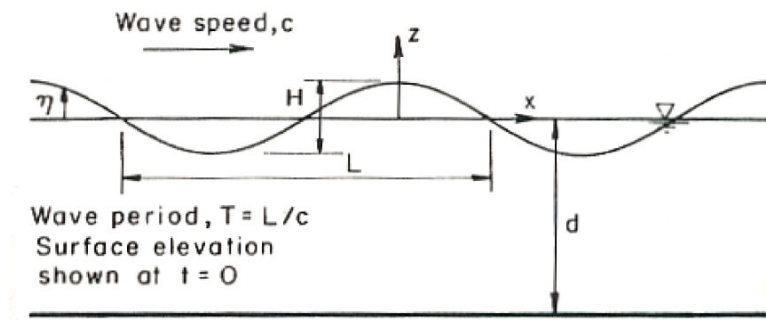


Figure 32: Coordinate system of wave propagation [194]

4.3.3.2 Formulation of Wave Theories

The existing different wave theories, attempt to determine the velocity potential Φ or equivalently, the stream function, Ψ pertaining to the fluid region. This should satisfy the Laplace equation:

$$\frac{\partial^2 \Phi}{\partial x^2} + \frac{\partial^2 \Phi}{\partial z^2} = 0 \quad (4-10)$$

Considering $\eta(x, t)$ to be the free surface elevation measured above the still water level $z = 0$, the following boundary conditions should be satisfied:

$$\frac{\partial \Phi}{\partial z} = 0 \text{ at } z = -d$$

$$\frac{\partial \eta}{\partial t} + \frac{\partial \Phi}{\partial x} \cdot \frac{\partial \eta}{\partial x} - \frac{\partial \Phi}{\partial z} = 0 \text{ at } z = \eta \quad (4-11)$$

$$\frac{\partial \Phi}{\partial t} + \frac{1}{2} \cdot \left[\left(\frac{\partial \Phi}{\partial x} \right)^2 + \left(\frac{\partial \Phi}{\partial z} \right)^2 \right] + g \cdot \eta = 0 \text{ at } z = \eta$$

From the above boundary conditions, the first one corresponds to the fact that at the seabed a zero vertical component on the fluid particle velocity is assumed, while the other two represent the kinematic and dynamic free surface boundary conditions respectively. Solution of this complicated problem is a difficult task because the free surface boundary conditions are nonlinear and must be satisfied at the free surface which is constantly changing. Analytical

methods for the wave modelling, corresponding to available wave theories, can be found to Appendix A of this Thesis.

4.3.3.3 Comparison and Application of Wave Theories

Selection of the most appropriate wave theory for each particular application is a significant decision as it will be shown later in this Thesis. Based on values of H , T and d , different wave theories are expected to describe differently the water particle motion. As mentioned in the introduction of this Chapter, empirical charts will prescribe the areas of applicability of each one of the methods, Figure 30, and Figure 31.

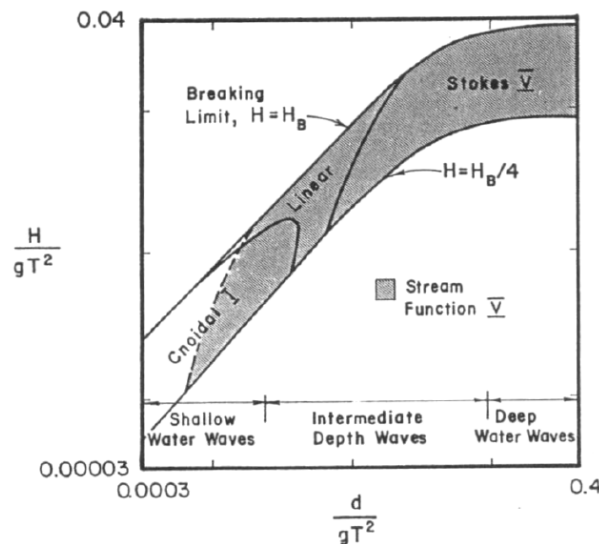


Figure 33: Applicability regions of wave theories based on the relative error on the fit of the two nonlinear free surface boundary conditions [195]

In [195], a comprehensive comparison of several available wave theories is presented. The wave theories examined include linear wave theory, Stokes third and fifth order theories, cnoidal, solitary and the stream function theories; the ranges of each theory is illustrated in Figure 33. Considering that the Laplace and bottom boundary condition are satisfied in all the theories included, the relative error of fit to the two nonlinear free surface boundary conditions was used in order to benchmark the performance of the methods. In the cumulative graphs that are available, the basic variables are combined in terms of H/gT^2

and d/gT^2 . It can be observed that all those charts relatively agree on the regions of applicability they indicate.

Once the water particles motion has been derived by applying the appropriate wave theory, hydrodynamic forces can then be calculated. The non-linear relation between water particle kinematics and water surface displacement, the turbulent flow process about a structural member, the natural variability of wave forces and the possibility of resonance between waves and structures are some of the difficulties imposed in the calculation of hydrodynamic forces.

4.3.3.4 Hydrodynamic Wave Forces

Based on the type and size of structural members on an offshore structure, different formulations for wave forces may be applicable. Mainly three different ways are applied for this calculation and a classification of those methods can be found, and are presented in [196]:

- Morison Equation
- Froude-Krylov theory
- Diffraction theory

Morison equation theory, as was presented in [197], describes the forces acting on a vertical pile subjected in a viscous, unsteady flow; this method is applied in cases when the structure is small compared to the water wave length and when the drag force is significant. In different cases, with small drag forces or inertia dominant, but still referring to relatively small structures, the Froude-Krylov theory is applicable. Finally, the diffraction theory is applied in cases when the size of the structure can be compared to that of the waves.

Morison proposed that the forces exerted on a vertical cylindrical pile which extends from the bottom to the free surface is composed of two components; that of drag and inertia. Combination of the two provides the total force as follows:

$$f = C_M A_I \frac{\partial \mathbf{u}}{\partial t} + C_D A_D |u|u \quad (4-12)$$

Where: C_M and C_D are the inertia and drag coefficients, u is the velocity of the wave particles, $\frac{\partial \mathbf{u}}{\partial t}$ is the local water particle acceleration at the centre line of the cylinder and A_I , A_D are the characteristic areas for each members calculated as:

$$A_I = \rho \frac{\pi}{4} D^2 \text{ and } A_D = \frac{1}{2} \rho D \quad (4-13)$$

Where: ρ is the mass density of water and D is the member's diameter. In the above equation, the inertia term is proportional to the acceleration of the water particles while the drag term is proportional to the square of the velocity. The absolute term is applied to ensure that the drag force will coincide with the direction of the flow. The wave velocity and acceleration of water particles decay with depth; therefore the force distribution is expected to follow the same pattern [198]. The previous expression provides the force for the unit length of a vertical cylinder; the total force will be derived by integration as follows:

$$F = \int_0^d f ds = \int_0^d \left[C_M A_I \frac{\partial \mathbf{u}}{\partial t} + C_D A_D |u|u \right] ds \quad (4-14)$$

In the above formulation of the total wave force, hydrodynamic coefficients C_M , C_D should be appropriately selected. Based on experimental research, those coefficients are found to be correlated to the Reynolds and Kuelegan-Carpenter (KC) numbers [194]; C_M increases with Re while K is related to the diameter D of the member and the amplitude of the wave A . Figure 34 and Figure 35, adopted from [199], show the correlation between coefficients and characteristic values. The analysis shows that at higher values of Re ($Re > 10^5$), C_D approaches 0.65 and C_M approaches 1.8. The coefficients C_M and C_D were also found to depend on both Re and a frequency parameter ($\beta = Re/KC$) when the coefficients were plotted against KC . Further extensive results based on field tests may be found at [200] showing extensive scatter of results due to the complexity of

wake structures in oscillatory flows which cannot be fully covered by Morison's equation.

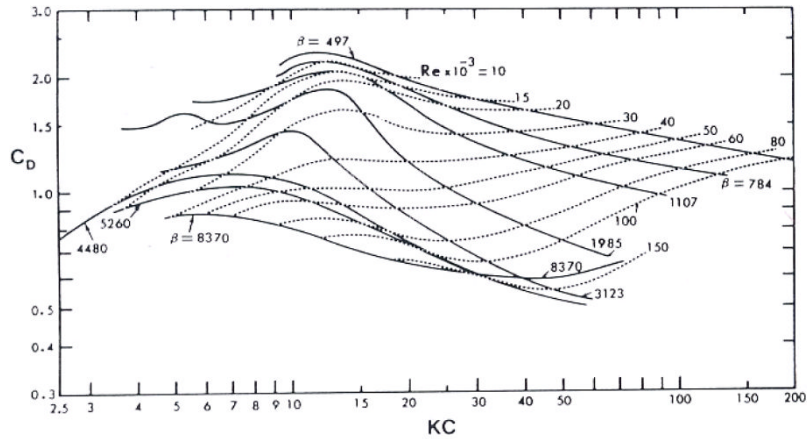


Figure 34: CD-KC number for different values of Re and $\beta=Re/KC$ [199]

Selection of hydrodynamic coefficients in practice is driven by the provisions of different standards and societies such as the American Petroleum Industry (API), Det Norske Veritas (DNV), International Organization for Standardization (ISO). A typical example is the classification of coefficients based on different roughness of the surface of the member; for a smooth cylinder, API suggests $C_D = 0.65$ and $C_M = 1.6$ while for rough cylinders $C_D = 1.05$ and $C_M = 1.2$.

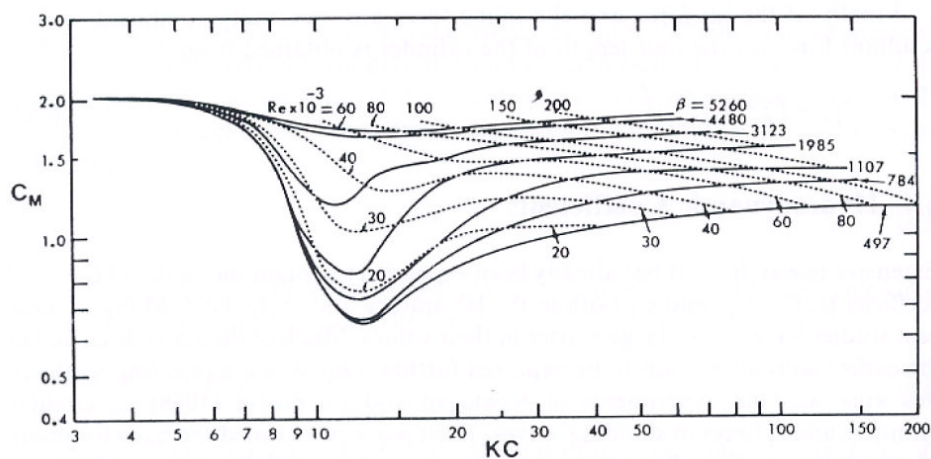


Figure 35: CM-KC number for different values of Re and $\beta=Re/KC$ [199]

A comparative study for the different proposed values for the hydrodynamic coefficients can be found in [201]. Design practice for global deterministic analysis combines a low drag factor with conservative estimates of the wave kinematics and current. API combines the wave kinematics factor with a low current value, current blockage and shielding.

Further literature, available in [184], considers that for tubular members of fixed offshore structures under extreme storm conditions, the Reynolds number lies in the post-critical regime ($Re > 2 \times 10^6$) and KC exceeds 10. Large scale laboratory experiments are presented in [202], for Re numbers exceeding this value, KC numbers up to 90 and including rough and smooth cylinders undergoing random oscillations in an attempt to realistically approximate tubular members of fixed offshore structures under extreme storm conditions. Table 12, summarizes the values of the hydrodynamic coefficients for smooth and rough cylinders as a function of the KC number. For the cases of rough cylinders, Re was found to have a low dependency on the value of the hydrodynamic coefficients.

KC Number	Smooth Force Coefficients		Rough Force Coefficients	
	C_d	C_m	C_d	C_m
0.0	0.7	2.0	1.5	2.0
6.0	0.7	2.0	1.5	2.0
30.0	0.7	1.7	1.3	1.5
60.0	0.7	1.6	1.2	1.3
90.0	0.7	1.6	1.2	1.3
high	0.6	1.6	1.1	1.3

Table 12: Values of hydrodynamic coefficient for circular cylinders [202]

Extensive research on oscillatory flows around cylinders have studied separation from the surface of the cylinder and formation of wake behind it, correlating vortex shedding behaviour at different values of the KC number [203]. An empirical formulation of the vortices formed around tubular sections is given in [191], correlating the Strouhal number valid for a range of Reynolds number between $60 - 2 \times 10^5$.

The majority of fixed offshore structures are drag dominated, considering ultimate limit state, and therefore the inertia coefficient has a lower influence. However, this becomes important for structures with large buoyancy legs and for other purposes such as fatigue design.

4.3.4 Joint Probability of Environmental Parameters

4.3.4.1 Wave Current Interaction

The first step in order to obtain the environmental design value is to consider the oceanographic data of the site where the structure is due to be deployed. The design wave method is a widely used method for the extrapolation of the data to obtain the extreme value for the environmental parameters; this has been an active research area, especially for the characterization of the extreme wave heights. Published research in [204], [205] and [206], have used real measurements to derive values from the meteocean data. The same method is also applicable for the estimation of extreme values for wind. The total loading experienced by the structure is based upon a set of design values of the individual environmental parameters such as the summation of the forces of wind, wave and current for the 50 or 100 year return period.

Drawback of the method is that it considers all the extreme environmental loads to occur at the same time, causing the worst case scenario to the structure. For example, occurrence of extreme wave current is not directly correlated to the instance of the extreme wind speed or extreme current speed. This implies that the initial assumption of simultaneous occurrence of all three extreme events, leads to over conservative consideration of forces.

Extensive studies have been carried out in order to systematically model the effects of joint probability of environmental loading on the structural response and are presented in [207] and [208]. Unlike the design wave method, a joint probability approach, assumes non correlated occurrence of the extreme events. The concept, widely used in the reliability analysis to quantify the design condition, has received increasing attention as the measured data set of the

metocean conditions becomes available and confidence in the hindcast model is constantly growing.

Over the years several techniques of joint probability have been developed. The joint probability of winds, waves and currents are mainly studied since these loads dominate the total loads applied on the structure. Combination of parameters in [208] have verified the model's ability to provide acceptably accurate results in cases of wave dominant structures, and describe complicated loading patterns for a wide range of environmental conditions. Application of the method has led to the reduction of loads which are exerted on the structure compared to the individual N -year wind, wave and current; in specific cases allowing reduction of even 20% [207]. Parallel studies for the Norwegian environments have concluded that wave and current loads during a storm rarely occur simultaneously at the same direction and therefore a more systematic consideration might substantially reduce the calculated hydrodynamic loads on drag dominated offshore structures [209]. Further studies [210] have verified this tendency for overestimation.

Another important issue that will be discussed in depth in the following sections is the incorporation of the design period in the extreme design conditions.

4.3.4.2 Wave Height- Period Joint Distribution

A systematic recording of environmental conditions for several locations in the North Sea is available in [211]. Most of the oceanographic data available are measured for typical time intervals of 10-20 minutes [212]. In cases of poor data, hind casting is the common method; different approximation methods are presented in [212]. In [213] and [214] where storm data have been studied, problems regarding limitations in computation of using hind casting and use of poor data are addressed and a threshold is proposed in order to obtain the joint probability of wave height and its period for the extreme waves.

For a probabilistic design of an offshore structure a joint distribution of significant wave height and wave period is required to describe the long term

wave climate. Those two variables are used as primary parameters to specify a set of stationary wave spectra, where the structural response is easily computed. [215], presents a review between the joint distributions of wave height and wave period, summarizing the work of several researchers. Among different available joint distribution models which may be applied, the applicability of each model should be checked for each specific location. Evaluation of different bi-variate distribution functions should be done empirically in order to ensure that the selected distribution provides a sufficient basis for the prediction of sea states.

Collected data for the significant wave height H and the spectral period T_p are classified in scatter diagrams which provide a convenient and simple to interpret way of summarizing pairs of random variables. The spectral peak period is chosen due to the fact that it is less correlated to the significant wave height [216]. The significant wave height and peak spectral period can adequately describe the sea state, and are important parameters in characterization of a wave spectrum [217].

Once the data are binned appropriately, the probability of occurrence of each is calculated. A three dimensional surface can be then constructed and smooth contour lines of same probability can be distinguished, giving an estimate of the bivariate probability distribution. Similar scatter diagrams and contour plots may be constructed from a fitted distribution and comparison between the two will show which bivariate probabilistic model has the best fit. Among several available bivariate probability density functions of the joint distribution available, three will be discussed here and will be applied in a later chapter.

4.3.4.2.1 Bivariate Log Normal Distribution

This model, proposed in [218] forms the joint probability density function based on five basic parameters ($\mu_x, \sigma_x, \mu_y, \sigma_y$ and P_{xy}), where $x = \ln X$, $y = \ln Y$ and the $\mu_x, \mu_y, \sigma_x, \sigma_y, P_{xy}$. Therefore the density function is formulated as:

$$f(x, y) = \frac{1}{2\pi\sigma_x \cdot \sigma_y \cdot XY \cdot \sqrt{1 - \rho_{xy}^2}} \cdot \exp \left\{ \frac{-1}{2(1 - \rho_{xy}^2)} \left[\left(\frac{x - \mu_x}{\sigma_x} \right)^2 - \frac{2\rho_{xy} \cdot (x - \mu_x)(y - \mu_y)}{\sigma_x \cdot \sigma_y} + \left(\frac{y - \mu_y}{\sigma_y} \right)^2 \right] \right\} \quad (4-15)$$

As would be considered for a bivariate normal probability density function, it is implied here that if the characteristic of wave height and wave period follow the log normal probability law, then the combined statistic properties should follow the bivariate log normal probability law.

4.3.4.2.2 Bivariate Weibull Distribution

Weibull distribution is widely used for the description and prediction of the extreme value of significant wave height. The form of the bivariate Weibull distribution is formulated as follows considering α, β, γ and λ are the parameters of the two distributions:

$$f_{xy}(x, y; \alpha, \beta, \gamma, \lambda) = \frac{\gamma y^{\gamma-1}}{\eta^\gamma} \cdot \exp \left\{ - \left(\frac{y}{\eta} \right)^\gamma \right\} \cdot \frac{\beta x^{\beta-1}}{\alpha^\beta} \cdot \exp \left\{ - \left(\frac{x}{\alpha} \right)^\beta \right\} \quad (4-16)$$

This bivariate distribution consists of a marginal Weibull distribution for the spectral peak period with parameters γ and η and the conditional Weibull distribution for significant wave height α, β ; these parameters may be estimated by the methods of moments.

4.3.4.2.3 Marginal Weibull and Conditional Log-Norma Distribution.

Combination of the above distributions derives the marginal Weibull and conditional log-normal distribution. This is one of the joint distributions which are used to describe the significant wave height and the spectral peak period, in cases where the 2-parameter Weibull distribution does not provide adequate results within the full range of wave heights. In [216] a combination between the 2-parameter Weibull distribution for large heights with a log-normal distribution for low heights is presented. An abbreviation of the method names it as the 'Lonowe' distribution (from LOGNormal and WEibull) and has shown to provide good fit to many sets of wave data. The transition point between the two

distributions is a decision that has some effect on the calculated probability of extreme wave heights. The joint probability density function is conveniently written:

$$f_{H_s T_p}(H_s, T_p) = f_{T_p/H_s}\left(\frac{T_p}{H_s}\right) f_{H_s}(H_s) \quad (4-17)$$

Where $f_{H_s}(H_s)$ and $f_{T_p/H_s}(T_p/H_s)$ are the marginal probability density function and the conditional probability density function for the significant wave height and the spectral peak period for a given wave height respectively. The probability density functions are fitted to the observations separately. Values of those probabilities are calculated as follows:

$$f_{H_s}(H_s) = \frac{1}{\sqrt{2\pi k H_s}} \cdot \exp\left\{-\frac{(\ln H_s - \theta)^2}{2k^2}\right\} \quad H_s \leq \eta_h \quad (4-18)$$

$$f_{H_s}(H_s) = \beta \cdot \frac{h_s^{\beta-1}}{\rho^\beta} \cdot \exp\left\{-\frac{H_s}{\rho}\right\} \quad H_s \leq \eta_h$$

Where: θ and k^2 are the mean and variance of $\ln(H_s)$ and where additionally, continuity is required for $f_{H_s}(H_s)$ at $H_s = \eta_h$, and β and ρ are the shape and scale parameter for the Lonowe model. Alternatively, the 3-parameter Weibull distribution may be adopted.

The conditional distribution of T_p given H_s is herein modeled by the lognormal distribution as follows:

$$f_{H_s T_p}(T_p/H_s) = \frac{1}{\sqrt{2\pi\sigma T_p}} \cdot \exp\left\{-\frac{(\ln T_p - \mu)^2}{2\sigma^2}\right\} \quad (4-19)$$

Where $\mu = E[\ln T_p]$ and $\sigma^2 = Var[\ln T_p]$

4.3.5 Estimation of Extreme and Design Values

Estimation of extreme values of environmental variables is defined by the marginal probabilities of exceedance which are determined by statistical

processing of an extreme value probability distribution of available data. Based on appropriate fitting, extrapolation of the data to small exceedance probabilities can be realized. Long term values of environmental variables can be obtained based on empirical procedures. In [219], the procedure of estimation of extreme values through statistical extrapolation distinguishes the following steps:

- Obtain a dataset through hind cast or measured data
- Statistical model fit
- Derive the required return value

In the following Sections, the above topics will be briefly discussed.

4.3.5.1 Data sampling

The most common methods to produce sub-sets of data for the derivation of extreme values are:

- Initial Distribution (ID) method
- Annual Maxima (AM) method
- Peaks Over Threshold (POT) method.

In the Initial Distribution (ID) method, as is presented in [212], all available data are considered for extrapolation, including data that might include multiple values generated by the same storm event. The estimation will be executed using an appropriate statistical model to a distribution of data that does not necessarily describe properly the distribution of extremes. This practice might impose an error in the derived extreme design values.

In the case of the Annual Maxima (AM) method, extremes are derived as the single most severe observation within a year period, providing a series of uncorrelated observations. Some issues raised from the definition of a year in temperate climates, such as the North Sea, and for significant rare events that do not occur in a location every year, in tropical climates such as the Gulf of Mexico [220].

In the Peaks Over Threshold (POT) method, the extremes are assumed to be generated differently than the other methods. Following this approach, an extreme is considered each time a value exceeds a given limit. The major issue in this method is an appropriate selection of this limit. Adequate time intervals can allow for several measurements to be taken, providing independent and uncorrelated observations. For the most important environmental variable which is the wave height in regions such as the Gulf of Mexico, this method is particularly applicable [205]. Further this method can distinguish severity of environmental phenomena.

4.3.5.2 Statistical model fit

Following the selection of the dataset, extreme values will be derived from statistical fitting based on an appropriate theoretical model. Selection of the most suitable fit should be done based on the best fit of available distributions [221]. Through the available probability distributions for the calculation of the extreme values the most widely used are the following:

- Log-Normal distribution
- Fisher – Tippett Type I (FT-I), Type II (FT-II), Type III (FT-III)
- Weibull 2 and 3 Parameter

Log-Normal Distribution is widely used in reliability analysis due to the fact that it can take only positive values and is the first to be used for extreme value calculation. Together with the Weibull distribution, those are the two representative distributions to describe the long-term behavior of the significant wave height. Apart from the selection of the selection of distribution functions, the following methods are used for the derivation of the parameters of the extreme distributions:

- Method of moments
- Least squares method
- Maximum likelihood method

The method of moments is simple and directly applicable and is based on the equation of the first two or three moments of the distribution to those of the data and therefore establishes relationships between estimated parameters and the sample mean, variance and skewness.

The least squares method is applicable to the Log-Normal, FT-I and FT-II distributions. This method initially transforms variables in a way that will linearize the cumulative density in a graph with a new set of variables; fitting a line to the transformed set will determine the parameters of the distribution. Although this method is widely used, it has the drawback of a bias [221].

The method of maximum likelihood may overcome this problem providing estimated parameters with small variance, based on the concept of constructing a likelihood function which depends on the probability density function of the observations, which are expressed in terms of the unknown parameters of the distribution; maximization of the logarithm of this function determines the value of the parameters. According to [222], advantage of this method is in its good asymptotic properties, since as the number of observations increases, the parameters estimators converge to the true values [223].

Further to the above, commonly used methods for the determination of the distribution parameters, combinations of the least squares method, least absolute deviation method and optimization method may be used. This method, proposed in [224], evaluates distribution parameters by automated search of optimal curve type based on the least absolute deviation between the empirical frequency point and distribution curve on ordinate.

The selection of an appropriate distribution for the estimation of extreme values is based on the level that data are represented by a line when variation of this line can be estimated by fitness tests. The advantage of using such methods is based on empirical distribution function (EDF). These EDF tests are distribution free and therefore could be useful for distinguishing between the various possible distributions [221]. Statistic tests that are used for this purpose are the Kolmogorov-Smirnov, the Crammer-Von Mises and the Anderson-Darling

statistic tests. Further reference to those tests is beyond the scope of this Thesis. An important note is the consistent selection of a single plotting position throughout the testing procedure [221].

4.3.5.3 Design Value

Once a particular probability distribution has been selected following the procedure that has been described above, the design value may be determined based on a return period, T_R or encounter probability, E_p . The return period, T_R , is defined as the average time interval between successive events being exceeded, and is directly related to the probability of exceedence as:

$$T_R = \frac{r}{Q(X)} = \frac{r}{1 - P(X)} \quad (4-20)$$

Where: r is the recorded interval associated with each data point and $Q(X)$ is the probability of exceedence. The probability E_p is defined as the probability that the successive event is exceeded during a prescribed period L_f , which will describe the design lifetime of a structure, and may be preferable instead of using T_R to correspond to the prescribed values of E_p and L_f and is defined with the following formula [225]:

$$E_p = 1 - \exp(-L_f/T_R) \quad (4-21)$$

4.3.6 Fluid Loading on Offshore Structures

In reliability analysis, loading is the most important concern to the response of the structure. During the operational life of a jacket structure, it is subjected to different loads depending on the type of service and the environmental conditions in the location of its deployment. The previous sections have covered the methods for the derivation of the environmental parameters. Some difficulties though arise from application of those parameters to structural analysis, setting the determination of analysis as an important step in the study of an offshore structure. Good engineering judgment combined with sound

scientific knowledge is essential for the validity of the results obtained in order to minimize errors.

The methods existing for the analysis of fluids can distinguish three main categories: deterministic, probabilistic and spectral. The deterministic approach [226], which is the simplest and most widely applied so far, analyses the fluid load by taking into account nonlinearities, but having the drawback of the restriction to incorporate uncertainties related to the sea state conditions [196]. Studies have shown that a deterministic model may produce unrealistic force distributions among the height of the structures, underestimating actual loads by 10% compared to a more advanced probabilistic model [227].

The probabilistic model is an extensively studied technique in the analysis of fluid loading, incorporating randomness of sea and wave forces with their statistical properties and enabling elaboration of the period's statistical properties prior to evaluation of the 50 or 100-year design wave. In the probabilistic method, a distribution is usually formed to describe the significant wave height, zero mean crossing period and the extreme conditions. In order to transfer from a deterministic to a probabilistic mode [228], some of the normal wave theories should be employed by selection of an appropriate wave height (eg. $H_{1/3}$, H_{10} , H_{max}). Having selected the appropriate design wave, a corresponding period can be allocated, as was described in the relevant section, based in studies such as [229], [230] and [231].

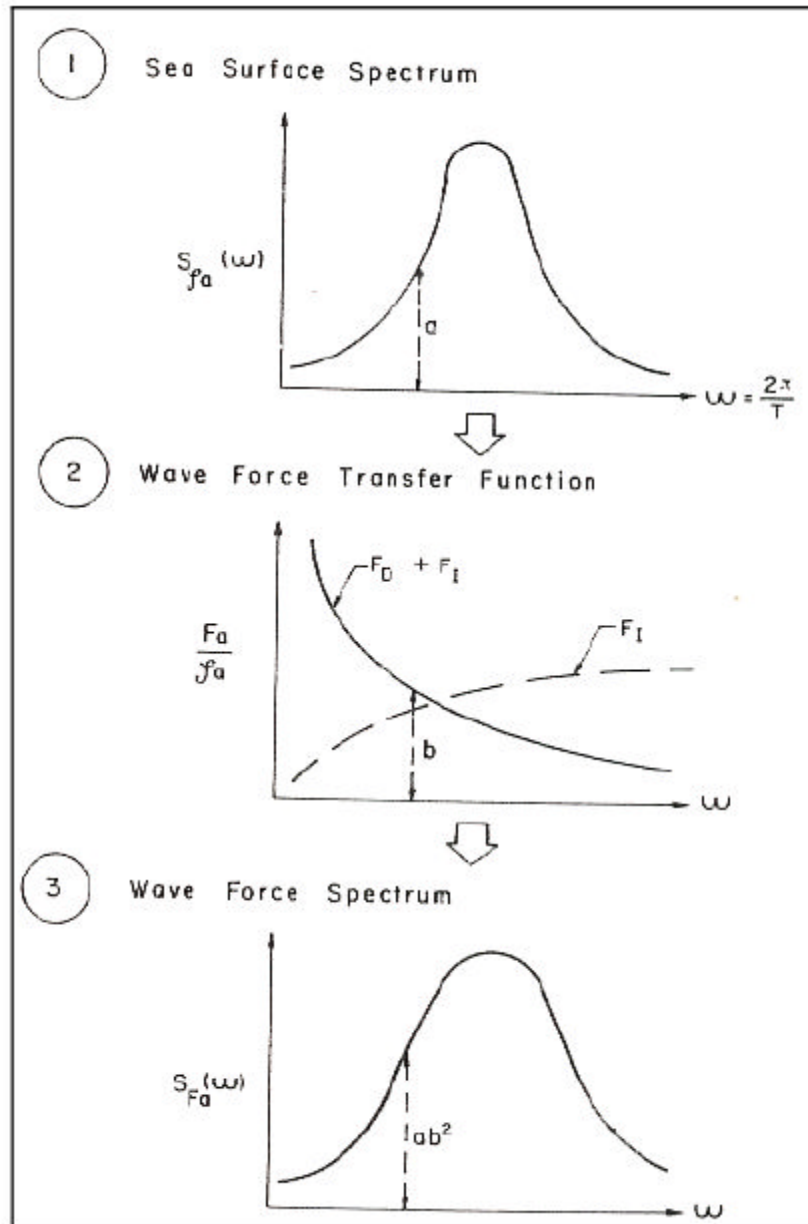


Figure 36: Frequency domain analysis [232]

Finally, the spectral method is the more comprehensive approach to the representation of the fluid loading, as it fully describes the loads and response of the structure statistically. It incorporates directly the variability of sea surface associated kinematics. Application of the method is based on linear superposition or linearization of non-linear processes. The method is often used for the dynamic and fatigue response assessment of deepwater structures in severe environmental conditions [233]. Figure 36, adopted from [232], illustrates

the sequence of spectral analysis; time discretization is applied to account for variation in time, and transfer functions are established to calculate the wave force response from the sea surface spectrum. The sea surface spectrum $S_W(\omega)$ is the input to the wave force transfer function while the $S_F(\omega)$ is the output. The wave force spectrum will be used in the structural analysis in order to obtain displacements by multiplying the wave force spectrum with the transfer function of the structure.

4.3.7 Response of Structure under Environmental Loading

In [194] and [232], the issue of structural loading is studied. Starting from definition of environmental conditions through elaboration of meteorological data, the wave conditions can be established. The appropriate wave theory will analyze the kinematics properties of the fluid, deriving the hydrodynamic forces and therefore calculating the structural response. It has been discussed in Chapter Two that static or dynamic approach can be followed for the structural analysis assessment and criteria for the selection of each approach, based on the natural frequency, have been established. In [196], the dynamic problem can be categorized as follows:

- Lowest natural frequency, which refers to the case where the natural frequency of the structure is lower than the resonance frequency. In such cases static analysis is sufficient; in different cases where the dynamic part of the load is significant then dynamic analysis might be required.
- One, or more, of the natural frequencies of the structure is in the range of the frequency of resonance. In such cases, dynamic analysis is definitely required.

A useful graph, presented in Figure 37, illustrates the areas of applicability of static and dynamic analysis. In cases where the response is controlled by stiffness, the analysis might follow the quasi-static method, while for the case where the response is controlled by mass and damping, the dynamic analysis should be employed. As far as dynamic analysis is concerned, it can be

classified in either frequency or time domain. The first method is more time and computationally efficient; however if the amount of data is restricted, the time domain analysis might be used, since it allows consideration of the drag term in the force equation without linearization, eliminating errors due to non linearity in sea states.

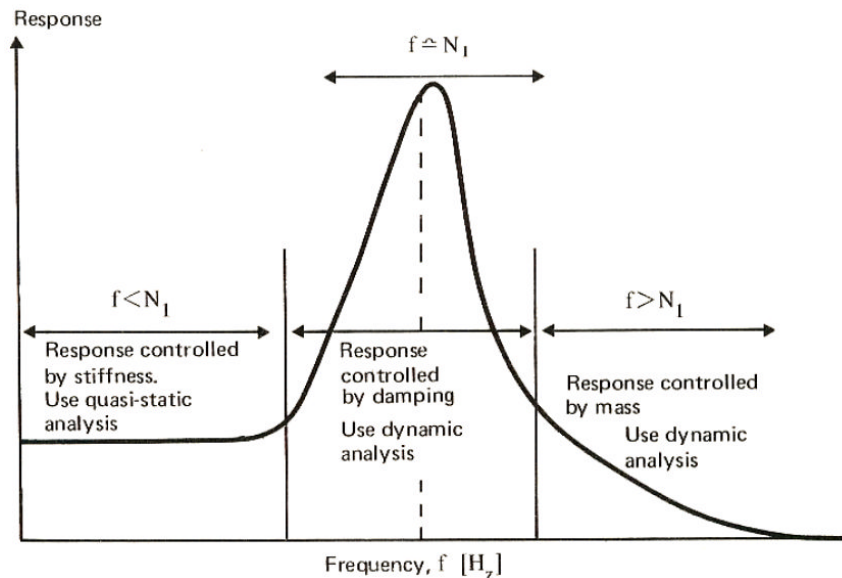


Figure 37: Static and Dynamic analysis response curve

4.4 Capacity of Offshore Structures

4.4.1 Resistance Model

Derivation of the resistance part of a limit state function defines the performance of a structure under specific load conditions, as a function of a number of different basic variables. For a realistic model of resistance, all the relevant variables should be identified and included, while the variables that have a lower significance on the model may be omitted.

Theoretical and empirical methods are available to derive a resistance model; however for a comprehensive selection, validation based on comparisons of the above techniques is essential. Comparison between the two sets of obtained data can be done using appropriate plots that will allow correlation between

variables. If the calculation method accounts adequately for the respective variables, correlation between theoretical and experimental values can be established. The types of plots that can be drawn are:

- Plot of the observed resistance values against the calculated values using the measured properties
- Plot of the observed resistance against each of the basic variables

Significant deviations in the plot of the second type should lead to reconsideration of the theoretical model. Insufficient consideration of all of the important variables and incompleteness of the resistance equation, without considering every design parameter, may impose a significant source of uncertainty on the reliability estimation.

4.4.2 Material Data

Material properties, for each grade of materials, are derived from relevant experiments on samples of sufficient number, following appropriate standardized procedures. For the reliability assessment, the properties of interest are the yield strength, Young's modulus, Poisson's ratio, and fracture toughness. Those properties are presented in this section.

4.4.2.1 Yield Strength of Steel Specimens

As it has been referred in the description of the Limit State Design Method in Chapter Two, the characteristic yield strength is defined as the 5 percent quantile of the test data [234] and [25]. In Table 13, the results of a study presented in [235] are presented. In this study, different grades of steel specimens have been tested and the Coefficient of variation has been derived showing that as the nominal value increases, this value decreases. Another interesting result of the experiments is that the yield strength follows a Log-Normal distribution; a fact that is countersigned by the DNV standards' provisions for reliability assessment of offshore structures [14].

<i>Material</i>	<i>Distribution</i>	<i>Yield Strength</i>	<i>CoV</i>
		(MPa)	(%)
Steel	Lognormal	<350	8.0
		350-400	6.0
		>400	5.0

Table 13: Yield Strength Properties [235]

4.4.2.2 Young's Modulus and Poisson's Ratio

The property of Young's modulus for steel specimens is found to follow a Normal distribution while for different materials, such as aluminium and concrete, a fixed value might be selected. In [236], a mean value of 2.1×10^{11} (Pa) with a coefficient of variation of 5% is proposed, while in [237] a value of 6%. Poisson's ratio can be represented by a fixed value of 0.3 for steel. Table 14 presents cumulatively data for Young's modulus and Poisson's ratio.

<i>Material</i>	<i>Distribution</i>	<i>Young's modulus</i>		<i>Poisson's ratio</i>	
		<i>Mean</i>	<i>CoV</i>	<i>Mean</i>	<i>CoV</i>
		(MPa)	(%)		(%)
Steel		210×10^3	5.0	0.3	-
Aluminium	Normal	7.0×10^4	-	0.3	-
Concrete		3.0×10^4	-	0.2	-

Table 14: Young's modulus and Poisson's ratio

4.4.2.3 Fracture Toughness

Fracture toughness in steel specimens is characterized by stress intensity factors K_{IC} and Crack Tip Opening Displacements (CTOD). Although initially considered to follow lognormal distributions, a two-parameter Weibull distribution was found to provide a better fit for (CTOD), as is documented in [238]. Due to the fact that fracture analysis will not be covered in this Thesis, further details for the consideration of fracture is beyond this scope and will not be included.

4.4.3 Geometry Data

Geometrical data refer to the physical quantities that describe the shape, size, cross sections and tolerances of members and structures. Compared to the material and loading properties, uncertainties in geometrical data are significantly less important since they depend on the production procedure of the elements and the quality of manufacturing and also the accuracy of the post-manufacture measurements; factors that can be efficiently controlled by means of quality assurance etc. Geometrical properties may be assumed to be deterministic variables, however in cases where their deviation has a significant effect on the structural response of the structure they can be considered as stochastic variables or as parameters of variables that describe actions or structural properties.

Eccentricities, misalignments, inclinations and curvatures are geometrical anomalies due to poor fabrication of members or inefficient assembly. Further than affecting the actual capacity of the members and as a result of the structure, eccentricities, misalignments and inclinations might amplify dynamic loads and therefore might cause fatigue issues on the structure while curvatures may have important influence in the buckling capacity of members.

<i>Material</i>	<i>Distribution</i>	<i>Thickness</i> (mm)	<i>CoV</i> (%)
		12.7	1.8
Steel	Normal	25.4	1.0
		50.8	0.7

Table 15: Variation in thickness of steel plates [239]

In the fabrication process of steel members, physical wearing in the shaping rollers of the steel mill will cause variation in the cross sectional dimensions of the members. Further, selection of the acceptable levels of tolerance will determine the accuracy of the manufacturing process. An extensive study made in [239] in I shaped beam elements has shown that the relative variation in height and flange width of the specimens is small, compared to the variation in thickness. Further, it is observed that flanges tend to be thinner while the web to

be thicker than its nominal values. Table 15 presents statistical properties of experimental data for specimens of different thicknesses [239].

4.4.4 Capacity of Members and Joints

This section deals with the buckling performance of structural members. Buckling curves illustrate the capacity performance of members to plastic deformation; extensive work is available in [239]. Design standards of steel structures extensively describe the consideration of buckling in members, while an important background reference is [240]. Further background literature in buckling curves is available in [241] and [242]. Although elastic analysis is used in traditional design, consideration of non-linear plastic analysis might be used in order to take advantage of post-buckling plastic performance of structural members. Due to the complicated requirements for the consideration of a non-linear performance several items should be considered in the implementation in conjunction to design standards [8]:

- Procedure for the identification of failure modes should be appropriately included taking into consideration the non-linear analysis.
- Modelling of joints should incorporate the effect of local details for end restraints or force-deformation relationships.
- Fabrication tolerances (member straightness and joint eccentricities) should be effectively included.
- Residual stresses on buckling capacity should also be considered.
- Failure criteria in terms of maximum strain at failure for components containing relevant imperfections from, e.g., welding and at regions containing notches.
- Repeated yielding in case of reversed loading due to, e.g., wave action.
- Sensitivity of input parameters and analysis assumption for evaluation of acceptance criteria.

Application of non-linear analysis definitely requires more effort and skill from the engineer than that of traditional deterministic analysis of working within the elastic region of materials; however if appropriately executed it might produce

more optimized structures. It should be noted that a systematic procedure for the use of non-linear analysis of offshore structures does not presently exist.

Regarding the axial capacity of stiffened plates a comparative study presented in [243] summarizes the provisions of different design codes. Data for those properties are essential for the design of floating structures and therefore will not be discussed further here. As far as the design of shell members and shell frame structures are concerned, several standards have been developed, while uncertainties have been studied in [244] and [245]. Most updated studies should be considered and design standards should be updated.

In [246] and [247], the design equations for static strength of grouted joints are derived. Test data for static capacity of tubular joints are available in [248]. Further work on the formulation of capacity equations is available in [244] and [249]. In a reliability assessment, background of the databases and equations used should illustrate the failure criterion used for each analysis. Therefore, definition of the characteristic design equations in various design standards varies since they are associated with different bias. Background literature for the derivation of those equations in standards can be found in [250] and [251].

4.4.5 Geotechnical Data

Modelling of geotechnical data may include aleatory and epistemic uncertainty; therefore stochastic representation can be applied through appropriate probability distribution functions. Statistical properties of soil depend on a number of parameters and can be obtained by several methods including a Monte-Carlo simulation scheme. Different statistical tools may be more suitable for problems of different nature and depending on the number of data points and simulations that can be realized. Although variables that are related to geotechnical data will not be considered in the application part of this Thesis, a brief reference will follow for reasons of completeness.

4.4.5.1 Soil Characteristics

An initial statistical approach is that of short-cut estimates, that can be used in cases of little data available. The method can obtain the mean and variance and gives a bound for standard deviation, and has been proven useful for cases of 'symmetrical' data. Benefit of the method is that it can be applied relatively quickly. The stochastic interpolation approach, proposed in [252] and [253] can be also applied to describe and present the properties of a site. The method can derive several soil properties but demands adequate data to be available. A more empirical method suggests use of histograms or fitted probability distribution functions. This method is maybe the most preferable one and should be used whenever the data sample allows so, deriving the distribution function by plotting in probability paper or by using statistical fit-tests.

Soil characteristics are summarized in Table 16 together with proposed appropriate probability distribution functions. Summary of statistical properties can be found in [254]. It can be observed that most of the characteristics follow a Normal or Lognormal distribution, however in specific cases may be described by uniform distributions. In the presence of adequate data, validation of the stochastic representation of each characteristic should be executed through appropriate distribution fit tests.

In cases of large soil volumes, in order to avoid local fluctuations of soil properties, the averaged property is used. In order to avoid negative values in a distribution, the lognormal distribution may be preferred. Therefore, characterization of the soil volume under consideration is an essential decision before proceeding to statistical analysis. In cases of large volumes, the site description strategy might be employed [252] and [253]; two steps are distinguished:

- Identification of the structure of the soil data.
- Use of the 'kriging' stochastic interpolation technique to estimate the soil property at the location of interest.

Soil Characteristic	Soil Type	Probability distribution function	Mean Values	CoV
Cone Resistance	Sand	Lognormal	*	*
	Clay	Normal/Lognormal	*	*
Undrained Shear Strength s_u	Marine Clay	Lognormal	*	5-20%
	Clay	Lognormal	*	10-35%
	Clay silt	Normal	*	10-30%
s_u normalised w.r.t. Vertical effective stress	Clay	Normal/Lognormal	**	5-15%
Plastic Limit	Clay	Normal	0.13-0.23	3-20%
Liquid Limit	Clay	Normal	0.30-0.80	3-20%
Submerged unit weight	All soils	Normal	4.5-11	0-10%
Friction angle	Sand	Normal	*	2-5%
Void ratio and porosity, including initial void ration	All soils	Normal	*	7-30%
Over consolidation ratio	Clay	Normal/Lognormal	1.2-40	10-35%

*: Site and Soil type-dependent

** : Function of over consolidation ratio

Table 16: Probability Density Function for Soil Characteristics [254]

Those methods can increase the quality of data and overcome the natural heterogeneity of the soil characteristics. The uncertainties involved in the soil characteristics, represent values for the parameters that are used for the analysis of bearing capacity of gravity structures, jack-up platforms and suction anchors, where "shallow" type of foundation failure is modelled. For piled structures, relevant uncertainties are studied in the following section.

4.4.5.2 Piled Foundations

Empirical methods derived from onshore tests on piles of small scale for the axial pile capacity have derived design parameters applicable to piles for offshore applications. The design variables considered for clay volumes are the skin friction factor along the pile, the undrained shear strength, the end bearing factor and appropriate factors to account for the correlation between site specific effects. As far as sand volumes are concerned, the design variables considered include coefficient of lateral soil stress, soil-pile friction angle, limiting skin friction, bearing capacity factor and limiting end bearing. API suggests values for pile design parameters in clay.

As far as sand characterization is considered, differences among available methods exist due to the following factors [8]:

- The value of the earth pressure coefficient, and thus the value of the effective stress, allowed in the calculations of axial pile capacity for compression and tension loading.
- The limiting side friction value, and the extent to which it depends on relative density.
- The limiting end bearing value and its dependence on relative density.

4.4.5.3 Uncertainty in Calculation Model and Load Effects

Uncertainties in the calculation model depend on the problem under consideration. The statistical properties of the soil model are difficult to determine, however a useful approximation can be based on literature review, comparisons of model test results with calculations, survey of expert opinions or relevant case studies and back-calculation. Further, discussion on studies of the uncertainty in different calculation models can be found in [255] while extensive studies exist for the modelling uncertainty for shallow types of foundations and quantification of model uncertainties [256] and [257]. Modelled uncertainty is characterised through the parameter of bias; value of bias greater than unity implies a conservative model, under predicting the actual capacity while a value

less than unity refers to a calculation model that over predicts the actual capacity.

Uncertainties in loads and load effects, either aleatory or epistemic, should be considered in a systematic way as they might significantly affect the geotechnical analysis. Engineering practice shows that load uncertainties are dominant in the structural response when compared to geotechnical uncertainties. Since influence of load effects depends on soil properties, parametric and sensitivity studies should be included to illustrate the actual effect of an incremental change on the deterministically modelled soil properties to the load effects.

4.4.6 Fatigue Data

Although fatigue limit states are not covered within this Thesis, this section will include some information regarding consideration of capacity of structures under fatigue loading. [258], gives S-N data for welded connections for different classes of structures in different environments (air, seawater and corrosion free) in the region between 10^5 - 10^7 cycles to failure. This is a common number for offshore structures. In cases where this range is exceeded, S-N data might be un-proportionally larger than that of the standard. Further data for crack growth parameters, such as C and m for Paris' crack growth formula are also included. From a stochastic perspective, m is modelled as a fixed parameter while $\ln C$ follows a normal distribution, implying that C follows a lognormal distribution. Further literature on the stochastic modelling of those variables can be found in [259] and [260].

It is common practice in offshore and further large scale structures to avoid using steel of normal grade and instead use high strength steel with yield strength of more than 450 MPa. Initiation period of this kind of steel will be longer and this should be taken into account since most of the available S-N data are derived from experiments in normal graded steel specimens. This fact may impose a level of extra conservatism.

Based on experimental work and finite element analysis models, starting from simpler geometries and moving to more complicated configurations, parametric formulas for the derivation of stress concentration factors are available in literature [261], [262], [263]. Stochastic properties of the ratio between measured and predicted values are summarized in [264]. This ratio indicates the bias of the experimental procedure. The derived mean values are in the range 0.81 – 1.01 and the corresponding COV's in the range 0.13 – 0.25.

Finally for the cumulative damage on a structure, the Miner-Palmgren Hypothesis can be applied for calculation of reliability. For steel structures, the Miner's damage ratio is proposed to follow a lognormal distribution with mean value 1 and CoV of 0.3 [265].

4.4.7 Corrosion Modelling

4.4.7.1 Definition of corrosion

Offshore and marine structures are designed to survive harsh and very corrosive environments. The level of capacity deterioration due to this effect should be considered throughout its service life, in order for the structure to sustain adequate safety levels. Systematic maintenance and corrosion protection systems, that refer to surface coating and cathodic protection arrangements are often employed to restrict the effect of corrosion on the structures. Extensive research is available regarding the performance of vessels or pipelines deployed offshore.

In [266], a classification of marine corrosion may be divided into the following categories, based on the deterioration mechanisms that are developed on the surface of plate materials:

- Immersion
- Splash/tidal zone
- Atmospheric
- Semi-enclosed space

Characterization of corrosion may be also based on the fact that the depth profile of a corrosion instance might distinguish a single defect or a cluster of defects through the thickness of the material. A definition based on this performance distinguishes [267]:

- Pitting corrosion, which refers to corrosion with length and width less than three times that of the un-corroded wall thickness.
- General corrosion (wastage), which refers to corrosion with length and width more than three times the un-corroded wall thickness.

From a structural reliability perspective, corrosion together with fatigue have time-dependent effects on the structure. In particular, there is a monotonic decreasing performance in the deterioration of Resistance as a function of time accompanied by an increase in uncertainty in the remaining strength. Figure 38 [268] and Figure 39 [269] present those two facts. In Figure 39, it can be observed that the distribution that describes the probability density function of the structural resistance 'flattens' with time and the mean value decreases, increasing the overlapping between the load (effect) and resistance curves.

There are a number of parameters that influence the corrosion performance of a structure. Environmental factors, such as biological, chemical factors and physical parameters might significantly determine the corrosion effect on structural members. From this category, the physical factors are the most important ones, since they account for temperature, pressure (significant in pipe lines), water velocity, suspended solids and percentage wetting. In general it has been observed that increased temperature will increase the corrosion rate, as it is observed in Figure 40 [269]. Water particles velocity has the same effect, as presented in Figure 41 [268], as increased velocity will increase corrosion losses. Further, factors such as pollution and water salinity may influence corrosion on the structure.

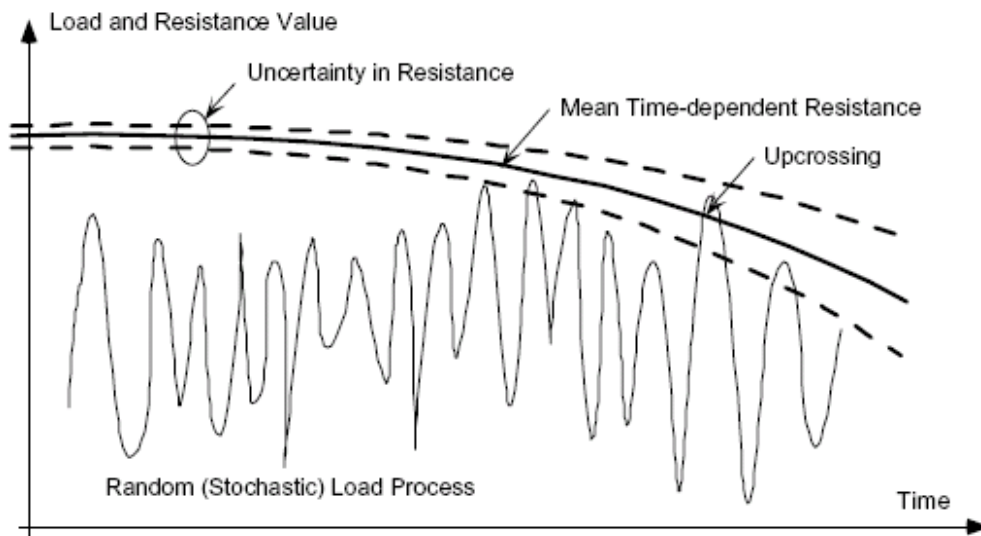


Figure 38: Continuous load process and potential exceedance of the deteriorating structural Resistance [268]

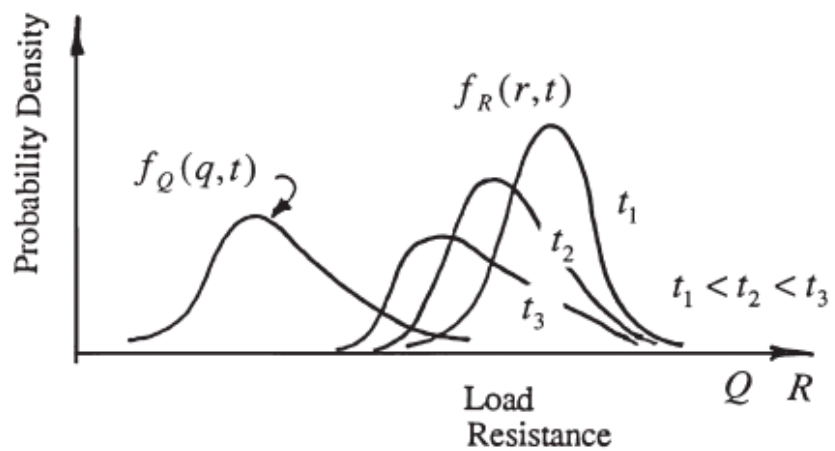


Figure 39: Strength Deterioration Structural Reliably Problem [269]

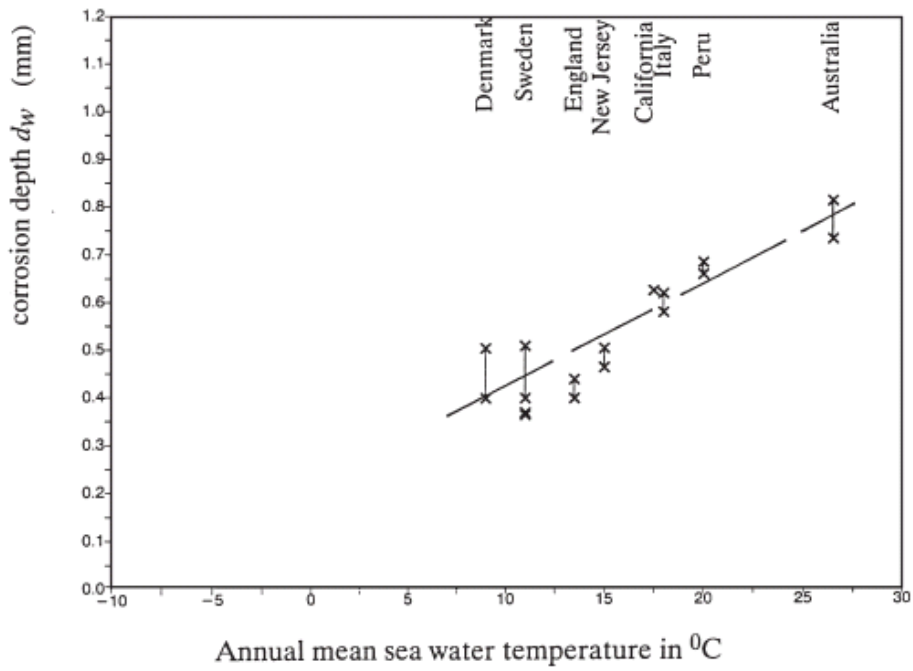


Figure 40: Corrosion depth as a function of sea water temperature [269]

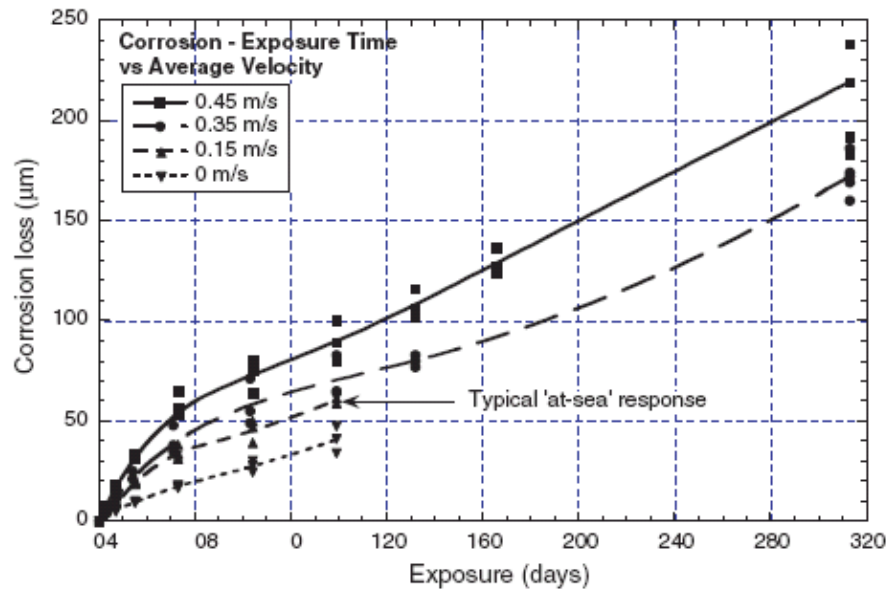


Figure 41: Effect of water velocity on early loss corrosion [268]

4.4.7.2 Corrosion Models

Several models have been proposed for consideration of thickness deterioration due to corrosion, both considering different periods of the life of the structure as well as for its whole service life. Most of the models are initially based in experimental work followed by scientific foundation of findings. The simplest way to account for corrosion is through constant annual rate deterioration. Based on the work of [270] and [271], typical values of annual deterioration can be found, and are illustrated in Table 17. Although those values can be reliable for initial design of structures, in case of reassessment of existing structures a more advanced model should be employed.

Environmental conditions	Corrosion rate (mm/year)
Immersed steel specimens, ocean conditions	0.05 – 0.20
Steel sheet piling – immersion zone	0.08
Tidal zone	0.10 – 0.25
Atmospheric zone	0.05 – 0.10
Ship deck plating (uncoated)	0.10 – 0.50

Table 17: Typical annual corrosion rates [270], [271]

Although in most of the studies executed so far the effect of corrosion is represented by a constant corrosion rate, which corresponds to a linear decrease of the plate thickness throughout its service period, there is experimental evidence that a non linear model would be more appropriate. Before proceeding to description of those models, a reference to the background of corrosion should be made. General corrosion is of main interest in this aspect since pitting corrosion cannot affect the main in plane stress distribution in a steel plate [272].

As it has already been mentioned, corrosion is affected by a number of parameters therefore a probabilistic model such as the one presented in [269] including a mean value expression and an expression for randomness and uncertainty can more systematically describe the expected corrosion:

$$C(t, P, E) = f_n(t, P, E) + \varepsilon(t, P, E) \quad (4-22)$$

Where: $C(t, P, E)$ is the total weight loss of material, $f_n(t, P, E)$ the mean function and $\varepsilon(t, P, E)$ the zero mean error function, t is the time parameter, P is a vector with parameters for the corrosion protection systems included, and E is a vector of environmental conditions. Throughout the service life of the structure, different corrosion processes can be distinguished and are illustrated in Figure 42 [269]:

- initial corrosion
- oxygen diffusion controlled by corrosion products and micro-organic growth
- limitation on food supply for aerobic activity
- anaerobic activity

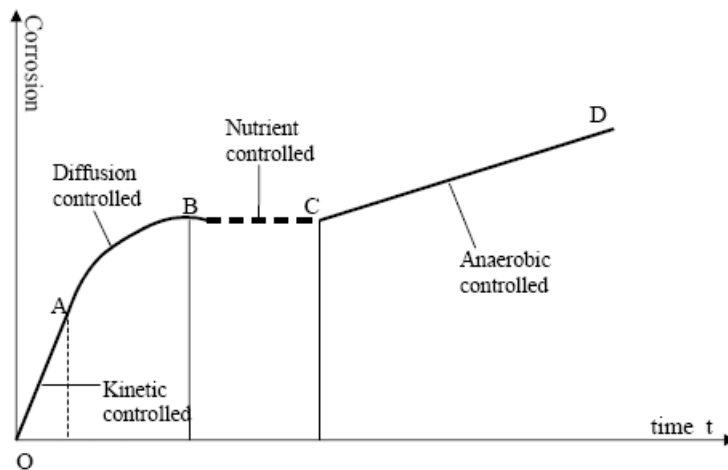


Figure 42: Different corrosion mechanism as a function of time [269]

For general corrosion several models exist for a more systematic description of corrosion deterioration. In [273], Southwell proposes a linear and a bilinear model while Melchers [269] extends this model, calculating coefficients based on available experimental data. As presented in [272], the extended Southwell linear model may be stochastically formulated as:

$$\mu_d(t) = 0.076 + 0.038t \quad (4-23)$$

$$\sigma_d(t) = 0.051 + 0.025t$$

Correspondingly, the extended Southwell bilinear model may be written as:

$$\mu_d(t) = \begin{cases} 0.09t, & 0 < t < 1.46 \text{ years} \\ 0.076 + 0.038t, & 1.46 < t < 16 \text{ years} \end{cases} \quad (4-24)$$

$$\sigma_d(t) = \begin{cases} 0.062t, & 0 < t < 1.46 \text{ years} \\ 0.035 + 0.017t, & 1.46 < t < 16 \text{ years} \end{cases}$$

The exponential model proposed by Melchers, based on the Southwell linear formulation, is the Melchers-Southwell non linear model, and is expressed as follows:

$$\mu_d(t) = 0.084t^{0.823}$$

$$\sigma_d(t) = 0.056t^{0.823} \quad (4-25)$$

Finally, in [274], a tri-linear and a different power approximation model are suggested for the corrosion wastage thickness as:

$$d(t) = \begin{cases} 0.170t, & 0 < t < 1 \\ 0.152 + 0.0186t, & 1 < t < 8 \\ -0.364 + 0.083t, & 8 < t < 16 \end{cases} \quad (4-26)$$

A different nonlinear model, based on observation data, has been proposed in [275]. According to this, the corrosion process is divided in three phases; the first where no corrosion is present due to effectiveness of corrosion protection means, the second which is initiated when the corrosion protection becomes damaged and the third which corresponds to the phase where the corrosion process stops. The practical interpretation of the last period implies that due to the corroded external surface of the plate, protection is provided. This should be taken into account since partial or full removal of this layer will initiate a new corrosion cycle in the corroded thickness of the plate. Appropriate formulations of the model can be described as the solution of a differential equation of the corrosion wastage:

$$d_\infty d(t) + \dot{d}(t) = d_\infty$$

Where: d_∞ is the long-term thickness of the corrosion wastage, $d(t)$ is the thickness of the corrosion wastage at time t , and $d(t)$ is the corrosion rate. The solution of the above equation leads to:

$$d(t) = \begin{cases} d_\infty(1 - e^{-(t-\tau_c)/\tau_t}), & t > \tau_c \\ 0, & t < \tau_c \end{cases} \quad (4-27)$$

$$\tau_t = \frac{d_\infty}{tg\alpha}$$

In the above equations, τ_c is the coating life (1.5-5.5 years), equal to the time interval between the painting of the surface and the time when its effectiveness is lost, and τ_t is the transition time (5-10 years) time and α is the angle as formed in Figure 43.

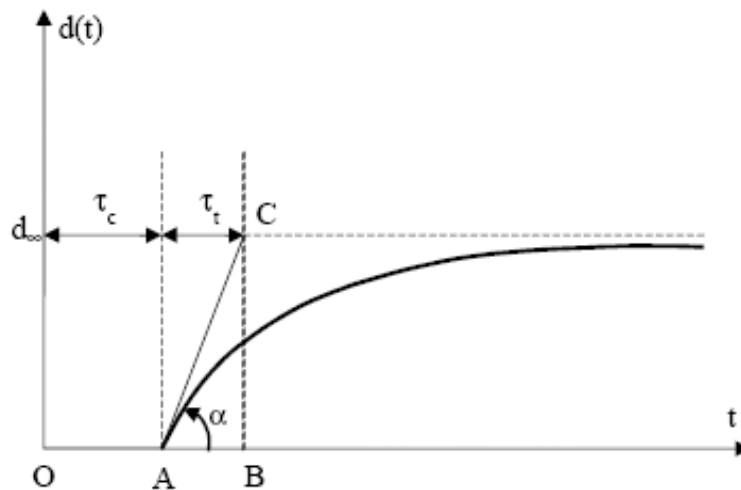


Figure 43: Thickness of corrosion wastage as a function of time [275]

Interesting work presented in [272], develops a parametric approach to the corrosion modelling introducing the Weibull function. The advantage of this distribution is that based on the values of specific parameters, different shapes of distributions can be derived. Further, by setting specific values in some of the parameters of the model, the more straight forward models that were described above can be obtained. Due to the strong mathematic formulation of this method, it will not be presented in this Thesis; however a comparative example that was executed among methods based on experimental data and using

statistical-fit methods to derive the best approach illustrates that this new method has a very good potential.

As far as pitting corrosion is considered, the problem that might be cause on the structure is deep holes that could lead to penetration. The local character of pitting corrosion makes it less significant than that of wastage corrosion. For reasons of completeness, following similar logic as for the general corrosion, a refined model is presented in Figure 44 [276], [277]. The parameters of this figure are explained in Table 18 together with a calculation model.

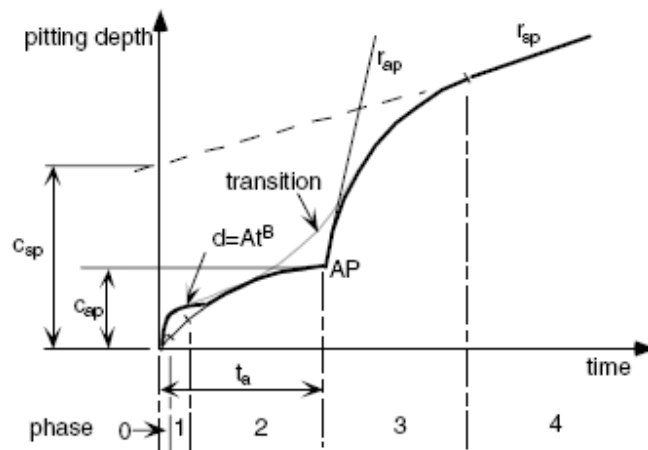


Figure 44: Model for maximum pit depth as a function of exposure period [276]

Phase	Phase description and corrosion controlling mechanism	Governing parameters as function of T
0	Initial pit growth	
1 and 2	Pit growth under overall aerobic conditions under rust cover	$t_a = 6.61 \cdot \exp \cdot (-0.088 \cdot T)$ $C_{ap} = 0.99 \cdot \exp \cdot (-0.052 \cdot T)$
3	Rapid pit growth under overall anaerobic conditions under rust cover	$r_{ap} = 0.596 \cdot \exp \cdot (0.0526 \cdot T)$
4	Steady-state pit growth under overall anaerobic conditions under rust cover	$C_{ap} = 0.641 \cdot \exp \cdot (0.0613 \cdot T)$ $r_{ap} = 0.353 \cdot \exp \cdot (-0.0436 \cdot T)$

Table 18: Phases in pitting corrosion and calibrated functions for model parameters [276]

4.4.7.3 Corrosion Protection Systems (CPS)

Painting coatings and cathodic protection schemes are the main techniques applied for the protection of steel members against corrosion, and are included in Appendix B of this Thesis. Those measures, together with appropriate maintenance, should be able to efficiently treat corrosion. However, practice from field observations shows that maintenance in offshore structures might not always be effective and CPS might be ineffective. Further, some parts of an offshore or marine structure are difficult to access and therefore apply any maintenance action.

4.5 Summary

This Chapter has presented the stochastic modelling of environmental loads and load bearing capacity of offshore structures. Wind, wave and current loads have been considered analytically. Especially for wave loads, after a thorough discussion of the transformation of sea state conditions to loads acting on the structural members, the joint probability modelling of environmental variables has been discussed. The capacity of offshore structures is also included in this Chapter. Stochastic modelling of material data has been presented in detail while geotechnical data are also briefly included. Finally, this chapter presents analytically the mechanisms of corrosion that lead to capacity deterioration of structures, and the available models to account for general corrosion during the design process.

5 APPLICATION OF THE RESPONSE SURFACE METHOD IN A TYPICAL JACKET STRUCTURE

5.1 Introduction

Based on the theory and methodology that has been presented previously, this chapter will present the application of structural reliability assessment for a typical reference offshore jacket structure. This analysis will start with a discussion on the analytical formulation of the limit state functions based on widely acceptable and used failure criteria. Following that, an application of the joint probability distribution of wave height and peak spectral period will be presented for a typical North Sea site, in order to determine an analytical relationship between the two correlated variables. Having obtained this, and after description of the reference structure that has been selected, its reliability will be derived in a local and later global-system level considering stochastic modelling of variables, based on the Stochastic Response Surface Method. Material properties, sea state conditions, selection of appropriate wave theory, effect of different statistical distributions in the modelling of the variables will be examined in addition to a thorough investigation of the effect of corrosion on structural members based on different thickness deterioration models.

5.2 Limit State Formulation

Appropriate formulation of limit states should link the performance of the structure with appropriate failure mechanisms that might occur on each member. For the scope of this PhD, limit state functions will be formulated based on the failure criteria commonly applied in structural design. For the reference structure that will be used, static analysis will determine its ultimate strength; therefore static strength will be of interest here.

Strength of a structural member is a property that is determined by its identity, the treatment and processing during and after manufacturing, and the loading at

which it will be subjected during its service life. For cases of complex structures, like the ones that will be studied here, the position of each element will also determine its criticality as a result of the effect of the loads acting on the whole structure.

Static loads refer to the case where a stationary force or a couple (moment) is applied to a member and remains unchanged in magnitude, point and direction of application. Result of a static load might be axial tension or compression, a shear load, a bending load, a torsional load, or any combination of these. In this section, the relation between static loading and strength is discussed, in order to later focus the attention on the predictability of potential failures that might result in degradation of reliability and eventually lead to failure.

In Chapter 2, reference has been made to brittle and ductile failure performance of structures. The same classification can be followed for members' failure, characterizing them in a way that will identify the member's loading performance and allocate appropriate applicable failure mechanisms in order to efficiently design against failure. Although structural members belong to one of those categories, a ductile material can fail in a brittle manner under specific loading conditions. The basic limit for the characterization of a material as ductile is based on the maximum strain (elongation) before failure ε_f and suggests [278]:

$$\varepsilon_f \geq 0.05 \quad (5-1)$$

Ductile materials have a yield strength which is considered the same for compressive and tensile loads $S_{yt} = S_{yc} = S_y$. Contrary to that performance, brittle materials do not have an identifiable yield strength, constituting engineering decision making more difficult, and are classified by individual consideration of ultimate tensile and compressive stresses S_{ut} and S_{uc} respectively. After years of engineering hypothesis, accepted practices have been formally developed to theories that are currently applied in modern engineering. Different theories are distinguished for different types of materials resulting to the following been proposed [278]:

Ductile materials (yield criteria):

- Maximum shear stress (MSS). Commonly referred to as the Tresca or Guest theory, it predicts that 'yielding begins whenever the maximum shear stress in any element equals or exceeds the maximum shear stress in a tension test specimen of the same material when that specimen begins to yield'.
- Distortion energy (DE). Alternatively called the von Mises or von Mises–Hencky theory, shear-energy theory or octahedral-shear-stress theory, it predicts that 'yielding occurs when the distortion strain energy per unit volume reaches or exceeds the distortion strain energy per unit volume for yield in simple tension or compression of the same material'.
- Ductile Coulomb-Mohr (DCM). Also known as internal-friction theory, it is applicable for materials with different tensile and compressive strength and provides a geometrical representation of stress states.

Brittle materials (fracture criteria):

- Maximum normal stress (MNS)
- Brittle Coulomb-Mohr (BCM)
- Modified Mohr (MM)

A universally applicable theory for any material is not currently available therefore different theories are more suitable for different problems. In the following sections, the above mentioned yield criteria will be briefly presented based on [278], [279] and [280]. After presentation of the criteria a critical comparison between them, will distinguish the applicability region of each of them. Presentation of the fracture criteria for brittle materials is beyond the scope of this work and therefore will not be included.

5.2.1 Maximum shear stress (MSS) – Tresca or Guest Theory

Following the observation that on an element that undergoes a tensile load, slip (Lüder) lines are formulated at approximately 45° with the axis of the strip declaring initiation of yield, and in parallel observations in cases of loading to fracture where shear stress is maximized at 45° from the axis of tension, a failure criterion is suggested to describe this failure mechanism. For the fundamental case of a simple tensile test, the corresponding stress might be given as:

$$\sigma = \frac{P}{A} \quad (5-2)$$

Considering the fact that the maximum shear stress occurs on a surface 45° from the tensile stress, the maximum shear stress should be described and correlated to yield strength S_y as follows:

$$\tau_{max} = \frac{\sigma}{2} = \frac{S_y}{2} \quad (5-3)$$

Following connotation from Mohr's circles for three dimensional stress, for a general stress state three principle stresses might be determined as $\sigma_1 \geq \sigma_2 \geq \sigma_3$. Expressing the shear stress using principal stresses, the above equation might be expressed as:

$$\tau_{max} = \frac{\sigma_1 - \sigma_3}{2} \quad (5-4)$$

And the corresponding failure criterion:

$$\tau_{max} \geq \frac{S_y}{2} \text{ or } \sigma_1 - \sigma_3 \geq S_y \quad (5-5)$$

An application of safety factor n might be considered for design purposes as:

$$\tau_{max} \geq \frac{S_y}{2n} \text{ or } \sigma_1 - \sigma_3 \geq \frac{S_y}{n} \quad (5-6)$$

Considering formulation of limit state functions in the form of the difference between supply (allowable load) and demand (actual load) the corresponding LSF is derived denoting failure for the MSS criterion:

$$G_{MSS} = \frac{S_y}{2n} - \tau_{max} \leq 0$$

$$G_{MSS} = \frac{S_y}{n} - (\sigma_1 - \sigma_3) \leq 0 \quad (5-7)$$

Plane stress (or membrane state stress) are problems which refer to cases where all loads applied, are symmetric to the mid-plane direction and at the same time in-plane displacements, strains and stresses can be considered to be uniform through the thickness, and the normal and shear stress components in the z direction are negligible. In such problems, one of the principal stresses is zero therefore only two components can be distinguished (σ_A and σ_B). Table 19, summarizes the formulation of the criterion for each case of principle stresses while Figure 45 represents the MSS theory in plane stress problems.

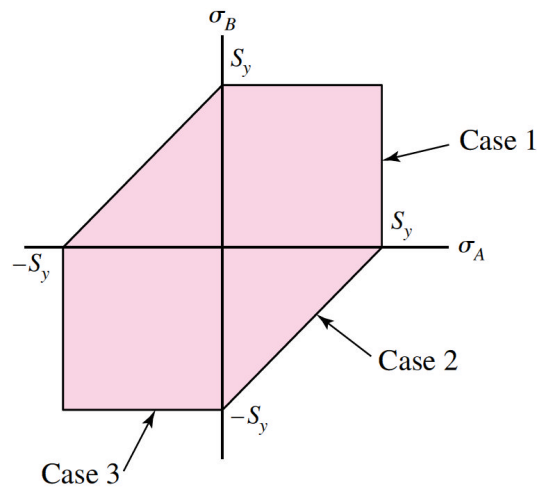


Figure 45: The MSS theory for plane stress problems (two nonzero principal stresses)

Case	Principle Stresses	Principle Stresses Correlation		Failure Criterion
1	$\sigma_A \geq \sigma_B \geq 0$	$\sigma_1 = \sigma_A$	$\sigma_3 = 0$	$\sigma_A \geq S_y$
2	$\sigma_A \geq 0 \geq \sigma_B$	$\sigma_1 = \sigma_A$	$\sigma_3 = \sigma_B$	$\sigma_A - \sigma_B \geq S_y$
3	$0 \geq \sigma_A \geq \sigma_B$	$\sigma_1 = 0$	$\sigma_3 = \sigma_B$	$\sigma_B \leq -S_y$

Table 19: MSS Failure Criterion for Plane stress problems

5.2.2 Distortion energy (DE) – von Mises Stress Theory

This theory was developed through the observation that ductile materials stressed hydrostatically exhibited greater yield strength compared to the values given by a simple tensile test. This phenomenon integrates the problem to a more complicated one, considering the yielding that is related to the angular distortion of the stressed element rather than been described as a simple tensile or compressive test. Introducing the term of hydrostatic stress σ_{av} in each principal direction of the three dimensional stress states, the correlation between principal stresses is given as:

$$\sigma_{av} = \frac{\sigma_1 + \sigma_2 + \sigma_3}{3} \quad (5-8)$$

Considering the above, in a member under tri-axial stress, that undergoes both volume change and energy distortion, each stress component can be described by a hydrostatic σ_{av} and a distortional component $(\sigma_i - \sigma_{av})$. For the three dimensional element, the strain energy per unit volume can be described as:

$$u = \frac{1}{2}(\varepsilon_1\sigma_1 + \varepsilon_2\sigma_2 + \varepsilon_3\sigma_3) = \frac{1}{2E}[\sigma_1^2 + \sigma_2^2 + \sigma_3^2 - 2\nu(\sigma_1\sigma_2 + \sigma_2\sigma_3 + \sigma_3\sigma_1)] \quad (5-9)$$

Substituting the above two equations, the strain energy for producing volume change u_v is given as:

$$u_v = \frac{3\sigma_{av}^2}{2E}(1 - 2\nu) = \frac{1 - 2\nu}{6E}[\sigma_1^2 + \sigma_2^2 + \sigma_3^2 + 2\sigma_1\sigma_2 + 2\sigma_2\sigma_3 + 2\sigma_3\sigma_1] \quad (5-10)$$

The distortion energy is obtained as:

$$u_d = u - u_v = \frac{1 + \nu}{3E} \left[\frac{(\sigma_1 - \sigma_2)^2 + (\sigma_2 - \sigma_3)^2 + (\sigma_3 - \sigma_1)^2}{2} \right] \quad (5-11)$$

Considering that for a simple tensile test, the distortion energy is given as:

$$u_d = \frac{1 + \nu}{3E} S_y^2 \quad (5-12)$$

The general state of stress the failure criterion is then formulated as:

$$\sigma' = \left[\frac{(\sigma_1 - \sigma_2)^2 + (\sigma_2 - \sigma_3)^2 + (\sigma_3 - \sigma_1)^2}{2} \right]^{1/2} \geq S_y \quad (5-13)$$

Where: σ' is the von Mises stress.

For a plane stress problem with two non zero principal stresses, as it was presented before, the expression for the von Mises stress is written as follows, representing a rotated ellipse as shown in Figure 46, including both DE and MSS theories:

$$\sigma' = (\sigma_A^2 - \sigma_A \sigma_B + \sigma_B^2)^{1/2} \quad (5-14)$$

Moving to a Cartecian coordinate system for the three dimensional stress state, the von Mises stress can be rewritten as:

$$\sigma'_{xyz} = \frac{1}{\sqrt{2}} \left[(\sigma_x - \sigma_y)^2 + (\sigma_y - \sigma_z)^2 + (\sigma_z - \sigma_x)^2 + 6(\tau_{xy}^2 + \tau_{yz}^2 + \tau_{zx}^2) \right]^{1/2} \quad (5-15)$$

And for plane stress problems:

$$\sigma'_{xyz} = (\sigma_x^2 - \sigma_x \sigma_y + \sigma_y^2 + 3\tau_{xy}^2)^{1/2} \quad (5-16)$$

Following the same principles for the formulations of the limit states for the failure region in reliability analysis:

$$G_{DE} = \frac{S_y}{n} - \sigma' \leq 0 \quad (5-17)$$

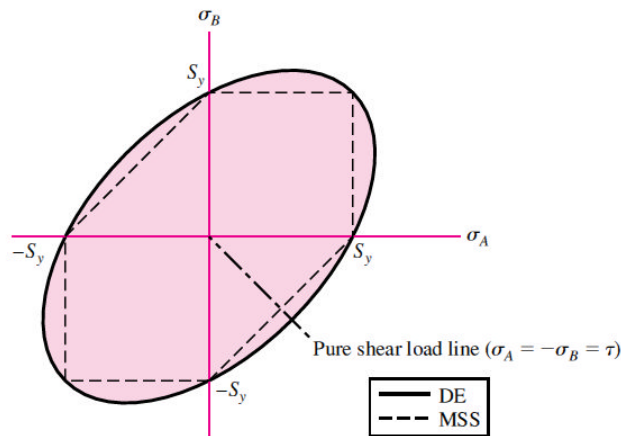


Figure 46: Distortion Energy Theory for plane stress problems

5.2.3 Ductile Coulomb-Mohr (DCM)

The ductile Coulomb-Mohr Theory is applicable for materials where strength against compression is different than that due to tension. Based on the Mohr theory of failure, it is a simplified procedure with results easy to be geometrically interpreted. The concept of the theory is based on combination of tension, compression, and shear tests observing performance to yield or fracture. Based on results of such tests, a graph such as the one in Figure 47 may be drawn and a closed region may be distinguished as the (non-straight) line ABCDE in the figure, above the σ axis in order to describe the stress state of a body.

This theory also known as the internal-friction theory, assumes that the BCD part of the envelop boundary is straight, implying that only tensile and compressive strengths are necessary. Considering a circle with centre C_2 , as illustrated in Figure 47, that connects the maximum and minimum principal stresses, geometrical relationships of similar triangles denote:

$$\frac{B_2 C_2 - B_1 C_1}{OC_2 - OC_1} = \frac{B_3 C_3 - B_1 C_1}{OC_3 - OC_1} \rightarrow \frac{\frac{\sigma_1 - \sigma_3}{2} - \frac{S_t}{2}}{\frac{S_t}{2} - \frac{\sigma_1 + \sigma_3}{2}} = \frac{\frac{S_c}{2} - \frac{S_t}{2}}{\frac{S_c}{2} + \frac{S_t}{2}} \rightarrow$$

$$\rightarrow \frac{\sigma_1}{S_t} - \frac{\sigma_3}{S_c} = 1 \quad (5-18)$$

Where: S_t and S_c denote the tensile and compressive strength respectively. As for the case of the MSS theory, Table 20 and Figure 48, summarize the stress state of the plane stress problem.

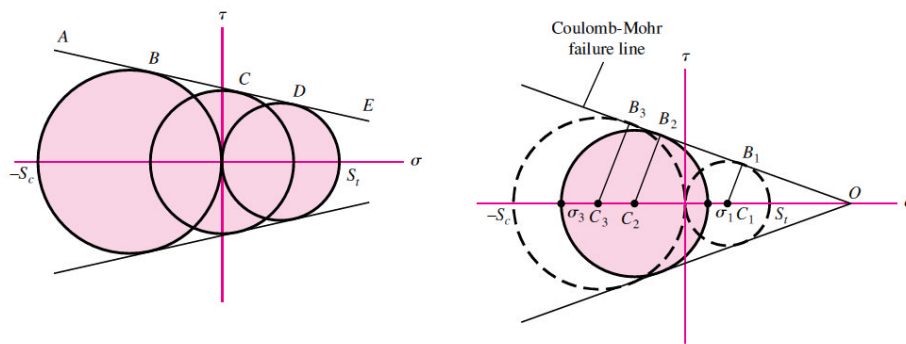


Figure 47: Mohr Cycles and Coulomb-Mohr Failure criterion

Case	Principle Stresses	Principle Stresses Correlation		Failure Criterion
1	$\sigma_A \geq \sigma_B \geq 0$	$\sigma_1 = \sigma_A$	$\sigma_3 = 0$	$\sigma_A \geq S_t$
2	$\sigma_A \geq 0 \geq \sigma_B$	$\sigma_1 = \sigma_A$	$\sigma_3 = \sigma_B$	$\frac{\sigma_A}{S_t} - \frac{\sigma_B}{S_c} \geq 1$
3	$0 \geq \sigma_A \geq \sigma_B$	$\sigma_1 = 0$	$\sigma_3 = \sigma_B$	$\sigma_B \leq -S_c$

Table 20: CM Failure Criterion for Plane stress problems

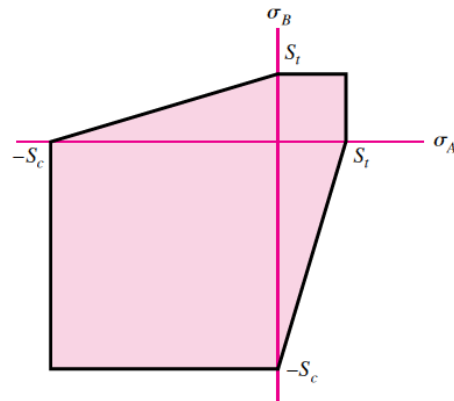


Figure 48: Coulomb-Mohr Failure criterion for Plane Stress problems

The corresponding limit state function G , will be formulated as follows for the failure region:

$$G_{CM} = \frac{1}{n} - \left(\frac{\sigma_1}{S_t} - \frac{\sigma_3}{S_c} \right) \leq 0 \quad (5-19)$$

5.2.4 Comments on Failure Criteria

Based mainly on work presented in [281], performance of different ductile materials has been studied in order to evaluate the applicability of each failure theory and corresponding design criteria. Elaboration of those experimental results illustrates that use of both the maximum shear stress theory and the distortion energy theory is applicable to the design and analysis of ductile materials. Selection of one theory rather than another is subjected to the engineer's decision and available tools. In general, the MSS theory is easier to implement but it is more conservative leading to overdesigned structures (by a percentage of approximately 15 %, which can be derived analytically for the simple case of a tensile specimen). Coulomb-Mohr's theory is applicable in cases of ductile materials with unequal tensile and compressive strengths, providing a simple equation where only those strengths participate and are compared with principal stresses.

A useful comment on the different failure criteria that have been presented above is that for the case of loaded members where stresses are present in one of the axis, and one principal stress is zero due to the two dimensional nature of the problem. The formulation of the principal stresses from the corresponding x-y-z directions can be expressed as:

$$\sigma_{1,2} = \frac{\sigma_x + \sigma_y}{2} \pm \sqrt{\left(\frac{\sigma_x - \sigma_y}{2}\right)^2 + \tau_{xy}^2} \quad (5-20)$$

Where for the axially loaded member:

$$\sigma_x = \sigma_{a,xx} + \sqrt{\sigma_{b,xy}^2 + \sigma_{b,xz}^2} \quad (5-21)$$

$$\sigma_y = 0$$

From (5-20), and neglecting shear stresses:

$$\sigma_1 = \sigma_x = \sigma_{a,xx} + \sqrt{\sigma_{b,xy}^2 + \sigma_{b,xz}^2} \quad (5-22)$$

$$\sigma_2 = 0$$

Applying the above in the limit state functions that have been derived earlier, the following expression can be derived, corresponding and verifying all of them:

$$G_{eq} = \frac{S_y}{n} - \sigma_1 = \frac{S_y}{n} - \sigma_{a,xx} - \sqrt{\sigma_{b,xy}^2 + \sigma_{b,xz}^2} \leq 0 \quad (5-23)$$

Or, alternatively expressed as:

$$G_{eq} = \frac{\sigma_{a,xx} + \sqrt{\sigma_{b,xy}^2 + \sigma_{b,xz}^2}}{S_y/n} \leq 1 \quad (5-24)$$

The above equation is adopted with minor alterations, mainly in the consideration of the safety factor of the material yield and the vectorial sum of

the two stresses due to bending moments, by the standards' provisions for ultimate limit state. The provisions of different standards will be presented in the next chapter. For cases where torsion and shear loads can be neglected, and only axial load and bending moment are present, as in the general case of frame structures, the above limit state corresponds to both the Tresca and the von Mises yield criteria.

Commercial FEA packages can provide values of principal stresses that will allow use of any of the criteria described above. Table 21, Summarizes the limit state functions derived, based on each of the failure criteria.

<p>Maximum shear stress (MSS) - Tresca or Guest theory</p>	$G_{MSS} = \frac{S_y}{2n} - \tau_{max} \leq 0$ $G_{MSS} = \frac{S_y}{n} - (\sigma_1 - \sigma_3) \leq 0$
<p>Distortion energy (DE) - von Mises–Hencky theory</p>	$G_{DE} = \frac{S_y}{n} - \sigma' \leq 0$
<p>Ductile Coulomb-Mohr (DCM)- Internal-friction theory</p>	$G_{CM} = \frac{1}{n} - \left(\frac{\sigma_1}{S_t} - \frac{\sigma_3}{S_c} \right) \leq 0$

Table 21: Limit states for different Failure Criteria

5.2.5 Buckling Limit state

Further to failure criteria for the ultimate strength of structural members, an additional limit state should be introduced for the analysis of members under compression in order to avoid buckling phenomenon. For the appropriate consideration of each case, members undergoing compressive loads should be categorized as either long or intermediate long, with central or eccentric loads. The term column is used for members where the principle stress derives mainly from axial forces that usually fall along the centreline of the member.

For a vertical column that undergoes an axial force P along its centroidal axis, simple compression will occur for relatively low values of this force. Increasing the value of P , and under specific conditions, the column might become

unstable, leading to extensive bending. The critical force between those two states, can be derived following the bending deflection equation of the member, providing a differential equation where appropriate boundary conditions may be applied for each problem and finally resulting in the critical load for unstable bending (Euler column formula):

$$P_{cr} = \frac{C\pi^2 EI}{l^2} \quad (5-25)$$

Where: E is the Young modulus of the material, I the moment of inertia and l the free length of the member. The parameter C , accounts for the end conditions of the member: $C = 1$ for both ends rounded or pivoted; $C = 4$ both ends fixed; $C = 0.25$ one end free and one end fixed; $C = 2$ one end rounded and pivoted, and one end fixed. An alternative useful expression for the critical load can be obtained as:

$$\frac{P_{cr}}{A} = \frac{C\pi^2 E}{(l/k)^2} \quad (5-26)$$

Considering: $I = AK^2$, where: A is the area and k the radius of gyration, and (l/k) is called the slenderness ratio which classifies the length of a column. The ratio P_{cr}/A is called 'crucial unit load'; it has the same units as strength and it represents the necessary load per unit area that should be applied on the column in order to exceed the stability equilibrium. It depends on Young modulus and slenderness ratio, implying that it is independent of the material yield strength.

Based on diagrams between the slenderness ratios and the unit load, also called PQR ratios, a critical value of the slenderness ratio is proposed, in order to distinguish different classes of beams (long, intermediate). A typical value selected for this scope denotes that the Euler's formula is applicable for cases where slenderness ratio is greater than that:

$$\left(\frac{l}{k}\right)_1 = \frac{2C\pi^2 E}{S_y} \quad (5-27)$$

Several formulas have been proposed for cases of slenderness ratio below $(l/k)_1$, most based on a linear relationship between slenderness ratio and unit load. Applying appropriate boundary conditions, the corresponding formula suggests:

$$\frac{P_{cr}}{A} = S_y - \left(\frac{S_y l}{2\pi k}\right)^2 \frac{1}{CE} \quad (5-28)$$

Formulation of the corresponding limit states, will be derived by comparison of the critical load to the actual axial force of each member. Therefore the following LS functions represent failure:

$$G_{b1} = P_{cr1} - N_{xx} = \frac{AC\pi^2 E}{(l/k)^2} - N_{xx}, \text{ for } \left(\frac{l}{k}\right) > \left(\frac{l}{k}\right)_1 \quad (5-29)$$

$$G_{b2} = P_{cr2} - N_{xx} = A \left[S_y - \left(\frac{S_y l}{2\pi k}\right)^2 \frac{1}{CE} \right] - N_{xx}, \text{ for } \left(\frac{l}{k}\right) \leq \left(\frac{l}{k}\right)_1$$

It should be noted that in most design standards, as it will be pointed out in the next chapter, distinguish between different classes of members is presented, following the above theory. This PhD has focused on the yield, buckling and corrosion which are the main failure mechanisms in the design of structural members. Further from that, for the comprehensive consideration of the integrity of structural members, additional mechanisms such as the following should be also considered:

- Creep, is a mechanism that forms gradually over time and can be described as the tendency of solid materials to deform permanently under the effect of stresses below the yield strength of materials. The magnitude and rate of this mechanism is influenced by exposure to high temperature and can lead to failure (ULS) or extensive deformation (SLS).
- Fatigue, is another progressive, localized effect occurring at members subjected in cyclic loading. The formation of the mechanism is initiated by microscopic cracks that are formed in the surface of a member, and it gradually propagates resulting to failure. Fatigue corrosion is another

mechanism that combines corrosion and cyclic loading. As it has already been mentioned, this failure mechanism is of great importance for offshore structures that undergo dynamic loads.

- Fracture, is described as the separation of a member subjected to stress in to two or more pieces. Ductile and brittle materials have a different fracture strength which is determined by tensile tests and stress-strain curves.
- Impact, is considered as a sudden force or acceleration applied on a member over a short period of time which forces the member to react in an unforeseen, and often non linear way. The load bearing capacity of a damaged member should be considered, in order to assess the performance of the structure throughout the rest of its service life.
- Wear, is the erosion of a member due to the action of another surface acting on it, due to the interaction of particles between the two surfaces. This mechanism might result to cross sectional loss of the material which might affect its load bearing capacity.
- In a global level de-pilling is another mechanism that might lead to global failure, when the extensive lateral loads or seabed movement, tends to dislocate the structure.

5.3 Application of Joint Probability Distribution

Before proceeding to the reliability assessment of the selected offshore jacket structure, an example of the application of the joint probability distribution between significant wave height and peak spectral period will be included, as it is required for the next steps of this application, in the formulation of the variable input matrix. Data for this analysis are obtained by [211] for a typical site (Grid Point 14212 - 61.507°N, 0.942°W) in a binned data form for H_s and T_p . For this analysis, different Matlab codes have been conducted and have been verified for the case presented in [282]. The matrix of the bivariate scatter diagram Z and the mean values of the classes are the input of the initial code that

processes the real data. Linear and logarithmic contours of equal probability are then drawn for this data; the later type deals with the fact that peaks that correspond to more observations that occur at regions of lower interest gather more of the contour lines underestimating the significance of lower probabilities regions. Figure 49 and Figure 50 present those plots.

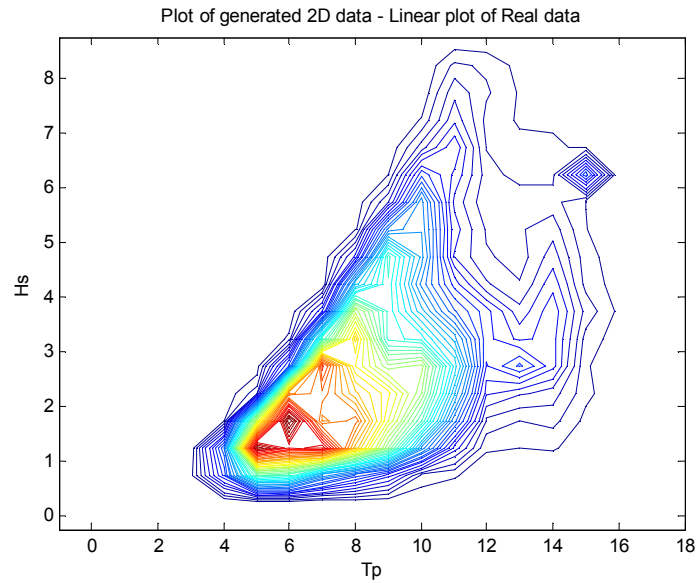


Figure 49: Linear Plot of real data (Hs (m), Tp (s))

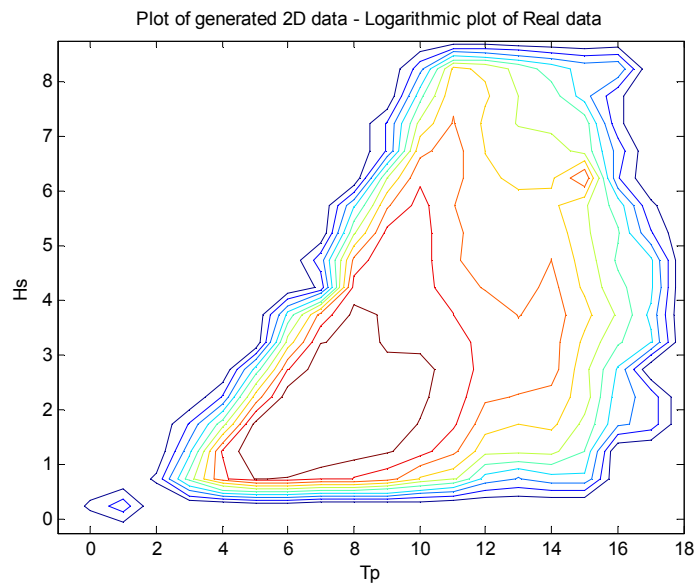


Figure 50: Logarithmic Plot of real data (Hs (m), Tp (s))

The next code that has been conducted, applies statistical fit in order to generate the coefficients of distribution for T_P and H_S for lognormal and Weibull distributions. Before proceeding to approximation of the joint distribution function, further analysis has been carried out in order to estimate the correlation between the two variables. In order to achieve this, the following procedure is introduced: starting from the scatter diagram, and taking the coordinates of the centre of each bin, Cartesian points with a number equalling to that of the observations were generated in order to apply the calculation formula. For the generation of those points, a routine was followed that produces points in a circular or elliptical pattern of radius equalling the half width of each bin dimension. The results of this approach, after verification, have been found to approximate the analytical solution sufficiently. Figure 51, presents a contour generated by those reconstructed data. Table 22, presents the coefficients estimated for this case.

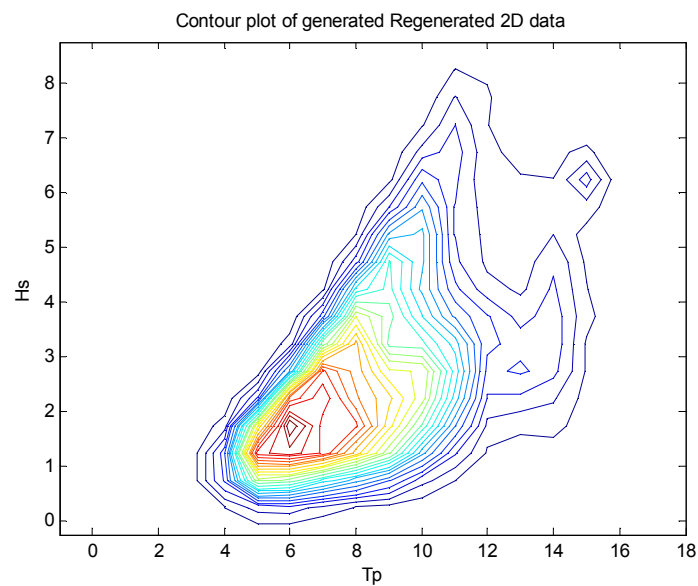


Figure 51: Linear Plot of regenerated data (Hs (m), Tp (s))

	Lognormal Approximation		Weibull Approximation		Correlation coefficient
TP	$\mu = 2.1805$	$\sigma = 0.2709$	$\lambda = 10.1157$	$\kappa = 3.9406$	ρ 0.5624
HS	$\mu = 0.9792$	$\sigma = 0.5027$	$\lambda = 3.4227$	$\kappa = 2.0934$	

Table 22: Distribution coefficients

Once the distributions' coefficients have been estimated, three different codes have been conducted in order to produce different contours that will allow selection of the most appropriate distribution. Each code will generate bivariate correlated random numbers. The procedure followed, starts with generation of a sequence of sets of values following normal distributions $N(0,1)$ taking into account a correlation coefficient. After that, for each set, the value of the Normal cumulative distribution function F_n is calculated and the final values of each distribution will be derived as the inverse cumulative distribution function of $F_n^{-1}(i)$ which corresponds accordingly to any statistical distribution. This is an easy procedure to program. The code will later bin data in a new scatter matrix and finally linear and logarithmic contours will be plotted. Using Lagrange interpolation, smoothed contours are produced. For the three different joint distribution functions, the results are presented in Figure 52 through Figure 54. Although linear plots are generated as well, the logarithmic ones will be presented since they include more information for the contours of lower probability.

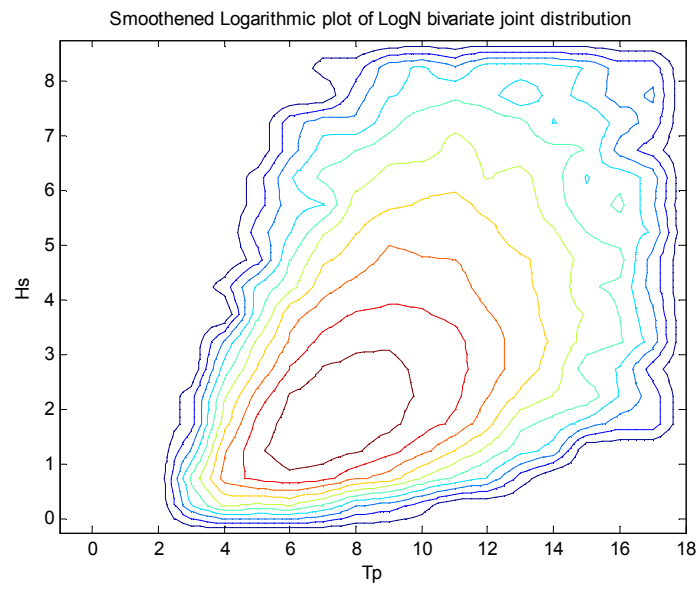


Figure 52: Logarithmic plot of LogN bivariate joint distribution (smoothened) (H_s (m), T_p (s))

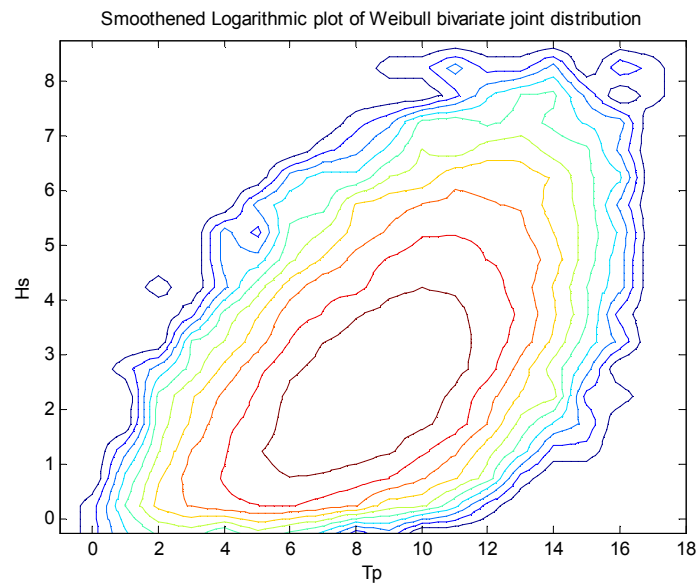


Figure 53: Logarithmic plot of Weibull bivariate joint distribution (smoothened) (H_s (m), T_p (s))

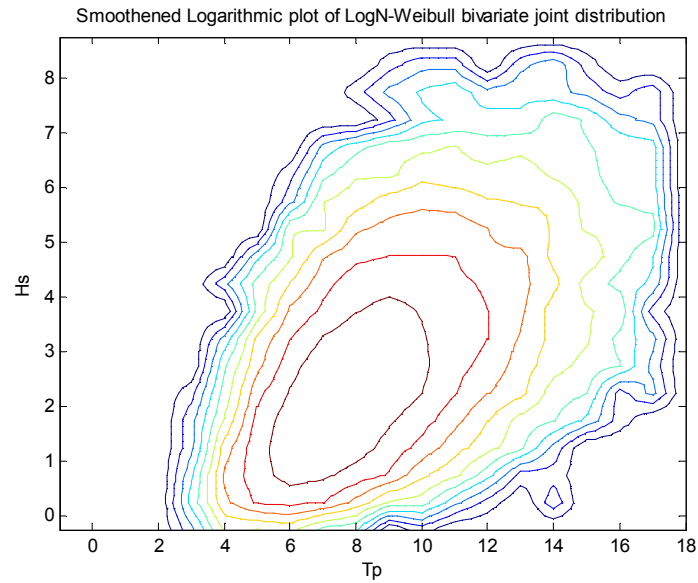


Figure 54: Logarithmic plot of LogN-Weibull bivariate joint distribution (smoothened) (H_s (m), T_p (s))

From the above plots, and based on visual observation [282], the bivariate Weibull distribution provides poor approximation of the original data underestimating the extreme values of T_p and allocating more points in H_s . Further, the area of the higher contour is larger, providing a less steep peak. The bivariate Lognormal and the marginal Lognormal-Weibull joint distributions provide a better fit on the approximation of the original data with the later having a close shape of the outer contour that is the one of interest, since it represents the area of low probability. The codes that have been conducted also provide the relative error contours between the original and the generated data in a logarithmic plot, distinguishing regions of greater error concentration. According to [283], the Lognormal distribution can provide good fit for cumulative probabilities below 0.99, while it deteriorates above this threshold. Figure 55, shows the comparison between the (reconstructed) original data, the Lognormal and the marginal Lognormal-Weibull cumulative distribution functions for the region of higher probabilities. It can be observed that the latter distribution function approximates better the curve of the original data.

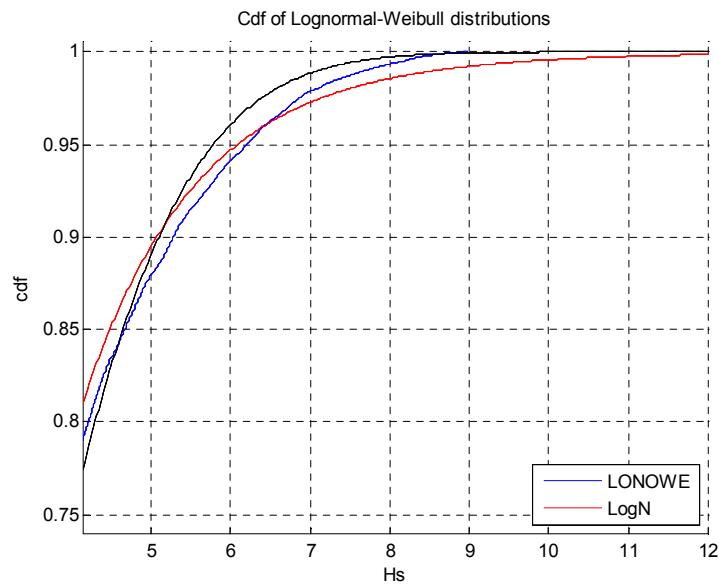


Figure 55: Comparison of best fit on the tail region of the CDF for H_s (m)

Having determined the most appropriate joint distribution model, the long term response of wave climate should be determined. There are two main approaches for the prediction of the design value of waves [284]; the 100 years storm and the 100 years design curve. The design curve approach refers to the use of the joint distribution function defining the region that the return period, which corresponds to the average period between exceedance of one value, probability is exceeded. This method will be followed here and the return period of 100 years will be selected since this is considered by most researchers and modern standards.

From the marginal Lognormal-Weibull distribution function, for the tail region of the cumulative distribution function, the extreme value corresponding to the 100 year return period can be evaluated, once the cumulative probability $[P(H_s)]_{T_r}$ of a given return period T_r is calculated as [285]:

$$[P(H_s)]_{T_r} = 1 - \frac{1}{8 \times 365 \times T_r} \quad (5-30)$$

Applying the inverse Weibull probability distribution function for the above probability, will derive the corresponding value for the significant wave height as

$H_s = 11.47$ m. The conditional probability of the spectral peak period for a given significant wave height is calculated as [283]:

$$T_p = \exp \left[\mu_{T|P} - \sqrt{1 - \rho_{HT}^2} \sigma_T \right]$$

Where: (5-31)

$$\mu_{T|P} = \mu_T + \rho_{HT} \frac{\sigma_T}{\sigma_H} (\ln H_s - \mu_H)$$

For the distributions that have been derived, and for the specific value of H_s the corresponding $T_p = 11.0$ sec. Based on literature [191], the results derived above, are reasonable. The extreme value with the return period of 100 years is a probabilistic value, so in order to derive a deterministic value of this value several approaches have been proposed and are presented in Table 23, [286]. From this table, that summarizes the work of several researchers [287], [288], [289], [290], [291], [292], [293], [294], Wiegel's work [295], the following formula correlates significant wave height to the maximum design wave height:

$$H_{max} = 1.87H_s \quad (5-32)$$

The procedure described and followed above has been verified with the example case presented in [230].

Reference	Data Type	H_s/H_0	$H_{1/10}/H_s$	H_{max}/H_s
Munk [287]	Field data	1.53	---	---
Seiwell [288]	Field data	1.57	---	---
Wiegel [290]	Field data	---	1.29	1.87
Barber [289]	Theoretical	1.61	---	1.50
Putz [292]	Field data	1.63	---	---
Longuet-Higgins [291]	Theoretical	1.60	1.27	1.77
Putz [292]	Theoretical	1.57	1.29	1.80
Darbyshire [293]	Field data	1.60	---	1.50
Hamada et al. [294]	Experimental	1.35	---	---

Table 23: Wave Height Statistical Correlations [286]

The values that are presented in Table 23, refer to a Reyleigh distribution fit of observed data, which stands as a special case of the Weibull distribution. The statistical values of interest of the Reyleigh distribution as presented in a parametric plot in Figure 56, are the following:

- The average wave height H_o
- The significant wave height H_s or $H_{1/3}$
- The 1/10 highest have height $H_{1/10}$

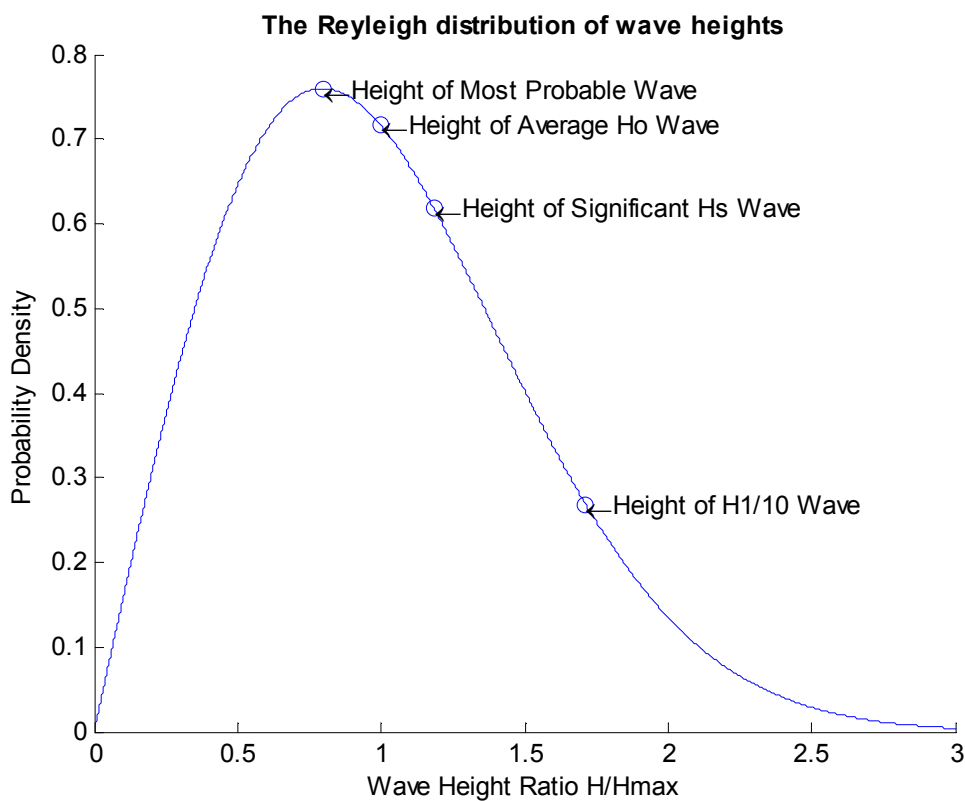


Figure 56: The Reyleigh distribution of wave heights

5.4 Reference Structure

Based on experience from offshore oil and gas platforms, the jacket-type support structure is a commonly selected configuration of subsea structures for medium and high water depths. Current interest for such locations considering

massive deployment of wind turbines, sets a reference depth between 40-50 m. Benefits of the jacket configuration compared to others, are discussed in [296] and [297]. Selection and implementation of a jacket support structure for the Beatrix wind farm, which has been deployed in a depth of 45 m, and stands as the deepest location so far, countersigns its applicability for this water depth [60].

For the application of the reliability assessment procedure that has been developed in the previous chapters, a typical structure will be examined for the reference depth of 50 m. The design depth in conjunction with the operational loads, will determine the general layout of the structure, in aspects of number of required legs, general layout and consideration of loading conditions. The depth of interest allows a four-legged configuration located in the corners of a square cross section at each elevation.

The structure is assumed to be constructed of tubular steel members of common 355 MPa steel with Young modulus of 200 GPa. Each of the legs is supported with a pile driven through the legs and extended to the seabed. The four legs are battered to achieve better stability against toppling, with a common bat angle with ratio 1:10. It has 5 elevations of horizontal and 4 of inclined full X bracing. The base elevation, which is positioned on the seabed, has dimensions of 25.0 m x 25.0 m and the structure extends above the water surface by 12 m, resulting to a total height of 62 m.

On top of the jacket support structure, an additional load will be considered to account for any operational loads acting on top of the support structure eg. the loads due to machinery on the top of an oil and gas platform, including the drag force imposed by the complicated geometry of the top side, or the aerodynamic loads induced by the operation of a wind turbine including the drag of the turbine tower. For this scope, an additional load will be applied on the top of the support structure proportional to the square of wind speed. The technique of ultra-stiff elements was employed in order to transfer the point loads to the legs, avoiding extensive stresses and deflection to the members of the top elevation.

The structure has been designed with the commercial software DNV SESAM [298], specialized for the design of offshore steel structures. This software allows efficient modelling of environmental loads, including wave loads and piling, providing the static and dynamic response of structural members in the form of, bending moments, axial forces and principal stresses. The basis for the design of this structure was selected to be API RP 2A WSD, since this is the most conservative existing design standard, as it will be discussed in the next chapter. Design according to the provisions of this standard, has ensured that both buckling and ultimate strength capacity of members have been achieved. Table 24, presents the design load input parameters for dimensioning of the structure. For the numbering of members the following common notation has been followed: for legs, the string $A0B$ characterizes the member, for horizontal braces, $A1B$, while for vertical braces $A5B$, where A represents the elevation and B the orientation of the member.

Although selection of different loading conditions describing the wave sea state is common in offshore structures taking into account deployment along preferential directions, having a greater significance for larger scale and more complicated structures, the symmetry of the reference structure allows consideration of two directions of 'wave attack' (0 and 45 degrees), and application of the same derived cross sections to the corresponding members. Having ensured that the operational loads have been considered in the worst case direction combined to the environmental loads, this simplification diminishes significantly the number of load cases that need to be examined, and in the present study will allow investigation of more parameters.

Figure 57, illustrates the structure of reference, while in Appendix C, details on the cross sections of members are included.

<i>Parameter</i>	<i>Value</i>	<i>Unit</i>
Significant Wave Height	11.47	m
Design Wave Height	21.46	m
Associated Wave Period	13.3	sec
Drag Coefficient	1.05	
Morison Coefficient	1.2	
Wind Speed	25	m/sec
Current Profile	MWL: 1 -25 m: 0.5	m/sec

Table 24: Design load input parameters for dimensioning of the structure

14 Sep 2010 14:34
baseline3
Analysis4
c1
FEM Loadcase = 4

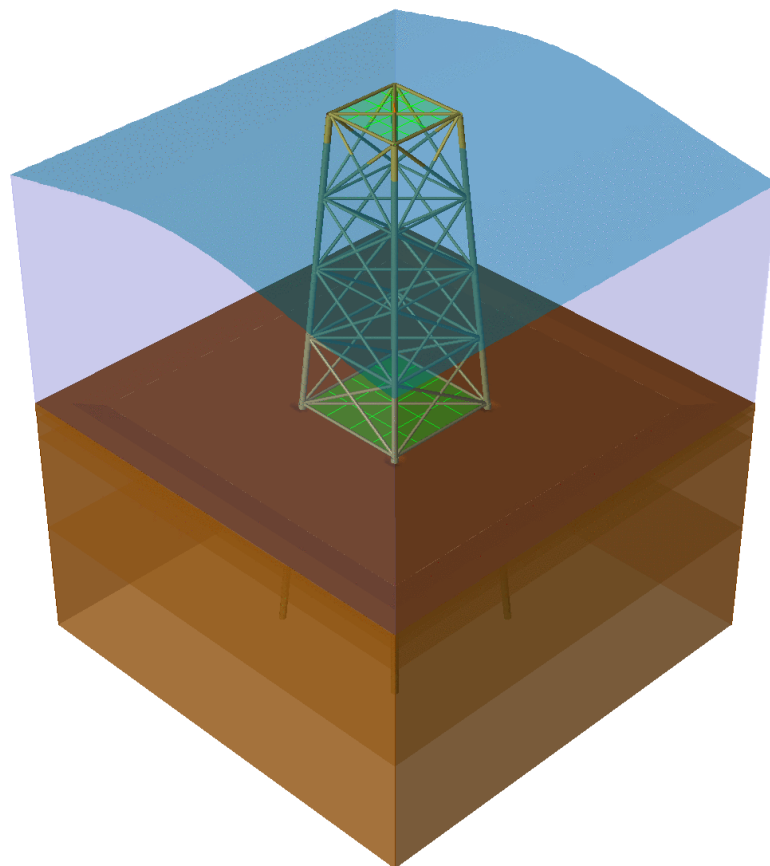


Figure 57: FEA model of a jacket structure developed in DNV GeniE software

5.5 Component Structural Reliability Assessment

5.5.1 Base case

The case that will stand as the basis for comparison in the later sections, accounts for four stochastic variables that will be considered in this analysis. Incorporation of more variables is feasible, however as it will be derived from the analysis, fewer variables should be modelled stochastically that have a greater effect on the structural response. For the derivation of the reliability indices of each member, several simulations have been executed in FEA software and the results are imported in the MATLAB code that has been developed for the data regression and later the calculation of the FORM and SORM reliability index. The four variables that are considered stochastically are summarized in Table 25.

	Variable	Distribution Type	Coefficients	Units
x_1	Wave height	Reyleigh	$A = 8.08$	m
x_2	Wind Force	Normal	(400,40)	kN
x_3	Current	Normal	(0.8,0.15)	m/sec
x_4	Yield	LogNormal	(2.55,1.398)	MPa

Table 25: Properties of stochastic variables

The structure has been modelled according to 5th order Stokes wave theory, considering drag and Morison coefficients for rough members' surfaces ($C_d = 1.05$ and $C_m = 1.2$). The effect of those assumptions, as well as the contributions of each of the variables will be examined in the later sections. Table 26 to Table 28, summarize the results of reliability indexes of members, for directions of 0 and 45 degrees for this base case.

Member ID	β		P_f		Member ID	β		P_f	
	0 degs	45 degs	0 degs	45 degs		0 degs	45 degs	0 degs	45 degs
b116	35.01	35.01	∞	∞	b316	20.87	9.05	4.83E-97	7.08E-20
b115	35.01	35.01	∞	∞	b315	20.86	14.8	6.64E-97	7.03E-50
b114	54.83	54.83	∞	∞	b314	6.94	7.68	1.99E-12	8.14E-15
b113	54.83	54.83	∞	∞	b313	10.48	7.52	5.40E-26	2.69E-14
b112	54.83	54.83	∞	∞	b312	6.96	7.5	1.65E-12	3.16E-14
b111	54.83	54.83	∞	∞	b311	10.46	7.76	6.55E-26	4.23E-15
b216	18.71	26.7	2.04E-78	2.30E-157	b416	8.37	6.02	2.84E-17	8.92E-10
b215	18.72	16.38	1.70E-78	1.43E-60	b415	8.36	9.64	3.03E-17	2.80E-22
b214	9.33	11.43	5.45E-21	1.45E-30	b414	5.76	6.91	4.24E-09	2.42E-12
b213	12.33	9.52	3.14E-35	8.36E-22	b413	8.98	6.7	1.31E-19	1.05E-11
b212	9.70	9.48	1.53E-22	1.27E-21	b412	6.00	6.72	9.61E-10	9.01E-12
b211	12.34	10.62	2.60E-35	1.14E-26	b411	8.98	7.04	1.36E-19	9.50E-13

Table 26: Reliability Index of Horizontal Members

Member ID	β		P_f		Member ID	β		P_f	
	0 degs	45 degs	0 degs	45 degs		0 degs	45 degs	0 degs	45 degs
b158	6.74	6.08	7.67E-12	5.96E-10	b358	6.16	5.37	3.62E-10	3.95E-08
b157	6.76	6.81	6.89E-12	4.93E-12	b357	6.16	5.24	3.59E-10	8.14E-08
b156	5.7	6.77	5.95E-09	6.48E-12	b356	5.31	5.12	5.46E-08	1.56E-07
b155	5.55	5.92	1.44E-08	1.64E-09	b355	5.33	5.19	5.04E-08	1.05E-07
b154	6.94	5.93	1.99E-12	1.48E-09	b354	6.09	5.21	5.69E-10	9.37E-08
b153	6.93	6.63	2.10E-12	1.64E-11	b353	6.08	5.14	6.04E-10	1.38E-07
b152	5.54	6.78	1.50E-08	6.10E-12	b352	5.33	5.2	5.02E-08	9.75E-08
b151	5.7	6.05	5.86E-09	7.08E-10	b351	5.3	5.35	5.65E-08	4.44E-08
b258	7.79	5.79	3.28E-15	3.62E-09	b458	3.72	4.48	9.86E-05	3.79E-06
b257	7.81	5.88	2.89E-15	2.06E-09	b457	3.72	4.48	9.99E-05	3.69E-06
b256	5.27	5.68	6.84E-08	6.58E-09	b456	6.37	4.35	9.53E-11	6.85E-06
b255	5.26	5.66	7.26E-08	7.37E-09	b455	6.34	4.64	1.18E-10	1.73E-06
b254	7.51	5.69	3.01E-14	6.38E-09	b454	3.79	4.69	7.65E-05	1.35E-06
b253	7.51	5.71	2.87E-14	5.70E-09	b453	3.79	4.32	7.57E-05	7.74E-06
b252	5.25	5.85	7.71E-08	2.47E-09	b452	6.33	4.45	1.22E-10	4.23E-06
b251	5.27	5.74	6.93E-08	4.78E-09	b451	6.37	4.51	9.75E-11	3.20E-06

Table 27: Reliability Index of Vertical Members

<i>Member ID</i>	β		P_f	
	<i>0 degs</i>	<i>45 degs</i>	<i>0 degs</i>	<i>45 degs</i>
b404	14.72	10.82	2.32E-49	1.40E-27
b403	10.66	10.20	7.76E-27	1.03E-24
b402	10.66	10.88	7.80E-27	7.17E-28
b401	14.73	19.52	2.13E-49	4.03E-85
b304	8.72	13.87	1.44E-18	4.54E-44
b303	8.14	7.36	1.99E-16	9.24E-14
b302	8.15	13.83	1.83E-16	7.84E-44
b301	8.71	7.23	1.54E-18	2.37E-13
b204	5.74	19.27	4.78E-09	4.54E-83
b203	7.45	6.26	4.52E-14	1.95E-10
b202	7.46	19.96	4.39E-14	5.78E-89
b201	5.74	5.72	4.76E-09	5.29E-09
b104	4.79	10.07	8.45E-07	3.93E-24
b103	5.23	4.50	8.62E-08	3.41E-06
b102	5.22	10.13	8.74E-08	2.09E-24
b101	4.79	4.66	8.41E-07	1.59E-06

Table 28: Reliability Index of Legs Members

From the results presented above it can be observed that reasonable values are derived for the reliability indices of the members. The large values that occur in members b1111-b1116 and refer to the horizontal members of the seabed elevation are due to the stiff piling conditions that have been selected in this analysis that result them to carry very small loads. In general, horizontal X brace elements are designed to carry small loads, but should be included in the design for practical reasons.

Variation in the direction of loading shows the worse case that should be considered in the minimum reliability that will eventually size the members. For the example of the legs, this fact is more obvious since in the 0 degrees of approach there is symmetry in loading for two sets of legs while in 45 degrees, two legs have symmetrically equal reliability, while the other two have different values referring to the different loads acting on them.

As far as the legs reliability index of different parts along its length is concerned, due to the uniform cross section that has been selected it is observed that reliability index values follow the cumulative load distributed along each of the

elevation of the structures; this indicates that members at lower elevations which suffer from greater stresses, will have lower values of reliabilities ($\beta = 4.79 - 14.73$ for 0 degrees and $\beta = 4.50 - 10.20$ for 45 degrees).

Smaller values that have can noticed on the top vertical X-braces of the structure (members b457-b458, $\beta = 3.72$), are due to the fact that the topside of the structure has not been analytically designed so those members locally suffer from increased loads that carry the loads of the topside. In a more realistic structure this phenomenon would have been avoided by appropriate design of the topside-structure interaction with adequate load paths that would transform those loads more uniformly to the rest of the structure.

Small deviations on the reliability indexes of symmetrical members in 45 degrees case is due to the fact that wind load is acting in a constant direction (0 degrees) compared to the different directions of the wave and current loads slightly “disturbing” this symmetry. However, the small scale of this deviation illustrates that the effect of the wind load is minimum compared to that of the sea state loads. Further, it should be essential to point out that the large values that are presented on the above tables refer only to two cases of loading where some of the members suffer more than others while considering the different directional load cases other members would be in this place. This means that in order to derive the total reliability index of each member, every possible direction of loading should be indentified and examined, and the final reliability of each member would equal the minimum of the values that have been partially calculated. For the case that has been examined, and due to the assumption that the same loading conditions act on the structure every 90 degrees, the final values of reliability indices can be derived based on the geometrical symmetry of the structure. Table 29, summarizes those results incorporating 8 different, but symmetrical, directions acting on the structure.

<i>Member ID</i>	<i>min(β)</i>						
b116	35.01	b416	6.02	b104	4.50	b252	5.25
b115	35.01	b415	6.02	b103	4.50	b251	5.25
b114	54.83	b414	5.76	b102	4.50	b358	5.12
b113	54.83	b413	5.76	b101	4.50	b357	5.12
b112	54.83	b412	5.76	b158	5.54	b356	5.12
b111	54.83	b411	5.76	b157	5.54	b355	5.12
b216	16.38	b404	10.20	b156	5.54	b354	5.12
b215	16.38	b403	10.20	b155	5.54	b353	5.12
b214	9.33	b402	10.20	b154	5.54	b352	5.12
b213	9.33	b401	10.20	b153	5.54	b351	5.12
b212	9.33	b304	7.23	b152	5.54	b458	3.72
b211	9.33	b303	7.23	b151	5.54	b457	3.72
b316	9.05	b302	7.23	b258	5.25	b456	3.72
b315	9.05	b301	7.23	b257	5.25	b455	3.72
b314	6.94	b204	5.72	b256	5.25	b454	3.72
b313	6.94	b203	5.72	b255	5.25	b453	3.72
b312	6.94	b202	5.72	b254	5.25	b452	3.72
b311	6.94	b201	5.72	b253	5.25	b451	3.72

Table 29: Minimum Reliability index of members, incorporating 8 different directions

Further to the above analysis for ultimate strength of members, reliability assessment for those under compression for buckling was performed. During the analysis, two different values of the parameter C in the critical buckling force calculation were considered, 1.2 (recommended value) and 4 (theoretical value) as it can be found in [278], in order to evaluate the effect of this parameter on the derived values of reliability indices. Results of this analysis for the 10 more critical members are presented in Table 30 which corresponds to vertical diagonal bracing members. From those values the conclusion that can be drawn is that coefficient C plays a significant role to the outcome of this analysis affecting significantly the value of β .

Member ID	$C = 4$		$C = 1.2$	
	0 degs	45 degs	0 degs	45 degs
b155	7.58	8.44	3.55	4.02
b152	7.58	10.82	3.55	5.25
b255	8.09	9.51	3.84	4.63
b252	8.09	10.61	3.85	5.17
b154	17.38	8.45	9.00	4.05
b355	9.04	10.72	4.45	5.38
b352	9.05	11.54	4.45	5.77
b254	28.32	9.53	15.10	4.68
b258	25.77	9.70	13.76	4.84
b257	25.74	10.65	13.76	5.25

Table 30: Reliability indices for buckling limit states (10 critical members)

5.5.2 Sensitivity analysis of design parameters

In this section, the effect of design parameters in the resultant values of reliability index will be investigated. Surface roughness, expressed through appropriate consideration of C_d and C_m coefficients, selection of wave modelling theory, effect of different statistical distributions and variation in stochastic loads properties are studied as the main model uncertainties; further sources of model uncertainty will not be investigated as they stand out of the scope of this contribution. A further analysis regarding the effect of corrosion modelling to the resulting values of β will show the reliability deterioration of the structure throughout its service life. For each case, the results with the major effect of the parameter examined will be illustrated.

5.5.2.1 Wave modelling

5.5.2.1.1 Effect of surface roughness

The effect of surface roughness of structural members will be examined based on provisions of standards for drag and inertial coefficients. Based on the fact that the base case accounts for rough cylinders ($C_D = 1.05$ and $C_M = 1.2$) according to API's provisions, smooth surface cylinders should be modelled with appropriate coefficients ($C_D = 0.65$ and $C_M = 1.6$). It is expected that members of greater surface roughness will generate greater drag force and therefore their relevant reliability index would be higher. Table 31 summarizes

the results of β and the related difference to the base case for the 30 members with the greatest effect for 0 degrees.

<i>Member ID</i>	β_{rough}	β_{smooth}	Relative error (%)	<i>Member ID</i>	β_{rough}	β_{smooth}	Relative error (%)
b415	8.36	15.05	80.03	b257	7.81	10.65	36.32
b416	8.37	15.06	79.98	b201	5.74	7.81	36.11
b301	8.71	13.62	56.33	b204	5.74	7.81	36.09
b304	8.72	13.63	56.29	b151	5.70	7.75	36.00
b158	6.74	9.61	42.62	b156	5.70	7.75	35.93
b157	6.76	9.63	42.53	b302	8.15	10.96	34.48
b404	14.72	20.54	39.54	b303	8.14	10.95	34.48
b401	14.73	20.55	39.50	b212	9.70	13.03	34.36
b357	6.16	8.56	39.02	b403	10.66	14.27	33.90
b358	6.16	8.56	38.99	b402	10.66	14.27	33.90
b458	3.72	5.13	37.80	b414	5.76	7.63	32.52
b457	3.72	5.12	37.67	b312	6.96	9.16	31.66
b152	5.54	7.56	36.55	b256	5.27	6.91	31.06
b155	5.55	7.58	36.49	b251	5.27	6.90	31.00
b258	7.79	10.62	36.39	b352	5.33	6.97	30.80

Table 31: Reliability index of smooth and rough cylinders (30 critical members)

The increase of reliability index is greater for members that have already greater values of β in both cases. Further, due to the increase to the distributed loads along the height of the structure, the resultant load acting on the structure with the rougher members will be greater on the members of the lower elevation, leading to greater difference of reliability compared to a structure with smoother components. This phenomenon, illustrates that as the structure ages, and the smoothness of the members' surfaces change due to corrosion, marine growth etc, the effect of environmental loads acting on the structure becomes more significant. This verifies the assumption presented in theory regarding deterioration of reliability due to decrease in the relative distance between load effect and resistance of the structure.

5.5.2.1.2 Different wave theories

Selection of the appropriate wave modelling theory is another decision that has a crucial impact on the accuracy of the prediction of the performance of the

structure for given input conditions. Increased complexity of more analytical methods may raise restriction to engineers, especially when appropriate software for modelling is not available; however, this fact might under or overestimate the actual performance of the structure. The effect of this inaccuracy is therefore transferred in the reliability calculation misjudging the actual performance of members. The base case has been modelled using 5th order Stokes equations model. Table 32, presents the results of the 20 members with the most significant deviation when modelled with different wave modelling theories, for the case of 0 degrees of wave angle. For this comparison, Airy wave theory and Stream function theory (3rd and 11th order) have been considered.

Member ID	β				Deviation from Stokes 5 th order		
	Stokes 5 th Order Theory	Airy Theory	Stream function (3 rd order)	Stream function (11 rd order)	Airy Theory (%)	Stream function (3 rd order) (%)	Stream function (11 rd order) (%)
b301	8.71	14.16	8.73	8.73	62.5	0.3	0.2
b304	8.72	14.17	8.74	8.74	62.5	0.2	0.2
b203	7.45	11.23	7.55	7.54	50.8	1.3	1.3
b202	7.46	11.24	7.55	7.55	50.6	1.2	1.2
b302	8.15	12.07	8.20	8.19	48.1	0.6	0.5
b303	8.14	12.05	8.19	8.18	48.0	0.6	0.5
b452	6.33	8.89	6.38	6.38	40.5	0.8	0.8
b455	6.34	8.90	6.39	6.39	40.4	0.7	0.7
b456	6.37	8.81	6.43	6.43	38.3	0.9	0.9
b451	6.37	8.80	6.42	6.42	38.2	0.9	0.8
b102	5.22	7.05	5.29	5.29	35.1	1.3	1.3
b103	5.23	7.05	5.29	5.29	34.9	1.1	1.1
b453	3.79	5.00	3.82	3.82	31.8	0.9	0.9
b454	3.79	4.99	3.82	3.82	31.7	0.8	0.8
b458	3.72	4.79	3.75	3.74	28.9	0.7	0.6
b457	3.72	4.79	3.74	3.74	28.8	0.6	0.5
b403	10.66	13.71	10.77	10.78	28.6	1.0	1.1
b402	10.66	13.71	10.77	10.77	28.6	1.0	1.1
b352	5.33	6.81	5.38	5.38	27.7	1.0	1.0
b355	5.33	6.81	5.38	5.38	27.7	1.0	1.0

Table 32: Reliability index for different wave theories (20 members with critical effect)

From the figures above, the conclusion that can be derived is that compared to the 5th order Stokes wave theory, Airy wave theory tend to underestimate the environmental loads, resulting to greater values of reliability indices. Greater deviation is found to occur in the mid elevation members. Stream function produces similar results than the base case with limited deviation (up to 4.3 %). The order of the stream function does not seem to provide a significant difference on the values of reliability index for the case studied. Finally from the sea state conditions that have been selected and the structure that has been examined, the results provided from the 5th order Stokes wave theory, which compiles to API's provisions for given environment, provide the most conservative results. This comparison illustrates the significance of the selection of the appropriate wave theory.

5.5.2.2 Effect of statistical distributions

Appropriate modelling of the stochastic variables is another issue that should be treated efficiently in the pre-processing of the reliability assessment. In the literature review of this Thesis, different statistical distributions have been proposed for different loads and design parameters. In the base case, relevant distributions have been selected based on the nature of the variables. In this section, the values of β that have been derived for the base case will be compared to values obtained by a new calculation of reliability derived by considering equivalent normal distributions for all of the variables modeled stochastically. Table 33 presents the properties of those equivalent normal distributions while Table 34 provides comparative results of the 20 members with greater deviations on the results (0 degrees).

	<i>Variable</i>	<i>Coefficients</i>	<i>Units</i>
<i>x1</i>	Wave height	(8.799,4.5932)	m
<i>x2</i>	Wind Force	(400,40)	kN
<i>x3</i>	Current	(0.8,0.15)	m/sec
<i>x4</i>	Yield	(355,25)	MPa

Table 33: Parameters of equivalent normal distributions

<i>Member ID</i>	β_{base}	β_{normal}	Deviation (%)	<i>Member ID</i>	β_{base}	β_{normal}	Deviation (%)
b101	4.79	5.19	8.4	b304	8.72	9.13	4.7
b104	4.79	5.19	8.4	b258	7.79	8.15	4.6
b201	5.74	6.20	8.0	b212	9.70	10.14	4.6
b204	5.74	6.20	8.0	b303	8.14	8.51	4.6
b415	8.36	8.96	7.2	b411	8.98	9.39	4.5
b416	8.37	8.96	7.1	b413	8.98	9.39	4.5
b404	14.72	15.49	5.2	b313	10.48	10.95	4.5
b401	14.73	15.49	5.2	b158	6.74	7.04	4.5
b402	10.66	11.19	5.0	b315	20.86	21.79	4.5
b403	10.66	11.19	5.0	b302	8.15	8.51	4.4

Table 34: Reliability indices for equivalent normal distributions

From the above results, it can be concluded that consideration of the equivalent normal variables overestimates values of reliability indices. This results in less conservative approximation of β . In the list provided, greater deviation occurs in the lower elevation legs members which are the most significant members in the design of a jacket structure. The maximum of 8.4 % in the value of β highlights the significance of appropriate statistical modeling of the stochastic variables.

5.5.2.3 Stochastic variables variation

5.5.2.3.1 Loading variables

Each of the variables that are considered stochastically in the reliability assessment of a structure, has a different contribution in the resultant value of β . This section presents the comparison of the base case, with three different simulations of cases where the three environmental loads, wave, wind and current, have been decreased by 25 %. The effect on β s are presented in Table 35, for the case of the 30 more critical members (lower values of β in the base case) and wave angle of 0 degrees.

<i>Member ID</i>	β_{base}	$\beta_{0.75 \times wave}$	$\beta_{0.75 \times wind}$	$\beta_{0.75 \times curr}$	<i>Member ID</i>	β_{base}	$\beta_{0.75 \times wave}$	$\beta_{0.75 \times wind}$	$\beta_{0.75 \times curr}$
b457	3.72	5.52	3.72	3.76	b352	5.33	7.67	5.33	5.35
b458	3.72	5.53	3.72	3.75	b355	5.33	7.66	5.33	5.35
b453	3.79	5.62	3.79	3.82	b152	5.54	7.96	5.55	5.57
b454	3.79	5.61	3.78	3.82	b155	5.55	7.96	5.56	5.57
b101	4.79	5.81	4.79	4.79	b151	5.70	8.18	5.71	5.71
b104	4.79	5.82	4.79	4.80	b156	5.70	8.18	5.71	5.73
b102	5.22	7.52	5.24	5.24	b201	5.74	7.09	5.73	5.74
b103	5.23	7.53	5.23	5.24	b204	5.74	7.08	5.74	5.74
b252	5.25	7.57	5.26	5.28	b414	5.76	8.23	5.75	5.80
b255	5.26	7.56	5.25	5.28	b412	6.00	8.56	6.00	6.05
b251	5.27	7.58	5.27	5.29	b353	6.08	8.68	6.09	6.13
b256	5.27	7.58	5.27	5.30	b354	6.09	8.67	6.09	6.13
b351	5.30	7.64	5.31	5.34	b357	6.16	8.77	6.16	6.20
b356	5.31	7.64	5.32	5.34	b358	6.16	8.78	6.16	6.21
b352	5.33	7.67	5.33	5.35	b452	6.33	9.01	6.34	6.36
b355	5.33	7.66	5.33	5.35	b455	6.34	9.01	6.34	6.36

Table 35: Reliability indices for cases of 25% reduced loads

The above results show that the wave loading has the most significant effect on the structure. A decrease in this load decreases crucially the loads acting on the structure and therefore increases the reliability indices of the members. This deviation increases to the members with higher reliability in the base case. The effect of wind and current is less important on the structure, verifying that the assumption made for symmetrical wave load sets every 90 degrees, is not influenced significantly by the different direction of the wind loads.

A useful note in this comparison is that the code that has been developed incorporating FORM and SORM can provide sensitivity factors of each of the variables, which illustrate the relative contribution of each to the calculated reliability index.

5.5.2.3.2 Material Yield

Different grades of steel, with different yield strength influence the reliability of the members since it directly forms the utilization ratio (ratio of actual stress to yield) that will later form the response surface of the structure. In this comparison, the S355 steel that has been used in the base case simulation is

compared to a steel of lower grade, S275, and the results are presented in Table 36.

<i>Member ID</i>	β_{355}	β_{275}	<i>Member ID</i>	β_{355}	β_{275}	<i>Member ID</i>	β_{355}	β_{275}
b101	4.79	4.11	b213	12.33	10.43	b353	6.08	5.06
b102	5.22	4.35	b214	9.33	7.94	b354	6.09	5.05
b103	5.23	4.36	b215	18.72	15.56	b355	5.33	4.43
b104	4.79	4.11	b216	18.71	15.53	b356	5.31	4.44
b111	54.83	36.36	b251	5.27	4.43	b357	6.16	5.07
b112	54.83	36.36	b252	5.25	4.38	b358	6.16	5.07
b113	54.83	36.36	b253	7.51	6.36	b401	14.73	12.43
b114	54.83	36.36	b254	7.51	6.37	b402	10.66	9.12
b115	35.01	22.57	b255	5.26	4.38	b403	10.66	9.13
b116	35.01	22.57	b256	5.27	4.43	b404	14.72	12.44
b151	5.70	4.82	b257	7.81	6.62	b411	8.98	7.57
b152	5.54	4.68	b258	7.79	6.63	b412	6.00	4.94
b153	6.93	5.91	b301	8.71	7.50	b413	8.98	7.57
b154	6.94	5.92	b302	8.15	6.96	b414	5.76	4.75
b155	5.55	4.69	b303	8.14	6.96	b415	8.36	7.10
b156	5.70	4.82	b304	8.72	7.50	b416	8.37	7.09
b157	6.76	5.80	b311	10.46	8.83	b451	6.37	5.38
b158	6.74	5.81	b312	6.96	5.92	b452	6.33	5.35
b201	5.74	4.91	b313	10.48	8.84	b453	3.79	3.13
b202	7.46	6.30	b314	6.94	5.87	b454	3.79	3.13
b203	7.45	6.30	b315	20.86	17.49	b455	6.34	5.35
b204	5.74	4.90	b316	20.87	17.50	b456	6.37	5.38
b211	12.34	10.41	b351	5.30	4.45	b457	3.72	3.05
b212	9.70	8.25	b352	5.33	4.43	b458	3.72	3.05

Table 36: Reliability indices for S355 and S275 steels

The results that have been derived illustrate as it was expected, that the steel of lower yield strength leads to lower values of target reliability. This deviation is greater in members of higher reliability. For the critical members (b457-b458) minimum derived values of β become very low form S275 steels, getting out of the acceptable limits set by standards, as it has been discussed earlier in this Thesis.

5.5.2.4 Corrosion models

Corrosion is one of the most important phenomena related to capacity deterioration of the structure. Different models for this time-dependent phenomenon have already been presented and express this problem as a time-independent one through a relative decrease in the thickness of members. In this section, different models have been considered in the reliability assessment and the corresponding reliability deterioration throughout the structure's service life is presented. In Figure 58, the cumulative relative degradation in members' thickness is expressed based on the models examined. For the models where thickness decrease is expressed through statistical distributions (mean value and standard deviation) the thickness value that corresponds to probability of occurrence of 95% is considered. From the results that have been collected, Figure 60 (i-iv) presents graphs that illustrate the degradation of the reliability index according to each method for 4 members of one leg, as they represent values of reliability index of different range. Table 37, shows the degradation of reliability between 0 and 20 years, since this is the most common prescribed life of offshore structures, for the 20 more critical members according to each method.

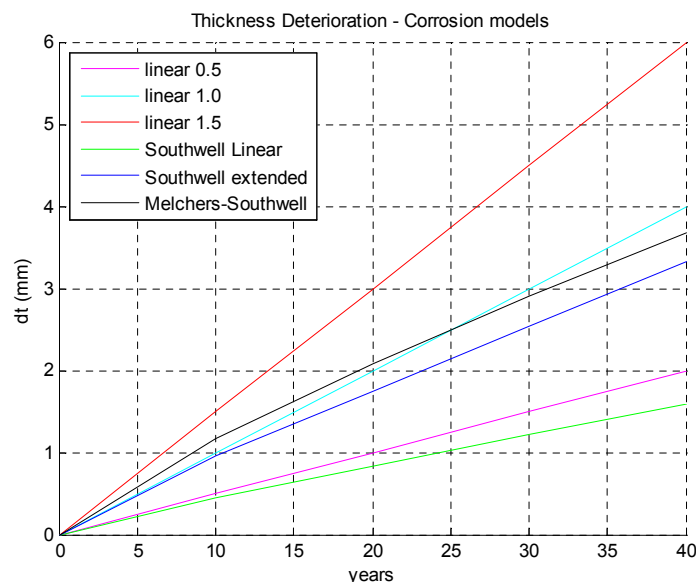


Figure 58: Thickness deterioration as a function of time

<i>Member ID</i>	<i>Base case</i>	<i>Linear 0.5</i>	<i>Linear 1.0</i>	<i>Linear 1.5</i>	<i>Southwell Linear</i>	<i>Southwell Extended</i>	<i>Melchers-Southwell</i>
b457	3.72	3.59	3.47	3.33	3.62	3.50	3.46
b458	3.72	3.60	3.47	3.33	3.62	3.50	3.46
b453	3.79	3.66	3.54	3.40	3.69	3.57	3.52
b454	3.79	3.66	3.53	3.40	3.69	3.57	3.53
b101	4.79	4.75	4.70	4.72	4.73	4.70	4.70
b104	4.79	4.75	4.70	4.72	4.73	4.70	4.70
b102	5.22	5.11	4.99	4.85	5.13	5.02	4.98
b103	5.23	5.11	4.99	4.86	5.13	5.02	4.98
b252	5.25	5.08	4.93	4.76	5.13	4.98	4.92
b255	5.26	5.09	4.94	4.77	5.14	4.99	4.92
b251	5.27	5.11	4.96	4.79	5.15	5.01	4.95
b256	5.27	5.11	4.97	4.79	5.16	5.01	4.95
b351	5.30	5.15	5.01	4.83	5.20	5.05	4.99
b356	5.31	5.15	5.01	4.84	5.20	5.05	4.99
b352	5.33	5.15	5.00	4.81	5.21	5.05	4.98
b355	5.33	5.15	5.00	4.81	5.21	5.04	4.99
b152	5.54	5.35	5.18	4.99	5.40	5.23	5.18
b155	5.55	5.36	5.19	5.00	5.41	5.24	5.17
b151	5.70	5.51	5.32	5.11	5.55	5.37	5.31
b156	5.70	5.50	5.32	5.11	5.55	5.37	5.31

Table 37: Reliability indices for 20 years for different corrosion models

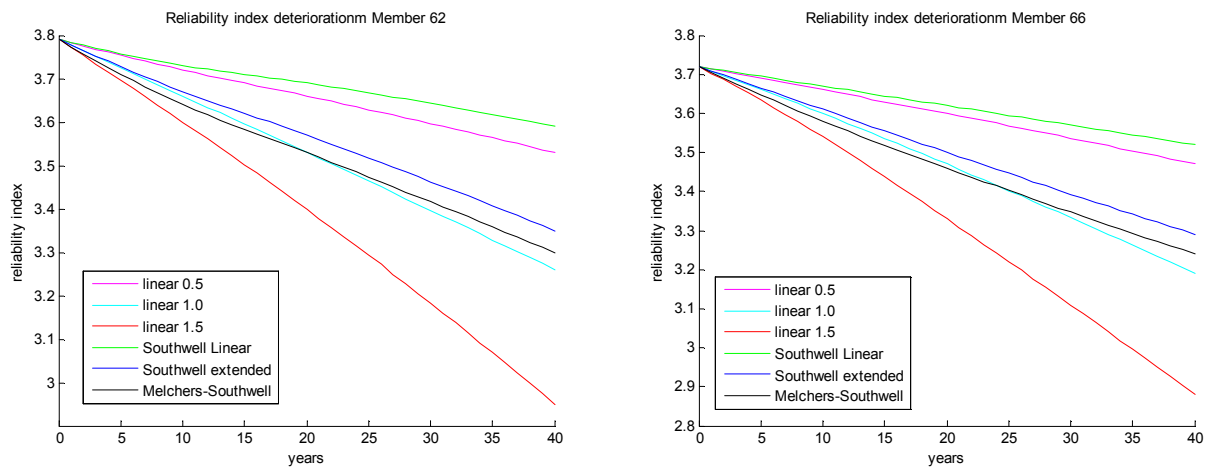


Figure 59: Reliability index deterioration of critical members (b454, b458)

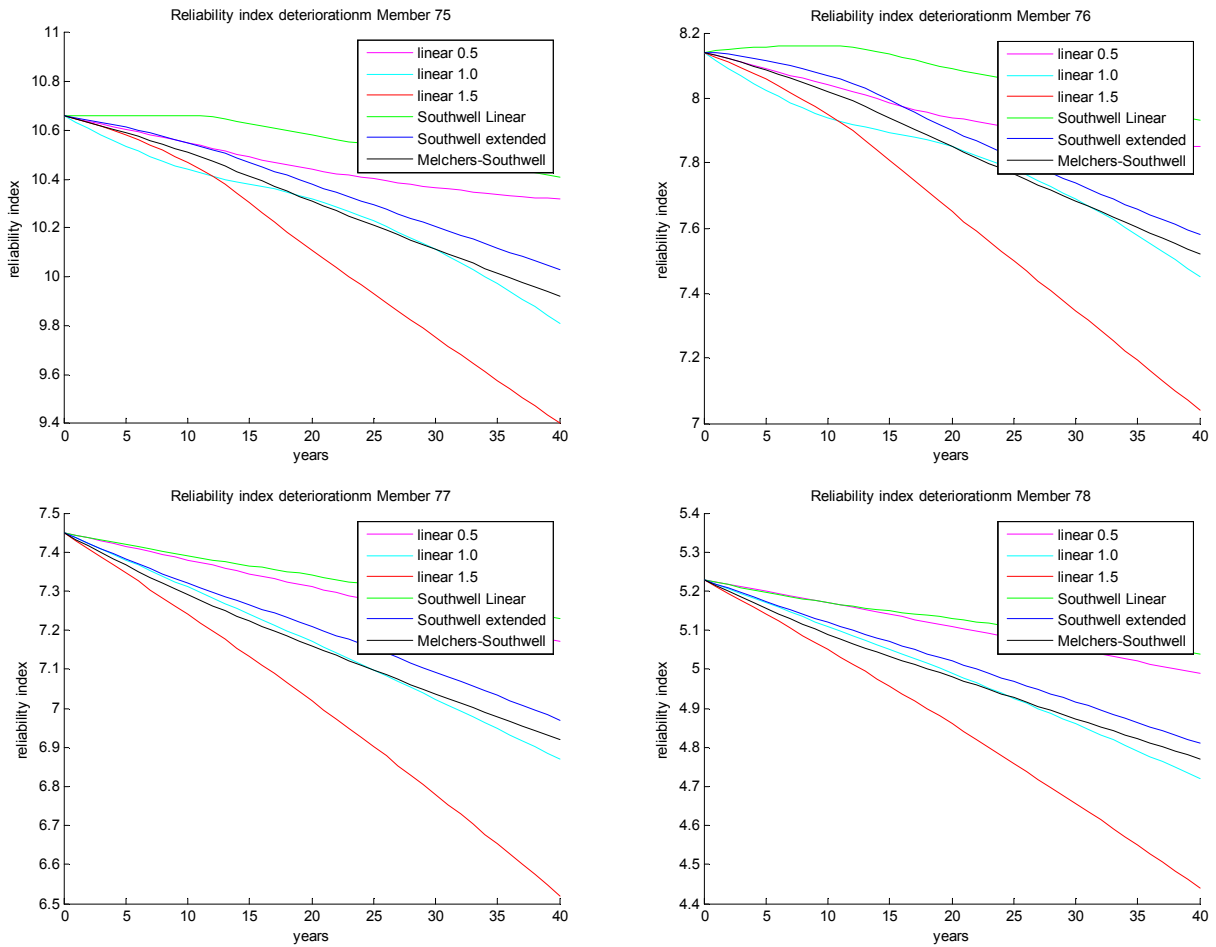


Figure 60: Reliability index deterioration of members (b403-b103)

From the simulations that have been executed and the results that are presented above, it can be pointed out that the effect of corrosion is significant in the reliability of the structure since its load bearing capacity is reduced. Selection of the appropriate corrosion model is essential since comparing different models it can double the effect of corrosion throughout its service life. This decision should be taken according to the type of the structure and the environment of deployment. The effect in reliability deterioration is more significant for thinner members and in members with greater values of reliability index. The fact that for specific members the deterioration rate changes, even implying small scale increase of reliability as time progresses, identifies load redistribution through alternative load paths of the structure, with different members suffering from greater loads than others as the thickness of members decreases uniformly.

For critical members, as it can be observed in Figure 59, appropriate modelling of the structures can classify them within an acceptable region of reliability or in an unsafe region yielding intervention when in operational phase or re-dimensioning when in the design phase. Further, in a more accurate assessment, different parts of the structure at different elevations shall be modelled according to different corrosion models.

The above analysis has considered general (wastage) corrosion on the structural members that accounts for wall thickness reduction and is considered by appropriate models. Additionally, pitting corrosion may occur locally on members leading to stress concentration effects. Wall thinning due to corrosion (of any type, including corrosion fatigue), can be largely mitigated against by use of an appropriate corrosion protection system, as it has been referred to earlier and is presented in Appendix B of the Thesis.

5.5.3 System Reliability Integration

Although the main interest of this Thesis is the estimation of reliability in a component level since this is the approach followed by design standards, in this section the effects of uncertainties on the structure as a system will be examined following the background theory that has been presented earlier.

For the purpose of this study, pushover analysis has been selected among other methods for the identification of the most dominant failure path of the structure. This analysis identifies in a deterministic way the most critical members of the structure forming a failure path that will derive the resultant global reliability of the structure. Available studies, verify that for cases of extreme loading conditions, the level of reliability of the identified failure path based on a pushover analysis is in accordance to values that may be obtained using extensive methods of search and simulations [299], [300].

Design simulation was combined with pushover analysis to address the stress variation on the structure and identify the sequence of failure of structural members as well as the global response of the structure. The difficulty of this

approach is that due to the simulations required, in structures of high complexity, the computational effort required increases; therefore it is not indicated for failure paths with large number of members. In [301] and [302], guidelines for simple methods of failure paths identification can be found.

An important assumption following this approach is that global failure occurs at one instance, for example in the case when the lateral wave load reaches its maximum, and all of the members of a failure paths fail at the same time. Failures are considered to occur over a short period of time during which the load is applied proportionally. This assumption transforms the problem to a time independent one, without demanding recalculation of reliability of the members of the damaged structure.

Once a member's failure is identified, its stiffness and therefore the global stiffness of the structure is modified by modelling a residual strength either by applying appropriate forces at the failed member or by changing its structural properties. Figure 61, presents the post-failure behaviour that has been considered in this analysis based on [86]. A new structural stress calculation is initiated and this loop continues until a successive sequence of members' failures is identified. The global response of the structure will illustrate the step where the global failure is considered to occur through criteria of extensive non linear deformation or displacements. In order to proportionally increase loads, the design case is selected as a base case and the loads are factored until the structure collapses.

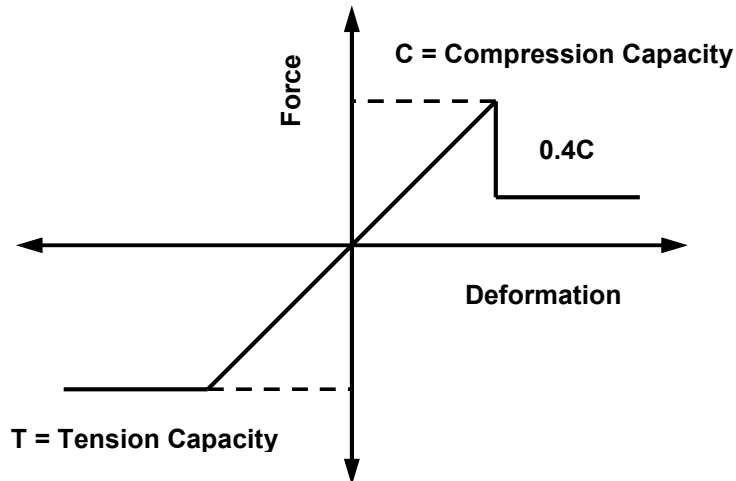


Figure 61: Post failure behaviour

For the reference structure that is examined, the resultant failure path, consisting of four different failure branches, 90 degrees apart for each load direction, that are been identified are presented in Figure 62. Error! Reference source not found.. In this graph, each of the branches is modelled as a sequence of parallel events, where they should all fail in order for the branch to fail, while branches are linked together in a series formation, indicating the once the weakest link has failed the whole structure fails. Graphs of displacement as a function of overturning moment and load factor are presented in Figure 63 and Figure 64.

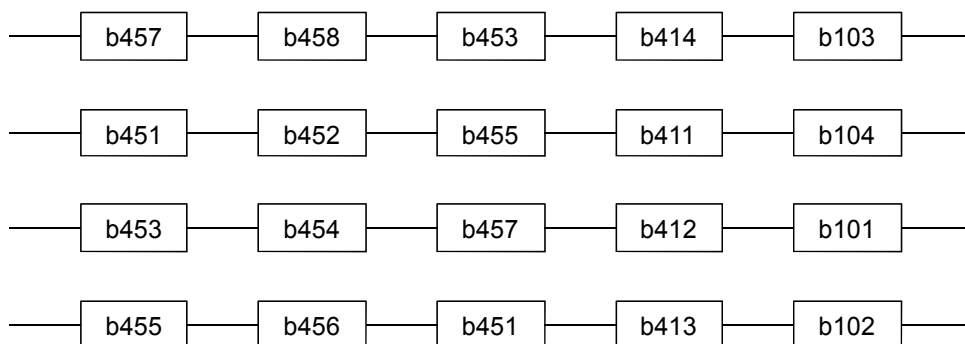


Figure 62: Critical Failure paths

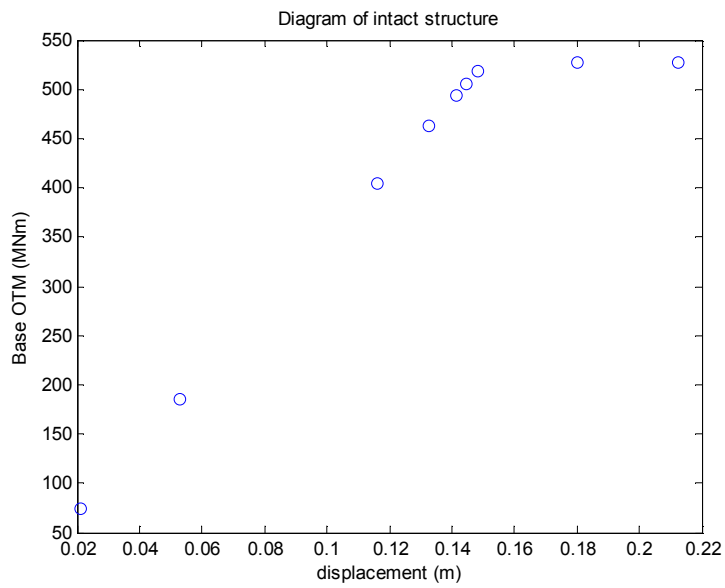


Figure 63: Displacement vs overturning moment (intact structure)

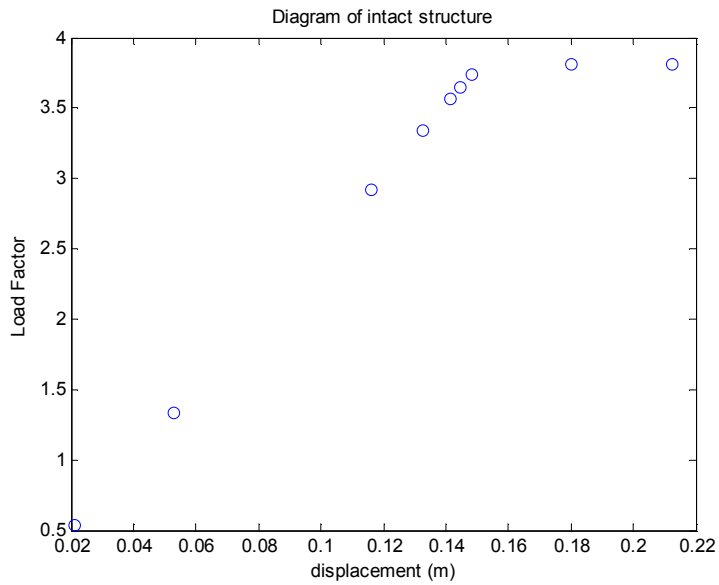


Figure 64: Displacement vs load factor (intact structure)

From the first failure path identified, failures of members 457-103 refer to the effective path of the structure. Failure of members 103 and 102, which refer to the legs of the lower elevation of the structure has the most significant effect on the global response of the structure since upon their failure, the structure stops

to deform linearly. For the case of 45 degrees, the first member to fail is 103, resulting to nonlinear displacement following the first failure of the structure, indicating absence of redundancy in this direction.

Calculation of the reserve strength ratio as the ratio of the base overturning moment of the ultimate resistance of the structure over that of the design load case derives a value of 3.7. The corresponding value for the case of 45 degrees is 3.1.

Further analysis has been executed for the case of damaged structure, by completely removing structural members, simulating the case when the two most likely to fail members are sequentially removed. The diagrams that correspond to those cases are presented in Figure 65 to Figure 68 presenting displacement as a function of overturning base moment and load factor.

From the results obtained, the capacity of the damaged structure can be determined and the residual strength can be expressed by calculation of the residual resistance factor (RIF) and the damage tolerance ratio (DTR). The RIF for the first case where the member b457 is removed is calculated as 0.96 while for the second case where additionally member b458 is removed, RIF is found to be 0.92. Those results show that for both damage scenarios, removal of members reduce the maximum environmental load the structure might resist. The DTR calculated for the first case is 0.92 while for the second case 0.88. Those numbers indicate the reduction in the reserve strength of the structure. The values of the DTR obtained, indicate that the platform has a high tolerance to damages.

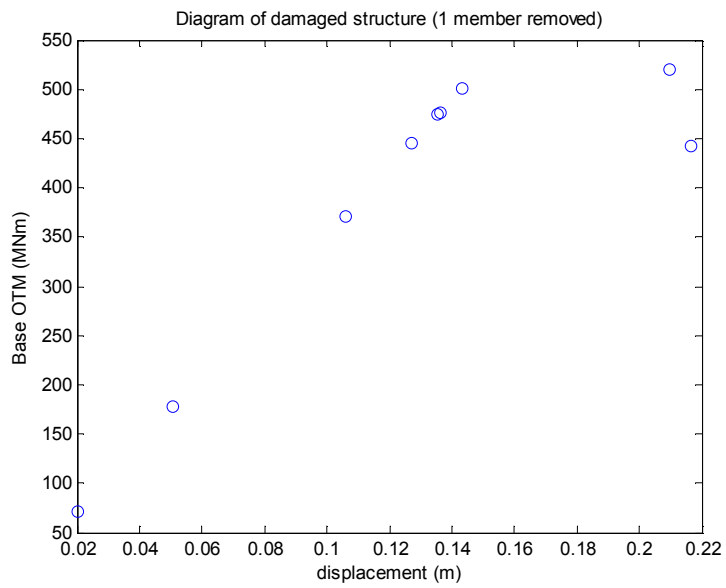


Figure 65: Displacement vs overturning moment (one member removed)

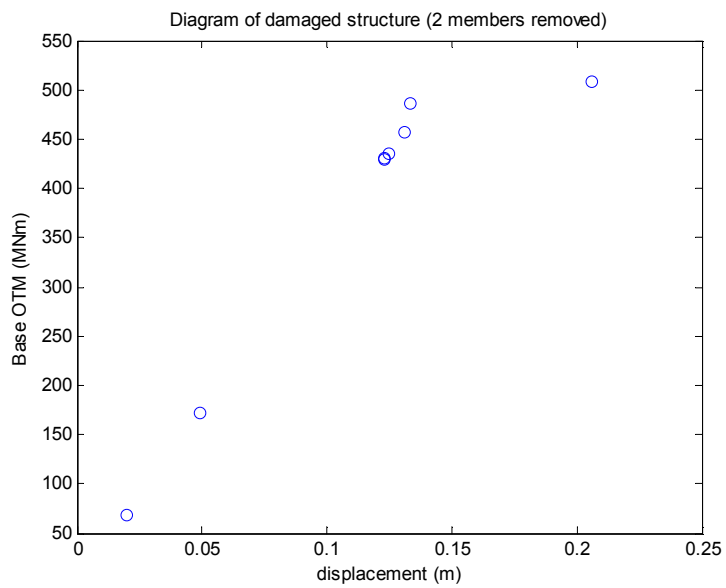


Figure 66: Displacement vs overturning moment (two members removed)

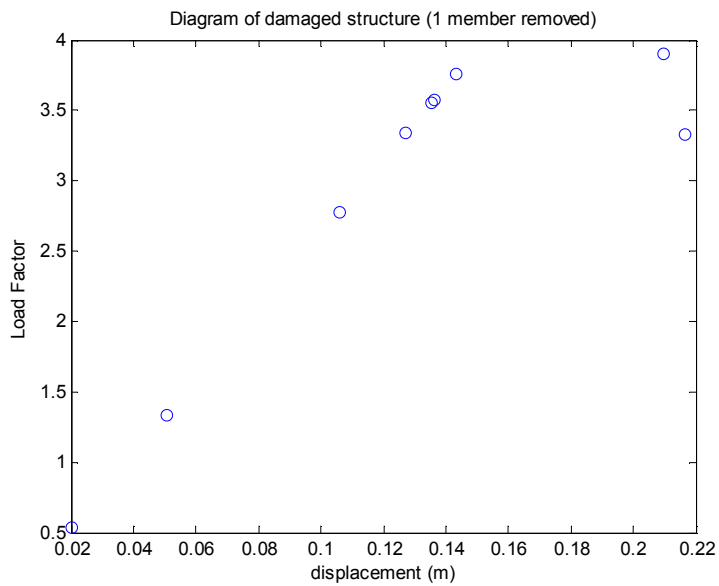


Figure 67: Displacement vs load factor (one member removed)

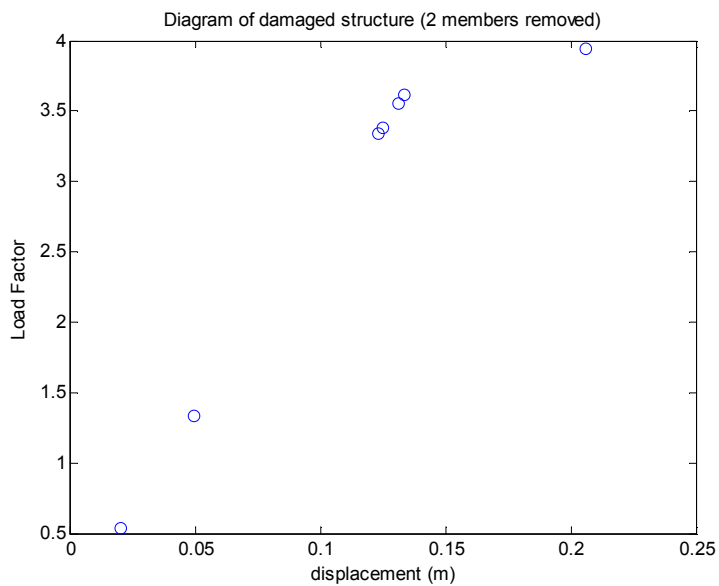


Figure 68: Displacement vs load factor (two members removed)

For a rough estimation of system reliability a simple bound approach is applied based on the assumptions stated earlier. Although this approach provides a wide range of the value of the system reliability it can derive an initial estimate of the system integrated reliability. Due to the fact that symmetric loads are

considered to act on the structure, the total reliability of the structure will equal that of anyone of the branches. For the calculation of the reliability of each branch, the laws of parallel systems are applied.

The values that have been derived both for the reserve strength ratio, residual resistance factor and damage tolerance ratio are reasonable and close to ones found in similar studies [92]. The value of the lower and upper bounds of the system reliability that have been calculated are presented in Table 38.

<i>Lower Bound</i>		<i>Upper Bound</i>	
β	P_f	β	P_f
10.97	2.66E-28	5.76	4.21E-09

Table 38: Bounds of System Reliability

The analysis that has been executed quantifies the level of system reliability of a typical jacket structure based on a simplified method. More accurate approximation of the index can be obtained through a more accurate method such as the Hobhenbicler approximation. The reliability index that has been calculated from the system of failure paths equals 5.76. This result, that equals the minimum reliability index of the members included in a failure path, is based on a new un-corroded platform. Capacity deterioration due to corrosion, weld imperfections, marine growth etc, will change the response of the structure and in some cases may create different load and failure paths; therefore an individual analysis should be executed varying members' thicknesses and surface properties in order to reflect the structure's deteriorated conditions.

5.6 A Note on the dynamic loading of structures

Although the main aim of this PhD has been the investigation of the response of the response of complex offshore structures due to static or quasi-static loads, dynamic loads might have significant effect on structures and therefore a separate complementary analysis should then be considered. This effect is due

to the inability of the structures to respond instantly to the loading applied. The increase of the effect in the response of a structure under dynamic load can be given by a Dynamic Amplification Factor (DAF) which will magnify stresses or displacements derived from static analysis to represent the corresponding values for dynamic loads:

$$DAF = \frac{u_{max}}{u_{static}} \quad (5-33)$$

The Dynamic Amplification Factor is practically a function of the geometry of the structure and the material properties, and corresponds to its ability to dissipate energy [303]. In [304], values for DAF are provided within a range of 1.10 – 1.30 based on a classification according to the scale of the structure, while in [305] values between 1.5 – 2.0 are given for wind turbine structures that are subjected to severe dynamic loads; the later values are considered as the most conservative ones [306].

Another effect of dynamic loads is the corrosion fatigue phenomenon. This refers to the mechanical deterioration of a material under combination of corrosion and cyclic loading. This phenomenon can be initiated by pitting, facilitating crack initiation and has a more significant effect to steels of higher grades, constituting a constraint on their extensive application. Fatigue corrosion can be avoided by addition of appropriate alloy or surface treatment of the members.

In those cases where cyclic loads are significant, direct application of the amplification factor to static loads obtained by ultimate strength do not produce accurate results; therefore a fatigue limit state should be employed as it can be found in literature [307], [308] and [309]. Further presentation of fatigue limit states is beyond the scope of this Thesis.

5.7 Summary

This Chapter has presented an application of the Stochastic Response Surface Method for the reliability assessment of ultimate strength for a typical offshore jacket structure, deployed in a hypothetical site in the North Sea. Basis of the analysis have been analytical limit states that have been derived, based on failure criteria of structural mechanics. An application of the joint probability distribution, which has been presented in Chapter 5, is included for the reference site. For a reference structure, the reliability of structural members has been executed, based on the theory and data, and using the computational tools that have been presented in the previous chapters considering four stochastic variables (wave, wind, current, material yield). Using a consistent methodology, a sensitivity analysis of the effect of different design parameters of the design, such as the angle of loads, buckling coefficients, statistical distribution and relative effect of variables has been presented. After an extensive investigation of different corrosion models and their effect on the estimated reliability indices, integration from a local to system reliability has been realized illustrating the structure's potential to redundancy.

6 COMPARISON OF THE ULTIMATE STRENGTH RELIABILITY PERFORMANCE OF RELEVANT DESIGN PROCEDURES

6.1 Introduction

In this Chapter, the reliability assessment of offshore jacket structures will be investigated based on limit states formulated by design standards' requirements. The basic clauses of each standard have been included in this Chapter. For the four standards that reference has been made in the first chapters of this Thesis, API LRFD [2], ISO 19902 [3], EN 1993 [5], AISC/ANSI [4], the applicable design provisions will be initially presented, resulting to the formulation of corresponding limit state functions. For the definition of loads and load combinations, load factors on both loads and material properties have been considered to equal unity, while reduction (resistance) factors for the strength of members under different loading modes have been selected deterministically following standards' recommendations.

Once this background is set, reliability indices for the members of the reference structure that was described in the previous Chapter will be calculated based on the new limit states. This study will illustrate the level of conservatism of standards, comparing obtained results to the ones that have been derived by the limit state that was based on the von Mises failure criterion in the previous Chapter. This study will focus on the component reliability assessment since this is the approach that design standards adopt; however following the procedure that was described and applied in the last section of the previous chapter, integration to a systemic level can be achieved.

6.2 API RP-2A: Recommended practice for planning, designing and constructing fixed offshore platforms LRFD

This section, will present the design procedure of tubular members subjected to tension, compression, bending, shear, hydrodynamic pressure, or combined action of the above loads, as included in Chapter D of the standard. Ultimate strength and stability criteria are derived. The recommendations provided, are considered to be applicable for stiffened or un-stiffened members with thickness of $t \geq 6 \text{ mm}$ and materials with yield of less than 414 MPa [2].

6.2.1 Design Provisions

6.2.1.1 Members in Tension

For cylindrical members that are subjected to tension, the condition that should be satisfied is:

$$f_t \leq \varphi_t F_y \quad (6-1)$$

Where:

F_y : Nominal yield strength (MPa)

f_t : Axial tensile stress (MPa)

φ_t : Resistance factor for axial tensile strength (= 0.95)

6.2.1.2 Members in Compression

For cylindrical members that are subjected to compression, the condition that should be satisfied is:

$$f_c \leq \varphi_c F_{cn} \quad (6-2)$$

Where:

F_{cn} : Nominal axial compressive strength (MPa)

f_c : Axial compressive stress (MPa)

φ_c : Resistance factor for axial compressive strength (= 0.85)

An additional check should take place for members subjected to column or local buckling. For column buckling, the nominal axial compressive strength F_{cn} should be determined as:

$$F_{cn} = [1.0 - 0.25\lambda^2]F_y, \text{ for } \lambda < \sqrt{2}$$

$$F_{cn} = \frac{1}{\lambda^2}F_y, \text{ for } \lambda \geq \sqrt{2} \quad (6-3)$$

$$\lambda = \frac{KL}{\pi r} \left[\frac{F_y}{E} \right]^{0.5}$$

Where:

λ : Column slenderness parameter (see Table 39)

E : Young's modulus of Elasticity (MPa)

K : Effective length factor

L : Un-braced Length (m)

r : Radius of gyration (m)

F_y : Nominal yield strength (smaller of F_{xe} and F_{xc})

The nominal elastic local buckling strength F_{xe} should be determined from:

$$F_{xe} = 2C_x E (t/D) \quad (6-4)$$

Where:

C_x : Critical elastic buckling coefficient (= 0.3 – 0.6)

D : Outside diameter (m)

t : Wall thickness (m)

x : Subscript for the member longitudinal axis

The nominal inelastic local buckling stress F_{xc} should be determined from:

$$F_{xc} = F_y, \text{ for } (D/t) \leq 60$$

$$F_{xc} = [1.64 - 0.23 \cdot (D/t)^{1/4}]F_y, \text{ for } (D/t) > 60 \quad (6-5)$$

6.2.1.3 Members in Bending

For cylindrical members subjected to bending stress, the condition that should be satisfied is:

$$f_b \leq \varphi_b F_{bn} \quad (6-6)$$

Where:

f_b : (= M/S) bending stress (MPa)

S : Elastic section Modulus (mm^3)

M : Applied bending moment (Nm)

φ_b : Resistance factor for bending strength (= 0.95)

F_{bn} : Nominal bending strength (MPa)

$$F_b = \frac{Z}{S} F_y, \text{ for } \frac{D}{t} \leq \frac{1500}{F_y}$$

$$F_b = \left[1.13 - 2.58 \cdot \frac{F_y \cdot D}{Et} \right] \frac{Z}{S} F_y, \text{ for } \frac{10340}{F_y} < \frac{D}{t} \leq \frac{20680}{F_y} \quad (6-7)$$

$$F_b = \left[0.94 - 0.76 \cdot \frac{F_y \cdot D}{Et} \right] \frac{Z}{S} F_y, \text{ for } \frac{20680}{F_y} < \frac{D}{t} \leq 300$$

Where:

Z : Plastic Section Modulus (mm^3)

6.2.1.4 Shear loads

For cylindrical members subjected to shear loads, the condition to be satisfied is:

$$f_v = \frac{2V}{A} \leq \varphi_v F_{vn} \quad (6-8)$$

Where:

F_{vn} : (= $F_y/\sqrt{3}$) Nominal Shear strength (MPa)

f_v : Maximum shear stress (MPa)

V : Beam shear (N)

A : Cross sectional area (m^2)

φ_v : Resistance factor for beam shear strength (= 0.95)

For cylindrical members subjected to torsional loads, the condition to be satisfied is:

$$f_{vt} = \frac{M_{vt}D}{2I_p} \leq \varphi_v F_{vtn} \quad (6-9)$$

Where:

F_{vtn} : ($= F_y/\sqrt{3}$) Nominal torsional strength (MPa)

f_{vt} : Torsional shear stress (MPa)

M_{vt} : Torsional moment (Nm)

I_p : Polar moment of inertia (m^4)

6.2.1.5 Hydrostatic Pressure

For the consideration of the hydrostatic pressure, the design hydrostatic head should be derived as:

$$p = \gamma_D w H_z$$
$$H_z = z + \frac{H_w}{2} \left[\frac{\cosh(k(d-z))}{\cosh(kd)} \right] \quad (6-10)$$

Where:

p : Hydrostatic Pressure (MPa)

γ_D : Hydrostatic pressure load factor

w : Sea water density (MN/m^3)

z : Depth below still water surface (m)

H_w : Wave Height (m)

k : ($= 2\pi/L$), where L : Wave length (m)

d : Still water depth (m)

For cylindrical members subjected to external (hydrostatic) pressure the condition to be satisfied is:

$$f_h = \frac{pD}{2t} \leq \varphi_b F_{hc} \quad (6-11)$$

Where:

f_h : Hoop stress due to factored hydrostatic pressure (MPa)

φ_b : Resistance factor for hoop buckling strength (= 0.80)

F_{hc} : Nominal critical hoop buckling strength

The elastic buckling nominal critical strength F_{hc} should be determined as:

$$F_{hc} = F_{he}, \text{ for } F_{he} \leq 0.55F_y \quad (6-12)$$

The inelastic buckling nominal critical strength F_{hc} should be determined as:

$$F_{hc} = 0.7F_y \left[\frac{F_{he}}{F_y} \right]^{0.4} \leq F_y, \text{ for } F_{he} > 0.55F_y \quad (6-13)$$

Where the elastic hoop buckling stress F_{he} is determined as:

$$F_{he} = 2C_h E (t/D)$$

$$C_h = \frac{0.44t}{D}, \text{ for } M \geq 1.6D/t$$

$$C_h = \frac{0.44t}{D} + \frac{0.21(D/t)^3}{M^4}, \text{ for } 0.825D/t \leq M \leq 1.6D/t \quad (6-14)$$

$$C_h = 0.737/(M - 0.579) \text{ for } 1.5D/t \leq M \leq 0.825D/t$$

$$C_h = 0.8 \text{ for } M < 1.5$$

Where:

$$M = \frac{L}{D} \sqrt{\frac{2D}{t}} : \text{Geometrical parameter}$$

L : Length of cylinder between stiffeners (m)

6.2.1.6 Members under combined loads

For cylindrical members under axial tension and bending loads, the condition that should be satisfied is:

$$U_m = 1 - \cos \left[\frac{\pi (f_t)}{2 \varphi_t F_y} \right] + \frac{[(f_{by})^2 + (f_{bz})^2]^{0.5}}{\varphi_b F_{bn}} \leq 1.0 \quad (6-15)$$

Where:

f_{by}, f_{bz} : Bending stresses about y and z- axis (MPa)

For cylindrical members under combined axial compressive and bending loads, the conditions that should be satisfied is:

$$U_m = \frac{f_c}{\varphi_c F_{cn}} + \frac{1}{\varphi_b F_{bn}} \left\{ \left[\frac{C_{my} \cdot f_{by}}{1 - \frac{f_e}{\varphi_c F_{ey}}} \right]^2 + \left[\frac{C_{mz} \cdot f_{bz}}{1 - \frac{f_e}{\varphi_c F_{ez}}} \right]^2 \right\}^{0.5} \leq 1.0 \quad (6-16)$$

$$U_m = 1 - \cos \left[\frac{\pi (f_c)}{2 \varphi_c F_{xc}} \right] + \frac{[(f_{by})^2 + (f_{bz})^2]^{0.5}}{\varphi_b F_{bn}} \leq 1.0 \quad (6-17)$$

$$F_c < \varphi_c F_{xc} \quad (6-18)$$

Where:

C_{my}, C_{mz} : Reduction factors (Table 39)

$F_{ey} = F_y / \lambda_y^2, F_{ez} = F_z / \lambda_z^2$: Euler buckling strengths (MPa)

λ_y, λ_z : Column slenderness parameters (eq. 7-3c)

Incorporating the hydrostatic pressure, the condition that should be satisfied for members subjected to longitudinal tensile stresses due to axial tension and bending, and hoop compressive strength is:

$$U_m = \left(\frac{f_t + f_b - (0.5f_h)}{\varphi_t F_y} \right)^2 + \left(\frac{f_h}{\varphi_h F_{hc}} \right)^{2n} + 2u \left| \frac{f_t + f_b - (0.5f_h)}{\varphi_t F_y} \right| \frac{f_h}{\varphi_h F_{hc}} \leq 1.0 \quad (6-19)$$

Where:

u : Poisson's Ration (= 0.3)

For members subjected to longitudinal compressive stresses due to axial compression, bending, and hoop compressive strength the fundamental equations for combined loads should be applied. Further, when the axial

utilization factor exceeds 0.5 ($f_x > 0.5\varphi_h F_{he}$), the following condition should be satisfied:

$$U_m = \frac{f_x - 0.5\varphi_h F_{he}}{\varphi_c F_{xe} - 0.5\varphi_h F_{he}} + \left(\frac{f_h}{\varphi_h F_{hc}} \right)^2 \leq 1.0 \quad (6-20)$$

Where: $f_x = f_c + f_b + (0.5f_h)$

Situation	K	C_m^I
Superstructure legs		
Braced	1.0	a)
Portal (un-braced)	K^2	a)
Structure legs and piling		
Grouted composite section	1.0	c)
Un-grouted legs	1.0	c)
Un-grouted piling between shim points	1.0	b)
Jacket Braces		
Face to face length of main diagonals	0.8	b) or c)
Face of leg to centerline of joint length of K-braces	0.8	c)
Longer segment Length of X-Braces	0.9	c)
Secondary Horizontals	0.7	c)
Deck Truss Chord Members	1.0	a) b) or c)
Deck truss web members		
In plane action	0.8	b)
Out of plane action	1.0	a) or b)

a. C_m values for the three cases defined in this table are as follows:

- 1) 0.85;
- 2) $0.40 < C_m = 0,6 - 0,4 \cdot M_1/M_2 < 0.85$, where M_1/M_2 is the ratio of smaller to larger moments at the ends of the unbraced portion of the member in the plane of bending under consideration. M_1/M_2 is positive when the member is bent in reverse curvature, negative when bent in single curvature.
- 3) $C_m = 1,0 - 0,4 \cdot (\sigma_c/f_e)$, or 0,85, whichever is less

b. Use effective length alignment chart. This may be modified to account for conditions different from those assumed in the development of the chart.

c. At least one pair of members framing into a joint shall be in tension, if the joint is not braced out-of-plane.

Table 39: Effective length and bending reduction factors

6.2.2 Numerical Results

Table 40, summarizes the limit states that have been considered in the reliability assessment of the reference structure. The corresponding paragraph and number of each limit state as it is referred to in the standard is included, as

well as the identification number that corresponds to this limit states in this Chapter. Following, in Table 41 to Table 43, the results of reliability analysis of each limit state are presented for the different classes of members.

Limit State	Description	Equation
ufShear	Usage factor due to shear action	6-8
ufTorsion	Usage factor due to torsional action	6-9
ufD211	Usage factor according to equation (D.2.1-1), i.e. axial tension	6-1
ufD252	Usage factor according to equation (D.2.5-2), i.e. hydrostatic pressure	6-11
ufD311	Usage factor according to equation (D.3.1-1), i.e. axial tension and bending	6-15
ufD321	Usage factor according to equation (D.3.2-1), i.e. axial compression and bending	6-16
ufD322	Usage factor according to equation (D.3.2-2), i.e. axial compression and bending	6-17
ufD323	Usage factor according to equation (D.3.2-3), i.e. axial compression	6-18
ufD331	Usage factor according to equation (D3.3-1), i.e. axial tension, bending and hydrostatic pressure	6-19
ufD341	Usage factor according to equation (D.3.4-1), i.e. axial compression, bending and hydrostatic pressure	6-20

Table 40: Limit States according to API-LRFD

	ufShear	ufTorsion	ufD211	ufD252	ufD311	ufD321	ufD322	ufD323	ufD331	ufD341
b101	0.00	21.43	5.97	0.00	15.30	7.80	13.26	10.78	0.00	0.00
b102	33.85	18.32	0.00	0.00	0.00	4.76	6.33	5.73	0.00	0.00
b103	33.82	18.33	0.00	0.00	0.00	4.76	6.32	5.74	0.00	0.00
b104	0.00	21.41	5.97	0.00	15.32	7.80	13.26	10.80	0.00	0.00
b201	0.00	26.62	7.06	0.00	0.00	7.36	12.81	10.05	0.00	0.00
b202	53.40	27.99	0.00	0.00	0.00	6.62	10.52	7.06	0.00	0.00
b203	53.33	28.00	0.00	0.00	0.00	6.62	10.51	7.07	0.00	0.00
b204	0.00	26.66	7.04	0.00	0.00	7.36	12.82	10.05	0.00	0.00
b301	37.35	30.82	10.49	0.00	9.56	0.00	0.00	29.69	0.00	0.00
b302	24.56	26.08	0.00	0.00	0.00	7.75	11.32	10.02	0.00	0.00
b303	24.56	26.06	0.00	0.00	0.00	7.76	11.30	10.03	0.00	0.00
b304	37.37	30.85	10.51	0.00	9.56	0.00	0.00	29.64	0.00	0.00
b401	16.84	11.74	0.00	0.00	0.00	31.61	17.49	0.00	0.00	0.00
b402	18.31	12.91	0.00	0.00	0.00	11.65	13.73	23.61	0.00	0.00
b403	18.32	12.91	0.00	0.00	0.00	11.65	13.73	23.58	0.00	0.00
b404	16.84	11.73	0.00	0.00	0.00	31.59	17.47	0.00	0.00	0.00

Table 41: Reliability indices for Leg Members

	ufShear	ufTorsion	ufD211	ufD252	ufD311	ufD321	ufD322	ufD323	ufD331	ufD341
b111	0.00	0.00	0.00	0.00	0.00	59.43	59.43	0.00	0.00	0.00
b112	0.00	0.00	0.00	0.00	0.00	59.43	59.43	0.00	0.00	0.00
b113	0.00	0.00	0.00	0.00	0.00	59.43	59.43	0.00	0.00	0.00
b114	0.00	0.00	0.00	0.00	0.00	59.43	59.43	0.00	0.00	0.00
b115	0.00	0.00	0.00	82.54	0.00	43.01	38.75	0.00	0.00	0.00
b116	0.00	0.00	0.00	82.54	0.00	43.01	38.75	0.00	0.00	0.00
b211	0.00	53.23	0.00	0.00	13.84	0.00	0.00	0.00	0.00	0.00
b212	30.24	30.21	13.24	0.00	14.53	0.00	0.00	0.00	0.00	0.00
b213	0.00	53.21	0.00	0.00	13.84	0.00	0.00	0.00	0.00	0.00
b214	31.94	31.94	57.97	0.00	6.50	10.28	0.00	12.49	0.00	0.00
b215	0.00	53.05	0.00	92.59	0.00	0.00	0.00	0.00	0.00	0.00
b216	80.00	44.07	0.00	92.64	0.00	0.00	0.00	0.00	33.45	0.00
b311	56.65	71.67	57.76	0.00	11.70	0.00	0.00	0.00	0.00	0.00
b312	20.90	20.89	15.89	0.00	8.75	0.00	0.00	0.00	0.00	0.00
b313	56.62	71.65	57.78	0.00	11.69	0.00	0.00	0.00	0.00	0.00
b314	22.57	22.58	32.73	0.00	6.15	7.24	0.00	14.18	0.00	0.00
b315	46.56	71.55	0.00	85.05	0.00	0.00	0.00	0.00	35.53	0.00
b316	46.60	71.61	0.00	85.06	0.00	0.00	0.00	0.00	35.58	0.00
b411	53.26	38.70	0.00	0.00	10.19	0.00	0.00	0.00	0.00	0.00
b412	18.54	18.53	20.55	0.00	7.00	0.00	0.00	0.00	0.00	0.00
b413	53.17	38.70	0.00	0.00	10.18	0.00	0.00	0.00	0.00	0.00
b414	17.75	17.74	36.06	0.00	0.00	4.29	4.69	17.09	0.00	0.00
b415	22.83	19.25	0.00	59.57	0.00	7.11	6.64	80.46	0.00	0.00
b416	22.81	19.27	0.00	59.60	0.00	7.11	6.63	80.39	0.00	0.00

Table 42: Reliability indices for Horizontal Brace Members

	ufShear	ufTorsion	ufD211	ufD252	ufD311	ufD321	ufD322	ufD323	ufD331	ufD341
b151	0.00	26.31	0.00	0.00	0.00	0.00	0.00	0.00	8.26	0.00
b152	0.00	0.00	0.00	82.54	0.00	0.00	8.63	6.11	0.00	18.92
b153	29.71	23.02	0.00	82.54	0.00	0.00	8.61	14.24	0.00	24.20
b154	29.69	23.01	0.00	82.53	0.00	0.00	8.62	14.24	0.00	24.20
b155	0.00	0.00	0.00	82.53	0.00	0.00	8.64	6.10	0.00	18.91
b156	0.00	26.33	0.00	0.00	0.00	0.00	0.00	0.00	8.26	0.00
b157	27.85	22.12	0.00	82.54	0.00	11.14	0.00	21.59	11.79	0.00
b158	27.83	22.12	0.00	82.54	0.00	11.14	0.00	21.52	11.80	0.00
b251	40.07	22.59	0.00	0.00	0.00	0.00	0.00	0.00	7.01	0.00
b252	0.00	29.70	0.00	92.69	0.00	0.00	7.47	6.00	0.00	18.38
b253	22.92	20.95	0.00	92.71	0.00	0.00	8.99	20.81	0.00	32.79
b254	22.93	20.96	0.00	92.70	0.00	0.00	8.99	20.80	0.00	32.77
b255	0.00	29.70	0.00	92.69	0.00	0.00	7.47	6.00	0.00	18.41
b256	40.07	22.62	0.00	0.00	0.00	0.00	0.00	0.00	7.01	0.00
b257	23.45	20.25	0.00	92.72	0.00	0.00	0.00	0.00	12.35	0.00

	ufShear	ufTorsion	ufD211	ufD252	ufD311	ufD321	ufD322	ufD323	ufD331	ufD341
b258	23.45	20.29	0.00	92.72	0.00	0.00	0.00	0.00	12.35	0.00
b351	65.11	23.30	0.00	0.00	0.00	0.00	0.00	0.00	7.10	0.00
b352	32.76	19.94	0.00	0.00	0.00	0.00	7.32	6.29	0.00	18.89
b353	19.72	14.84	0.00	11.15	0.00	0.00	7.33	16.61	0.00	20.05
b354	19.73	14.83	0.00	11.15	0.00	0.00	7.34	16.61	0.00	20.05
b355	32.73	19.95	0.00	0.00	0.00	0.00	7.32	6.30	0.00	18.91
b356	65.14	23.31	0.00	0.00	0.00	0.00	0.00	0.00	7.11	0.00
b357	46.43	0.00	0.00	17.12	0.00	0.00	9.25	0.00	0.00	21.42
b358	46.44	0.00	0.00	17.15	0.00	0.00	9.25	0.00	0.00	21.43
b451	0.00	0.00	6.68	0.00	7.85	0.00	0.00	0.00	0.00	0.00
b452	59.92	29.74	0.00	0.00	0.00	4.56	18.59	7.40	0.00	0.00
b453	13.68	11.57	0.00	0.00	0.00	3.03	4.40	0.00	0.00	0.00
b454	13.68	11.56	0.00	0.00	0.00	3.02	4.41	0.00	0.00	0.00
b455	59.86	29.73	0.00	0.00	0.00	4.56	18.58	7.41	0.00	0.00
b456	0.00	0.00	6.67	0.00	7.84	0.00	0.00	0.00	0.00	0.00
b457	9.80	9.81	0.00	15.57	0.00	4.45	4.10	24.76	0.00	0.00
b458	9.81	9.82	0.00	15.57	0.00	4.44	4.10	24.73	0.00	0.00

Table 43: Reliability indices for Vertical Brace Members

The final value of the reliability index for every member will be derived as the minimum value calculated from each of the limit states examined. Results referring to the legs members, starting from the first elevation, distinguish one set of members in axial compression and bending (b102-b103) with $\beta = 4.76$ and one set in axial tension (b101-b104) with $\beta = 5.97$. Due to the uniform cross section of the legs, it is expected that the values of β of this elevation will be the lowest one, sizing the rest of the corresponding leg parts. Moving to the second elevation the same pattern is followed with members (b202-b203) in axial compression and bending with $\beta = 6.62$ and the second set (b201-b204) in axial tension with $\beta = 7.06$. The same pattern can be observed in the third elevation with the set of members (b302-b303) subjected to axial compression and bending with $\beta = 7.75$ and the set of (b301-b304) subjected to axial tension with $\beta = 10.51$. A different behaviour can be observed in the fourth elevation leg members which are characterized by their performance to torsion with $\beta = 11.73$ for (b401-b404) and $\beta = 12.91$ for (b402-b403); this varying pattern is due to the fact that topside loads have been incorporated in the design using ultra

stiff elements. An analytical representation of those loads would reduce this effect on the reliability assessment.

Horizontal bracing members of the first elevation, have great values of reliability due to the insignificant loads they carry based on the piling conditions that have been applied. Members of the first elevation that stand parallel to the flow (b211-b213) have $\beta = 13.24$ due to axial tension and bending, while for the members vertical to the flow, the one that meets the flow first (b214) has a lower value of $\beta = 6.50$ due to axial tension and bending and the second one (b212) has $\beta = 13.24$ due to axial tension. The two X-bracing members (b215-b216) have great values of reliability since they carry minimum loads as they have a non functional load to the operation of the structures. In the third elevation, the reliability indices of all of the members forming the square braces are determined by the axial tension and bending limit states where the two symmetrical members, parallel to the flow (b311-b313) have $\beta = 11.69$, the first vertical to the flow (b314) $\beta = 6.15$ and the second (b312) $\beta = 8.75$. The members parallel to the flow of the fourth elevation (b411-b413) have $\beta = 10.18$ due to axial tension and bending, the first member vertical to the flow (b414) $\beta = 4.29$ due to axial compression and bending while the second member (b412) $\beta = 7.00$ due to axial tension and bending. At this elevation, the X brace members show values of $\beta = 6.63$ due to the axial compression and bending criterion, due to the loads transmitted by the topside loads.

For the vertical X-braces of the first elevation, the two symmetrical sets of members parallel to the flow, have one of their member (b152-b155) defined by the axial compression limit state with $\beta = 6.10$ and the other of their members (b151-b156) with $\beta = 8.26$ subjected to axial tension, bending and hydrodynamic pressure. From the sets vertical to the flow, the first (b157-b158) has $\beta = 11.14$ due to axial compression and bending, while the second one (b153-b154) has $\beta = 8.61$ due to axial compression and bending. From the members of the second elevation that stand parallel to the flow, members (b252-b255) are subjected to axial compression with $\beta = 6.00$ while members (b251-b256) are subjected in axial tension, bending and hydrostatic pressure

with $\beta = 7.01$. From the sets vertical to the flow, the first (b257-b258) has $\beta = 12.35$ due to axial tension, bending and hydrostatic pressure, while the second one (b253-b254) has $\beta = 8.99$ due to axial compression and bending. From the members of the third elevation that stand parallel to the flow, members (b352-b355) are subjected to axial compression with $\beta = 6.29$ while members (b351-b356) are subjected in axial tension, bending and hydrostatic pressure with $\beta = 7.10$. From the sets vertical to the flow, the first (b357-b358) has $\beta = 9.25$ due to axial compression and bending, while the second one (b353-b354) has $\beta = 7.33$ due to axial compression and bending. Finally for the members of the fourth elevation, those that stand parallel to the flow, (b452-b455) are subjected to axial compression and bending with $\beta = 4.56$ while members (b451-b456) are subjected in axial tension with $\beta = 6.68$. From the sets vertical to the flow, the first (b457-b458) has $\beta = 4.44$ due to axial compression and bending, while the second one (b453-b454) has $\beta = 3.02$ due to axial compression and bending.

6.3 ISO 19902:2002: Petroleum and natural gas industries- general requirements for offshore structures

In this section, the relevant provisions of ISO 19902 will be presented, as they are included in Chapter 13 of this standard. After an initial reference to the design requirements of members subjected to individual tension, compression, bending, shear or hydrostatic pressure, and provisions for combined forces results, of the numerical application will be presented [3].

6.3.1 Design Provisions

6.3.1.1 Members in Axial Tension

For members subjected to axial tension, the design condition that should be satisfied is:

$$\sigma_t \leq \frac{f_t}{\gamma_{R,t}} \quad (6-21)$$

Where:

σ_t : Axial tensile stress (MPa)

f_t : Representative Axial tensile strength $f_t = f_y$ (MPa)

f_y : Representative yield strength (MPa)

$\gamma_{R,t}$: Partial resistance factor for axial tensile strength (= 1.05)

The derived utilization of a member subjected to tension is therefore:

$$U_m = \frac{\sigma_t}{\frac{f_t}{\gamma_{R,t}}} \quad (6-22)$$

6.3.1.2 Members in Axial Compression

Members subjected to axial compression should be checked both for ultimate as well as buckling strength. The corresponding utilization factor for ultimate strength would be:

$$U_m = \frac{\sigma_c}{\frac{f_c}{\gamma_{R,c}}} \quad (6-23)$$

Where:

σ_c : Axial compressive stress (MPa)

f_c : Representative Axial compressive strength as will be derived below (MPa)

$\gamma_{R,c}$: Partial resistance factor for axial compressive strength (= 1.18)

The representative axial compressive strength for tubular members f_c without hydrostatic pressure would be derived by the smallest values of the following equations:

$$f_c = (1.0 - 0.278\lambda^2)f_{yc}, \text{ for } \lambda \leq 1.34$$

$$f_c = \frac{0.9}{\lambda^2} f_{yc}, \text{ for } \lambda \leq 1.34 \quad (6-24)$$

$$\lambda = \sqrt{\frac{f_{yc}}{f_e}} = \frac{KL}{\pi r} \sqrt{\frac{f_{yc}}{E}}$$

Where:

f_{yc} : Representative local buckling strength, as will be derived below (MPa)

λ : Column Slenderness parameter

f_e : Euler buckling strength (MPa)

E : Young's Modulus of Elasticity (MPa)

K : Effective length factor

L : Un-braced length (m)

r : Radius of gyration ($= \sqrt{I/A}$) (m)

I : Moment of inertia ($\text{kg}\cdot\text{m}^2$)

A : Cross-sectional area (m^2)

The representative local buckling strength f_{yc} shall be determined as:

$$f_{yc} = f_y, \text{ for } \frac{f_y}{f_{xe}} \leq 0.170 \quad (6-25)$$

$$f_{yc} = \left(1.047 - 0.274 \frac{f_y}{f_{xe}}\right) f_y, \text{ for } \frac{f_y}{f_{xe}} > 0.170$$

$$f_{xe} = 2C_x Et/D \quad (6-26)$$

Where:

f_{xe} : Representative elastic local buckling strength (MPa)

C_x : Elastic critical buckling coefficient ($= 0.3 - 0.6$)

D : Outside diameter of member (m)

t : Wall thickness of member (mm)

6.3.1.3 Bending

The corresponding utilization factor for members subjected to bending should be:

$$U_m = \frac{\sigma_b}{\frac{f_b}{\gamma_{R,b}}} = \frac{M/Z_e}{\frac{f_b}{\gamma_{R,b}}} \leq 1.0 \quad (6-27)$$

Where:

σ_b : Bending stress (MPa)

f_b : Representative bending strength (MPa)

$\gamma_{R,b}$: Partial resistance factor for bending strength (= 1.05)

M : Bending moment (Nm)

Z_e : Elastic section modulus (mm³)

The representative bending strength should be determined as:

$$f_b = \left(\frac{Z_p}{Z_e}\right) f_y, \text{ for } \frac{f_y D}{Et} \leq 0.0517$$

$$f_b = \left[1.13 - 2.58 \left(\frac{f_y D}{Et}\right)\right] \left(\frac{Z_p}{Z_e}\right) f_y, \text{ for } 0.0517 < \frac{f_y D}{Et} \leq 0.1034 \quad (6-28)$$

$$f_b = \left[0.94 - 0.76 \left(\frac{f_y D}{Et}\right)\right] \left(\frac{Z_p}{Z_e}\right) f_y, \text{ for } 0.1034 < \frac{f_y D}{Et} \leq 120 \frac{f_y}{E}$$

6.3.1.4 Shear

For members, subjected to shear force, the utilization factor should be derived as:

$$U_m = \frac{\tau_b}{\frac{f_v}{\gamma_{R,v}}} = \frac{2V/A}{\frac{f_v}{\gamma_{R,v}}} \leq 1.0 \quad (6-29)$$

Where:

τ_b : Maximum beam shear stress (MPa)

f_v : Representative shear strength (= $f_y/\sqrt{3}$) (MPa)

$\gamma_{R,v}$: Partial resistance factor for shear strength (= 1.05)

V : Beam shear (N)

For members subjected to torsional shear force, the utilization factor should be derived as:

$$U_m = \frac{\tau_t}{\frac{f_v}{\gamma_{R,v}}} = \frac{M_{v,t}D/2I_p}{\frac{f_v}{\gamma_{R,v}}} \leq 1.0 \quad (6-30)$$

Where:

τ_t : Torsional shear stress (MPa)

$M_{v,t}$: Torsional moment due to factored actions (Nm)

$I_p = \frac{\pi}{21} [D^4 - (D - 2t)^4]$: Polar moment of inertia (m³)

6.3.1.5 Hydrostatic Pressure

Provisions of ISO 19902 for calculation of hydrostatic pressure and formulation of utilization criteria for hoop buckling stress are exactly the same as the ones included in API RP-2A LRFD and have been presented in the previous section. Therefore, they will not be analytically presented here. The utilization factor of a member under external pressure is derived as:

$$U_m = \frac{\sigma_h}{\frac{f_h}{\gamma_{R,h}}} = \frac{pD/2t}{\frac{f_h}{\gamma_{R,h}}} \leq 1.0 \quad (6-31)$$

6.3.1.6 Members subjected to combined forces without hydrostatic pressure

For tubular members subjected to combined axial tension and bending forces, without hydrostatic pressure, the condition that should be satisfied is:

$$U_m = \frac{\gamma_{R,t} \cdot \sigma_t}{f_t} + \frac{\gamma_{R,d} \cdot \sqrt{\sigma_{b,y}^2 + \sigma_{b,z}^2}}{f_b} \leq 1.0 \quad (6-32)$$

Where:

$\sigma_{b,y}, \sigma_{b,z}$: Bending stress about the member y and z-axis (MPa)

For tubular members subjected to combined axial compression and bending forces without hydrostatic pressure, the condition that should be satisfied is:

$$U_m = \frac{\gamma_{R,c} \cdot \sigma_c}{f_c} + \frac{\gamma_{R,b}}{f_b} \cdot \left[\left(\frac{C_{m,y} \cdot \sigma_{b,y}}{1 - \sigma_c / f_{e,y}} \right)^2 + \left(\frac{C_{m,z} \cdot \sigma_{b,z}}{1 - \sigma_c / f_{e,z}} \right)^2 \right]^{0,5} \leq 1.0 \quad (6-33)$$

$$U_m = \frac{\gamma_{R,c} \cdot \sigma_c}{f_{yc}} + \frac{\gamma_{R,b} \cdot \sqrt{\sigma_{b,y}^2 + \sigma_{b,z}^2}}{f_b} \leq 1.0 \quad (6-34)$$

Where:

$C_{m,y}$, $C_{m,z}$: Moment reduction factors corresponding to the member y- and z-axes (see Table 44)

$f_{e,y} = \frac{\pi^2 E}{(K_y \cdot L_y / r)^2}$, $f_{e,z} = \frac{\pi^2 E}{(K_z \cdot L_z / r)^2}$: Euler buckling strengths corresponding to the member y- and z-axes (MPa)

K_y , K_z : Effective length factors for the y- and z-directions (see Table 44)

L_y , L_z : Un-braced lengths in the y- and z-directions (m)

6.3.1.7 Members subjected to combined forces with hydrostatic pressure

In the presence of hydrostatic pressure, for tubular members subjected to combined axial tension, bending and hydrostatic pressure shall be designed to satisfy:

$$U_m = \frac{\gamma_{R,t} \cdot \sigma_{t,c}}{f_{t,h}} + \frac{\gamma_{R,b} \cdot \sqrt{\sigma_{b,y}^2 + \sigma_{b,z}^2}}{f_{b,h}} \leq 1.0 \quad (6-35)$$

Where:

$f_{t,h} = f_y \cdot \left(\sqrt{1 + 0,09 \cdot B^2 - B^{2\eta}} - 0,3 \cdot B \right)$: Representative axial tensile strength in the presence of external hydrostatic pressure

$f_{b,h} = f_b \cdot \left(\sqrt{1 + 0,09 \cdot B^2 - B^{2\eta}} - 0,3 \cdot B \right)$: Representative bending strength in the presence of external hydrostatic pressure

$$B = \frac{\gamma_{R,h} \cdot \sigma_h}{f_h} \leq 1.0, \eta = 5 - 4 \cdot \frac{f_h}{f_y}$$

For tubular members subjected to combined axial compression, bending and hydrostatic pressure shall be designed to satisfy:

$$U_m = \frac{\gamma_{R,c} \cdot \sigma_{c,c}}{f_{yc}} + \frac{\gamma_{R,b} \cdot \sqrt{\sigma_{b,y}^2 + \sigma_{b,z}^2}}{f_{b,h}} \leq 1.0 \quad (6-36)$$

$$U_m = \frac{\gamma_{R,c} \cdot \sigma_c}{f_{c,h}} + \frac{\gamma_{R,b}}{f_{b,h}} \cdot \left[\left(\frac{C_{m,y} \cdot \sigma_{b,y}}{1 - \sigma_c / f_{e,y}} \right)^2 + \left(\frac{C_{m,z} \cdot \sigma_{b,z}}{1 - \sigma_c / f_{e,z}} \right)^2 \right]^{0,5} \leq 1.0 \quad (6-37)$$

$$U_m = \frac{\sigma_x - 0,5 \cdot f_{he} / \gamma_{R,h}}{f_{xe} / \gamma_{R,c} - 0,5 \cdot f_{he} / \gamma_{R,h}} + \left(\frac{\gamma_{R,h} \cdot \sigma_h}{f_{he}} \right)^2 \leq 1.0 \quad (6-38)$$

Where:

$f_{c,h}$: Representative axial compressive strength in the presence of external hydrostatic pressure (MPa)

$$f_{c,h} = \frac{1}{2} f_{yc} \left[(1,0 - 0,278\lambda^2) - \frac{2\sigma_q}{f_{yc}} + \sqrt{(1,0 - 0,278\lambda^2)^2 + 1,12\lambda^2 \frac{\sigma_q}{f_{yc}}} \right],$$

$$\text{for } \lambda \leq 1,34 \sqrt{\left(1 - \frac{2\sigma_q}{f_{yc}}\right)^{-1}} \quad (6-39)$$

$$f_{c,h} = \frac{0,9}{\lambda^2} \cdot f_{yc}, \text{ for } \lambda \leq 1,34 \sqrt{\left(1 - \frac{2\sigma_q}{f_{yc}}\right)^{-1}}$$

$\sigma_q = 0.5\sigma_h$: Compressive axial strength due to capped end hydrostatic action (MPa)

σ_h : Hoop stress due to forces from factored hydrostatic pressure (MPa)

Structural component	K	C_m^a
Topsides legs		
Braced	1,0	1)
Portal (unbraced)	K^b	1)
Structure legs and piling		
Grouted composite section	1,0	3)
UngROUTED legs	1,0	3)
UngROUTED piling between shim points	1,0	2)
Structure brace members		
Primary diagonals and horizontals	0,7	2) or 3)
K-braces ^c	0,7	2) or 3)
X-braces		
Longer segment length ^c	0,8	2) or 3)
Full length ^d	0,7	2) or 3)
Secondary horizontals	0,7	2) or 3)
a. C_m values for the three cases defined in this table are as follows:		
1) 0,85;		
2) for members with no transverse loading, other than self weight,		
$C_m = 0,6 - 0,4 \cdot M_1/M_2$		
where M_1/M_2 is the ratio of smaller to larger moments at the ends of the unbraced portion of the member in the plane of bending under consideration;		
M_1/M_2 is positive when the member is bent in reverse curvature, negative when bent in single curvature.		
C_m shall not be larger than 0,85;		
3) for members with transverse loading, other than self weight,		
$C_m = 1,0 - 0,4 \cdot (\sigma_c/f_e)$, or 0,85, whichever is less,		
and $f_e = f_{ey}$ or f_{ez} as appropriate.		
b. See effective length alignment chart in A.13.5. This may be modified to account for conditions different from those assumed in the development of the chart.		
c. For either in-plane or out-of-plane effective lengths, at least one pair of members framing into a K- or X-joint shall be in tension, if the joint is not braced out-of-plane.		
d. When all members are in compression and the joint is not braced out-of-plane.		

Table 44: Effective length and moment reduction factors for member strength checking

6.3.2 Numerical Results

Table 45, summarizes the limit states that have been considered in the reliability assessment of the reference structure. The corresponding paragraph and number of each limit state, as it is referred to in the standard, is included, as well as the identification number that corresponds to this limit state in this

Chapter. Following, in Table 46 to Table 48, the results of reliability analysis of each limit state are presented for the different classes of members.

Limit State	Description	Equation
(13.2-2)	Usage factor according to (13.2-2) – Axial Tension	6-22
(13.2-4)	Usage factor according to (13.2-4) – Axial compression	6-23
Euler	Usage factor with respect to Euler load capacity	
(13.2-12)	Usage factor according to (13.2-12) – Bending	6-27
(13.2-17)	Usage factor according to (13.2-17) – Shear	6-29
(13.2-19)	Usage factor according to (13.2-19) – Torsion	6-30
(13.3-2)	Usage factor according to (13.3-2) – Tension and bending	6-32
(13.3-7)	Usage factor according to (13.3-7) – Compression and bending	6-33
(13.3-8)	Usage factor according to (13.3-8) – Compression and bending	6-34
(13.2-31)	Usage factor according to (13.2-31) – Hoop Buckling	6-31
(13.4-12)	Usage factor according to (13.4-12) – Tension, Bending, hydrostatic pressure	6-35
(13.4-19)	Usage factor according to (13.4-19) – Compression, Bending, hydrostatic pressure	6-36
(13.4-20)	Usage factor according to (13.4-20) – Compression, Bending, hydrostatic pressure	6-37
(13.4-21)	Usage factor according to (13.4-21) – Compression, Bending, hydrostatic pressure	6-38

Table 45: Limit States according to ISO 19902

	(13.2-2)	(13.2-4)	Euler	(13.2-12)	(13.2-17)	(13.2-19)	(13.3-2)	(13.3-7)	(13.3-8)	(13.2-31)	(13.4-12)	(13.4-19)	(13.4-20)	(13.4-21)
b101	6.16	9.64	25.02	11.88	32.06	22.76	5.41	7.26	8.92	0.00	0.00	0.00	0.00	0.00
b102	0.00	5.52	15.22	12.22	33.82	21.42	0.00	4.71	4.95	0.00	0.00	0.00	0.00	0.00
b103	0.00	5.52	15.21	12.20	33.85	21.42	0.00	4.71	4.96	0.00	0.00	0.00	0.00	0.00
b104	6.16	9.64	24.99	11.89	32.04	22.78	5.41	7.26	8.91	0.00	0.00	0.00	0.00	0.00
b201	6.86	10.22	24.99	18.22	25.38	33.66	6.05	16.55	13.07	0.00	0.00	0.00	0.00	0.00
b202	0.00	6.82	18.75	39.88	53.37	33.69	0.00	6.56	6.85	0.00	0.00	0.00	0.00	0.00
b203	0.00	6.82	18.72	39.94	53.36	33.68	0.00	6.56	6.85	0.00	0.00	0.00	0.00	0.00
b204	6.88	10.24	25.00	18.19	25.36	33.68	6.05	16.51	13.07	0.00	0.00	0.00	0.00	0.00
b301	10.49	41.79	90.92	10.16	19.35	0.00	7.17	0.00	0.00	0.00	0.00	0.00	0.00	0.00
b302	0.00	9.42	22.84	27.19	50.18	0.00	0.00	7.75	9.01	0.00	0.00	0.00	0.00	0.00
b303	0.00	9.42	22.85	27.20	50.19	0.00	0.00	7.75	9.02	0.00	0.00	0.00	0.00	0.00
b304	10.48	41.76	90.96	10.18	19.37	0.00	7.17	0.00	0.00	0.00	0.00	0.00	0.00	0.00
b401	0.00	0.00	0.00	17.02	25.49	19.43	0.00	35.07	29.35	0.00	0.00	0.00	0.00	0.00
b402	0.00	19.06	40.03	18.01	25.52	20.11	0.00	11.05	12.79	0.00	0.00	0.00	0.00	0.00
b403	0.00	19.09	40.04	18.04	25.52	20.08	0.00	11.05	12.79	0.00	0.00	0.00	0.00	0.00
b404	0.00	0.00	0.00	17.03	25.51	19.42	0.00	35.08	29.34	0.00	0.00	0.00	0.00	0.00

Table 46: Reliability indices for Leg Members

	(13.2-2)	(13.2-4)	Euler	(13.2-12)	(13.2-17)	(13.2-19)	(13.3-2)	(13.3-7)	(13.3-8)	(13.2-31)	(13.4-12)	(13.4-19)	(13.4-20)	(13.4-21)
b111	0.00	0.00	0.00	63.25	0.00	0.00	0.00	63.25	63.25	0.00	0.00	0.00	0.00	0.00
b112	0.00	0.00	0.00	63.25	0.00	0.00	0.00	63.25	63.25	0.00	0.00	0.00	0.00	0.00
b113	0.00	0.00	0.00	63.25	0.00	0.00	0.00	63.25	63.25	0.00	0.00	0.00	0.00	0.00
b114	0.00	0.00	0.00	63.25	0.00	0.00	0.00	63.25	63.25	0.00	0.00	0.00	0.00	0.00
b115	0.00	0.00	0.00	40.05	0.00	0.00	0.00	0.00	0.00	82.54	0.00	37.50	0.00	0.00
b116	0.00	0.00	0.00	40.05	0.00	0.00	0.00	0.00	0.00	82.55	0.00	37.50	0.00	0.00
b211	0.00	0.00	0.00	13.85	0.00	80.45	13.77	0.00	0.00	0.00	0.00	0.00	0.00	0.00
b212	13.45	0.00	0.00	15.61	30.22	0.00	9.90	0.00	0.00	0.00	0.00	0.00	0.00	0.00
b213	0.00	0.00	0.00	13.86	0.00	80.44	13.80	0.00	0.00	0.00	0.00	0.00	0.00	0.00
b214	57.94	7.96	9.26	15.74	31.93	0.00	6.43	9.44	0.00	0.00	0.00	0.00	0.00	0.00
b215	0.00	0.00	0.00	20.97	79.86	53.37	0.00	0.00	0.00	92.58	22.67	0.00	0.00	0.00
b216	0.00	0.00	0.00	20.99	79.92	53.38	0.00	0.00	0.00	92.68	22.72	0.00	0.00	0.00
b311	57.73	0.00	0.00	11.70	56.63	0.00	11.48	0.00	0.00	0.00	0.00	0.00	0.00	0.00
b312	15.89	0.00	0.00	8.85	20.89	0.00	7.57	0.00	0.00	0.00	0.00	0.00	0.00	0.00
b313	57.71	0.00	0.00	11.71	56.68	0.00	11.48	0.00	0.00	0.00	0.00	0.00	0.00	0.00
b314	32.77	8.32	9.54	9.26	23.55	0.00	6.02	7.01	0.00	0.00	0.00	0.00	0.00	0.00
b315	0.00	0.00	0.00	19.59	0.00	46.39	0.00	0.00	0.00	85.05	27.92	0.00	0.00	0.00
b316	0.00	0.00	0.00	19.59	0.00	46.42	0.00	0.00	0.00	85.06	27.94	0.00	0.00	0.00
b411	0.00	0.00	0.00	10.31	53.22	0.00	10.37	0.00	0.00	0.00	0.00	0.00	0.00	0.00
b412	18.98	0.00	0.00	7.45	18.54	0.00	6.75	0.00	0.00	0.00	0.00	0.00	0.00	0.00
b413	0.00	0.00	0.00	10.31	53.27	0.00	10.38	0.00	0.00	0.00	0.00	0.00	0.00	0.00
b414	36.09	11.42	13.16	7.14	17.76	0.00	0.00	4.28	4.55	0.00	0.00	0.00	0.00	0.00
b415	0.00	0.00	0.00	9.70	21.95	44.36	0.00	0.00	0.00	59.63	9.65	0.00	0.00	0.00
b416	0.00	0.00	0.00	9.70	21.96	44.37	0.00	0.00	0.00	59.60	9.65	0.00	0.00	0.00

Table 47: Reliability indices for Horizontal Brace Members

	(13.2-2)	(13.2-4)	Euler	(13.2-12)	(13.2-17)	(13.2-19)	(13.3-2)	(13.3-7)	(13.3-8)	(13.2-31)	(13.4-12)	(13.4-19)	(13.4-20)	(13.4-21)
b151	6.44	0.00	0.00	13.73	0.00	25.38	0.00	0.00	0.00	0.00	5.67	0.00	0.00	0.00
b152	0.00	0.00	3.23	0.00	84.93	80.48	0.00	0.00	0.00	83.16	0.00	6.03	2.20	20.07
b153	0.00	0.00	8.34	22.20	0.00	37.33	0.00	0.00	0.00	0.00	0.00	11.60	5.10	0.00
b154	0.00	0.00	8.34	22.21	0.00	37.42	0.00	0.00	0.00	0.00	0.00	11.59	5.09	0.00
b155	0.00	0.00	3.23	0.00	84.83	80.48	0.00	0.00	0.00	83.15	0.00	6.04	2.20	20.06
b156	6.45	0.00	0.00	13.72	0.00	25.39	0.00	0.00	0.00	0.00	5.66	0.00	0.00	0.00
b157	13.34	0.00	0.00	8.90	27.85	37.39	0.00	0.00	0.00	82.53	6.08	0.00	0.00	0.00
b158	13.34	0.00	0.00	8.90	27.87	37.39	0.00	0.00	0.00	82.54	6.08	0.00	0.00	0.00
b251	6.71	0.00	0.00	11.32	40.11	29.49	0.00	0.00	0.00	10.69	5.43	0.00	0.00	0.00
b252	0.00	0.00	3.47	60.04	84.98	40.61	0.00	0.00	0.00	0.00	0.00	5.99	2.24	23.17
b253	0.00	0.00	13.88	14.80	0.00	42.39	0.00	0.00	0.00	0.00	0.00	12.34	6.76	0.00
b254	0.00	0.00	13.88	14.80	0.00	42.35	0.00	0.00	0.00	0.00	0.00	12.35	6.76	0.00
b255	0.00	0.00	3.47	60.07	84.98	40.64	0.00	0.00	0.00	0.00	0.00	5.99	2.24	23.19
b256	6.71	0.00	0.00	11.32	40.12	29.50	0.00	0.00	0.00	10.68	5.44	0.00	0.00	0.00

	(13.2-2)	(13.2-4)	Euler	(13.2-12)	(13.2-17)	(13.2-19)	(13.3-2)	(13.3-7)	(13.3-8)	(13.2-31)	(13.4-12)	(13.4-19)	(13.4-20)	(13.4-21)
b257	26.77	0.00	0.00	9.08	23.47	42.44	0.00	0.00	0.00	92.66	6.31	0.00	0.00	0.00
b258	26.77	0.00	0.00	9.07	23.47	42.41	0.00	0.00	0.00	92.68	6.32	0.00	0.00	0.00
b351	6.84	0.00	0.00	9.88	38.75	30.01	0.00	0.00	0.00	17.32	5.41	0.00	0.00	0.00
b352	0.00	0.00	4.01	15.59	30.27	30.10	0.00	0.00	0.00	0.00	0.00	5.93	2.65	26.79
b353	0.00	0.00	19.92	9.72	84.91	32.76	0.00	0.00	0.00	0.00	0.00	9.02	6.36	46.37
b354	0.00	0.00	19.93	9.71	84.97	32.81	0.00	0.00	0.00	0.00	0.00	9.02	6.35	46.44
b355	0.00	0.00	4.01	15.62	30.28	30.07	0.00	0.00	0.00	0.00	0.00	5.91	2.65	26.74
b356	6.84	0.00	0.00	9.89	38.74	30.03	0.00	0.00	0.00	17.35	5.40	0.00	0.00	0.00
b357	28.38	0.00	99.26	5.85	11.76	18.34	0.00	0.00	0.00	0.00	4.71	0.00	0.00	0.00
b358	28.40	0.00	99.28	5.85	11.78	18.35	0.00	0.00	0.00	0.00	4.71	0.00	0.00	0.00
b451	7.91	0.00	0.00	12.75	31.73	25.50	0.00	0.00	0.00	80.91	6.51	0.00	0.00	0.00
b452	0.00	5.28	5.05	25.72	53.41	30.05	0.00	4.73	9.25	0.00	0.00	7.91	3.87	46.46
b453	0.00	7.64	26.26	3.86	10.12	22.95	0.00	2.82	3.28	0.00	0.00	0.00	0.00	0.00
b454	0.00	7.64	26.26	3.86	10.12	22.95	0.00	2.83	3.28	0.00	0.00	0.00	0.00	0.00
b455	0.00	5.28	5.05	25.73	53.39	30.07	0.00	4.72	9.25	0.00	0.00	7.91	3.87	46.42
b456	7.90	0.00	0.00	12.75	31.75	25.47	0.00	0.00	0.00	80.83	6.52	0.00	0.00	0.00
b457	0.00	9.44	0.00	4.38	11.42	80.38	0.00	4.90	8.32	0.00	0.00	4.53	4.66	13.16
b458	0.00	9.43	0.00	4.39	11.42	80.43	0.00	4.91	8.32	0.00	0.00	4.53	4.65	13.15

Table 48: Reliability indices for Vertical Brace Members

The final value of the reliability index for every member will be derived as the minimum value calculated from each of the limit states examined. Results referring to the leg members, starting from the first elevation, distinguish one set of members in axial compression and bending (b102-b103) with $\beta = 4.71$ and one set in axial tension and bending (b101-b104) with $\beta = 5.41$. Due to the uniform cross section of the legs, it is expected that the values of β of this elevation will be the lowest one, sizing the rest of the leg members. Moving to the second elevation a different pattern is followed with members (b202-b203) in axial compression and bending with $\beta = 6.56$ having a greater value of reliability index than the second member (b201-b204) subjected in axial tension and bending with $\beta = 6.05$. The same pattern as in the second elevation can be observed in the third elevation with the set of members (b302-b303) subjected to axial compression and bending with $\beta = 7.75$ and the set of (b301-b304) subjected to axial tension and bending with $\beta = 7.17$. A slightly different behaviour can be observed in elevation 4 leg members with the set of members

(b402-b403) subjected to axial compression and bending with $\beta = 11.05$ and the set of (b401-b404) subjected to bending with $\beta = 17.02$.

Horizontal bracing members of the first elevation, have great values of reliability due to the insignificant loads they carry due to the piling conditions that have been applied. Members of the first elevation that stand parallel to the flow (b211-b213) have $\beta = 13.77$ due to axial tension and bending, while for the members vertical to the flow, the one that meets the flow first (b214) has a lower value of $\beta = 6.43$ and the second one (b212) has $\beta = 9.90$ both due to axial tension and bending. The two X-bracing members (b215-b216) have great values of reliability since they carry minimum loads as they have a non functional load to the operation of the structures. In the third elevation, the reliability indices of all of the members forming the square braces are determined by the axial tension and bending limit states where the two symmetrical members, parallel to the flow (b311-b313) have $\beta = 11.48$, the first vertical to the flow (b314) $\beta = 6.02$ and the second (b312) $\beta = 7.57$. The members parallel to the flow of the fourth elevation (b411-b413) have $\beta = 10.31$ due to bending, the first member vertical to the flow (b414) $\beta = 4.28$ due to axial compression and bending while the second member (b412) $\beta = 6.75$ due to axial tension and bending. At this elevation the X brace members show values of $\beta = 9.65$ due to the axial compression and bending criterion, due to the loads transmitted from the topside loads.

For the vertical X-braces of the first elevation, the two symmetrical sets of members parallel to the flow, have one of their members (b152-b155) defined from the axial compression, bending and hydrodynamic limit state with $\beta = 2.20$ and the other of their members (b151-b156) with $\beta = 5.67$ subjected to axial tension, bending and hydrodynamic pressure. From the sets vertical to the flow, the first (b157-b158) has $\beta = 6.08$ due to axial tension, bending and hydrostatic pressure, while the second one (b153-b154) has $\beta = 5.10$ due to axial compression, bending and hydrostatic pressure. From the members of the second elevation that stand parallel to the flow, members (b252-b255) are subjected to axial compression, bending and hydrodynamic pressure with

$\beta = 2.24$ while members (b251-b256) are subjected in axial tension, bending and hydrodynamic pressure with $\beta = 5.43$. From the sets vertical to the flow, the first (b257-b258) has $\beta = 6.31$ due to axial tension, bending and hydrostatic pressure, while the second one (b253-b254) has $\beta = 6.76$ due to axial compression, bending and hydrodynamic pressure. From the members of the third elevation that stand parallel to the flow, members (b352-b355) are subjected to axial compression, bending and hydrodynamic pressure with $\beta = 2.65$ while members (b351-b356) are subjected in axial tension, bending and hydrostatic pressure with $\beta = 5.41$. From the sets vertical to the flow, the first (b357-b358) has $\beta = 4.71$ due to axial tension, bending and hydrodynamic pressure, while the second one (b353-b354) has $\beta = 6.35$ due to axial compression, bending and hydrostatic pressure. Finally for the members of the fourth elevation, those that stand parallel to the flow, (b452-b455) are subjected to axial compression, bending and hydrodynamic pressure with $\beta = 3.87$ while members (b451-b456) are subjected in axial tension, bending and hydrodynamic pressure with $\beta = 6.51$. From the sets vertical to the flow, the first (b457-b458) has $\beta = 4.38$ due to bending, while the second one (b453-b454) has $\beta = 2.82$ due to axial compression and bending.

6.4 BS EN 1993-1-1:2005 Eurocode 3: Design of Steel Structures

In this section, the design requirements of Eurocode 3 will be discussed. Provisions for cylindrical cross sections will be presented resulting to derivation of limit states that will be used later in the analysis. The basic requirement demands that 'the design value of one or several action effects in each cross section shall not exceed the corresponding design resistance for that action or the corresponding combination' [5]. The design values of resistance should depend on the classification of the cross-section, while four classes can be distinguished:

- Class 1 cross-sections are those which can develop their plastic moment capacity and provide significant amount of rotation resistance.
- Class 2 cross-sections are those which can develop their plastic moment resistance, but have limited rotation capacity because of local buckling.
- Class 3 cross-sections are those in which the stress in the extreme compression fibre of the steel member assuming an elastic distribution of stresses can reach the yield strength, but local buckling is liable to prevent development of the plastic moment resistance.
- Class 4 cross-sections are those in which local buckling will occur before the attainment of yield stress in one or more parts of the cross-section.

Table 49, presents the criteria for classification of members based on design yield and geometrical properties.

Class	Section in bending and/or compression					
1	$d/t \leq 50\varepsilon^2$					
2	$d/t \leq 70\varepsilon^2$					
3	$d/t \leq 90\varepsilon^2$					
	f_y	235	275	355	420	460
$\varepsilon = \sqrt{235/f_y}$	ε	1,00	0,92	0,81	0,75	0,71
	ε^2	1,00	0,85	0,66	0,56	0,51

Table 49: Classification of members

6.4.1 Design Provisions

For elastic verification, the following conservative yield criterion should be satisfied along the length of the member under consideration:

$$\left(\frac{\sigma_{x,Ed}}{f_y/\gamma_{M0}}\right)^2 + \left(\frac{\sigma_{z,Ed}}{f_y/\gamma_{M0}}\right)^2 - \left(\frac{\sigma_{x,Ed}}{f_y/\gamma_{M0}}\right) \cdot \left(\frac{\sigma_{z,Ed}}{f_y/\gamma_{M0}}\right) + 3 \cdot \left(\frac{\tau_{Ed}}{f_y/\gamma_{M0}}\right)^2 \leq 1 \quad (6-40)$$

Where:

$\sigma_{x,Ed}$: Design value of the longitudinal stress at the point of consideration (MPa)

$\sigma_{z,Ed}$: Design value of the transverse stress at the point of consideration (MPa)

τ_{Ed} : Design value of the shear stress at the point of consideration (MPa)

γ_{M0} : Resistance partial factor of cross section applicable to all classes (1.00)

Another conservative approximation applicable to all cross section classes introduces a linear summation of the utilization ratios for each stress resultant.

$$\frac{N_{Ed}}{N_{Rd}} + \frac{M_{y,Ed}}{M_{y,Rd}} + \frac{M_{z,Ed}}{M_{z,Rd}} \leq 1 \quad (6-41)$$

Where:

$N_{Rd}, M_{y,Rd}, M_{z,Rd}$: Design values of the resistance depending on the cross sectional classification and including any reduction that may be caused by shear effects

$N_{Ed}, M_{y,Ed}, M_{z,Ed}$: Design values of the action at point of consideration

6.4.1.1 Members in Tension

For members in tension, the design value of the tension force N_{Ed} at each cross section should satisfy:

$$\frac{N_{Ed}}{N_{t,Rd}} \leq 1.0 \quad (6-42)$$

Where,

$$N_{t,Rd} = \min \left(N_{pl,Rd} = \frac{A \cdot f_y}{\gamma_{M0}}, N_{u,Rd} = \frac{0,9 A_{net} \cdot f_u}{\gamma_{M2}} \right)$$

γ_{M2} : Resistance of cross section in tension to fracture

6.4.1.2 Members in Compression

For members in compression, the design value of the compression force N_{Ed} at each cross-section should satisfy:

$$\frac{N_{Ed}}{N_{c,Rd}} \leq 1.0 \quad (6-43)$$

Where:

$$N_{c,Rd} = \frac{A \cdot f_y}{\gamma_{M0}}, \text{ for class 1, 2 or 3 cross-sections}$$

$$N_{c,Rd} = \frac{A_{eff} \cdot f_y}{\gamma_{M0}}, \text{ for class 4 cross-sections}$$

6.4.1.3 Bending

For members under bending moment, the design value of the bending moment M_{Ed} at each cross-section should satisfy:

$$\frac{M_{Ed}}{M_{c,Rd}} \leq 1.0 \quad (6-44)$$

$$M_{c,Rd} = M_{pl,Rd} = \frac{W_{pl} \cdot f_y}{\gamma_{M0}}, \text{ for class 1 or 2 cross sections}$$

$$M_{c,Rd} = M_{el,Rd} = \frac{W_{el,min} \cdot f_y}{\gamma_{M0}}, \text{ for class 3 cross sections}$$

$$M_{c,Rd} = \frac{W_{eff,min} \cdot f_y}{\gamma_{M0}}, \text{ for class 4 cross sections}$$

Where: $W_{el,min}$ and $W_{eff,min}$ is the maximum elastic stress (MPa).

6.4.1.4 Shear

For members under shear loads, the design value of the shear force V_{Ed} at each cross section should satisfy:

$$\frac{V_{Ed}}{V_{c,Rd}} \leq 1.0 \quad (6-45)$$

Where: $V_{c,Rd}$ is the design shear resistance (N)

In the absence of torsion the design plastic shear resistance is given by:

$$V_{pl,Rd} = \frac{A_V (f_y / \sqrt{3})}{\gamma_{M0}} \quad (6-46)$$

Where: $A_V = 2A/\pi$ is the shear area for cylindrical cross sections.

A conservative verification based on elastic design, suggests:

$$\frac{\frac{V_{Ed} \cdot S}{I \cdot t}}{f_y / (\sqrt{3} \cdot \gamma_{M0})} \leq 1.0 \quad (6-47)$$

V_{Ed} : Design value of the shear force (N)

S : First moment of area about the centroidal axis of that portion of the cross-section between the point at which the shear is required and the boundary of the cross-section (m³)

I : Second moment of area of the whole cross section (mm⁴)

t : The thickness at the examined point (mm)

6.4.1.5 Torsion

For members subject to torsion for which distortional deformations may be disregarded the design value of the torsional moment T_{Ed} at each cross-section should satisfy:

$$\frac{T_{Ed}}{T_{Rd}} \leq 1.0 \quad (6-48)$$

Where:

T_{Rd} : Design torsional resistance of the cross section.

For the elastic verification the yield criterion, eq. (6-40) can be applied.

6.4.1.6 Buckling Resistance of members

Members in compression should also be verified against buckling as follows:

$$\frac{N_{Ed}}{N_{b,Rd}} \leq 1.0 \quad (6-49)$$

Where:

N_{Ed} : Design value of the compression force (N)

$N_{b,Rd}$: Design buckling resistance of the compression member (N)

The design buckling resistance of a compression member $N_{b,Rd}$ should be taken as:

$$N_{b,Rd} = \frac{\chi \cdot A \cdot f_y}{\gamma_{M1}}, \text{ for class 1,2 and 3 cross sections}$$

$$N_{b,Rd} = \frac{\chi \cdot A_{eff} \cdot f_y}{\gamma_{M1}}, \text{ for class 4 cross sections}$$

Where:

γ_{M1} : Resistance of members to instability (1.00)

χ : Reduction factor for the relevant buckling mode and should be determined as follows based on the relevant buckling curve according to:

$$\chi = \frac{1}{\Phi + \sqrt{\Phi^2 - \bar{\lambda}^2}} \leq 1.0 \quad (6-50)$$

$$\Phi = 0,5 \cdot [1 + \alpha \cdot (\bar{\lambda} - 0,2) + \bar{\lambda}^2]$$

The non-dimensional slenderness $\bar{\lambda}$ is given by:

$$\bar{\lambda} = \sqrt{\frac{A \cdot f_y}{N_{cr}}} = \frac{L_{er}}{i} \cdot \frac{1}{\lambda_1}, \text{ for class 1,2 and 3 cross sections}$$

$$\bar{\lambda} = \sqrt{\frac{A_{eff} \cdot f_y}{N_{cr}}} = \frac{L_{er}}{i} \cdot \frac{\sqrt{\frac{A_{eff}}{A}}}{\lambda_1}, \text{ for class 4 cross sections}$$

$$\lambda_1 = \pi \sqrt{\frac{E}{f_y}} = 93, \quad \varepsilon = \sqrt{\frac{235}{f_y}} \quad (f_y \text{ in } N/mm^2)$$

Where:

α : Imperfection factor (see Table 50)

N_{cr} : Elastic critical force for the relevant buckling mode based on the gross cross sectional properties.

L_{er} : Buckling length in the buckling plane (m)

i : Radius of gyration about the relevant axis, determined using the properties of the gross cross-section (m)

Buckling curve	a_0	a	b	c	d
Imperfection factor α	0,13	0,21	0,34	0,49	0,76

Table 50: Imperfection factors for buckling curves

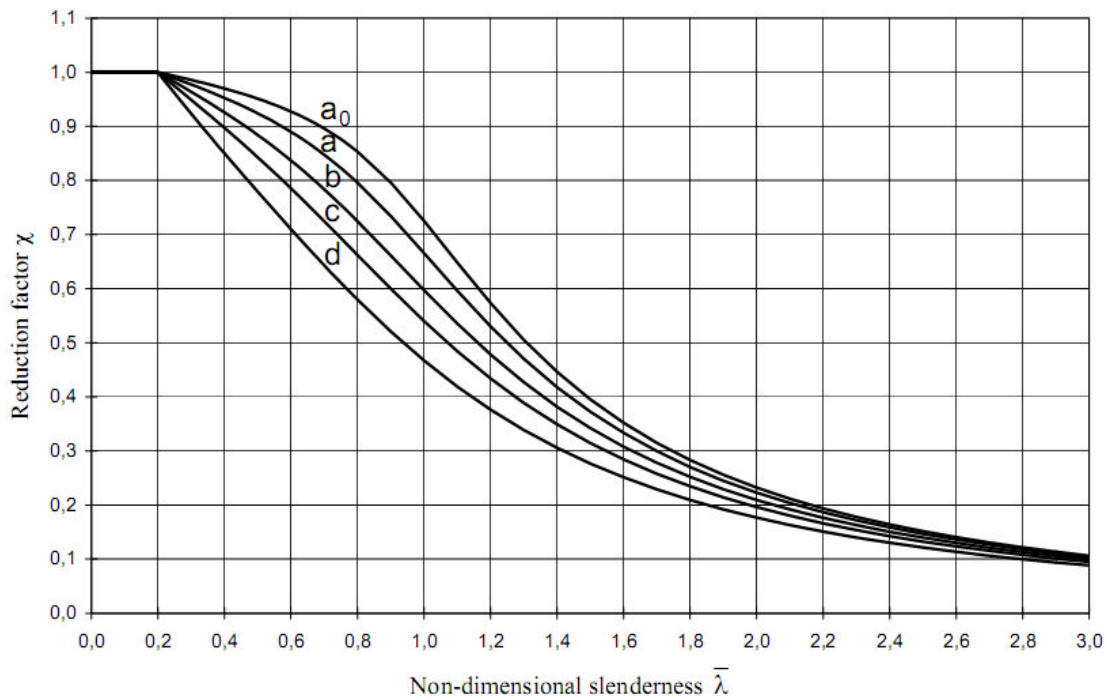


Figure 69: Buckling curves

Buckling effects may be ignored for slenderness $\bar{\lambda} \leq 0,2$ or for $\frac{N_{Ed}}{N_{cr}} \leq 0,04$.

For a laterally unrestrained member subject to major axis bending should be verified against lateral-torsional buckling as:

$$\frac{M_{Ed}}{M_{b,Rd}} \leq 1.0 \quad (6-51)$$

Where:

M_{Ed} : Design value of the moment (Nm)

$M_{b,Rd}$: Design buckling resistance moment (Nm)

The design buckling resistance moment should be considered as:

$$M_{b,Rd} = \chi_{LT} \cdot W_y \cdot \frac{f_y}{\gamma_{M1}} \quad (6-52)$$

Where:

W_y : Appropriate section modulus as follows:

$$W_y = W_{pl,y}, \text{ for Class 1 or 2 cross-sections}$$

$W_y = W_{el,y}$, for Class 3 cross-sections

$W_y = W_{eff,y}$, for Class 4 cross-sections

χ_{LT} : Reduction factor for lateral-torsional buckling.

γ_{M1} : Resistance of members to instability

Estimation of χ_{LT} for lateral torsional buckling should be determined as:

$$\chi_{LT} = \frac{1}{\Phi_{LT} + \sqrt{\Phi_{LT}^2 - \bar{\lambda}_{LT}^2}} \leq 1.0 \quad (6-53)$$

$$\Phi_{LT} = 0,5 \cdot [1 + \alpha_{LT} \cdot (\bar{\lambda}_{LT} - 0,2) + \bar{\lambda}_{LT}^2]$$

$$\bar{\lambda}_{LT} = \sqrt{\frac{W_y \cdot f_y}{M_{cr}}}$$

Where:

α_{LT} : Imperfection factor (see Table 50)

M_{cr} : Elastic critical moment for lateral-torsional buckling

For slenderness $\bar{\lambda}_{LT} \leq \bar{\lambda}_{LT,0}$ or for $\frac{M_{Ed}}{M_{er}} \leq \bar{\lambda}_{LT,0}^2$ lateral torsional buckling effects may be ignored and only cross sectional checks apply.

6.4.1.7 Bending and axial force

In the case of axial force acting on members, its effect on plastic resistance should be investigated. For class 1 and 2 cross sections, the following criterion shall be satisfied:

$$M_{Ed} \leq M_{N,Rd} \quad (6-54)$$

Where:

$M_{N,Rd}$: design plastic moment resistance reduced due to the axial force N_{Ed}

For circular cross sections, the criterion applied for bi-axial bending denotes:

$$\left[\frac{M_{y,Ed}}{M_{N,y,Rd}} \right]^2 + \left[\frac{M_{z,Ed}}{M_{N,z,Rd}} \right]^2 \leq 1 \quad (6-55)$$

$$M_{N,y,Rd} = M_{N,z,Rd} = M_{pl,Rd} \cdot (1 - n^{1,7})$$

For Class 3 and class 4 cross sections, in the absence of shear force, the maximum longitudinal stress shall satisfy the criterion:

$$\sigma_{x,Ed} \leq \frac{f_y}{\gamma_{M0}} \quad (6-56)$$

Where:

$\sigma_{x,Ed}$: Design value of the longitudinal stress due to moment and axial force

In the presence of shear, provided that the design value of shear force does not exceed 50% of the design plastic shear resistance, no reduction to the resistances defined for bending and axial force should be made. In the opposite case, a reduction in yield strength should be employed as:

$$(1 - \rho) \cdot f_y \quad (6-57)$$

$$\rho = (2V_{Ed}/V_{pl,Rd} - 1)^2$$

6.4.1.8 Members in bending and axial compression

For members which are subjected to combined bending and axial compression should satisfy:

$$\frac{N_{Ed}}{\chi_y \cdot N_{Rk}} + k_{yy} \cdot \frac{M_{y,Ed} + \Delta M_{y,Ed}}{\chi_{LT} \cdot \frac{M_{y,Rk}}{\gamma_{M1}}} + k_{yz} \cdot \frac{M_{z,Ed} + \Delta M_{z,Ed}}{\chi_{LT} \cdot \frac{M_{z,Rk}}{\gamma_{M1}}} \leq 1 \quad (6-58)$$

$$\frac{N_{Ed}}{\chi_z \cdot N_{Rk}} + k_{zy} \cdot \frac{M_{y,Ed} + \Delta M_{y,Ed}}{\chi_{LT} \cdot \frac{M_{y,Rk}}{\gamma_{M1}}} + k_{zz} \cdot \frac{M_{z,Ed} + \Delta M_{z,Ed}}{\chi_{LT} \cdot \frac{M_{z,Rk}}{\gamma_{M1}}} \leq 1$$

Where:

N_{Ed} , $M_{y,Ed}$, $M_{z,Ed}$: Design values of the compression force and the maximum moments about the y-y and z-z axis along the member, respectively

$\Delta M_{y,Ed}$, $\Delta M_{z,Ed}$: Moments due to the shift of the centroidal axis (=0 for classes 1, 2, 3; $=e_{N,y(z)}N_{ed}$ for class 4)

χ_y , χ_z : Reduction factors due to flexural buckling

χ_{LT} : Reduction factor due to lateral torsional buckling

k_{yy} , k_{yz} , k_{zy} , k_{zz} : Interaction factors (App. A and B of standard)

6.4.2 Numerical Results

Table 51, summarizes the limit states that have been considered in the reliability assessment of the reference structure. The corresponding paragraph and number of each limit state, as it is referred to in the standard, is included, as well as the identification number that correspond to this limit state in this Chapter. Following, in Table 52 to Table 54, the results of reliability analysis of each limit state are presented for the different classes of members.

Limit State	Description	Equation
ufEuler	Usage factor equal ratio for axial compression / Euler capacity	6-43
ufAxial	Usage factor equal ratio for axial load / design resistance for axial loading	6-42
ufTorsion	Usage factor due to torsion	6-48
ufShearz	Usage factor due to shear in local z direction	6-45
ufSheary	Usage factor due to shear in local y direction	6-45
ufXSection	Cross section usage factor according to section 6.2.9 (Bending and Axial Froce) and 6.2.10 (Bending Shear and axial Force)	6-54/6-56
uf646	Usage factor according to equation (6.46) (Buckling Resistance - Compression)	6-49
uf655	Usage factor according to equation (6.55) (Buckling Resistance - Bending)	6-51
uf661	Usage factor according to equation (6.61) (Bending and Axial Compression)	6-58a
uf662	Usage factor according to equation (6.62) (Bending and Axial Compression)	6-58b

Table 51: Limit States according to EN 1993

	ufEuler	ufAxial	ufTorsion	ufShearz	ufSheary	ufXSection	uf646	uf655	uf661	uf662
b101	25.00	5.44	22.26	0.00	80.60	0.00	10.54	0.00	7.69	8.18
b102	15.21	6.31	23.19	44.40	44.44	11.21	6.09	0.00	5.16	5.21
b103	15.22	6.32	23.17	44.36	44.45	11.19	6.09	0.00	5.17	5.21
b104	25.01	5.45	22.27	0.00	80.51	0.00	10.53	0.00	7.69	8.18
b201	25.01	5.85	29.45	30.33	53.38	17.81	11.32	0.00	21.35	19.14
b202	18.74	7.69	37.43	56.85	0.00	17.99	7.46	0.00	7.19	7.20
b203	18.72	7.69	37.43	56.78	0.00	17.99	7.45	0.00	7.19	7.20
b204	24.99	5.86	29.50	30.34	53.44	17.77	11.31	0.00	21.34	19.18

	ufEuler	ufAxial	ufTorsion	ufShearz	ufSheary	ufXSection	uf646	uf655	uf661	uf662
b301	91.11	10.30	0.00	25.06	37.39	11.57	0.00	0.00	0.00	0.00
b302	22.83	10.67	0.00	53.38	72.05	23.69	10.39	0.00	8.38	8.45
b303	22.86	10.67	0.00	53.39	71.98	23.69	10.39	0.00	8.38	8.44
b304	90.97	10.29	0.00	25.07	37.43	11.59	0.00	0.00	0.00	0.00
b401	0.00	0.00	19.70	31.16	36.07	20.54	0.00	0.00	23.90	24.45
b402	40.06	21.84	19.73	40.55	29.01	21.94	19.20	0.00	11.55	11.58
b403	40.04	21.83	19.76	40.56	29.01	21.97	19.20	0.00	11.54	11.57
b404	0.00	0.00	19.73	31.15	36.04	20.55	0.00	0.00	23.88	24.44

Table 52: Reliability indices for Leg Members

	ufEuler	ufAxial	ufTorsion	ufShearz	ufSheary	ufXSection	uf646	uf655	uf661	uf662
b111	0.00	0.00	0.00	0.00	0.00	68.20	0.00	0.00	0.00	0.00
b112	0.00	0.00	0.00	0.00	0.00	68.20	0.00	0.00	0.00	0.00
b113	0.00	0.00	0.00	0.00	0.00	68.20	0.00	0.00	0.00	0.00
b114	0.00	0.00	0.00	0.00	0.00	68.20	0.00	0.00	0.00	0.00
b115	0.00	0.00	0.00	0.00	0.00	41.17	0.00	0.00	0.00	0.00
b116	0.00	0.00	0.00	0.00	0.00	41.17	0.00	0.00	0.00	0.00
b211	0.00	0.00	80.56	56.72	0.00	20.19	0.00	0.00	0.00	0.00
b212	0.00	13.87	0.00	0.00	33.83	19.49	0.00	0.00	0.00	0.00
b213	0.00	0.00	80.46	56.67	0.00	20.19	0.00	0.00	0.00	0.00
b214	9.25	13.39	0.00	80.26	33.88	46.12	8.30	0.00	10.72	7.78
b215	0.00	0.00	53.41	0.00	56.88	24.63	0.00	0.00	0.00	0.00
b216	0.00	0.00	53.36	0.00	56.83	24.65	0.00	0.00	0.00	0.00
b311	0.00	0.00	0.00	0.00	72.00	13.67	0.00	0.00	0.00	0.00
b312	0.00	16.23	0.00	0.00	30.93	7.00	0.00	0.00	0.00	0.00
b313	0.00	0.00	0.00	0.00	71.97	13.68	0.00	0.00	0.00	0.00
b314	9.54	14.92	0.00	46.27	30.94	8.87	8.74	0.00	9.18	6.81
b315	0.00	0.00	46.35	57.72	72.00	33.86	0.00	0.00	0.00	0.00
b316	0.00	0.00	46.43	57.77	72.07	33.86	0.00	0.00	0.00	0.00
b411	0.00	0.00	0.00	0.00	72.00	10.01	0.00	0.00	0.00	0.00
b412	0.00	21.24	0.00	32.77	22.86	7.65	0.00	0.00	0.00	0.00
b413	0.00	0.00	0.00	0.00	72.01	10.01	0.00	0.00	0.00	0.00
b414	13.15	16.53	0.00	53.24	24.61	7.06	11.94	0.00	4.64	4.18
b415	46.43	0.00	53.36	0.00	20.57	10.29	40.18	0.00	6.26	5.89
b416	46.46	0.00	53.42	0.00	38.81	32.04	40.19	0.00	6.25	5.89

Table 53: Reliability indices for Horizontal Brace Members

	ufEuler	ufAxial	ufTorsion	ufShearz	ufSheary	ufXSection	uf646	uf655	uf661	uf662
b151	0.00	7.00	96.23	80.22	56.85	10.61	0.00	0.00	0.00	0.00
b152	3.11	6.72	80.52	84.92	80.48	0.00	2.81	0.00	2.53	2.54
b153	8.07	15.07	42.41	0.00	33.87	7.96	7.54	0.00	5.44	5.11
b154	8.07	15.07	42.41	0.00	33.85	7.96	7.53	0.00	5.44	5.11

	ufEuler	ufAxial	ufTorsion	ufShearz	ufSheary	ufXSection	uf646	uf655	uf661	uf662
b155	3.11	6.71	80.51	85.04	80.42	0.00	2.81	0.00	2.53	2.54
b156	0.00	7.01	96.18	80.32	56.91	10.60	0.00	0.00	0.00	0.00
b157	12.71	11.91	42.40	0.00	33.88	8.37	11.71	0.00	0.00	0.00
b158	12.70	11.91	42.38	0.00	33.87	8.37	11.72	0.00	0.00	0.00
b251	0.00	6.72	31.86	56.75	71.96	9.18	0.00	0.00	0.00	0.00
b252	3.39	6.61	31.14	0.00	80.47	15.32	3.05	0.00	2.59	2.58
b253	13.51	25.14	50.22	0.00	32.80	8.92	12.64	0.00	7.79	6.94
b254	13.49	25.13	50.14	0.00	32.81	8.92	12.63	0.00	7.78	6.94
b255	3.39	6.61	31.17	0.00	80.47	15.33	3.05	0.00	2.59	2.59
b256	0.00	6.72	31.86	56.75	72.06	9.17	0.00	0.00	0.00	0.00
b257	0.00	35.90	42.46	0.00	30.27	9.20	0.00	0.00	0.00	0.00
b258	0.00	35.90	42.44	0.00	30.33	9.20	0.00	0.00	0.00	0.00
b351	0.00	6.99	28.73	53.31	0.00	9.35	0.00	0.00	0.00	0.00
b352	3.95	6.93	28.77	40.33	0.00	10.55	3.55	0.00	2.90	2.89
b353	18.60	28.23	36.05	0.00	26.36	8.23	16.80	0.00	7.86	6.41
b354	18.56	28.26	36.08	0.00	26.35	8.22	16.81	0.00	7.87	6.41
b355	3.95	6.93	28.76	40.29	0.00	10.56	3.55	0.00	2.90	2.89
b356	0.00	6.99	28.73	53.34	0.00	9.35	0.00	0.00	0.00	0.00
b357	0.00	0.00	36.11	56.80	26.34	8.32	0.00	0.00	11.80	8.26
b358	0.00	0.00	36.03	56.81	26.36	8.32	0.00	0.00	11.79	8.27
b451	0.00	8.11	26.98	40.50	44.43	14.52	0.00	0.00	0.00	0.00
b452	5.02	8.00	28.74	36.07	0.00	11.91	4.57	0.00	3.84	3.82
b453	26.27	40.14	0.00	30.30	20.10	5.83	24.86	0.00	5.22	4.14
b454	26.24	40.10	0.00	30.30	20.09	5.84	24.84	0.00	5.23	4.14
b455	5.02	8.01	28.77	36.04	0.00	11.91	4.57	0.00	3.84	3.82
b456	0.00	8.10	26.97	40.50	44.43	14.52	0.00	0.00	0.00	0.00
b457	0.00	0.00	80.59	53.27	20.76	5.81	0.00	0.00	5.36	4.13
b458	0.00	0.00	80.56	53.34	20.79	5.82	0.00	0.00	5.36	4.13

Table 54: Reliability indices for Vertical Brace Members

The final value of the reliability index for every member will be derived as the minimum value calculated from each of the limit states examined. Results referring to the leg members, starting from the first elevation, distinguish one set of members in axial compression and bending (b102-b103) with $\beta = 5.16$ and one set in axial tension (b101-b104) with $\beta = 5.44$. Due to the uniform cross section of the legs, it is expected that the values of β of this elevation will be the lowest one, sizing the members. Moving to the second elevation, a different pattern is followed with members (b202-b203) in axial compression and bending with $\beta = 7.19$ having a greater value of reliability index than the second member

(b201-b204) subjected in axial tension with $\beta = 5.85$. The same pattern as in the second elevation can be observed in the third elevation with the set of members (b302-b303) subjected to axial compression and bending with $\beta = 8.38$ and the set of (b301-b304) subjected to axial tension with $\beta = 10.30$. A different behaviour can be observed in the fourth elevation leg members with the set of members (b402-b403) subjected to axial compression and bending with $\beta = 11.54$ and the set of (b401-b404) subjected to torsion with $\beta = 19.70$.

Horizontal bracing members of the first elevation, have great values of reliability due to the insignificant loads they carry, according to the piling conditions that have been applied. Members of the first elevation that stand parallel to the flow (b211-b213) have $\beta = 20.19$ due to the cross section usage factor limit state, while for the members vertical to the flow, the one that meets the flow first (b214) has a lower value of $\beta = 7.78$ due to bending and axial compression and the second one (b212) has $\beta = 13.87$ due to axial tension. The two X-bracing members (b215-b216) have great values of reliability since they carry minimum loads, as they have a non functional load to the operation of the structure. In the third elevation, the two symmetrical members, parallel to the flow (b311-b313) have $\beta = 13.67$ due to the cross section usage factor limit state, the first vertical to the flow (b314) $\beta = 6.81$ due to axial compression and bending, and the second member (b312) $\beta = 7.00$ due to the cross section usage factor limit state. The members parallel to the flow of the fourth elevation (b411-b413) have $\beta = 10.01$ due to the cross section usage factor limit state, the first member vertical to the flow (b414) $\beta = 4.18$ due to axial compression and bending while the second member (b412) $\beta = 7.65$ due to the cross section usage factor limit state. At this elevation the X brace members show values of $\beta = 5.89$ due to axial compression and bending criterion, due to the loads transmitted from the topside loads.

For the vertical X-braces of the first elevation, the two symmetrical sets of members parallel to the flow, have one of their member (b152-b155) defined from the axial compression and bending limit state with $\beta = 2.53$ and the other of their members (b151-b156) with $\beta = 7.00$ subjected to axial tension. From

the sets vertical to the flow, the first (b157-b158) has $\beta = 8.37$ due to the cross section usage factor limit state, while the second one (b153-b154) has $\beta = 5.11$ due to axial compression and bending. From the members of the second elevation that stand parallel to the flow, members (b252-b255) are subjected to axial compression and bending with $\beta = 2.59$ while members (b251-b256) are subjected in axial tension with $\beta = 6.72$. From the sets vertical to the flow, the first (b257-b258) has $\beta = 9.20$ due to the cross section usage factor limit state, while the second one (b253-b254) has $\beta = 6.94$ due to axial compression and bending. From the members of the third elevation that stand parallel to the flow, members (b352-b355) are subjected to axial compression and bending with $\beta = 2.89$ while members (b351-b356) are subjected in axial tension with $\beta = 6.99$. From the sets vertical to the flow, the first (b357-b358) has $\beta = 8.26$, while the second one (b353-b354) has $\beta = 6.41$ both due to axial compression and bending. Finally for the members of the fourth elevation, those that stand parallel to the flow, (b452-b455) are subjected to axial compression and bending with $\beta = 3.82$, while members (b451-b456) are subjected in axial tension with $\beta = 8.10$. From the sets vertical to the flow, the first (b457-b458) has $\beta = 4.13$, while the second one (b453-b454) has $\beta = 4.11$ both due to axial compression and bending.

6.5 ANSI/AISC 360-05: Specification for structural steel buildings

The design procedure for the design of members under load actions is described in Chapters A-H of this standard. Axial force and bending (flexure as it will be referred to herein) about one or both axes, with or without torsion, and to members subject to torsion only is analytically derived both in a limit state and in a working state design. In this section, the limit state provisions will be presented for symmetric members subjected to bending and axial force, since the members of the structure of reference is of this type. Different sections in this standard include modified provisions for unsymmetrical members. Finally,

provisions for members under combined torsion, flexure, shear and/or axial force will be presented [4].

6.5.1 Design Provisions

The standard defines that design according to its provisions should be satisfied when 'the design strength of each structural component equals or exceeds the required strength determined on the basis of the load combinations considered'.

The typical for LRFD standard basic equation that should be satisfied is:

$$R_u \leq \phi R_n \quad (6-59)$$

Where:

R_u : Required strength (MPa)

R_n : Nominal strength, as specified for each case of loading (MPa)

ϕ : Resistance factor, as specified for each case of loading

ϕR_n : Design strength (MPa)

6.5.1.1 Members in tension

For members in tension, the design tensile strength $\phi_t P_n$ shall be derived by the lower value of the limit states corresponding to tensile yielding and tensile rupture:

$$P_n = F_y A_g, \phi_t = 0.90 \quad (6-60)$$

$$P_n = F_u A_e, \phi_t = 0.75$$

Where:

A_e : Effective net area (mm²), calculated as the product of the net area A_n and the shear lag factor U specified for different connections of tension members.

A_g : Gross area of member (mm²)

F_y : Specified minimum yield stress (MPa)

F_u : Specified minimum tensile stress (MPa)

6.5.1.2 Members in compression

For design of members in compression the design compressive strength $\phi_c P_n$ shall be determined as the lowest value obtained by the limit states of flexural buckling, torsional buckling and flexural - torsional buckling. The reduction factor referring to compression is $\phi_t = 0.90$. The nominal compressive strength P_n for the case of flexural buckling should be:

$$P_n = F_{cr} A_g \quad (6-61)$$

Where the flexural buckling is determined as:

$$F_{cr} = \begin{cases} 0.658 \frac{F_y}{F_e} F_y, & \text{when } F_e \geq 0.44 F_y \\ 0.877 F_e, & \text{when } F_e < 0.44 F_y \end{cases} \quad (6-62)$$

$$F_e = \frac{\pi^2 E}{\left(\frac{KL}{r}\right)^2}$$

Where:

F_e : Elastic critical buckling (MPa)

L : Laterally un-braced length of member (mm)

r : Radius of gyration (mm)

K : Effective length factor in plane of bending equals 1 unless different analysis indicates a smaller value

6.5.1.3 Members in Flexure

For the design of flexural strength, $\phi_B M_n$, the corresponding reduction factor would be $\phi_t = 0.90$. The nominal flexural strength M_n should be determined by the lower value obtained by the limit states corresponding to yielding and plastic buckling as follows:

$$M_n = M_p = F_y Z \quad (6-63)$$

$$M_n = \left(\frac{0.021E}{\frac{D}{t}} + F_y \right) S, \text{ for non-compact sections}$$

$$M_n = F_{cr} S = \frac{0.33E}{\frac{D}{t}} S, \text{ for sections with slender walls}$$

Where:

S : Elastic section modulus (mm^3)

Z : Plastic section modulus about the axis of bending (mm^3)

6.5.1.4 Members in Shear

Design shear strength, $\phi_v V_n$ should be determined by applying $\phi_v = 0.90$ and for cylindrical cross sections, the nominal shear strength should be determined according to limit states of shear yielding and shear buckling as:

$$V_n = \frac{F_{cr} A_g}{2} \quad (6-64)$$

Where F_{cr} should be derived by the maximum of the values:

$$F_{cr} = \frac{1.60E}{\sqrt{\frac{L_v}{D}} \left(\frac{D}{t} \right)^{\frac{5}{4}}} \quad (6-65)$$

$$F_{cr} = \frac{0.78E}{\left(\frac{D}{t} \right)^{\frac{3}{2}}}$$

Where:

A_g : Gross area of section based on design wall thickness (mm^2)

D : Outside diameter (mm)

L_v : Distance from maximum to zero shear force (mm)

$t = (0.93 - 1)t_n$: Design wall thickness (mm)

6.5.1.5 Members subject to Flexure and Axial Force

The fundamental relationship that should constrain the interaction between axial force and flexure is:

$$U_m = \frac{P_r}{P_c} + \frac{8}{9} \cdot \left(\frac{M_{rx}}{M_{cx}} + \frac{M_{ry}}{M_{cy}} \right) \leq 1.0, \text{ For } \frac{P_r}{P_c} \geq 0.2$$

$$U_m = \frac{P_r}{2P_c} + \frac{8}{9} \cdot \left(\frac{M_{rx}}{M_{cx}} + \frac{M_{ry}}{M_{cy}} \right) \leq 1.0, \text{ For } \frac{P_r}{P_c} < 0.2$$
(6-66)

Where:

P_r : Required axial compressive (tensile) strength, (N)

$P_c = \varphi_c P_n$: Available axial compressive strength, (N)

$P_c = \varphi_t P_n$: Available axial tensile strength, (N)

$\varphi_c = 0.90$: Resistance factor for compression

φ_t : Resistance factor for tension (as described above)

$\varphi_b = 0.90$: Resistance factor for flexure

M_r : Required flexural strength (N-mm)

$M_c = \varphi_b M_n$: Available flexural strength (N-mm)

x : Subscript relating symbol to strong axis bending

y : Subscript relating symbol to weak axis bending

6.5.1.6 Members under torsion and combined torsion, shear and/or axial force

The design torsional strength, $\varphi_T T_n$ should consider $\varphi_T = 0.90$ and nominal torsional strength:

$$T_n = F_{cr} \cdot C$$
(6-67)

Where:

$C = \frac{\pi \cdot (D-t)^2 \cdot t}{2}$: Torsional constant

F_{cr} : The greatest of (without exceeding $0.6F_y$):

$$F_{cr} = \frac{1.23E}{\sqrt{\frac{L}{D}} \cdot \left(\frac{D}{t}\right)^{\frac{5}{4}}}$$
(6-68)

$$F_{cr} = \frac{0.60E}{\left(\frac{D}{t}\right)^{\frac{3}{2}}}$$

Where:

L : Length of the member (mm)

D : Outside diameter (mm)

For cylindrical members subjected to combined torsion, shear, flexure and axial force: when $T_r \leq 20$, provisions of the fundamental relationship between axial force and flexure should be followed. In the case when $T_r > 20$, interaction of torsion, shear, flexure and/or axial force shall be limited by:

$$\left(\frac{P_r}{P_c} + \frac{M_r}{M_c}\right) + \left(\frac{V_r}{V_c} + \frac{T_r}{T_c}\right)^2 \leq 1.0 \quad (6-69)$$

Where:

P_r : Required axial strength (N)

$P_c = \varphi \cdot P_n$, design tensile or compressive strength (N)

M_r : Required flexural strength (N-mm)

$M_c = \varphi_b \cdot M_n$, Design flexural strength (N-mm)

V_r : Required shear strength (N)

$V_n = \varphi_v \cdot V_n$: Design shear strength (N)

T_r : Required torsional strength (N-mm)

$T_c = \varphi_T \cdot T_n$ Design torsional strength (N-mm)

6.5.2 Numerical Application

Table 55, summarizes the limit states that have been considered in the reliability assessment of the reference structure. For this standard, the final value of the reliability index for each member is determined by dominant limit state referring to symmetrical members subjected to bending and axial force. Therefore this case will describe the effect of any action or combination of

actions. Following, in Table 56 to Table 58, the results of reliability analysis of each limit state are presented for the different classes of members.

Limit State	Description	Equation
ufH1	Usage factor according to section H1	6-66

Table 55: Limit States according to ANSI/AISC 360-05

	ufH1		ufH1
b101	4.64	b301	9.78
b102	4.25	b302	8.65
b103	4.26	b303	8.65
b104	4.64	b304	9.79
b201	7.62	b401	14.91
b202	5.47	b402	10.90
b203	5.47	b403	10.92
b204	7.63	b404	14.88

Table 56: Reliability indices for Leg Members

	ufH1		ufH1
b111	61.99	b311	10.26
b112	61.99	b312	8.90
b113	61.99	b313	10.26
b114	61.99	b314	6.06
b115	37.69	b315	17.11
b116	37.69	b316	17.11
b211	10.99	b411	9.01
b212	10.58	b412	6.30
b213	10.97	b413	8.99
b214	7.54	b414	5.42
b215	15.82	b415	8.59
b216	15.81	b416	8.59

Table 57: Reliability indices for Horizontal Brace Members

	ufH1		ufH1
b151	4.90	b351	4.85
b152	2.07	b352	2.64
b153	4.40	b353	5.80
b154	4.40	b354	5.80
b155	2.06	b355	2.64
b156	4.90	b356	4.85
b157	7.52	b357	6.27
b158	7.52	b358	6.28

	uffH1		uffH1
b251	4.79	b451	7.43
b252	2.26	b452	3.50
b253	7.40	b453	3.82
b254	7.39	b454	3.82
b255	2.26	b455	3.50
b256	4.79	b456	7.43
b257	8.58	b457	3.88
b258	8.58	b458	3.88

Table 58: Reliability indices for Vertical Brace Members

Investigating results for the leg members, starting from the first elevation, distinguish one set of members (b102-b103) with $\beta = 4.25$ and one set (b101-b104) with $\beta = 4.64$. Due to the uniform cross section of the legs, it is expected that the values of β of this elevation will be the lowest one, sizing the members. Moving to the second elevation, members (b202-b203) have $\beta = 5.47$ while (b201-b204) have $\beta = 7.63$. In the third elevation, members (b302-b303) have $\beta = 8.65$ and the set of (b301-b304) has $\beta = 9.78$. For members in the fourth elevation, the set of (b402-b403) is found to have $\beta = 10.90$ and the set of (b401-b404) with $\beta = 14.88$.

Horizontal bracing members of the first elevation, have great values of reliability due to the insignificant loads they carry, according to the piling conditions that have been applied. Members of the second elevation that stand parallel to the flow (b211-b213) have $\beta = 10.99$, while for the members vertical to the flow, the one that meets the flow first (b214) has a lower value of $\beta = 7.54$ and the second one (b212) has $\beta = 10.58$. The two X-bracing members (b215-b216) have great values of reliability since they carry minimum loads, as they have a non functional load to the operation of the structures. In the third elevation, the two symmetrical members, parallel to the flow (b311-b313) have $\beta = 10.26$, the first vertical to the flow (b314) $\beta = 6.06$, and the second member (b312) $\beta = 8.90$. The members parallel to the flow of the fourth elevation (b411-b413) have $\beta = 9.01$, the first member vertical to the flow (b414) $\beta = 5.42$ while the second member (b412) $\beta = 6.30$. At this elevation the X brace members show values of $\beta = 8.59$, due to the loads transmitted from the topside loads.

For the vertical X-braces of the first elevation, the two symmetrical sets of members parallel to the flow, have one of their members (b152-b155) with $\beta = 2.07$ and the other of their members (b151-b156) with $\beta = 4.90$. From the sets vertical to the flow, the first (b157-b158) has $\beta = 7.52$, while the second one (b153-b154) has $\beta = 4.40$. From the members of the second elevation that stand parallel to the flow, members (b252-b255) have $\beta = 2.26$ while members (b251-b256) have $\beta = 4.79$. From the sets vertical to the flow, the first (b257-b258) has $\beta = 8.58$, while the second one (b253-b254) has $\beta = 7.40$. From the members of the third elevation that stand parallel to the flow, members (b352-b355) have $\beta = 2.64$ while members (b351-b356) have $\beta = 4.85$. From the sets vertical to the flow, the first (b357-b358) has $\beta = 6.27$, while the second one (b353-b354) has $\beta = 5.80$. Finally for the members of the fourth elevation, those that stand parallel to the flow, (b452-b455) have $\beta = 3.50$ while members (b451-b456) have $\beta = 7.43$. From the sets vertical to the flow, the first (b457-b458) has $\beta = 3.88$, while the second one (b453-b454) has $\beta = 3.82$.

6.6 Discussion

Table 59 to Table 61, summarize the minimum values of reliability indices based on different limit states that have been investigated based on provisions of different standards as well as values obtained by the analytical limit state derived in the previous Chapter (based on the von Mises failure criterion). Although in general similar trends of figures can be observed, differences in individual members are found due to the different design considerations that each standard suggests. The basic difference in those design provisions relates to the reduction (or resistance) factors that are used in each of the potential load actions, and are listed in Table 62. EN and AISC, propose more conservative reduction factors for members under tension (0.8 and 0.9-0.75 respectively), while API LRFD and ISO propose more conservative values for members in compression (0.85 for both). API LRFD and ISO have propose the same values for bending, shear and torsion (0.95), and for hoop buckling (0.80).

EN's values for bending, shear and torsion is 1.00 while AISC/ANSI proposes a value equals to 0.90. Work on the derivation of the strength reduction factors has been performed in the background documents of the API standards [310]. For every case of action, von Mises criterion has not accounted for any reduction factor. Further, differences in the expressions for combinations of actions in standards provide different results, distinguishing from a simple summation, vectorial summation or weighted summation of action resultants. It should also be noted here that application of EN and ANSI/AISC is not directly applicable to offshore structure since they are generic documents for steel structures and do not have special clauses for actions such as external pressure on members etc; however useful conclusions can be derived by including them in this analysis.

For leg members, difference in the pattern of minimum value of reliability is observed between members in axial tension and compression, combined with bending, based on reduction of members' strengths. The lowest elevation members, which will eventually size the rest of the member' parts, based on von Mises criterion, indicate a minimum value of $\beta = 4.79$ based on member in tension, while API and ISO derive values of 4.76 and 4.71 respectively based on members in compression. Respective values derived by EN and AISC/ANSI are 5.16 and 4.25 based on members in compression. For the second elevation leg members, von Mises criteria follow the same trend, dominated by members in tension, with a minimum $\beta = 5.74$. The same trend is followed by ISO (6.05), EN (5.85) and AISC/ANSI (5.47), while API LRFD members are characterized by their members in axial compression (6.62). For the members of the third elevation, all standards (8.15, 8.38, 8.65 respectively) and the von Mises limit state (8.15), are dominated by their members in axial compression, apart from ISO (7.17) where axial compression prevails. Finally, for the fourth elevation both the von Mises limit states (10.66) and the standards minimum limit states (API LRFD: 11.65, ISO: 11.05, EN: 11.54 AISC/ANSI: 10.90) are determined by their members in axial compression.

For the horizontal brace members of the first elevation, all standards agree in great values of β ; those values imply zero value of probability of failure and therefore great numerical differences are insignificant. From the six members of the horizontal bracing of the second elevation, the most severe effect is for all cases derived by the first member located vertical to the flow (API LRFD: 6.50, ISO: 6.43, EN: 7.78, AISC/ANSI: 7.54, v.Mises: 9.33) suffering from axial tension. X braces show great values of β due to the lower acting stresses. The members of the third elevation are dominated by the ones subjected to axial compression and bending while members of the fourth elevation are dominated by the ones subjected to axial tension and bending (el3: API LRFD: 6.14, ISO: 6.02, EN: 6.81, AISC/ANSI: 6.06, v.Mises: 6.94 / el4: API LRFD: 4.29, ISO: 4.28, EN: 4.18, AISC/ANSI: 5.42, v.Mises: 5.76). X bracing members on the fourth elevation, affected by the topside loads, have a lower value of β based on EN (5.89) while other values derived are (API LRFD: 6.63, ISO: 9.62, AISC/ANSI: 8.41, v.Mises: 8.37).

Vertical X brace members present lower values of reliability index, illustrating greater differences between standards. For the members of the first elevation, AISC/ANSI provides the most conservative values of β , apart from the case of the set of members located vertical to the flow where ISO provides more conservative values. All values derived, agree that the most critical members are those subjected in axial compression and bending (API LRFD: 6.10, ISO: 2.20, EN: 2.53, AISC/ANSI: 2.06, v.Mises: 5.55). The same pattern is followed for the second and third elevations where ISO and AISC/ANSI provide the most conservative results based on the members parallel to the flow, subjected in axial compression and bending (el3: API LRFD: 6.00, ISO: 2.24, EN: 2.59, AISC/ANSI: 2.26, v.Mises: 5.25 / el4: API LRFD: 6.29, ISO: 2.65, EN: 2.89, AISC/ANSI: 2.64, v.Mises: 5.33). Finally, the most critical members of the fourth elevations, are the second vertical to the flow (API LRFD: 3.02, ISO: 2.83, EN: 4.14, AISC/ANSI: 3.82, v.Mises: 3.79).

The above analysis concludes that a global characterization between the most or least conservative standard cannot be made since different standards are

more conservative in different classes of members than others. The general comment that can be concluded from the values obtained is that the ISO and AISC/ANSI standards provide more conservative results than API LRFD and EN respectively. As far as the von Mises criterion is concerned, in most of the cases, the values derived lay between minimum and maximum of the values derived by design standards, therefore providing a good initial estimate of β . The benefit of the use of this limit state is that it can account universally for different actions and combinations of actions of members, allowing simulation of the response with any non specialized software.

From the application of the derived methodology in the analysis above, both considering the global von Mises criterion, as well as the different limit states proposed by each standard, have proven the efficiency of this method to rapidly calculate reliability in structural design. Further, it can be concluded that the implied reliability of different standards can be achieved by procedures that do not necessarily follow their provisions. The procedure that has been derived can be also applied for the evaluation of the minimum levels of reliability that is achieved, by assessing the reliability of structures that are designed in a way that the utilization factor is lower, but as close as possible to unity. This comparison which could benchmark the performance of design standards, would verify that certain standards' provisions are followed, once the provisions of a different less conservative standards are met.

	vMises	API	ISO	EN	AISC		vMises	API	ISO	EN	AISC
b101	4.79	5.97	5.41	5.44	4.64	b301	8.71	9.56	7.17	10.30	9.78
b102	5.22	4.76	4.71	5.16	4.25	b302	8.15	7.75	7.75	8.38	8.65
b103	5.23	4.76	4.71	5.17	4.26	b303	8.14	7.76	7.75	8.38	8.65
b104	4.79	5.97	5.41	5.45	4.64	b304	8.72	9.56	7.17	10.29	9.79
b201	5.74	7.06	6.05	5.85	7.62	b401	14.73	11.74	15.00	15.11	13.14
b202	7.46	6.62	6.56	7.19	5.47	b402	10.66	11.65	11.05	11.55	10.90
b203	7.45	6.62	6.56	7.19	5.47	b403	10.66	11.65	11.05	11.54	10.92
b204	5.74	7.04	6.05	5.86	7.63	b404	14.72	11.73	14.98	15.10	13.14

Table 59: Minimum Reliability indices for Leg Members

	vMises	API	ISO	EN	AISC		vMises	API	ISO	EN	AISC
b111	54.83	59.43	63.25	68.20	61.99	b311	10.46	11.70	11.48	13.67	10.19
b112	54.83	59.43	63.25	68.20	61.99	b312	6.96	8.75	7.57	7.00	8.90
b113	54.83	59.43	63.25	68.20	61.99	b313	10.48	11.69	11.48	13.68	10.26
b114	54.83	59.43	63.25	68.20	61.99	b314	6.94	6.14	6.02	6.81	6.06
b115	35.01	38.75	37.50	41.17	37.69	b315	20.86	35.53	19.59	33.86	15.39
b116	35.01	38.75	37.50	41.17	37.69	b316	20.87	35.58	19.59	33.86	15.38
b211	12.34	13.84	13.77	20.19	10.86	b411	8.98	10.19	10.31	10.01	9.01
b212	9.70	13.24	9.90	13.87	10.58	b412	6.00	7.00	6.75	7.65	6.30
b213	12.33	13.84	13.80	20.19	10.87	b413	8.98	10.18	10.30	10.01	8.99
b214	9.33	6.50	6.43	7.78	7.54	b414	5.76	4.29	4.28	4.18	5.42
b215	18.72	53.05	20.16	24.63	15.47	b415	8.36	6.64	9.63	5.89	8.40
b216	18.71	53.45	20.17	24.65	15.49	b416	8.37	6.63	9.62	5.89	8.41

Table 60: Minimum Reliability indices for Horizontal Brace Members

	vMises	API	ISO	EN	AISC		vMises	API	ISO	EN	AISC
b151	5.70	8.26	5.67	7.00	4.90	b351	5.30	7.10	5.41	6.99	4.85
b152	5.54	6.11	2.20	2.53	2.07	b352	5.33	6.29	2.65	2.89	2.64
b153	6.93	8.61	5.10	5.11	4.40	b353	6.08	7.33	6.36	6.41	5.80
b154	6.94	8.62	5.09	5.11	4.40	b354	6.09	7.33	6.35	6.41	5.80
b155	5.55	6.10	2.20	2.53	2.06	b355	5.33	6.30	2.65	2.89	2.64
b156	5.70	8.26	5.66	7.01	4.90	b356	5.31	7.11	5.40	6.99	4.85
b157	6.76	7.41	6.08	8.37	7.52	b357	6.16	9.25	4.71	7.35	6.27
b158	6.74	7.40	6.08	8.37	7.52	b358	6.16	9.25	4.71	7.35	6.28
b251	5.27	7.01	5.43	6.72	4.79	b451	6.37	6.68	6.51	8.11	7.43
b252	5.25	6.00	2.24	2.58	2.26	b452	6.33	4.56	3.87	3.82	3.50
b253	7.51	8.99	6.76	6.94	7.40	b453	3.79	3.03	2.82	4.14	3.82
b254	7.51	8.99	6.76	6.94	7.39	b454	3.79	3.02	2.83	4.14	3.82
b255	5.26	6.00	2.24	2.59	2.26	b455	6.34	4.56	3.87	3.82	3.50
b256	5.27	7.01	5.44	6.72	4.79	b456	6.37	6.67	6.52	8.10	7.43
b257	7.81	12.35	6.31	9.20	8.47	b457	3.72	4.10	4.38	4.13	3.84
b258	7.79	12.35	6.32	9.20	8.47	b458	3.72	4.10	4.39	4.13	3.84

Table 61: Minimum Reliability indices for Vertical Brace Members

	API	ISO	EN	AISC
Tension	0.95	1/1.05	1/1.25	0.9/0.75
Compression	0.85	1/1.18	1	0.9
Bending	0.95	1/1.05	1	0.9
Shear	0.95	1/1.05	1	0.9
Torsion	0.95	1/1.05	1	0.9
Hoop Buckling	0.8	1/1.25		

Table 62: Reduction factors of different standards

6.7 Summary

This Chapter has performed a comparison of the ultimate strength reliability performance of structural members, based on relevant procedures proposed by design standards. Based on a consistent methodology, the minimum values of reliability indices have been derived, giving the opportunity for direct comparison of the obtained results. This study has shown that, although design standards meet minimum levels of reliability, they do not perform in a uniform way, in order to classify one of the standards as the more or least conservative. Further, the von Mises criterion that has been derived earlier, seems to provide an accurate estimate of β , accounting for multiple actions on members.

7 CONCLUSIONS AND RECCOMENTATIONS

This final chapter will summarize what has been presented in the previous chapters of this Thesis and will identify the contribution of the research that has been carried out. The main aim of this PhD has been to study the design of offshore structures through a stochastic perspective and provide a generic methodology that will efficiently assess reliability levels of structural members, allowing combination and integration with available design methods and numerical tools/procedures. Application of the methodology on a hypothetical jacket structure, deployed in a theoretical site, has provided useful results and conclusions. Finally, some recommendations for future work will illustrate aspects of potential improvements and extensions of the method established, as well as different applications that this method might be related to.

7.1 Summary

The First Chapter of this Thesis has presented the background of structural reliability and has set the context of structural safety. Through an initial presentation of the evolution of design methods, development of design standards was presented. With a view to performance-based-design, which is freely followed by modern design standards, target reliability requirements are introduced based on commonly accepted sources, in order to set the threshold which the reliability performance of structures should aim to meet.

The Second Chapter has presented a review of reliability assessment of steel and offshore structures, providing fundamental formulations of reliability calculation and analyzing important decisions for comprehensive reliability analysis. Selection of the appropriate type of response analysis and integration from component to system reliability has been discussed. Finally, an initial review of the Stochastic Methods for reliability assessment will provide the background for the development of the methodology that will be applied later in this Thesis.

The Third Chapter introduced the numerical procedures for the computation of structural reliability. First and Second Order Reliability Methods (FORM/SORM) as well as Simulation Methods are presented, setting the background of the codes that have been developed for the scope of this Thesis, and are followed by the established tools that have been used in order to verify the different steps of the methodology that is proposed. A review of the development of the Stochastic Response Surface Method (SRS) and the methodology that has been applied in the reference application has been analytically discussed. Regression techniques have been included as fundamentals of the regression analysis that has been applied in the SRS, and a variation of the conventional least square method (LSM) has been proposed for more efficient regression and prevention from ill conditioned systems of equations. Verification of the codes for the FEA simulation, the multivariate polynomial regression, and the FORM/SORM estimation routine that have been developed, based on commercially available software, have shown that the codes written provide sufficiently accurate results and can be later used in the analysis. Validation of the SRS method, based on results obtained by direct simulations for a reference structure, have given proof that the SRS methodology provides accurate results, and can be confidently used for the later application chapters.

In the Fourth Chapter, the environmental loading of offshore structures has been presented, considering modelling of wave loads according to different wave theories and a procedure for the correlation between significant wave height and peak spectral period based on the joint distribution of statistical distributions. Modelling of wind and current loading have also been covered. Further, modelling of capacity of offshore structures has been included, through an extensive review of literature data for material properties and methodologies for the consideration of capacity deterioration due to corrosion.

The Fifth chapter presents the assessment of the reliability of structural tubular members of a typical offshore structure based on ultimate strength under stochastically represented loads and capacity properties. Analytical derivation of limit states based on yield failure criteria has been presented for ductile materials providing the limit state according to which reliability of the structure

has been evaluated. An application of the procedure for the correlation between the significant wave height and peak spectral period for the calculation of the joint probability distribution function has been also presented. A sensitivity analysis of the main variables and different models of corrosion has been included. Finally, integration from component to system reliability, based on the reliability performance of the structural members and the failure mechanism of the structure, has been discussed.

Chapter Six, introduces the design requirements of the most widely used standards for the design of offshore structures API RP 2A [1], [2], and ISO 19902 [3]. Further, ANSI/AISC 360-05 [4], and EUROCODE 3 [5], have been included as generic codes of the design of steel structures with strong probabilistic background. Based on their provisions, limit states were formulated based on different actions or combinations of actions that members are subjected to. For the same reference case structure, the minimum reliability index of each member according to those standards was calculated, drawing conclusions from the results obtained.

7.2 Contribution of this PhD

Design of offshore and steel structures is currently based on provisions of relevant design standards. This practice can achieve compliance to minimum levels of reliability; however their generalized character imposes a degree of conservatism, often overestimating members and structures. Modern standards derive safety factors based on probabilistic and statistical procedures, therefore having a reliability based background, but express them deterministically restricting potential of optimization. This yields for a procedure to be developed allowing validation of partial factors based on the fundamental requirement of target reliability. Verification and calibration of design standards is mainly based on simplistic models considering fewer variables, or even statistical approximations of resistance and loading performance for a specific set of loads, representing them with distributions that can explicitly be transformed to values of reliability index. This method, although significantly easier to

implement, lacks flexibility and, especially moving towards limit state formats of standards, should be expressed with a stronger mathematical formulation.

The contribution of this PhD research can be summarized in the following:

- The methodology that is proposed allows reliability assessment of structural components through a sequence of individual steps that permit calculation of reliability, based on easy to program procedures. After execution of a finite series of simulations, the response of each member can be identified and a quadratic polynomial response surface based on the values of the limit states that are examined through data regression analysis can be formulated. Later, a separate routine can account for the estimation of the reliability index based on one of the available numerical techniques. Due to the linear nature of the response surfaces of the problem investigated, deterministic methods are proven to calculate adequately values of reliability indices. This methodology was proven to be efficient, allowing accurate and rapid calculation of reliability. Those discrete steps, which may employ different tools and procedures for each task, can handle several problems that are difficult to be modelled in one unified simulation code. For the problem of the design of offshore structures that has been studied, reliability analysis took place using the specialized software DNV SESAM for a confident representation of the response of structural members through appropriate modelling of the environmental loads acting on the structure. Following this methodology, specialized commercial tools for different applications may be employed for the probabilistic assessment of several engineering problems.
- Due to combined actions on structural members, different limit states should be examined in order to derive the minimum reliability index of a structural member. Analytical derivation of limit states based on widely accepted failure criteria can account for combinations of actions on a structural member incorporating multiple limit states into one. This facilitates representation of the response of structural members since

principal stresses or even equivalent von Mises stresses are easy to be obtained through available commercial tools. Application of such limit states in this analysis has provided results that can be compared with the ones derived from analytical limit states following guidelines of design standards, suggesting a simplified methodology for the consideration of limit states. Incorporation of a more analytical or stochastic representation of members' strength under different actions (tension, compression, bending, etc.) or employment of resistance factors for the correction of the stochastic distribution of yield strength could provide even more accurate results for the calculation of reliability.

- Based on the von Mises limit state that has been analytically derived, a reference structure has been introduced and based on stochastic representation of the basic design variables (wave, wind, current, yield strength), the reliability indices of each member has been calculated for two different angles of load application (0 and 45 degrees) in order to obtain the minimum value. Further, a buckling limit state has been introduced and applied for different values of buckling coefficient. For the base case of the 0 degrees angle of approach, and based on the consistent methodology that has been developed, a sensitivity analysis was executed benchmarking the effect of variation of loads magnitude on the structure. This analysis has illustrated that for the load cases and materials studied, the wave load and material yield strength are the most important factors in the formulation of the reliability index of the structure, while the current and wind loads play an insignificant role. The effect of accurate modelling of statistical distributions was also examined and found to affect the derived results. A separate analysis has shown that roughness of the surface of members has a considerable effect on the reliability index of the structure, contributing to the increase of the effect of environmental loads on members as the structure ages. Different wave theories have also been examined illustrating that appropriate selection of the most suitable theory can provide different results. Finally, capacity deterioration of structural members has been studied for

different corrosion models and the corresponding variation of the reliability index has been illustrated.

- From the procedure that has been established, different limit states were formulated according to different provisions of widely used design standards for different potential actions and combinations of actions on members. API RP 2A, ISO 19902, ANSI/AISC 360-05 and EUROCODE 3 have been studied. For the base case of the reference structure that has been considered, reliability indices for all different limit states proposed in each standards' have been calculated, obtaining the minimum value of reliability index for each member and each standard. This has allowed comparison of standards performance, illustrating that ISO and AISC/ANSI provide more conservative results than API LRFD and EN. A different conclusion of this study illustrates that although standards meet relative levels of reliability, they do not perform uniformly among different classes of members.
- This Thesis illustrates a different approach on the use of design standards. Towards performance-based-design, where values of target reliability suggest the main design constraint, this methodology can use fundamental expressions of standards that incorporate scientific evidence as well as previous experience information for the calculation of reliability. Therefore, instead of designing for compliance to maximum permitted strength requirements, design could aim to achieve additionally minimum levels of reliability. This approach will provide a better understanding of the actual structural performance. Further, as it can be derived from the results of the analysis, transferring from a deterministic analysis that considers maximum strength to a probabilistic-stochastic that characterizes members' performance through reliability indices, different members are found to be the critical ones. Figure 70, Figure 71 and Table 63, present the stress distribution and the reliability indices of the reference structure based on the von Mises limit state function, illustrating different sequence of critical members.

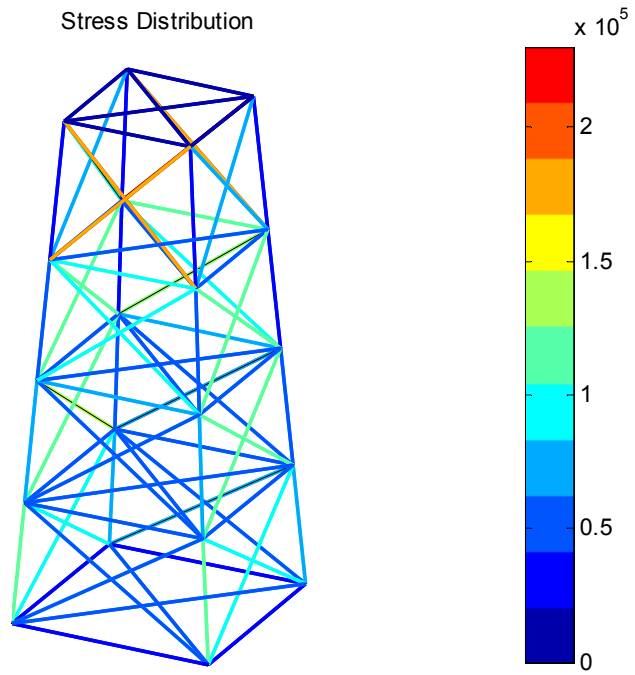


Figure 70: Stress distribution

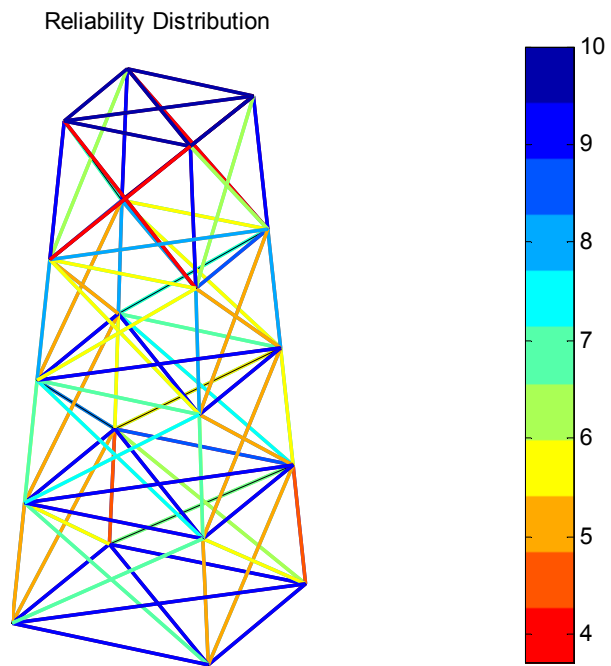


Figure 71: Reliability distribution

	β	$vMises$ (MPa)	β	$vMises$ (MPa)
1	b457	3.72	b458	230278
2	b458	3.72	b457	230277
3	b453	3.79	b453	219414
4	b454	3.79	b454	219414
5	b101	4.79	b102	140430
6	b104	4.79	b103	140430
7	b102	5.22	b252	136741
8	b103	5.23	b255	136741
9	b252	5.25	b352	136389
10	b255	5.26	b355	136389
11	b251	5.27	b414	132287
12	b256	5.27	b356	129416
13	b351	5.30	b351	129415
14	b356	5.31	b251	128804
15	b352	5.33	b256	128804
16	b355	5.33	b412	125771
17	b152	5.54	b357	122132
18	b155	5.55	b358	122132
19	b151	5.70	b152	118106
20	b156	5.70	b155	118106

Table 63: Critical Members

From the above results, excluding the top elevation braces where extreme values are obtained due to the topside loads, the next elements in the list follow a different pattern when comparing reliability indices rather than maximum stresses. This fact implies that throughout the service life of the structure, the members that will require maintenance are the ones with lower levels of reliability rather than those that suffer from greater stresses.

- From the results that have been derived, both using the von Mises limit state as well as the analytical limit states dictated by the provisions of design standards, are found to follow a similar trend. A different conclusion that can be drawn is that the implied reliability of each standard can be met by procedures that do not necessarily follow their provisions. The level of minimum reliability that standards aim to achieve can be estimated using the method described and has been followed in Chapter 6, by assessing the reliability of structures that are designed in a way that the utilization factor is lower, but as close as possible to unity. This comparison, which could benchmark the performance of design standards, would verify that certain standards' provisions are followed, once the provisions of a different but less conservative standard are met.

7.3 Future recommendations:

This study has derived some useful conclusions that might initiate further work on several aspects. Potential topics of interest might be found among the following:

- Although deterministic methods were found to provide efficient calculation for the type of limit state functions that were considered in this application, simulation methods can be also included, allowing handling of more complicated types of statistical distributions where the cumulative distribution functions cannot be directly derived as well as consideration of more complicated limit state functions, including highly correlated stochastic variables. Subset simulation is a method that could provide adequate approximation of the reliability index of members having relatively low computational requirements.
- For the reliability assessment that took place, deterministic values of the reduction factors of the different actions that members are subjected to have been used. Those values account for different sources of uncertainty due to geometrical and structural imperfections, residual stresses etc. Application of those values on the representative value of yield strength, in order to derive the design value of resistance of each action, which is stochastically modelled, transforms the distribution properties of strength for each different action. Following a fully probabilistic approach, different statistical distributions should be considered for different actions adequately describing strength for each action, as is described in relevant clauses regarding “Design assisted by testing”.
- Based on the derivation of the limit state functions that were used in this Thesis, relevant limit states can be derived for brittle materials, corresponding to appropriate fracture criteria. This practice will allow assessment of various problems including the continuously evolving application of composite materials. The special performance of those

materials that combine brittle and ductile behaviour before failure can be adequately assessed in the absence of specific design rules.

- Incorporation of the methodology in one unified code for a specific application (eg. steel structures) will allow automated iterations of required simulations for the reliability assessment of members. This will allow consideration of numerous stochastic variables providing even more accurate results. Further, combination of such code in a multi-disciplinary optimization routine (MDO), can automate a procedure that will lead to a robust design of an optimized structure compromising, but achieving, minimum acceptable levels of target reliability for the lowest possible weight. Although the mathematic skills for such an endeavour are high, the tools and procedures required are already available constituting incorporation in an iterative design routine feasible. Figure 72, presents a block diagram of the reliability based design approach concept in structural design. This is an approach that provides significant advantages for the design of novel and special structures or the verification of structures in new design environments where data from previous experience are not available.
- Combining a methodology that allows efficient calculation of reliability of structural members with techniques that provide real-time data of a structure (eg. thickness deterioration, surface condition, etc), its reliability evaluation can be updated for any given time instance. This practice would provide a more accurate understanding of the actual performance of the structure, allowing modification of its maintenance schedule, extending or reducing the intervals between interventions as indicated, and restoring its safety levels.
- Finally, design standards focus their analysis in a component level, implying that the minimum system reliability will equal that of the minimum value of the reliability of the sum of the components. This fact restricts application of techniques of structural design such as structural redundancy through alternative load paths. In such cases, the acceptable

reliability requirements in a component level may be considered lower than in the case where the whole structure is considered failed, following failure of the first member. Therefore, methodical investigation of structural reliability in a system level can show potential benefits, as it may prove to have a better reliability performance for the same total cost of the structure.

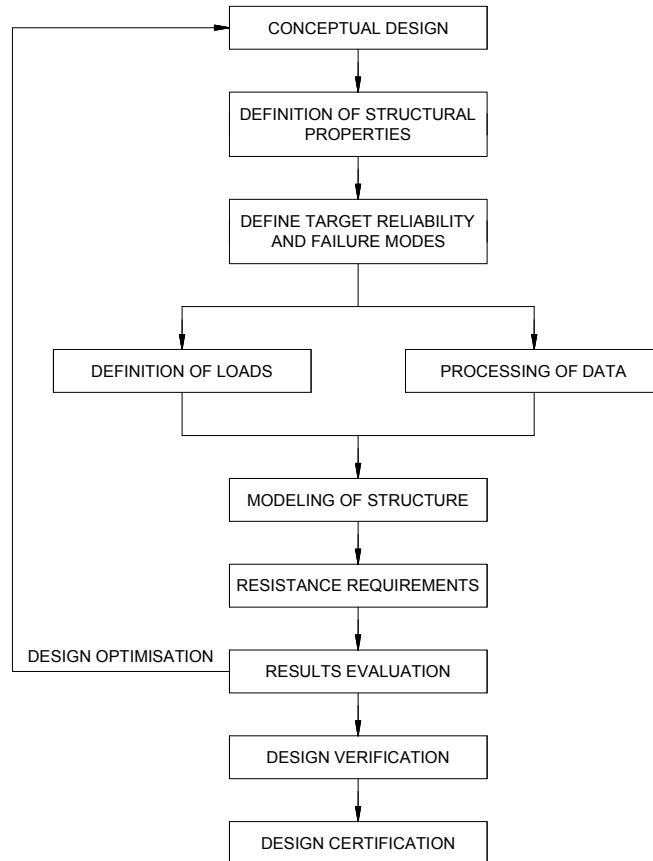


Figure 72: Reliability Based Optimization

REFERENCES

- [1] **American Petroleum Insitute.** Recommended Practice for Planning, Designing and Constructing Fixed Offshore Platforms - Working Stress Design. 01-Dec-2000. API RP 2A-WSD.
- [2] **American Petroleum Institute.** Recommended Practice for Planning, Designing and Constructing Fixed Offshore Platforms - Load and Resistance Factor Design . 01-Jul-1993 . API RP 2A-LRFD.
- [3] **International Standardization Organization.** Petroleum and natural gas industries-general requirements for offshore structures. 2002. ISO 19000:2002.
- [4] **American Institute of Steel Construction.** Specification for structural steel buildings. March 2005. ANSI/AISC 360-05.
- [5] **Comité Européen de Normalisation.** Eurocode 3: Design of Steel Structures. 2005. CEN 1993-1-1:2005 .
- [6] **International Standardization Organization.** General principles on reliability for structures. 2008. ISO 2394:2008.
- [7] **Comité Européen de Normalisation.** Basis of Structural Design. 2002. CEN Eurocode 1990.
- [8] **Det Norske Veritas.** Guideline for Offshore Structural Reliability Analysis. Norway : DNV, 1995. DNV Report No. 95-2018.
- [9] **T. Bayes.** An essey towards solving a problem in the doctrine of chance. Philosophical Transaction of the Royal Social Society, 1763.
- [10] **D. V. Lindley.** Making Decisions. New York : Wiley-interscience, 1985.
- [11] **B. D. Finetti.** Theory of Probability. New York : Wiley, 1974.
- [12] **S. Kaplan, and B. J. Garrick.** On the quantitative definition of Risk. Risk Analysis. 1981, Vol. 1.

- [13] **National Physics Laboratory.** Manual of Codes of Practice for the Determination of Uncertainties in Mechanical Tests on Metallic Materials. UK-EU, 2000.
- [14] **Det Norske Veritas.** Structural Reliability Analysis of Marine Structures. Norway. Classification No. 30.6. July 1992
- [15] **T. Onoufriou,** Reliability based inspection optimization planning for offshore structures. Journal of Marine Structures. Vol. 12. 521-539. 1999.
- [16] **G. Sigurdsson, R. Skjong, B. Skallerud, and J. Amdahl.** Probabilistic Collapse Analysis of Jackets. In: Schuëller, Shinozuka and Yao. Structural Safety and Reliability. Rotterdam: Balkema. 1994.
- [17] **P. Thoft-Christensen, and Y. Murotsy.** Application of Structural Systems Reliability Theory. Berlin. Springer-Verlag. 1986.
- [18] **M. Holicky, and T. Vrouwenvelder.** "Chapter I-Basic Concepts of Structural Reliability", Leonardo DaVinci Pilot Project CZ/02/B/F/PP-134007, Handbook 2-Reliability Backgrounds. 2005.
- [19] **H. Gulvanesian, and M. Holicky.** Annex C – Calibration Procedure, . Leonardo DaVinci Pilot Project CZ/02/B/F/PP-134007, Handbook 2-Reliability Backgrounds. 2005.
- [20] **Det Norske Veritas.** DNV-OS-C101 Design of Offshore Steel Structures. General (LRFD method). Hovik, Norway : Det Norske Veritas, 2008.
- [21] **T. Moan.** Safety of offshore structures. Center for Offshore Research & Engineering, University of Singapore. Coder Report No. 2005-04. 2005
- [22] **F. M. Burdekin.** General Principles of the use of safety factors in design and assessment. Journal of Engineering Failure Analysis. 2006.

[23] **R. C. Turner, C. P. Ellinas, and G. A. N. Thomas.** Worldwide Calibration of API RP2A-LRFD. Journal of Waterway, Port, Coastal and Ocean Engineering. Vol. 120. 1994.

[24] **BOMEL Ltd, Helth & Safety Executives.** System-based calibration of North West European annex environmental load factors for the ISO fixed steel offshore structures code 19902. Berkshire : HSE Books. Research Report 087. 2003.

[25] **Comité Européen de Normalisation.** Eurocode 1990:2002 Basis of structural design . EU : CEN. 2002.

[26] **DG Enterprise and Industry Joint Research Centre.** B1: The EUROCODES: Implimentation and Use. EU. JRC 42745. 2008.

[27] **Lloyds Registers.** LRS code for offshore Platforms. London. 1998.

[28] **Germanischer Lloyd.** Guidelines for offshore technology, Part IV – Industrial Services, Part 6: Offshore Technology. GL. 2007.

[29] **Det Norske Veritas.** DNV: Rules for the classification of Offshore Installations. DNV. 1989.

[30] **Det Norske Veritas.** DNV Offshore Standard OS-C101: Design of offshore steel structures, General – LRFD Method. DNV. 2008.

[31] **Norwegian Oil industry Association and The Federation of Norwegian Industry.** NORSOK N-001 Integrity of offshore structures. Norway. 2008.

[32] **A. Kolios, and F. P. Brennan.** Reliability Based Design for Novel Offshore Structures . Porto, Portugal : proceedings of the 3rd International Conference of Integrity, Reliability and Failure, 20 - 24 July 2009.

[33] **T. Moan.** Target levels for reliability based reassessment of offshore structures. Kyoto, Japan : Proceedings of the seventh international conference on structural safety and reliability. 1997.

- [34] **T. Moan.** Current trends in the safety of offshore structures. Honolulu : Proceedings of the Eighth International Offshore and Polar Engineering Conference, 1997.
- [35] **B. Bhattacharya, R. Basu, and K. Ma.** Developing target reliability for novel structures: the case of the Mobile Offshore Base. Marine Structure. 13; 37-58, 2001.
- [36] **A. E. Mansour.** An introduction to structural reliability theory. Washington : Ship structure committee. Report SSC-351. 1990.
- [37] **Committee IV.** Design Principles and criteria. Trondheim, Norway : Proceedings of the 13th International Ship and Offshore Structures Congress, 1997.
- [38] **American Association of State Highway and Transportation Officials.** LRFD bridge design specifications, AASHTO. Washington, DC. 1994.
- [39] **A. S. Nowak, N. M. Szerszen, and C. H. Park.** Target safety levels for bridges. Kyoto, Japan : Proceedings of the Seventh International Conference on Structural Safety and Reliability. 1997.
- [40] **C. G. Ramsaya, A. J. Bolsovera, R. H. Jonesa, and W. G. Medlanda.** Quantitative risk assessment applied to offshore process installations. Challenges after the piper alpha disaster . Journal of Loss Prevention in the Process Industries. Volume 7, Issue 4, Pages 317-330. 1994.
- [41] **R. Whitman.** Evaluating calculated risk in geotechnical engineering. J Geotech Engng, ASCE. 110; 20:145-88, 1984.
- [42] **H. N. Cullen,** The public inquiry into the Piper Alpha disaster. UK : The Parliament by the Secretary of the State for Energy, 1990.
- [43] **R. G. Bea.** Reliability Based design criteria for coastal and ocean structures. Australia : The Institution of Engineers. 1990.

[44] **A. H. S. Ang, and D. De Leon.** Determination of optimal target reliabilities for design and upgrading of structures. Struct Safety. 19:91-103. 1997.

[45] **D. L Keese, and W. R. Barton.** Risk assessment and its application to flight safety analysis. SANDIA National Laboratories. SAND 89. 1982.

[46] **Construction Industry Research and Information Association.** Rationalization of safety and serviceability factors in structural codes. London : CIRIA. Report No 63. 1977.

[47] **D. E. Allen.** Criteria for design safety factors and quality assurance expenditure. Trondheim, Norway : Proceedings of the Third International Conference on structural safety and reliability. 1981.

[48] **International Standardization Organization.** ISO/IEC Guide 51:1999 - Safety aspects - Guidelines for their inclusion in standards. 1999.

[49] **S. G. Stiansen, and A. K. Thamyambali.** Lessons Learnt from Structural Reliability Research & Applications in Marine Structures. Marine Structural Reliability Symposium. 5th – 6th October 1987. New Jersey: Society of Naval Architects and Marine Eng, 1987.

[50] **A. M. Freudenthal.** The safety of structures. Transc. ASCE, vol. 112, 1947.

[51] **C. A. Cornell.** A probability-based structural code. J. Am. Concr. Inst. . 66, pp. 974–985. 1969.

[52] **A. M. Hasofer, and N. C. Lind.** Exact and Invariant Second Moment code format. Journal of the Engineering Mechanics Division. 100 (EM), ASCE, 1974.

[53] **R. Rackwitz.** Reliability Analysis-Past, Present and Future. USA: ASCE. 8th ASCE Specialty Conference on Probabilistic Mechanics and Structural Reliability, 24th – 26th July, 2000.

- [54] **R. Stocki, K. Kolanek, S. Jendo, and M. Kleiber.** Study on discrete optimization techniques in reliability based optimization of truss structures. Computers & Structures. 79; 2235-2247. 2001.
- [55] **G.H. Sterling, B.E. Cox, and R.M. Warrington, Shell Oil Co.** Design of the COGNAC PLATFORM for 1025 feet water Depth, GULF OF MEXICO. Houston, Texas : Proceedings of the Offshore Technology Conference, 30 April-7 May 1979.
- [56] **D. I. Karsan,** Handbook of Offshore Engineering . Houston, TX, USA : AMEC Paragon, 2005.
- [57] **W. R. Ulbricht, M. A. Ripping, E. H. Doyle, J. W. Stevens, and J. G. Mayfield.** Design Fabrication and Installation of the Auger TLP Foundation System. Houston, Texas, USA : Proceedings of the Offshore Technology Conference (OTC 7626), 2-5 May 1994.
- [58] **J. J.S.Daniel, R and M. Knight.** World trends in major offshore structures: 1970-1999. London: Marine Management (Holdings) Ltd. : Proceedings of Offshore 1993 IMARE/RINA, Joint Offshore Group 3rd International Conference. 17th – 18th February, 1993.
- [59] **J. R. Beck.** Worldwide Petroleum Industry Outlook: 2001-2005 projection to 2010. 17th ed. United States of America: Pen Well Publishing, 2000.
- [60] **Talisman Energy.** Beatrice Wind Farm Demonstrator Project Scoping Report. UK. 2005.
- [61] **F. Moses.** Application of Reliability to Formulation of Fixed Offshore Design Codes. New Jersey: SNAME. 15-30. : Marine Structural Reliability Symposium. 5th – 6th October, 1987.
- [62] **J. C. P. Kam, M. Birkinshaw, and J. V. Sharp.** Review of the Applications of Structural Reliability Technologies in Offshore Structural Safety. Proceedings of the 12th International Conference on Offshore Mechanics and Arctic Engineering. Vol 2. Unit. 1993.

- [63] **A. E. Mansour.** Combining Extreme Environmental Loads for Reliability-Based Designs. Arlington VA: SNAME. : Extreme Loads Response Symposium. 19th – 20th Oct, 1981.
- [64] **A. E. Mansour, H. Y. Jan, C. I. Zigelman, Y. N. Chen, and S. J. Harding.** Implementation of Reliability Methods to Marine Structures. Transaction SNAME. 353-380. 1984.
- [65] **R. Aggarwal, R. G. Bea, B. C Gerwick, C. W. Ibbs, R. B. Reimer, and G.C. Lee.** Development of a Methodology for Safety Assessment of Existing Steel Jacket Offshore Platforms. Houston : 22th Annual Offshore Technology Conference. 7th – 10th May 1990.
- [66] **R. G. Bea.** Reliability Based Requalification Criteria for Offshore Platforms. Proceedings of the 12th International Conference on Offshore Mechanics and Artic Engineering. Vol 2. 351-361. 1993.
- [67] **L. Manuel, D. G. Schmucker, C. A. Cornell, and J. E. Carballo.** A Reliability-based design format for Jacket Platforms under Waves Loads. Journal Marine Structures. Vol (11). 413-428. 1998.
- [68] **L. Tvedt.** Proban – probabilistic analysis . Structural Safety. Volume 28, Issues 1-2. 2006.
- [69] **S. Gollwitzer, B. Kirchgäßner, R. Fischer, and R. Rackwitz.** PERMAS-RA/STRUREL system of programs for probabilistic reliability analysis. Structural Safety. Volume 28, Issues 1-2. 2006.
- [70] **R. Skjong, E. B. Gregersen, E. Cramer, A. Croker, O. Hagen, G. Korneliussen, S. Lacasse, I. Lotsberg, F. Nadim, K. O. Ronold.** Guideline for Offshore Structural Reliability Analysis - General. DNV. Report No. 95-2018. 1995.
- [71] **K. Bell, B. Hatlestad, O. E. Hansteen, and P. O. Araldsen.** NORSAM User Manual, Part 1, General Description. 1970.

- [72] **N. D. P. Barltrop, and A.J. Adams.** Dynamics of Fixed Marine Structures. Butterworth-Heinemann Ltd., Reprint. 1991.
- [73] **D. Faulkner, M. J. Cowling, and P. A. Fierze.** Integrity of Offshore Structures - 4. Applied Science Publishers. 1990.
- [74] **Society of Naval Architects and Marine Engineers.** Site Specific Assessment of Mobile Jackup Units Guideline, R.P. and Commentaries, Example calc. S.N.A.M.E. Technical & Research Bulletin 5-5. 1993.
- [75] **City University.** Joint Industry Project. Jackup site Assessment Procedures - Establishment of an International Recommended Practice. City University, London, England. Seminar, 1993.
- [76] **T. Onoufriou, and V. J. Forbes.** Developments in Structural System Reliability Assessments of Fixed Steel Offshore Platforms. Reliability Engineering and System Safety. Vol. (71). 189-199. 2001.
- [77] **Y. Murotsu, and H. Okada.** Application of Reliability Assessment Methods to Marine Frame Structures Based on Ultimate Strength Analysis. New Jersey: S.N.A.M.E. Marine Structural Reliability Symposium. 5th – 6th October, 1987.
- [78] **N. K. Shetty.** Selective enumeration method for identification of dominant failure paths of large structures. Huston, USA : Proceedings of the International Conference on Offshore Mechanics and Arctic and Engineering. 1994.
- [79] **P. Thoft-Christensen, and Y. Murotsy.** Application of Structural Systems Reliability Theory. Berlin : Springer-Verlag. 1986.
- [80] **G. Sigurdsson, R. Skjong, B. Skallerud, and J. Amdahl.** Probabilistic Collapse Analysis of Jackets. Rotterdam: Balkema. 535-543. Schuëller, Shinozuka and Yao. Structural Safety and Reliability. 1994.
- [81] **P. S. Tromans, and J. W. Van de Graaf.** Substantiated Risk Assessment of Jacket Structure. Journal of Waterway, Port Coastal and Ocean Engineering. Vol 120 (6). 535-555, 1992.

[82] **J. W. Van de Graaf, P. S. Tromans, and M. Efthymiou.** The Reliability of Offshore Structures and Its Dependence on Design Code and Environment. Houston: OTC. 105-118 : 26th Annual Offshore Technology Conference. 2nd – 5th May, 1994.

[83] **R. G. Bea, and M. M. Mortazavi.** ULSLEA: A Limit Equilibrium procedure to determine the Limit State Loading of Template-type Platforms. Journal of Offshore Mechanics and Arctic Engineering. Transactions of the ASME. Volume 118(4). 267-275. 1996.

[84] **P. A. Frieze, A. C. Morandi, M. Birkinshaw, D. Smith, and A. T. Dixon.** Fixed and Jack-up Platforms: Basis for Reliability Assessment. Journal of Marine Structure. volume 10. 263-284. 1997.

[85] **H. Nordal, C. A. Cornell, and A. Karamchandani.** A Structural System Reliability Case Study of an Eight-leg Steel Jacket Offshore Production Platform. Marine Structural Reliability Symposium. New Jersey: Society of Naval Architect. 5-6 October, 1987.

[86] **R. S. De, A. Karamchandari, and C. A. Cornell.** Offshore Structural System Reliability under Changing Load Pattern. Applied Ocean Research. Vol. 13 (3). 145-157. 1991.

[87] **M. Hohenbichler.** An Approximation to the Multivariate Normal Distribution. Lyngby : DIA-LOG 6-82, Danish Academy of Engineers, pp. 79-100. 1982.

[88] **H. Pham.** Handbook of reliability engineering . London : Springer. 2003.

[89] **O. Ditlevsen.** Narrow reliability bounds for structural systems. J. Struct. Mech. 7, pp. 453–472 1979.

[90] **G. Sigurdsson, R. Skjong, B. Skallerud, and J. Amdahl.** Probabilistic Collapse Analysis of Jackets. In: Schuëller, Shinozuka and Yao. Structural Safety and Reliability. Rotterdam: Balkema. 535-543. 1994.

- [91] **R. K. Aggarwal, R. G. Bea , B. C. Gerwic. C. W. Ibbs, R. B. Reimer, and G.C. Lee.** Development of a Methodology for Safety Assessment of Existing Steel Jacket Offshore Platforms. 22th Annual Offshore Technology Conference. Houston. 7th – 10th May, 1978. 1990.
- [92] **Health & Safety Executive.** Offshore Technology Report-OTO 2000 037 (a Review of Reliability Considerations for Fixed Offshore Platforms). UK: University of Surrey. HSE. 2000.
- [93] **S-K Choi, R. V. Grandhi, and R. A. Canfield.** Structural reliability under non-Gaussian stochastic behavior. Computers & Structures. 82 (2004) 1113–1121. 2004.
- [94] **G. I. Schueller.** A state-of-the-art report on computational stochastic mechanics. Journal of Probabilistic Engineering Mechanics. 12(4):197-313. 1997.
- [95] **R. G. Spanos, and P. D. Ghanem.** Spectral stochastic finite-element formulation for reliability analysis. J. Engrg. Mech. ASCE 117 (10), pp. 2351–2372. 1991.
- [96] **R. G. Ghanem and W. Brzakala.** Stochastic finite-element analysis of soil layers with random interface. J. Engrg. Mech. ASCE 122 (4), pp. 361–369. 1996.
- [97] **R. G. Ghanem.** Stochastic finite elements with multiple random non-normal properties. J. Engrg. Mech. ASCE 125 (1), pp. 26–40. 1999.
- [98] **C. G. Soares, and N.-Z. Chena.** Spectral stochastic finite element analysis for laminated composite plates . Computer Methods in Applied Mechanics and Engineering. Volume 197, Issues 51-52, Pages 4830-4839. 2008.
- [99] **M. A. Tatang.** Direct Incorporation of Uncertainty in Chemical and Environmental Engineering Systems, Ph.D. Dissertation. Massachusetts Institute of Technology, Cambridge, MA. 1995.

- [100] **S. S. Isukapalli.** Uncertainty Analysis of Transport-Transformation Models, Ph.D . Dissertation. Rutgers, The State University of New Jersey, New Brunswick, NJ. 1999.
- [101] **C. L. Pettit, R. A. Canfield, and R. Ghanem.** Stochastic Analysis of an Aeroelastic System. New York. 15th ASCE Engineering Mechanics Conference, Columbia University. June 2-5, 2002.
- [102] **D. Xiu, and G. Karniadakis,.** The Wiener-Askey Polynomial Chaos for Stochastic Differential Equations. SIAM Journal on Scientific Computing. Vol. 24, (2), pp. 619-644. 2002.
- [103] **R. Ghanem, and P. D. Spanos.** Stochastic Finite Elements: A Spectral Approach. NY. Springer-Verlag, 1991.
- [104] **I. Babuska, R. Tempone, and G. E. Zouraris.** Galerkin Finite Element Approximations of Stochastic Elliptic Differential Equations. SIAM Journal on Numerical Analysis. Vol. 42, pp. 800-825. 2004.
- [105] **I. Elishakoff.** Simulation of space-random fields for solution of stochastic boundary-value problems. J. Acous. Soc. Am. 65. 399-403. 1979.
- [106] **B. Ellingwood, and J. Zhang.** Orthogonal series expansion of random fields in first-order reliability analysis. ASCE J. Engrg. Mech. 1994.
- [107] **M. Grigoriu.** Simulation of nonstationary Gaussian processes by random trigonometric polynomials. ASCE J. Engrg. Mech. 119(2). 328-343. 1993.
- [108] **H. Hotelling.** Analysis of a Complex of Statistical Variables into Principle components. Journal of Educational Psychology. Vol.24, pp.498-520. 1933.
- [109] **R. L. Iman, and W. J. Conover.** A distribution free approach to inducing Rank Correlation among input variables. Communications in statistics: Simulation and Computation. B11, pp.311-334. 1982.

- [110] **M. Stein.** Large Sample Properties of Simulations Using Latin Hypercube Sampling. *Technometrics*. Vol.29, (2), pp. 143-151. 1987.
- [111] **S. Choi, R. A. Canfield, and R. V. Grandhi.** Estimation of Structural Reliability for Gaussian Random Fields. *Structure & Infrastructure Engineering*. Nov. 2005.
- [112] **S. Choi, R. V. Grandhi, and R. A. Canfield.** Robust Design of Mechanical Systems via Stochastic Expansions. *International Journal of Materials and Product Technology*. Vol. 25, pp. 127-143. 2006.
- [113] **S. Choi, R. V. Grandhi, R. A. Canfield, and C. L. Pettit.** Polynomial Chaos Expansion with Latin Hypercube Sampling for Estimating Response Variability. *AIAA Journal*. Vol. 42, pp. 1191-1198. 2004.
- [114] **E. Cureton, and R. D'Agostino.** Factor Analysis: An applied approach. NJ : Lawrence Erlbaum Associates. 1983.
- [115] **W. T. Martin, and R.H. Cameron.** The orthogonal development of nonlinear functionals in series of Fourier-Hermite functionals. *Ann. Math.* 48 385-392. 1974.
- [116] **S-K. Choi, R. Grandhi, and R. Canfield.** Reliability-based Structural Design. USA. Springer. 2006
- [117] **Society of Automotive Engineers.** Integration of Probabilistic Methods into the Design Process. Aerospace Information Report 5080. 1997.
- [118] **A. M. Freudenthal, J. M. Garrelts, and M. Shinozuka.** The Analysis of Structural Safety. *Journal of the Structural Division*. ASCE. Vol. 92. 1966.
- [119] **M. Rosenblatt.** Remarks on a Multivariate Transformation. *The Annals of Mathematical Statistics*. Vol. 23. 1952.

- [120] **M. Hohenbichler, and R. Rackwitz.** Non-normal Dependent Vectors in Structural Safety. Journal of the Engineering Mechanics Division. ASCE. Vol. 107, No. EM6. 1981.
- [121] **R. E. Merchelers.** Structural Reliability Analysis and Prediction. UK. Ellis Horwood Limited. 1987.
- [122] **L. Wang, and R. V. Grandhi.** Reliability-based structural optimization using improved two-point adaptive nonlinear approximations . Finite Elements in Analysis and Design. Volume 29, Issue 1, Pages 35-48. 1998.
- [123] **K. Breitung.** Asymptotic Approximations for Multinormal Integrals. Journal of the Engineering Mechanics Division. Vol. 110. 1984.
- [124] **L. Tvedt.** Two Second-order Approximations to the Failure Probability - Section on Structural Reliability. Norwar. DNV. 1984.
- [125] **L. Tvedt.** Distribution of Quadratic Forms in Normal Space Applicationsto Structural Reliability. Journal of the Engineering Mechanics Division. ASCE. Vol. 116. 1990.
- [126] **M. Hohenbichler, and R. Rackwitz.** Improvement of Second-order Reliability Estimates by Importance Sampling. Journal of Engineering Mechanics Division. ASCE. Vol. 116. 1990.
- [127] **H. U. Koyluoglu, S. R. K. Nielsen.** New Approximations for SORM Integrals. Structural Safety. Vol. 13. 1994.
- [128] **G. Q. Cai, and I. Elishakoff.** Refined Second-order Approximations Analysis. Structural Safety. Vol. 14. 1994.
- [129] **L. P. Wang, and R. V. Grandhi.** Improved Two-point Function Approximation for Design Optimizaation. AIAA Journal. Vol. 32. 1995.
- [130] **A. Der Kiureghian, H. Z. Lin, and S. J. Hwang.** Second Order Reliability Approximations. Journal of Engineering Mechanics. Vol. 113. 1987.

- [131] **J. Todd.** Survey of Numerical Analysis. New York : McGraw Hill. 1962.
- [132] **K. Breitung.** Asymptotic Approximations for Multinormal Integrals. Journal of the Engineering Mechanics Division. ASCE, Vol. 110, No. 3. pp 357-366. 1984.
- [133] **Det Norske Veritas.** PROBAN Theory Manual. DNV. DNV Software Report No.: 96-7017. 2004.
- [134] **J. von Neumann, and S. Ulam.** The Monte Carlo Method. Bulletin AMS,51-0-165. 1945.
- [135] **M. D. McKay, R. J. Beckman, and W. J. Conover.** A comparison of three methods for selecting valuesm of input variables in the analysis of output from a computer code. Technometrics. Vol.21, (2), pp. 239-245. 1979.
- [136] **D. C. Champis and G. I. Schuëller.** Using Monte Carlo Simulation to Treat Physical Uncertainties in Structural Reliability. Lecture Notes in Economics and Mathematical Systems. Volume 581, Part II, 67-83. 2006.
- [137] **E. C. Anderson,** Monte Carlo Methods and Importance Sampling. Notes, 1999.
- [138] **R. E. Guerra, T. N. Saleem, and T. D. Savitsky.** Importance Sampling. Rice University, Lecture Notes. 2008.
- [139] **T.S. Doorn, E.J.W. ter Maten, J.A. Croon, A. Di Bucchianico, and O. Wittich.** Importance Sampling Monte Carlo simulations for accurate estimation of SRAM yield. Eindhoven University of Technology, 2008.
- [140] **S-K Au, and J. L. Beck.** Estimation of small failure probabilities in high dimensions by subset simulation. Probabilistic Engineering Mechanics Volume 16, Issue 4, Pages 263-277. October 2001.

- [141] **G. I. Schuëller, H. J. Pradlwarter, and P. S. Koutsourelakis.** A critical appraisal of reliability estimation procedures for high dimensions. Probabilistic Engineering Mechanics Volume 19, Issue 4, Pages 463-474. October 2004.
- [142] **M. Shinozuka.** Basic analysis of structural safety. Journal of Structural Engineering. ASCE, Vol 109(3), pp. 721-740. 1983.
- [143] **I. Deak.** Three digit accurate multiple normal probabilities. Numerische Mathematik. Vol. 35, pp. 369-380. 1980.
- [144] **M. Hohenbichler, and R. Rackwitz.** Sensitivity and importance measures in structural reliability. Civil Engineering Systems. Vol. 3(4), pp. 203-209. 1986.
- [145] **G. Schall, S. Gollwitzer, and R. Rackwitz.** Integration of multinormal densities on surfaces. Proceedings of the 2nd IFIP Working Conference on Reliability and Optimization on Structural Systems. P. Thoft-Christensen. ed. Springer Verlag, 1988.
- [146] **P. Bjerager, and S. Krenk.** Sensitivity measures in structural reliability analysis. Proceedings of the 1st IFIP Working Conference on Reliability and Optimization on Structural Systems. P. Thoft-Christensen, ed. Springer Verlag, Berlin, pp 459-470. 1987.
- [147] **R. Y. Rubinstein.** Simulation and the Monte Carlo Method. s.l. : John Wiley & Sons Ltd, New York. pp. 115-118. 1981.
- [148] **R. E. Melcher.** Structure Reliability Analysis and Prediction, 2nd ed. England : John Wiley & Sons Ltd. 1999.
- [149] **W. C. Broding, F. W. Diederich, and P. S. Parker.** Structural optimization and design based on a reliability design criterion. J. Spacecraft. 1(1), 56–61. 1964.
- [150] **L. Faravelli.** Response Surface Approach for Reliability Analysis. J Eng Mech. 115(12):2763-81. 1989.

- [151] **M. Lemaire.** Finite element and reliability - Combined methods by response surface PROBAMAT-21st century: Probabilities and materials - Tests, models and applications for the 21st century; Proceedings of the NATO Advanced Research Workshop, Perm, Russia; NETHERLANDS; 10-12 Sept. 1997. pp. 317-331. 1998
- [152] **D. C. Cox, and P Baybutt.** Methods for uncertainty analysis: a comparative survey. *Risk Anal* . 1(4):251–8. 1981.
- [153] **S. H. Kim, and S. W. Na.** Response surface method using vector projected sampling points. *Struct Saf.* 19:3–19. 1997.
- [154] **K. Breitung, and L. Faravelli.** Log-likelihood maximization and response surface reliability assessment. *Nonlinear Dyn.* 4:273–86. 1994.
- [155] **C. G. Bucher, and U. Bourgund.** A fast and efficient response surface approach for structural reliability problems. *Struct Saf* . 7:57–66. 1990.
- [156] **S. Gupta, and C. S. Manohar.** An improved response surface method for the determination of failure probability and importance measures. *Struct Saf* . 26:123–39. 2004.
- [157] **V. W. Liu, and F. A. Moses.** A sequential response surface method and its application in the reliability analysis of aircraft structural systems. *Struct Saf.* 16:39–46. 1994.
- [158] **M. R. Rajashekhar, and B. R. Ellingwood.** A new look at the response surface approach for reliability analysis. *Struct Saf* . 12:205–20. 1993.
- [159] **L. Olivi.** Response surface methodology in risk analysis. In: Apostolakis G, Garribba S, Volta G, editors. *Synthesis and analysis methods for safety and reliability studies.* Plenum Press, 1980.
- [160] **H. P. Gavin, and S. C. Yau.** High-order limit state functions in the response surface method for structural reliability analysis. *Structural Safety.* 30, 162-179. 2008.

- [161] **S. Engelund, and R. Rackwitz.** Experiences with experimental design schemes for failure surface estimation and reliability. In: Proceedings of the sixth speciality conference on probabilistic mechanics and structural and geotechnical reliability. ASCE. 1992.
- [162] **I. Enevoldsen, M. H. Faber, and J. D. Sorensen.** Adaptive response surface technique in reliability estimation. *Structural Safety*. 1257–64. Schuëller, Shinozuka, Yao. 1994.
- [163] **N. Devictor, M. Marques, and M. Lemaire.** Utilisation des surfaces de réponse dans le calcul de la fiabilité des composants mécaniques. *Revue Française de Mécanique*. 1:43–51. 1997.
- [164] **S. H. Kim, and S. W. Na.** Response surface method using vector projected sampling points. *Structural Safety* . 19:3–19. 1997.
- [165] **P. K. Das, and Y. Zheng.** Cumulative formation of response surface and its use in reliability analysis. . *Probabilistic Engineering Mechanics* . 15:309–15. 2002.
- [166] **N. Impollonia, and A. Sofi.** A response surface approach for the static analysis of stochastic structures with geometrical nonlinearities. *Computer Methods in Applied Mechanics and Engineering* . 192:4109–29. 2003.
- [167] **A. I. Khuri, and J. A. Cornell.** Response surfaces designs and analyses. 2nd ed. Marcel Dekker, 1996.
- [168] **I. Kaymaz, and C. A. McMihon.** A response surface mehtod based on weighted regression for reliability analysis. *Probabilistic Engineering Mechanics*. 20;11-17. 2005.
- [169] **A.S.Nguyen, A. Sellier, F. Duprat, and G. Pons.** Adaptive response surface method based on a double regression technique. *Probabilistic Engineering Mechanics*. 135-143. 2009.

- [170] **B. Sudret, and A. Der Kiureghian.** A stochastic Finite Elements methods and reliability. State of the art report. University of California. 2000.
- [171] **N. Gayton, J. M. Bourinet, and M. Lemaire.** CQ2RS: A new statistical approach to the response surface method for reliability analysis. *Structural Safety*. 25: 99-121. 2003.
- [172] **R. H. Myers.** Response Surface Methodology. Boston. Allyn and Bacon Inc. 1971.
- [173] **J. A. Nelder.** Inverse polynomials, a useful group of multifactor response functions. *Biometrics*. 22, 128-141, 1966.
- [174] **D. J. J. Toal, N. W. Bressloff, and A.J. Keane.** Kriging hyperparameter tuning strategies. *AIAA Journal*. vol. 46:pp. 1240–1252. 2008.
- [175] **D. R. Jones.** A taxonomy of global optimization methods based on response surfaces. *Journal of Global Optimization*. vol. 21:pp. 345–383. 2001.
- [176] **A. Forrester, A. Sobester, and A. Keane.** Engineering design via surrogate modelling: a practical guide. Chichester, UK. Wiley, 2008.
- [177] **A. Sobey, J. Underwood, J. Blake, and & A. Sheno.** Reliability analysis of damaged steel structures using finite element analysis. Scotland, UK. Proceeding of 5th International ASRANet Conference, 2010.
- [178] **O. C. Zienkiewicz, and R. L. Taylor.** The Finite Element Method. 5th. Butterworth-Heinemann. Vol. 2: Solid Mechanics. 2000.
- [179] **S. S. Rao.** The Finite Element Method in Engineering. 4th. Elsevier Science & Technology Books, Dec. 2004.
- [180] **R. T. Fenner.** Finite Element Methods for Engineers. Imperial College Press. 1996.
- [181] **A. J. M. Ferreira.** MATLAB code for Finite Element Analysis. Springer. 2009.

[182] **A. S. Nowak, and K. R. Collins.** Reliability of structures. United States of America. McGraw Hill. 2000.

[183] **B. J. Muga, and J. F. Wilson.** Dynamic Analysis of Ocean Structure. New York. Plenum Press. 1970.

[184] **M. Efthymiou, and C. G. Graham.** Environmental Loading on Fixed Offshore Platforms. Netherlands: SUT : Environmental Forces on Offshore Structures and their Prediction. 1990.

[185] **J. Gaythwaite.** The Marine Environment and Structural Design. New York : Van Nostrand Reinhold Co. 1981.

[186] **N. P. D. Baltrop, G. M. Mitchell, and J. B. Arkins.** Fluid Loading on Fixed Offshore Structure. London : Department of Energy. 1990.

[187] **O. T. Gusmestad, and D. Karunakaran.** Wave Current Interaction. London : Proceedings of the Society of Underwater Technology, 81-110. 1990.

[188] **S. K. Chakrabati.** Nonlinear Methods in Offshore Engineering. New York : Elsevier. 1990.

[189] **D. H. Peregrine.** Interaction of Water Waves and Currents. Advances in Applied Mechanics. 16: 9-117. 1976.

[190] **R. A. Dalrymple.** Models for Nonlinear Water Waves in Shear Currents. Houston. OTC, 843-856 : Proceedings of the 6th Annual Offshore Technology Conference. 1974.

[191] **M. H. Patel.** Offshore Structures. N. Morgan. Marine Technology Reference Book. London. Butterworth. 1990.

[192] **P. Pagrut, and M. C. Deo.** Extreme Wave Height Estimates. San Francisco:ISOPE, 186, 193 : Proceedings of the 2nd International Offshore and Polar Engineering Conference. 1992.

- [193] **B. Le. Mehaute.** An Introduction to Hydraulodynamics and Water Waves. Dusseldorf. Springer-Verlag. 1976.
- [194] **T. Sarpkaya, and M. Isaacson.** Mechanics of Wave Forces on Offshore Structures. New York. Van Nostrand Reinhold, 1981.
- [195] **R. G. Dean.** Relative Validities of Water Wave Theories. Journal of Waterways, Harbors and Coastal Engineering Division. 96(WWI): 105-119. 1970.
- [196] **J. H. Vugts.** A Review of Hydrodynamic Loads on Offshore Structures and Their Formulation. London: BOSS, 693-708 : Proceedings of the 2nd International Conference on Behaviour of Offshore Structures. 1979.
- [197] **J. R. Morison, M. P. O'Brien, J. W. Johnson, and S. A. Schaaf.** The Force Exerted by Surface Waves on Piles. Petroleum Transactions. 189:149-157. 1950.
- [198] **T. H. Dawson.** Offshore Structural Engineering. Englewood Cliffs: Prentice Hall. 1983.
- [199] **T. Sarpkaya.** In-Line and Transverse Forces on Cylinders in Oscillatory Flow at High Reynolds Numbers. Huston: OTC, 95-108. Proceedings of 8th Annual Offshore Technology Conference. 1976.
- [200] **R. L. Wiegel.** Oceanographical Engineering. New Jersey. Prentice Hall. 1964.
- [201] **O. T. Gusmestad, and D. Karunakaran.** Wave Current Interaction. London: Society for Underwater Technology: 81-110 : Proceedings of the Environmental Forces on offshore structures and their Prediction. 1990.
- [202] **G. Rodenbusch, and C. Kallstorm.** Forces on a Large Cylinder in Random Two-Dimension Flows. Huston. OTC. Proceedings of 18th Annual Offshore Technology Conference. 1986.

- [203] **M. de St. Q. Isaacson, and D. J. Maulli.** Transverse Forces on Vertical Cylinders in Waves. Journal of Waterways, Harbors and Coastal Engineering Division. 102 (WW1). 49-60. 1976.
- [204] **C. Petruskas, and P. M. Aagaard.** Extrapolation of Historical Storm Data for Estimating Design - Wave Heights. Society of Petroleum Engineers Journal. 11(1): 23-37. 1971.
- [205] **R. E. Haring, and J. C. Heidenman.** Gulf of Mexico Rare Wave Return Periods. Journal of Petroleum Technology. 32(1): 35-47. 1980.
- [206] **G. P. V. Vledder, and T. J. Zitman.** Design Waves: Statistics and Engineering Practice. San Francisco, USA: The International Society of Offshore and Polar Engineering : Proceedings of the 2nd International Offshore and Polar Engineering Conference. 1992.
- [207] **M. N. Madsen, J. B. Nielsen, P. Klinting, and J. Knudsen.** A Design Load Method For Offshore Structures Based Upon the Joint Probability of Environmental Parameters. USA: ASME, 75-80 : Proceedings of 7th International Conference on Offshore Mechanics and Arctic Engineering. 1988.
- [208] **E. M. Bitner-Gregersen, and S. Haver.** Joint Environmental Model for Reliability Calculations. UK. The international Society of Offshore Conference. Proceedings of the First International Offshore and Polar Engineering Conference. 1991.
- [209] **J. C. Heideman, O. Hagen, C. Cooper, and D. Finn-Erik.** Joint Probability of Extreme Waves and Currents on Norwegian Shelf. Journal of Waterway, Port, Coastal and Ocean Engineering. Vol.115(4). 534-546. 1989.
- [210] **P. S. Tromas, and L. Vanderschuren.** Response Based Design Conditions in the North Sea: Application of the New Method. Houston. OTC. 287-297. Proceedings of 27th Annual Offshore Technology Conference. 1995.
- [211] **Fugro GEOS.** Wind and wave frequency distributions for sites around the British Isles. London. Health and Safety Executives. 2001.

- [212] **M. J. Tucker.** Waves in Ocean Engineering: Measurements, Analysis, Interpretation. Chichester. Ellis Horwood Ltd. 1991.
- [213] **D. Myrhaug, and S. P. Kjeldsen.** Parametric Modeling of joint Probability density distributions for steepness and asymmetry in deep water waves. Applied Ocean Research. Vol. 6 (4). 207-220. 1984.
- [214] **M. A. Srokosz.** A Note on the Joint Distribution of Wave Height and Period During the Growth Phase of a Storm. Journal of Ocean Engineering. Vol. 15 (4). 379-387. 1988.
- [215] **M. A. Skrokosz, and P. G. Challenor.** Joint Distribution of Wave Height and Period: A Critical Comparison. Journal of Ocean Engineering. Vol.14(4). 296-311. 1987.
- [216] **S. Haver.** Wave Climate of Northern Norway. Applied Ocean Research. Vol. 14 (5). 359-376. 1985.
- [217] **S. Haver.** On the Joint Distribution of Heights and Periods of Sea Waves. Journal of Ocean Engineering. Vol.14 (5) 359-376. 1987.
- [218] **M. K. Ochi.** On Long-term Statistics for Ocean and Coastal Waves. Proceedings of 16th Coastal Engineering Conference. Vol.1. 59-75. 1978.
- [219] **G. P. van Vledder, and T. J. Zitman.** Design Waves: Statistics and Engineering Practice. San Francisco: ISOPE, 170-178 : Proceedings of the 2nd International Offshore and Polar Engineering Conference. 1992.
- [220] **J. N. Sharma, and W. G. Grosskopf.** Practical Considerations in Preparing Extreme Wind, Wave and Current Criteria. Houston: OTC, 377-386 : Proceedings of the 26th Annual Offshore Technology Conference. 1994.
- [221] **L. R. Muir, and A. H. El-Shaarawi.** On the calculation of Extreme Wave Heights: A Review. Ocean Engineering. 13(1): 93-118. 1986.

- [222] **C. G. Soares, and M. Scotto.** Modelling Uncertainty in Long-Term Predictions of Significant Wave Height. *Journal of Offshore Mechanics and Arctic Engineering.* 118: 284-291. 1996.
- [223] **D. J. T. Carter, and P. G. Challenor.** Methods of Fitting the Fisher-Tippett Type I Extreme Value Distribution. *Ocean Engineering.* 10(3): 191-199, 1983.
- [224] **G. Q. Yao, B. C. Ding, J. Y. Wang, and Z. X. Ma.** Statistic Analysis of Wave Parameters for the China Sea. Singapore: ISOPE, 22-26 : Proceedings of the 3rd International Offshore and Polar Engineering Conference. 1993.
- [225] **L. E. Borgman.** Risk Criteria. *Journal of Waterways and Harbors Division.* 89(WW3): 1-35. 1963.
- [226] **R. C. Turner, and M. J. Baker.** A Probabilistic Wave Model and Reliability Analysis. Berlin : Proceedings IFIP Working Conference on Reliability and Optimization of Structural Systems. In *Lecture Notes in Engineering.* Springer-Verlag. 1988.
- [227] **P. M. Hagemeyer.** A Comparison between a Deterministic and Probabilistic Fluid Loading Model for a Jacket Structure. The Hague: OMAE. 89-97 : Eight International Conference on Offshore Mechanics and Arctic Engineering. 1989.
- [228] **M. K. Ochi.** Probabilistic Extreme Values and Their Implication for Offshore Structure Design. Houston: OTC. 987-989 : Proceedings of 10th Offshore Technology Conference. 1978.
- [229] **M. S. Longuet-Higgins.** On the Joint Distribution of wave periods and Amplitudes in a Random Wave Field. London. 241-258 : Proceedings of the Royal Society of London. 1983.
- [230] **J. Mathisen, and E. Bitner-Gregersen.** Joint distribution for Significant Wave Height and Wave Zero-Up-Crossing Period. *Applied Ocean Research.* Vol.12, (2), 93-103. 1990.

- [231] **D. M. Constantine, and K. Tzanis.** Numerical Results of the Joint Probability of Heights and Periods of Sea Waves. Coastal Engineering. Vol. 22. 217-235. 1994.
- [232] **M. G. Hallam, N. J. Heaf, and L. R. Wootton.** Dynamics of Marine Structures: Methods of calculating the dynamic response of fixed structures subjected to wave and current action. London : Ciria Underwater Engineering Group. 1977.
- [233] **R. G. Bea, and N. W. Lai.** Hydrodynamic Loadings on Offshore Platforms. Houston: OTC, 155-164. Proceedings of 10th Annual Offshore Technology Conference. 1978.
- [234] **Norwegian Petroleum Directorate.** Regulations Relating to Loadbearing Structures in the Petroleum Activities. Norway. NPD. 1994.
- [235] **D. K. Hart, S. E. Rutherford, and A. H. S. Wickham.** Structural Reliability Analysis of Stiffened Panels. UK. The Royal Institute of Naval Architects. 1985.
- [236] **D. Smith, A. Csenki, C. P. Ellinas.** Ultimate Limit State Analysis of Unstiffened Structural Components. Glasgow, UK. IOS' 87. 1987.
- [237] **T. V. Galambos, and M. K. Ravindra.** Properties of Steel for Use in LRFD. Journal of Structural Division. ASCE, Vol. 104, No. ST9. 1978.
- [238] **J. P. Tronskar, A. Karlsen, H. Bratfos, M. Hauge.** Probabilistic Fracture Mechanics Analysis of Welded K-node: Significance of Local Brittle Zones. Calgary, Alberta, Canada : Proceedings of 11th International Conference on Offshore Mechanics and Arctic Engineering, OMAE. 1992.
- [239] **ECCS.** Manual on Stability of Steel Structures. European Convention for Constructural Steelwork. 1976.
- [240] **V. Galambos.** Guide to stability Design Criteria for Metal Structures. s.l. : Fourth Edition. John Wiley & Sons. 1988.

- [241] **R. Bjorhovde.** Chapter 2.3 - Compression Members. J. E. Harding, and R. Bjorhovde P. J. Dowling. *Constructional Steel Design - an International Guide.* Elsevier Applied Science. 1992.
- [242] **R. D. Sherman.** Chapter 2.4 - Tubular Members. *Constructional Steel Design - An International Guide.* P. J. Dowling, J. E. Harding, and R. Bjorhovde. Elsevier Applied Science. 1992.
- [243] **M. A. Bonello, M. K. Chryssanthopoulos, and P. J. Dowling.** Ultimate Strength Design of Stiffened Plates under Axial Compression and Bending. *Marine Structures.* Vol. 6, Nos. 5&6, pp. 533-552. 1993.
- [244] **C. P. Ellinas, M. Lalani, M., and J. V. Sharp.** Tubular Joint Strength Formulations. The Implication for Harmonisation. London, England : Proceedings, SUT Int. Conf. on API RP 2A-LRFD, Its Present and Future Role in Offshore Safety Cases. 1993.
- [245] **D. Faulkner.** Efficient Design of Orthogonally Stiffened Cylinders. London, England : Proceedings, BOSS conference. 1992.
- [246] **M. B. Gibstein.** Static Strength of Tubular Joints. Norway : Det Norske Veritas. Report No. 73-86-C. 1973.
- [247] **M.B. Gibstein.** The Static Strength of T-Joints Subjected to In-plane Bending Moments. Norway : Det Norske Veritas. Report No. 76-137. 1976.
- [248] **Department of Energy.** Background to New Static Strength Guidance for Tubular Joints in Steel Offshore Structures. 1990.
- [249] **MSL Engineering.** Static Strength of Tubular Joints in Offshore Structures. Report Health & Safety Executive. 1992.
- [250] **J. A. Yura, N. Zettlemyer, and I. F. Edwards.** Ultimate Capacity Equations for Tubular Joints. Houston, Texas. Proceedings, Offshore Technology Conference, OTC Paper No. 3690. 1980.

- [251] **I. Lotsberg**. Design of Tubular Joints. Norway. NIF Course. 1990.
- [252] **F. Nadim**. Geotechnical Site description using stochastic interpolation. Oslo, Norway. 10th Geotechnical Meeting (NGM-88). 1988.
- [253] **J. M. Keaveny, F. Nadim, and S. Lacasse**. Autocorrelation function for offshore geotechnical data. San Francisco. Proceedings of the 5th International Conference on Structural Safety and Reliability. ICOSSAE '89. 1989.
- [254] **T. R. Guttormsen**. Reliability analysis for offshore foundations — uncertainty in soil parameters. Oslo. NGI Report No. 51411-3. 1987.
- [255] **Norwegian Geotechnical Institute**. Reliability-based design of offshore foundations - model uncertainty in axial pile capacity calculations. London : HSE Books. Offshore Technology Report OTN 95 145. 1994.
- [256] **K. H. Andersen, , R. Dyvik, R. Lauritzsen, D. Heien, L. Hårvik, and T. Amundsen**. Model tests of gravity platforms: Interpretation. J. Geotech. Engrg. ASCE, Vol. 115, No. 11, pp. 1550-1568. 1989.
- [257] **K. H. Andersen, R. Dyvik, K. Schrøder, O.E. Hansteen, and S. Bysveen**. Field tests of anchors in clay - II: Predictions and interpretation. J. Geotech. Engrg. ASCE, Vol. 119, No. 10. 1993.
- [258] **Det Norske Veritas**. Fatigue Strength Analysis for Mobile Offshore Units. Høvik, Norway : DNV. DNV Classification Note 30.2. 1984.
- [259] **British Standards Institution**. Guidance on Methods for Assessing the Acceptability of Flaws in Fusion Welded Structures. UK. PD 6493. 1991.
- [260] **H. O. Madsen, S. Krenk, and N. C. Lind**. Methods of Structural Safety. N.J. Prentice-Hall Ltd, Englewood Cliffs. 1986.
- [261] **J. G. Kuang, A. B. Potvin, and R. D. Leick**. Stress Concentrations in Tubular Joints. Houston, Texas : Proceedings, Offshore Technology Conference, OTC Paper No. 2205. 1975.

- [262] **M. B. Gibstein** Parametric Stress Analysis of T-Joints. Cambridge, England : Proceedings, European Offshore Steel Research Seminar. Paper 26. 1978.
- [263] **M. Efthymiou**. Development of SCF Formulae and Generalised Influence Functions for Use in Fatigue Analysis. Surrey, England : OTJ'88 Recent Developments in Tubular Joints Technology. 1988.
- [264] **A. K. Hellier, M. P. Conolly, and W. D. Dower**. Stress Concentration Factors for Tubular T and Y Joints. Int. Journal of Fatigue. Vol. 12, No. 1. 1990.
- [265] **P. H. Wirsching**. Fatigue Reliability of Offshore Structures. Journal of Structural Engineering. ASCE, Vol. 110, pp. 2340-2356. 1984.
- [266] **R. E. Melchers**. Modeling of marine corrosion of steel specimens. W. T. Young, and R. M. Kain. Corrosion testing in natural waters. Philadelphia: ASTM STP 1300, p. 20-33. 1997.
- [267] **A. Cosham, P. Hopkins, and K. A. Macdonald**. Best practice for the assessment of defect in pipelines - Corrosion. Engineering Failure Analysis. 14 1245-1265, 2007.
- [268] **R. E. Melchers**. The effect of corrosion on the structural reliability of steel offshore structures. Corrosion Science. 47, 2391-2410. 2005.
- [269] **R. E. Melchers**. Corrosion uncertainty modelling for steel structures. Journal of Constructional Steel Research. 52, 3-19. 1999.
- [270] **F. L. LeQue**. Marine Corrosion: causes and prevention. New York. Wiley Interscience. 1975.
- [271] **B. D. Craig**. Handbook of corrosion data. Ohio : ASM International. 1989.
- [272] **S. Qin, and W. Cui**. Effect of corrosion models on the time dependent reliability of steel plated elements. China. 16, 15-34. 2003.

- [273] **C. R. Southwell, J. D. Bultman, and C. W. Hummer Jr.** Estimating of service life of steel in sea water. M. Schumacher. Seawater corrosion Handbook. New Jersey. Noyes Data Corporation. 1979.
- [274] **R. E. Melchers.** Probabilistic Modeling of immersion marine corrosion. M. Shinozuka, Y. K. Wen, and N. Shiraishi. Structural Safety and Reliability. Rotterdam: Balkema. 1998.
- [275] **C. G. Soares, and Y. Garbatov.** Reliability on maintained, corrosion protected plates subjected to non linear corrosion and compressive loads. Mar Struct. 12: 425-45. 1999.
- [276] **R. E. Melchers.** Pitting Corrosion of mild steel in marine immersion environment-1: maximum pit depth corrosion. NACE. 60 (9) 824-836. 2004.
- [277] **R. E. Melchers.** Pitting Corrosion of mild steel in marine immersion environment-2: variability of maximum pit depth. NACE. 60 (10) 937-944. 2004.
- [278] **J. Shigley, C. Mischke, and R. Budynas.** Shigley's Mechanical Engineering Design, 8th Edition. USA : McGraw.Hill Primis, 2006.
- [279] **G. Tsamasfyros.** Mechanics of Deformable Bodies 1 (Greek edition). Athens, Greece. Symmetria Publications. 1990.
- [280] **G. Tsamasfyros.** Mechanics of Deformable Bodies 2 (Greek Edition). Athens, Greece. Symmetria Publications. 1990.
- [281] **J. Marine.** Engineering Materials. Englewood Cliffs, N.J. Prentice-Hall. 1952.
- [282] **J. Mathisen, and E. Bitner-Gregersen.** Joint distribution for significant wave height and wave zero-up-crossing period. Applied Ocean Research. Vol.12 No.2. 1990.
- [283] **S. K. Chakrabarti.** Nonlinear Methods in Offshore Engineering. Netherlands. Elsevier Science Publishing Company Inc. 1990.

- [284] **S. Havier.** On the Joint Distribution of Heights and Periods of Sea Waves. Journal of Ocena Engineering. Vol.14(5), 359-376. 1987.
- [285] **P. Pagrut, and M. C. Deo.** Extreme Wave Height Estimates. 2nd International Offshore and Polar Engineering Conference. USE: ISOPE. 186-193. 1992.
- [286] **J. F. Wilson.** Dynamics of Offshore Structures. New Jersey : Johny Wiley and Sons. 1984.
- [287] **W. H. Munk.** Proposed Uniform Procedure for Observing Waves and Interpreting Instrument Records. Scripps Institute of Oceanography. Wave Report 26. 1944.
- [288] **H. R. Seiwell.** Sea Surface Roughness Measurements in Theory and Practice, Annals. New York Academy of Science. 51 (3). 1949.
- [289] **N. F. Barber.** Ocean Waves and Swell, Proceedings of the Institution of Civil Engineers. Marine and Waterways Division. 1950.
- [290] **R. R. Putz.** Wave-Height Variability; Prediction of Distribution Function, Technical Report No. HE 116-318, Series No. 3, Issue No. 318, Institute of Engineering Research. Berkeley, CA. University of California. 1950.
- [291] **M. S. Longuet-Higgins.** On the Statistical Distribution of the Heights of Sea Waves. Journal of Marine Research . 2 (3). 1952.
- [292] **R. R. Putz.** Statistical Distribution for Ocean Waves. Transactions, American Geophysical Union . 33 (5). 1952.
- [293] **J. Darbyshire.** The Generation of Waves by Wind. Proceedings of the Royal Society Ser. A 215. 1952.
- [294] **T. Hamada, H. Mitsuyasu, H., and N. Hose.** An Experiemental Study of Wind Effect upon Water Surface. Tokyo : Transportation Technical Research Institute. 1953.

- [295] **R. L. Wiegel.** An Analysis from Data Wave Recorders on the Pacific Coast of the United States. Transactions, American Geophysical Union. 30, 1949.
- [296] **A. Kolios, M. Collu, A. Chahardehi, F. P. Brennan, M.H. and Patel.** Multi-Criteria Decision Making Method to Compare Support Structures for Offshore Wind Turbines. Warsaw : European Wind Energy Conference - EWEC, April 2010.
- [297] **W. Musial, S. Butterfield, and B. Ram.** Energy from offshore wind. Houston, Texas. Offshore Technology Conference. NREL/CP-500-39450. May 1–4, 2006.
- [298] <http://www.dnv.co.uk/services/software/products/sesam/>. [Online]
- [299] **J. C. P. Kam, M. Birkinshaw, and J. V. Sharp.** Review of the Applications of Structural Reliability Technologies in Offshore Structural Safety. USA : Proceedings of the 12th International Conference on Offshore Mechanics and Arctic Engineering, Vol 2. 1993.
- [300] **G. Sigurdsson, R. Skjong, B. Skallerud, and J. Amdahl.** Probabilistic Collapse Analysis of Jackets. Shinozuka, Yao, and Schueller. Structural Safety and Reliability. Rotterdam: Balkema. 1994.
- [301] **P. S. Tromans, and J. W. Van de Graaf.** Substantiated Risk Assessment of Jacket Structure. Journal of Waterway, Port Coastal and Ocean Engineering. Vol 120 (6). 535-555. 1992.
- [302] **P. A. Frieze, A. C. Morandi, M. Birkinshaw, D. Smith, and A. T. Dixon.** Fixed and Jack-up Platforms: Basis for Reliability Assessment. Journal of Marine Structure. Vol 10, 263-284. 1997.
- [303] **Det Norske Veritas.** Fatigue Design of Offshore Steel Structures. DNV. DNV-RP-C203 . April 2010 .

- [304] **Det Norske Veritas.** Rules for the Classification of Steel Ships. DNV, April 2005.
- [305] **Det Norske Veritas.** Design of Offshore Wind Turbine Structures. DNV, DNV-OS-J101. October 2007.
- [306] **M-H Tsai.** An analytical methodology for the dynamic amplification factor in progressive collapse evaluation of building structures. Mechanics Research Communications. Volume 37, Issue 1, Pages 61-66 , January 2010.
- [307] **M. K. Chryssanthopoulos, and T. D. Righiniotis.** Fatigue Reliability of welded steel structures. Journal of Constructional Steel Research. Vol. 62, pp. 1199-1209. 2006.
- [308] **E. Ayala-Uruga, and T. Moan.** Fatigue reliability-based assessment of welded joints applying consistent fracture mechanics formulations. International Journal of Fatigue. Vol. 29, pp. 444-456. 2007.
- [309] **T. Moan, G. O. Godve, and A. M. Blanker.** Reliability based fatigue design criteria for offshore structures considering the effect of inspection and repair. Offshore Technology Conference 7189. pp. 591-600. 1993.
- [310] **F. Moses.** Final Reports for API PRAC 79-22 (1980), 80-22 (1981), 81-22 (1982), 82-22 (1983), 83-22 (1985), 85 –22 (1986), 87-22 (1987). Dallas : American Petroleum Institute.
- [311] **S. K. Chakrabati.** Hydrodynamics of Offshore Structures. Boston : Computational Mechanics Publications. 1987.
- [312] **L. Skjelbreia, and J. A. Hendrickson.** Fifth-order Gravity Wave Theory. Netherlands: ASCE, 184-196. Proceedings of the 7th Conference on Coastal Engineering. 1961.
- [313] **R. G. Dean.** Stearn Function Representation of Nonlinear Ocean Waves. Journal of Geophysical Research. 70(18): 4561-4572. 1965.

- [314] **S. N. Rasmussen.** Corrosion Protection of Offshore Structures. Denmark : HEMPEL A/S. 2005.
- [315] **Norwegian Technology Standards Institution.** M-501 - Surface preparation and protective coating. Norway. NORSOK. June 2004 .
- [316] **International Standardization Organization.** ISO 12944:1998 (part 1 –8) - Paints and varnishes - Corrosion protection of steel structures by protective paint systems. Geneve, Switzerland : ISO. 1998.
- [317] **International Standardization Organization.** ISO 20340:2003-Paints and varnishes - Performance requirements for protective paint systems for offshore and related structures. Geneve, Switzerland : ISO. 2003.
- [318] **A. W. Peabody.** Peabody's Control of Pipeline Corrosion, 2nd Ed. s.l. : NACE International. 2001.
- [319] **American Society for Testing and Materials.** B843 - 07-Standard Specification for Magnesium Alloy Anodes for Cathodic. ASTM . 1998.
- [320] **American Society for Testing and Materials.** B418 - 09 Standard Specification for Cast and Wrought Galvanic Zinc Anodes. ASTM , 2009.
- [321] **R. L. Kean, and K. G. Davies.** Cathodic Protection. DTI under contract from NPL. 2000.

APPENDICES

APPENDIX A

In this Appendix, complementary to what has been presented in Chapter Four, the different wave theories will be briefly presented in a way that program modelling for combination with FEA is feasible.

A.1. Linear Wave Theory

This theory, also known as amplitude, sinusoidal or Airy wave theory is based on the assumption that the wave height is much smaller than both the wave length and the water depth. Considering the boundary conditions set, the free surface boundary conditions can be linearized by neglecting the wave height term beyond the first order and are satisfied at the mean water level, rather than at the oscillating free surface. Considering small amplitude waves, the free surface boundary conditions are reduced to:

$$\begin{aligned}\frac{\partial\Phi}{\partial z} - \frac{\partial\eta}{\partial t} &= 0 \text{ at } z = 0 \\ \frac{\partial\Phi}{\partial t} + g \cdot \eta &= 0 \text{ at } z = 0\end{aligned}\tag{A.1-1}$$

The free surface profile is given by the following equation:

$$\eta = -\frac{1}{g} \cdot \left(\frac{\partial\Phi}{\partial t}\right) \text{ at } z = 0\tag{A.1-2}$$

Combining the two boundary conditions, eliminating η , gives:

$$\frac{\partial^2\Phi}{\partial t^2} + g \cdot \frac{\partial\Phi}{\partial z} = 0 \text{ at } z = 0\tag{A.1-3}$$

Assuming the velocity potential Φ to be described with the following formula and substituting to the basic Laplace equation:

$$\Phi = Z(z)\Phi(x - ct)\tag{A.1-4}$$

$$\frac{\partial^2 Z}{\partial z^2} - k^2 Z = 0$$

$$\frac{\partial^2 \Phi}{\partial x^2} - k^2 \Phi = 0$$

Where: k^2 is a constant suitably chosen. Integrating the above differential equations, the general solutions of Z and Φ are:

$$Z = A_1 \cdot \cosh(kz) + A_2 \cdot \sinh(kz) \quad (\text{A.1-5})$$

$$\Phi = A_3 \cdot \cos[k(x - ct)] + A_4 \cdot \sin[k(x - ct)] \quad (\text{A.1-6})$$

Where: A_1 , A_2 , A_3 and A_4 are constants to be determined by the boundary conditions, therefore:

$$\begin{aligned} A_2 &= A_1 = \tanh(kd) \\ t = 0 \rightarrow x = 0 \rightarrow A_3 &= 0 \end{aligned} \quad (\text{A.1-7})$$

Rewriting the above equations, the velocity potential maybe written in the form:

$$\Phi = A \cdot \frac{\cosh[k(z + d)]}{\sinh(kd)} \cdot \sin[k(x - ct)] \quad (\text{A.1-8})$$

Where: $A = A_1 \cdot A_4$. A can be derived as a function of H , $k(L, T)$, and $c(L, T)$ as follows in order to derive A_4 :

$$A = \frac{gH}{2kc}, A_4 = \frac{gH}{2kct \tanh(kd)} \quad (\text{A.1-9})$$

The velocity potential may finally be derived as:

$$\Phi = \frac{gH \cdot \cosh(ks)}{2\omega \cdot \sinh(kd)} \cdot \sin \theta = \frac{\pi H \cdot \cosh(ks)}{kT \cdot \sinh(kd)} \cdot \sin \theta$$

(Error!
Reference
source not
found.Error!
Reference
source not
found.-10)

Where: $s = z + d$ and $\theta = k \cdot (x - ct) = kx - \omega t$ is the wave phase angle.

Having obtained a solution for Φ , other variables of interest might be calculated based on formulations presented in Table 64 [194].

	Shallow Water	Deep Water
Range of validity	$kd < \frac{\pi}{10}, \frac{d}{L} < \frac{1}{20}, \frac{d}{gT^2} < 0.0025$	$kd < \pi, \frac{d}{L} < \frac{1}{2}, \frac{d}{gT^2} < 0.08$
Velocity potential	$\varphi = \frac{\pi H}{k^2 T d} \cdot \sin \theta = \frac{gH}{2\omega} \cdot \sin \theta$	$\varphi = \frac{\pi H}{kT} \cdot e^{kz} \cdot \sin \theta = \frac{gH}{2\omega} \cdot e^{kz} \cdot \sin \theta$
Dispersion relation	$c^2 = \frac{\omega^2}{k^2} g d$	$c^2 = c_0^2 \cdot \frac{\omega^2}{k^2} = \frac{g}{k}$
Wave length	$L = T \sqrt{g d}$	$L = L_0 = g T^2 / 2\pi$
Surface elevation	$\eta = \frac{H}{2} \cdot \cos \theta$	$\eta = \frac{H}{2} \cdot \cos \theta$
Horizontal particle displacement	$\xi = -\frac{H}{2kd} \cdot \sin \theta$	$\xi = -\frac{H}{2kd} \cdot e^{kz} \cdot \sin \theta$
Vertical particle displacement	$\zeta = \frac{H}{2} \cdot \left(1 + \frac{z}{d}\right) \cdot \cos \theta$	$\zeta = \frac{H}{2} \cdot e^{kz} \cdot \cos \theta$
Horizontal particle velocity	$u = \frac{\pi H}{T(kd)} \cdot \cos \theta$	$u = \frac{\pi H}{T} \cdot e^{kz} \cdot \cos \theta$
Vertical particle velocity	$w = \frac{\pi H}{T} \cdot \left(1 + \frac{z}{d}\right) \cdot \sin \theta$	$w = \frac{\pi H}{T} \cdot e^{kz} \cdot \sin \theta$
Horizontal particle acceleration	$\frac{\partial u}{\partial t} = \frac{2\pi^2 H}{T^2(kd)} \cdot \sin \theta$	$\frac{\partial u}{\partial t} = \frac{2\pi^2 H}{T^2} \cdot e^{kz} \cdot \sin \theta$
Vertical particle acceleration	$\frac{\partial w}{\partial t} = -\frac{2\pi^2 H}{T^2} \cdot \left(1 + \frac{z}{d}\right) \cdot \cos \theta$	$\frac{\partial w}{\partial t} = -\frac{2\pi^2 H}{T^2} \cdot e^{kz} \cdot \cos \theta$
Pressure	$p = -\rho g z + \frac{1}{2} \rho g H \cdot \cos \theta$	$p = -\rho g z + \frac{1}{2} \rho g H e^{kz} \cdot \cos \theta$
Group velocity	$C_G = C$	$C_G = 1/2 C$
Average energy density	$E = 1/8 \rho g H^2$	$E = 1/8 \rho g H^2$
Energy flux	$P = E C$	$P = 1/2 E C$
Radiation stress	$S_{XX} = 3/2 E, S_{XY} = S_{YX} = 0,$ $S_{YY} = 1/2 E$	$S_{XX} = 1/2 E, S_{XY} = S_{YX} = 0$ $S_{YY} = 0$

Table 64: Shallow and deep water approximation to linear wave theory
[194]

A.2. Stokes Finite Amplitude Wave Theory

The linear wave theory, as it was presented in the previous section, can provide an initial, rather simplistic approximation of the water particles motion due to wave loading. For a more accurate and complete solution, the perturbation technique might be used [311]. Stokes, has proposed an extension of the linear wave theory for waves of finite height when the following conditions are met:

$$\frac{H}{d} \ll (kd)^2 \text{ for } kd < 1, \text{ and } \frac{H}{L} \ll 1 \quad (\text{A.2-1})$$

The velocity potential maybe written as:

$$\Phi = \sum_{n=1}^{\infty} \varepsilon^n \Phi_n \quad (\text{A.2-2})$$

Where: ε is the perturbation parameter, defined in terms of wave slope (H/L) as $\varepsilon = kH/2$, and Φ_n is the n th order solution for Φ . Substituting the above expression in the basic Laplace equation and considering the boundary conditions at the seabed and separation of terms of different polynomial orders, the following equations may be derived:

$$\begin{aligned} \frac{\partial^2 \Phi_n}{\partial x^2} + \frac{\partial^2 \Phi_n}{\partial z^2} &= 0 \text{ for } n = 1, 2, \dots \\ \frac{\partial \Phi_n}{\partial z} &= 0 \text{ at } z = -d \text{ for } n = 1, 2, \dots \end{aligned} \quad (\text{A.2-3})$$

From the above equations set, the difficulty of defining the free surface boundary conditions due to nonlinear term consisting of product exists, in order to apply them to the unknown surface elevation rather than mean waterline. In [312], an expansion of the Stokes wave theory to the fifth order has raised a widely used method in engineering practice. The velocity potential Φ and the free surface elevation η , are written in a series form of fifth order as:

$$\Phi = \frac{c}{k} \sum_{n=1}^5 \Phi'_n \cosh(nks) \sin(n\theta) \quad (\text{A.2-4})$$

$$\eta = \frac{1}{k} \sum_{n=1}^5 \eta'_n \cos(n\theta) \quad (\text{A.2-5})$$

In the above formulas, the coefficients Φ'_n and η'_n are expressed as functions of λ and a series of coefficients A and B, as are presented in Table 65, Table 66 and Table 67. The wave celerity is now:

$$c^2 = C_0^2 \cdot (1 + \lambda^2 \cdot C_1 + \lambda^4 \cdot C_2) \quad (\text{A.2-6})$$

Where: C_0 is the celerity given by linear wave theory for the same depth and wave number:

$$C_0^2 = (g/k) \cdot \tanh kd \quad (\text{A.2-7})$$

Considering appropriate values for the coefficients B and C , parameters λ and k should be initially defined solving the system:

$$\begin{aligned} \frac{1}{kd} \cdot [\lambda + B_{33}\lambda^3 + (B_{35} + B_{55}) \cdot \lambda^5] &= \frac{H}{2d} \\ kd \cdot \tanh(kd) \cdot [1 + C_1\lambda^2 + C_2\lambda^4] &= 4\pi^2 \cdot \frac{d}{gT^2} \end{aligned} \quad (\text{A.2-8})$$

The final values of λ and k are determined from above equation through an iterative procedure.

$\varphi'_1 = \lambda A_{11} + \lambda^3 A_{13} + \lambda^5 A_{15}$	$\eta'_1 = \lambda$
$\varphi'_2 = \lambda^2 A_{22} + \lambda^4 A_{24}$	$\eta'_2 = \lambda^2 B_{22} + \lambda^4 B_{24}$
$\varphi'_3 = \lambda^3 A_{33} + \lambda^5 A_{35}$	$\eta'_3 = \lambda^3 B_{33} + \lambda^5 B_{35}$
$\varphi'_4 = \lambda^4 A_{44}$	$\eta'_4 = \lambda^4 B_{44}$
$\varphi'_5 = \lambda^5 A_{55}$	$\eta'_5 = \lambda^5 B_{55}$

Table 65: Φ'_n and η'_n the coefficients [194]

Velocity potential, φ	$\frac{k\varphi}{c} = \sum_{n=1}^5 \varphi'_n \cdot \cosh(nks) \cdot \sin(n\theta)$
Wave length, c	$\frac{c^2}{gd} = \frac{\tanh(kd)}{kd} \cdot [1 + \lambda^2 C_1 + \lambda^4 C_2]$
Surface elevation, η	$k\eta = \sum_{n=1}^5 \eta'_n \cdot \cos(n\theta)$
Horizontal particle velocity, u	$\frac{u}{c} = \sum_{n=1}^5 n\varphi'_n \cdot \cosh(nks) \cdot \cos(n\theta)$
Vertical particle velocity, w	$\frac{w}{c} = \sum_{n=1}^5 n\varphi'_n \cdot \sinh(nks) \cdot \sin(n\theta)$
Horizontal particle acceleration, $\partial u/\partial t$	$\frac{\partial u/\partial t}{\omega c} = \sum_{n=1}^5 n^2 \varphi'_n \cdot \cosh(nks) \cdot \sin(n\theta)$
Vertical particle acceleration, $\partial w/\partial t$	$\frac{\partial w/\partial t}{\omega c} = - \sum_{n=1}^5 n^2 \varphi'_n \cdot \sinh(nks) \cdot \cos(n\theta)$
Temporal derivative of φ	$\frac{\partial \varphi/\partial t}{c^2} = - \sum_{n=1}^5 n\varphi'_n \cdot \cosh(nks) \cdot \cos(n\theta)$
Pressure, p	$\frac{p}{\rho g d} = 1 - \frac{s}{d} - \frac{c^2}{gd} \left\{ \frac{\partial \varphi/\partial t}{c^2} + \frac{1}{2} \left[\left(\frac{u}{c} \right)^2 + \left(\frac{w}{c} \right)^2 \right] \right\}$

Table 66: Stokes fifth-order wave theory [194]

$$A_{11} = 1/S$$

$$A_{13} = \frac{-C(5C^2 + 1)}{8S^2}$$

$$A_{15} = \frac{-(1184C^{10} - 1440C^8 - 1992C^6 + 2641C^4 - 249C^2 + 18)}{1536S^{11}}$$

$$A_{22} = 3/8S^4$$

$$A_{24} = \frac{(192C^8 - 424C^6 - 312C^4 + 480C^2 - 17)}{768S^{10}}$$

$$A_{33} = \frac{(13 - 4C^2)}{64S^7}$$

$$A_{35} = \frac{(512C^{12} - 4224C^{10} - 6800C^8 - 12,808C^6 + 16,704C^4 - 3154C^2 + 107)}{4096S^{13} \cdot (6C^2 - 1)}$$

$$A_{44} = \frac{(80C^6 - 816C^4 + 1338C^2 - 197)}{1536S^{10} \cdot (6C^2 - 1)}$$

$$A_{55} = \frac{-(2880C^{10} - 72,480C^8 + 324,000C^6 - 432,000C^4 + 163,470C^2 - 16,245)}{61,440S^{11} \cdot (6C^2 - 1) \cdot (8C^4 - 11C^2 + 3)}$$

$$B_{22} = C \cdot \frac{(2C^2 + 1)}{4S^3}$$

$$B_{22} = C \cdot \frac{(272C^8 - 504C^6 - 192C^4 + 322C^2 + 21)}{384S^9}$$

$$B_{33} = \frac{3 \cdot (8C^6 + 1)}{64S^6}$$

$$B_{35} = \frac{(88,128C^{14} - 208,224C^{12} + 70,848C^{10} + 54,000C^8 - 21,816C^6 + 6264C^4 - 54C^2 - 81)}{12,288S^{12} \cdot (6C^2 - 1)}$$

$$B_{44} = \frac{C \cdot (768C^{10} - 448C^8 - 48C^6 + 48C^4 + 106C^2 - 21)}{384S^9 \cdot (6C^2 - 1)}$$

$$B_{55} = \frac{(192,000C^{16} - 262,720C^{14} + 83,680C^{12} + 20,160C^{10} - 7280C^8)}{12,288S^{10} \cdot (6C^2 - 1) \cdot (8C^4 - 11C^2 + 3)}$$

$$+ \frac{(7160C^6 - 1800C^4 - 1050C^2 + 225)}{12,288S^{10} \cdot (6C^2 - 1) \cdot (8C^4 - 11C^2 + 3)}$$

$$C_1 = \frac{8C^4 - 8C^2 + 9}{8S^4}$$

$$C_2 = \frac{(3840C^{12} - 4096C^{10} + 2592C^8 - 1008C^6 + 5944C^4 - 1830C^2 + 147)}{512S^{10} \cdot (6C^2 - 1)}$$

$$C_3 = -1/4SC$$

$$C_4 = \frac{(12C^8 + 36C^6 - 162C^4 + 141C^2 - 27)}{192CS^9}$$

Table 67: The coefficients for Stokes fifth-order wave theory [311]

A.3. Stream Function Wave Theory

A different method for the representation of non linear waves is that of the steam function wave theory [313]. Two different types of this theory distinguish:

- Symmetric or Regular Stream Function Theory that describes periodic waves of symmetric, permanent form with prescribed period, height and still water depth.
- Irregular Stream Function Theory that represents a stream function and associated kinematics of a wave with a predetermined profile. This theory is suitable in analyzing wave tank or field test data.

The Irregular Stream Function wave theory sets no restrictions on the wave form; therefore the wave can change form as it propagates through its motion. It is more suitable in cases were a measured wave surface profile is available and the water particle kinematics and dynamics are required for this wave profile and is applied to a single wave in the wave profile (eg. the largest wave). The Symmetric or Regular Stream Function Theory is the one tackled by other wave theories which assumed to propagate at a constant speed and without a change in its form.

This method will be presented for the special case of a constant free surface pressure, neglecting any underlying current. Moving from a Cartesian to a relative coordinates system, considering \bar{c} to be the speed vector, the problem is reduced to a steady flow, with the horizontal component of velocity to move in the $u-c$ plane. Proportionally to the previous theories, for the two dimensional flow, a steam function Ψ can be formulated, satisfying the Laplace equation as follows:

$$\frac{\partial^2 \Psi}{\partial x^2} + \frac{\partial^2 \Psi}{\partial z^2} = 0 \quad (\text{A.3-1})$$

Assuming Q to be the Bernoulli's constant, the corresponding boundary conditions are:

$$\begin{aligned}\frac{\partial \Psi}{\partial x} &= 0 \text{ at } z = -d \\ \frac{w}{u-c} &= \frac{\partial \eta}{\partial x} \text{ at } z = \eta \\ \eta + \frac{1}{2g} \left[\left(\frac{\partial \Psi}{\partial x} \right)^2 + \left(\frac{\partial \Psi}{\partial z} \right)^2 \right] &= Q \text{ at } z = \eta\end{aligned}\tag{A.3-2}$$

In the Cartesian, two dimensional (x, z) system, the N -order symmetric stream function Ψ is given as follows, satisfying the bottom boundary condition and the kinematic free surface condition:

$$\Psi(x, z) = cz + \sum_{n=1}^N X_n \cdot \sinh[nk \cdot (z + d)] \cdot \cos(nkx)\tag{A.3-3}$$

Where: the coefficients X_n , the wave number k and the surface value of stream function are determined using the dynamic free surface boundary condition for a given H , T and d . Differentiation of the stream function can give the individual horizontal and vertical water particle velocities as:

$$\begin{aligned}u - c &= -\frac{\partial \cdot \Psi}{\partial \cdot z} = -c - \sum_{n=1}^N nkX_n \cdot \cosh[nk(z + d)] \cdot \cos(nkx) \\ w &= \frac{\partial \cdot \Psi}{\partial \cdot x} = -\sum_{n=1}^N nkX_n \cdot \sinh[nk(z + d)] \cdot \sin(nkx)\end{aligned}\tag{A.3-4}$$

For the Bernoulli constant Q , the mean square value E , is defined as:

$$\bar{E} = \frac{1}{l} \sum_{n=1}^l (Q_i \cdot \bar{Q})^2\tag{A.3-5}$$

Where: $i=1, \dots, l$, x takes successive values spanning one complete wave length, and \bar{Q} represents the average value of the Bernoulli constant. Then, X_n , k and Ψ are obtained in an iterative way with an initial estimate derived from linear theory of the wave number, k and the stream function, Ψ such that \bar{E} is minimized.

APPENDIX B

B.1. Painting coatings

Coatings and combinations of coatings with cathodic protection (for the immersion zone of the structure) is the most common method employed for the protection of structures from corrosive environments. The actual performance of coating systems and thus the efficiency of the CPS is subjected on several fundamental parameters that should be considered in the design process. The most important of those are the following:

- Type and condition of the substrate
- Environment and possible additional stresses
- Surface preparation
- Quality of the coatings
- Selection of the coating systems (Generic types, thickness etc.)
- Application
- Quality control

The substrate of interest in offshore structures is steel. This parameter refers to the state where the structure is in the fabrication process and should illustrate the basic specification of the coating system to be applied. The parameter of environment includes apart from the obvious loading conditions, different sources of stresses due to thermal, chemical or different nature. The preparation of the surface is the most important parameter since it can significantly damage the applied coating. The degree of cleaning (removal of rust, particles, grease, salts etc.), the final roughness and the preparation of sharp edges, welding seams and imperfections are critical elements towards this scope. Selection of coatings should be appropriate and paint of good quality should be selected and usually certified by appropriate classification bodies. Coating systems, is the parameter that refers to the combination of different layers of appropriate coating each providing a different level of protection to the structure. In conjunction with coatings that target to limit corrosion, for the

immersion zone anti-fouling coatings should be used in order to delay or ease removal of fouling. Table 68, proposes typical coating types and systems for each of the areas of the offshore structure.

Proper application of the coating or the coating systems is crucial for the maximization of the efficiency of the protection. It is important to apply the prescribed thickness of film (within the tolerance range) since smaller thickness might lead to premature corrosion while thicker layers might result in undesirable effects such as solvent retention, reduced adhesion etc. [314]. The problem of variation of the film thickness during application can be avoided by applying more coats of the same total thickness distributing the variation to all over the member.

Area	Coating types	Coating system
Atmospheric zone	Zinc-rich primer, Epoxies and UV durable topcoat	Minimum 320 μm /13 mils in minimum 3 coats.
Splash zone	Epoxy or Polyester	Minimum 600 μm /24 mils in minimum 2 coats.
Immersion	Epoxy	Minimum 450 μm /18 mils in minimum 2 coats.

Table 68: Typical coating systems used for offshore structures

Since coatings are applied most of the times manually, areas of the structure where proper access is not available should be pointed out. Critical points of this category are welding seams, edges, and corners. For those cases, stripe coating, corrosion protection schemes or application of CPS within manufacturing phase should be considered in order to sufficiently protect the structure.

The wide application and great significance of the painting coatings has raised an interest for systematic recording of the procedures and the requirements into design and application standards. NORSOK [315] has published a standard describing the surface preparation and protective coatings. Within its provisions, different steps in the coating process are illustrated and the qualifications of the painters, inspectors and coating systems are included. ISO [316] has published a standard that illustrates the basic factors that determines the effectiveness of

the paint coating systems. These are summarised to the 'choice and formulation of the products used in differently classified environments and the standard of workmanship and execution of their contract'. An additional relevant standard published by ISO, [317], is a complementary standard to the previous one referring to the special offshore environment, proposing tougher testing of the coating systems. Finally, a series of publications from NACE (National Association of Corrosion Engineers) are available covering different aspects of application of the method.

B.2. Cathodic protection

Cathodic protection is a widely used technique nowadays to control the corrosion on a metal surface by transforming it to the cathode of an electrochemical cell [318]. Initially introduced in the early 1820s by Davy, it became practically applicable in 1945 and had a rapid development since then. Application of the method can be found in pipelines, ship hulls, storage tanks, harbour structures, tubular and foundation pilings and offshore platforms, floating and subsea structures.

The basic concept of cathodic protection requires connection of the metal to be protected to another more easily corroded metal that will act as an anode of the electrochemical cell, as is presented in Figure 73. Three different types of cathodic protection methods are available:

- Galvanic or Sacrificial Corrosion Protection
- Impressed-Current Corrosion Protection
- Galvanization

For the Galvanic or Sacrificial Corrosion Protection, reactive metals are employed as anodes that are directly electrically connected to the steel that needs to be protected. In order to achieve transformation of the structure to a cathode, it becomes negatively charged by considering the natural potentials between the anode and the steel, causing a positive current to flow in the electrolyte, from the anode to the steel. Metals commonly used as sacrificial

anodes are zinc, aluminium and magnesium. Standards that describe application of cathodic protection can be found in [319] and [320].

Impressed-Current Corrosion Protection Systems, that refer mainly to structures of larger scale, where application of Galvanic anodes is not economically feasible, employ inert (zero or low dissolution) anodes and use an external source of dc power (rectified ac) to impress a current from an external anode onto the cathode surface. Those anodes are of tubular, rod-type shaped or continuous ribbons of materials such as high silicon cast iron, graphite, mixed metal oxide, platinum and niobium wires.

Galvanizing is a technique that accounts for coating steel with a layer of metallic zinc. This coating is very durable even in harsh environments, since they combine benefits of coating and cathodic protection. Even in cases with local damage to the treatment, the method retains effectiveness since the surrounded areas of the 'wounded' one form a galvanic cell with the exposed steel and protect it from corrosion, as a form of corrosion protection where zinc acts as an anode.

A very important parameter that should be considered for the more effective performance of the cathodic protection is the cathodic 'shielding effect'. This is based on the fact that in practice solid film backed anti-corrosion coatings such as polyethylene tapes, shrinkable pipeline sleeves, and factory applied single or multiple solid film coatings are used. The high electrical resistivity of those patches protects electrical current to flow from the cathodic protection, blocking it from reaching to the metal to be protected.

Table 69, adopted by [321], presents the requirements of a Galvanic and an Impressed-Current Corrosion Protection System.

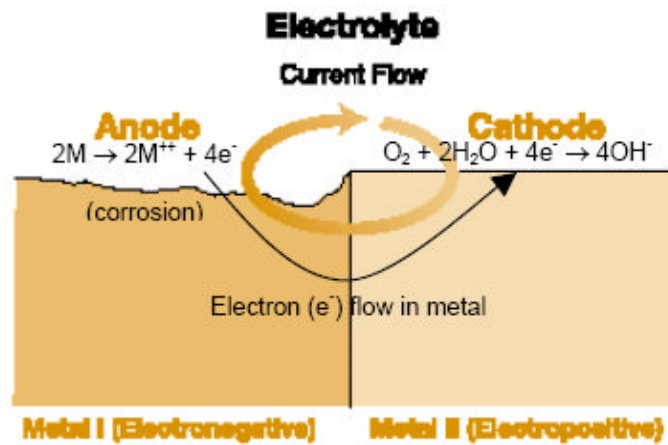


Figure 73: Corrosion Cell

Galvanic System	Impressed-Current System
Sacrificial anodes	Inert anodes (clusters of which, connected together often in a backfill, are called the "groundbed")
Direct welding to the structure or a conductor connecting the anode to the structure	A dc power source.
Secure and minimum resistance connections between conductor and structure, and between conductor and anode.	Electrically well insulated, minimum resistance and secure conductors between anodes and power source
	Secure and minimum resistance connections between power source and structure

Table 69: Requirements of Galvanic and an Impressed-Current Corrosion Protection System

APPENDIX C

In this Appendix, the details regarding the geometry of the reference structure is given. In Figure 74, the numbering of the structural members is presented. Further in Table 70, the dimension of each group of members is included.

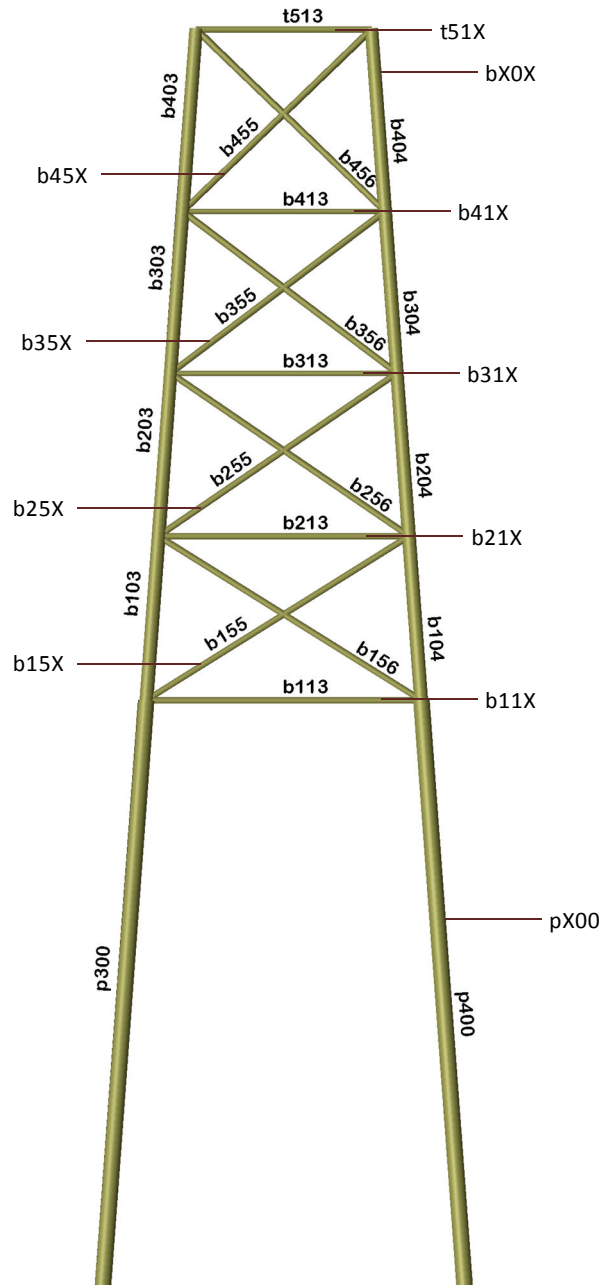


Figure 74: Numbering of the structural members

Type	ID	Diameter (m)	Thickness (mm)
Legs	bX0X	1.25	0.028
Piles	pX00	1.5	0.024
V1	b15X	0.6	0.018
V2	b25X	0.6	0.018
V3	b35X	0.6	0.018
V4	b45X	0.6	0.018
H1	b11X	0.6	0.018
H2	b21X	0.6	0.018
H3	b31X	0.5	0.016
H4	b41X	0.5	0.016
Topside	t51X	0.6	0.016

Table 70: Dimension of group of members

APPENDIX D

```
% Matlab Code for the Response Surface Method
% This code requires input of a matrix with the geometry of the
% structure, and the corresponding loads and properties as well as a
% complementary FEA code for the execution of simulations and a code
% for regression analysis.
% Output of the code is a vector of PFs and Betas for each of the
% members of the complex structure.
%
% Athanasios Kolios - Cranfield University 2010

clear
clc
format long e
tic

a=open('Data23.mat');
Coord=a.Coords;
Con=a.Connections;
Re=a.BC;
Load=a.Loading;
E=a.Elasticity;
A=a.Area;

er=10^-50;

x1_m=500;
x2_m=21e10;
x3_m=0.5;
x4_m=1000000;
x1_s=200;
x2_s=0.1e10;
x3_s=0.01;
x4_s=100000;

A=[x1_m-3*x1_s x1_m x1_m+3*x1_s];
B=[x2_m-3*x2_s x2_m x2_m+3*x2_s];
```

```

D=[x3_m-3*x3_s x3_m x3_m+3*x3_s];
E=[x4_m-3*x4_s x4_m x4_m+3*x4_s];

c=num2cell([A; B; D; E],2);
[c{:}] = ndgrid(c{:});
c=reshape(cat(length(c)+1,c{:}),[],length(c));
siz=size(c);

[nel,~]=size(Con);
[n,~]=size(c);
[xL,yL]=size(Load);

for i=1:n
    L=Load;
    for k=1:xL
        for l=1:yL
            if L(k,l)~=0
                L(k,l)=c(i,1);
            end
        end
    end
    [~,~,SAX]=FEA(Coord,Con,Re,L*c(i,1),c(i,2)*ones(nel,1),c(i,3)*ones(nel,1),1);
    S_all=c(i,4)*ones(1,nel);
    G(i,:)=abs(SAX)./S_all;
end

for i=1:nel
    y_var=G(:,i);
    x_var=c;
    b=reg_an(x_var,y_var,2);
    [Pf_form,b_form]=FORM_SORM(b,x1_m,x2_m,x3_m,x4_m,x1_s,x2_s,x3_s,x4_s);
    Pf(i)=Pf_form;
    beta(i)=b_form;
end
toc
%end of program

```

```

% Matlab Code for Adaptive Response Surface Method
% This code requires input of a matrix with the geometry of the
% structure, and the corresponding loads and properties as well as a
% complementary FEA code for the execution of simulations and a code
% for regression analysis.
% Weighted Regression is incorporated after the first iteration in
% order to 'tune' the accuracy of the response surface.
% Output of the code is a vector of PFs and Betas for each of the
% members of the complex structure.
%
% Athanasios Kolios - Cranfield University 2010

clear
clc
format long e
tic

a=open('Data23.mat');
Coord=a.Coords;
Con=a.Connections;
Re=a.BC;
Load=a.Loading;
E=a.Elasticity;
A=a.Area;

x1_m=1;
x2_m=21e10;
x3_m=1;
x4_m=100000;
x1_s=0.2;
x2_s=1e10;
x3_s=0.01;
x4_s=10000;

[nel,~]=size(Con);
[xL,yL]=size(Load);

er=10^-40;

```

```

% Step 1.1
[~,~,SAX]=FEA(Coord,Con,Re,Load,x2_m*ones(nel,1),A,1);
S_all=x4_m*ones(1,nel);
Gmean=abs(SAX)./S_all;

%Step 1.2-1.5 : Load
L=Load;
for k=1:xL
    for l=1:yL
        if L(k,l)~=0
            L(k,l)=(x1_m-3*x1_s)*Load(k,l);
        end
    end
end
[~,~,SAX]=FEA(Coord,Con,Re,L,x2_m*ones(nel,1),A,1);
S_all=x4_m*ones(1,nel);
GL=abs(SAX)./S_all;
if GL(18)<Gmean(18)
    kLoad=-3;
else
    kLoad=3;
end

%Step 1.2-1.5 : Elasticity
[~,~,SAX]=FEA(Coord,Con,Re,Load,(x2_m-3*x2_s)*ones(nel,1),A,1);
S_all=x4_m*ones(1,nel);
GE=abs(SAX)./S_all;
if GE(18)<Gmean(18)
    kElast=-3;
else
    kElast=3;
end

%Step 1.2-1.5 : Area
[~,~,SAX]=FEA(Coord,Con,Re,Load,x2_m*ones(nel,1),(x3_m-3*x3_s)*A,1);
S_all=x4_m*ones(1,nel);
GA=abs(SAX)./S_all;
if GA(18)<Gmean(18)
    kArea=-3;
end

```

```

else
    kArea=3;
end

%Step 1.2-1.5 : Stress Allowed
[~,~,SAX]=FEA(Coord,Con,Re,Load,x2_m*ones(nel,1),A,1);
S_all=(x4_m-3*x4_s)*ones(1,nel);
GSA=abs(SAX)./S_all;
    if GSA(18)<Gmean(18)
        kSall=-3;
    else
        kSall=3;
    end

%Step 1.6 Calculation of ybest
L=Load;
for k=1:xL
    for l=1:yL
        if L(k,l)~=0
            L(k,l)=(x1_m+kLoad*x1_s)*Load(k,l);
        end
    end
end
[~,~,SAX]=FEA(Coord,Con,Re,L,(x2_m+kElast*x2_s)*ones(nel,1),(x3_m+kArea*x3_s)*A,1);
S_all=(x4_m+kSall'*x4_s)*ones(1,nel);
ybest=abs(SAX)./S_all+er*ones(1,nel);

%Design matrix
c=[x1_m x2_m x3_m x4_m;
    x1_m+kLoad*x1_s x2_m x3_m x4_m;
    x1_m x2_m+kElast*x2_s x3_m x4_m;
    x1_m x2_m x3_m+kArea*x3_s x4_m;
    x1_m x2_m x3_m x4_m+kSall*x4_s];
[n,~]=size(c);
%Step 1.6 Calculation of W
W=zeros(n,nel);
for j=1:n
    L=Load;

```

```

for k=1:xL
    for l=1:yL
        if L(k,l)~=0
            L(k,l)=c(j,1)*Load(k,l);
        end
    end
end

end

[~,~,SAX]=FEA(Coord,Con,Re,L,c(j,2)*ones(nel,1),c(j,3)*A,1);
S_all=c(j,4)*ones(1,nel);
G(j,:)=abs(SAX)./S_all;
W(j,:)=exp(-(G(j,:)-ybest)./ybest);
end

%Step 2-3 Weighted regression, FORM/SORM
for j=1:nel
    x_var=c;
    [xs,ys]=size(x_var);
    regs=ys+1;
    for i=1:xs;
        X=x_var;
        X(i,regs)=1;
    end;
    Y=G(:,j);
    Weight=diag(W(:,j));
    b(:,j)=(X'*Weight*X)\(X'*Weight*Y);
    %b(:,j)=inv(X'*Weight*X)*(X'*Weight*Y);

    % Definition of Limit State Functions
    syms x1 x2 x3 x4
    a1=b(1,j)+er;
    a2=b(2,j)+er;
    a3=b(3,j)+er;
    a4=b(4,j)+er;
    a5=b(5,j)+er;
    %a6=b(6,j)+er;
    %a7=b(7,j)+er;
    %a8=b(8,j)+er;
    %a9=b(9,j)+er;

```

```

%g=1-(a1*x1^2+a2*x1+a3*x2^2+a4*x2+a5*x3^2+a6*x3+a7*x4^2+a8*x4+a9);
g=1-(a1*x1+a2*x2+a3*x3+a4*x4+a5);

% Calculation of Partial derivatives
dgx1=diff(g,x1);
dgx2=diff(g,x2);
dgx3=diff(g,x3);
dgx4=diff(g,x4);

% Express functions in a matlab complex form
g_m=matlabFunction(g);
dgx1_m=matlabFunction(dgx1);
dgx2_m=matlabFunction(dgx2);
dgx3_m=matlabFunction(dgx3);
dgx4_m=matlabFunction(dgx4);

% First Iteration
i=1;

%Initial point (mean)
x1_v(i,j)=x1_m;
x2_v(i,j)=x2_m;
x3_v(i,j)=x3_m;
x4_v(i,j)=x4_m;

g_v(i,j)=g_m(x1_v(i,j),x2_v(i,j),x3_v(i,j),x4_v(i,j));
%dgx1_v(i)=dgx1_m();
%dgx2_v(i)=dgx2_m();
%dgx3_v(i)=dgx3_m();
%dgx4_v(i)=dgx4_m();

b_v(i,j)=g_v(i,j)/((((dgx1_m()*x1_s)^2)+(dgx2_m()*x2_s)^2)+(dgx3_m()*x3_s)^2)+(dgx4_m()*x4_s)^2)^0.5);

a1_v(i,j)=-
(dgx1_m()*x1_s)/((((dgx1_m()*x1_s)^2)+(dgx2_m()*x2_s)^2)+(dgx3_m()*x3_s)^2)+(dgx4_m()*x4_s)^2)^0.5);

```

```

a2_v(i,j)=-
(dgx2_m()*x2_s)/((((dgx1_m()*x1_s)^2)+((dgx2_m()*x2_s)^2)+((dgx3_m()*x
3_s)^2)+((dgx4_m()*x4_s)^2))^0.5);
a3_v(i,j)=-
(dgx3_m()*x3_s)/((((dgx1_m()*x1_s)^2)+((dgx2_m()*x2_s)^2)+((dgx3_m()*x
3_s)^2)+((dgx4_m()*x4_s)^2))^0.5);
a4_v(i,j)=-
(dgx4_m()*x4_s)/((((dgx1_m()*x1_s)^2)+((dgx2_m()*x2_s)^2)+((dgx3_m()*x
3_s)^2)+((dgx4_m()*x4_s)^2))^0.5);

```

```

%New design point

```

```

x1_v(i+1,j)=x1_m+b_v(i,j)*x1_s*a1_v(i,j);
x2_v(i+1,j)=x2_m+b_v(i,j)*x2_s*a2_v(i,j);
x3_v(i+1,j)=x3_m+b_v(i,j)*x3_s*a3_v(i,j);
x4_v(i+1,j)=x4_m+b_v(i,j)*x4_s*a4_v(i,j);
g_v(i+1,j)=g_m(x1_v(i+1),x2_v(i+1),x3_v(i+1),x4_v(i+1));

```

```

end

```

```

%Step 4 New centre point

```

```

Xmean=[x1_v(1,:); x2_v(1,:); x3_v(1,:); x4_v(1,:)];
Xdesign=[x1_v(2,:); x2_v(2,:); x3_v(2,:); x4_v(2,:)];

```

```

for i=1:nel

```

```

alpha(i)=g_v(1,i)/(g_v(1,i)-g_v(2,i));

```

```

for j=1:4

```

```

Xnew(j,i)=Xmean(j,i)+(Xdesign(j,i)-Xmean(j,i))*alpha(i);

```

```

end

```

```

end

```

```

for i=1:nel

```

```

%Step 5 New design matrix

```

```

c2=[x1_m x2_m x3_m x4_m;

```

```

x1_m+kLoad*x1_s x2_m x3_m x4_m;

```

```

x1_m x2_m+kElast*x2_s x3_m x4_m;

```

```

x1_m x2_m x3_m+kArea*x3_s x4_m;

```

```

x1_m x2_m x3_m x4_m+kSall*x4_s

```

```

Xnew(1,i) x2_m x3_m x4_m;

```

```

x1_m Xnew(2,i) x3_m x4_m;
x1_m x2_m Xnew(3,i) x4_m;
x1_m x2_m x3_m Xnew(4,i)];

[n,~]=size(c2);

%Step 6 Calculation of W
W=zeros(n,nel);
for j=1:n
    L=Load;
    for k=1:xL
        for l=1:yL
            if L(k,l)~=0
                L(k,l)=c2(j,1)*Load(k,l);
            end
        end
    end
    [~,~,SAX]=FEA(Coord,Con,Re,L,c2(j,2)*ones(nel,1),c2(j,3)*A,1);
    S_all=c2(j,4)*ones(1,nel);
    G(j,:)=abs(SAX)./S_all;
    W(j,:)= exp(-(G(j,:)-
Gmean+er*ones(1,nel))./(Gmean+er*ones(1,nel)));
end

%Step 7 Reliability Calculations
xexp=c2;
[xs,ys]=size(xexp);
regs=2*ys+1;
for k=1:xs;
    X(k,regs)=1;
    for j=1:ys;
        X(k,2*j-1)=xexp(k,j)^2;
        X(k,2*j)=xexp(k,j)^1;
    end;
end;

Y=G(:,i);
Weight=diag(W(:,i));
b2=(X'*Weight*X)\(X'*Weight*Y);

```

```
[Pf_form,b_form]=FORM_SORM(b2,x1_m,x2_m,x3_m,x4_m,x1_s,x2_s,x3_s,x4_s)
;
    Pf(i)=Pf_form;
    beta(i)=b_form;
end

toc
```

```

% This code performs multivariate polynomial regression (MPR)
% analysis.
% A scaling of the design parameters is included in order to prevent
% from ill-conditioned systems.
% The vector y_var, includes values of dependent variables (y) while
% the matrix x_var includes the values of independent variables (xi).
%
% An example of 3 variables is included.
%
% Athanasios Kolios - Cranfield University 2010 (R)

clc
clear

format short g

% Input of dependent variables
x_var=[15  15  15  10  10  10  5  5  5  15  15  15  10  10  10  5
5  5  15  15  15  10  10  10  5  5  5;
15  10  5  15  10  5  15  10  5  15  10  5  15  10  5  15  10  5
15  10  5  15  10  5  15  10  5;
600000  600000  600000  600000  600000  600000  600000  600000  600000
700000  700000  700000  700000  700000  700000  700000  700000  700000
800000  800000  800000  800000  800000  800000  800000  800000
800000;]';

%Input of independent variables
y_var=[0.784426667  0.655335  0.527383333  0.652808333  0.522951667
0.394113333  0.522345  0.39159  0.261475  0.672365714  0.561715714
0.452042857  0.55955  0.448244286  0.337811429  0.447724286  0.335648571
0.224121429  0.58832  0.49150125  0.3955375  0.48960625  0.39221375
0.295585  0.39175875  0.2936925  0.19610625]';

% power_f: This matrix is formed as the exponential factor of each of
the % variables for each coefficient.
% For the example of a 4th order regression and 2 variables, the
results will % return:
% power_f=[1,0;0,1;2,0;0,2;3,0;0,3;4,0;0,4;0,0;];

```

```

% obtain sizes
[n,p] = size(x_var);
% model terms loop
nv=p;
np=2; % degree of the polynomial

% Size of matrix transpose
k=nv*np;

% Formation of matrix with I's
B= repmat(eye(nv),np,1);

% Scaling of variables
std_s = sqrt(diag(cov(x_var)));
x_var_s = x_var*diag(1./std_s);

% Vector of coefficients
F=(1:1:np);
FT=transpose(F);
FTT=zeros(k,1);

% Expand F
for i=1:nv;
    for j=1:np;
        FTT(i+(j-1)*nv)=FT(j);
    end;
end;

% Multiply with B and get BT
for i=1:k;
    for j=1:nv;
        power_f(i,j)=B(i,j)*FTT(i);
    end;
end;

for i=1:nv;
power_f(k+1,i)=0;

```

```

end;

nt = size(power_f,1);

% build the design matrix
M = ones(n,nt);
sf = ones(1,nt);
for i = 1:nt;
    for j = 1:p;
        M(:,i) = M(:,i).*x_var_s(:,j).^power_f(i,j);
        sf(i) = sf(i)/(std_s(j)^power_f(i,j));
    end;
end

% Calculation of Coeff_fact
Coeff= M\y_var;
y_calc = M*Coeff(:);
Coeff_fact=transpose(Coeff)

% Reverse scaling
Coeff_fact=Coeff_fact'*sf;

% variance of the regression parameters
s_var = norm(y_var - y_calc);

% R^2
R2 = 1 - (s_var/norm(y_var-mean(y_var)) )^2;

% RMSE
RMSE = sqrt(mean((y_var - y_calc).^2));

clear B Coeff F FT FTT M i j k n p np nt nv

% End of code

```

```

% FORM-SORM_v1_0.m
%
% This code calculates the reliability of a four variable function,
% with second order polynomials, where variables are normal, according
% to the Hasofer, Lind, Rackwitz and Fiessler index method.
% A convergence criterion for the FORM is included in the code.
% SORM has been also incorporated.
%
% This version of the code has been verified with DNV PROBAN Software
% Example of 3 variables incorporated
%
% Athanasios Kolios - Cranfield University 2010

tic
clear
clc

er=10^-50;

% Input of dependent variables - Load patterns
xinp=[15    15  15  10  10  10  5  5  5  15  15  15  10  10  10  5
5  5  15  15  15  10  10  10  5  5  5;
15  10  5  15  10  5  15  10  5  15  10  5  15  10  5  15  10  5
15  10  5  15  10  5  15  10  5;
600000  600000  600000  600000  600000  600000  600000  600000  600000
700000  700000  700000  700000  700000  700000  700000  700000  700000
800000  800000  800000  800000  800000  800000  800000  800000
800000;];

x_var=xinp';
%Input of independent variables - Response
yinp=[0.784426667  0.655335  0.527383333 0.652808333 0.522951667
0.394113333 0.522345  0.39159 0.261475  0.672365714 0.561715714
0.452042857 0.55955 0.448244286 0.337811429 0.447724286 0.335648571
0.224121429 0.58832 0.49150125 0.3955375  0.48960625 0.39221375
0.295585  0.39175875 0.2936925  0.19610625];

y_var=yinp';

```

```

[xs,ys]=size(x_var);

%Definition of Variables
x1_m=12;
x2_m=12;
x3_m=700000;
x4_m=er;
x1_s=2;
x2_s=2;
x3_s=80000;
x4_s=er;

% Expand x_var to X
regs=2*ys+1;
xexp=x_var;

for i=1:xs;
    X(i,regs)=1;
    for j=1:ys;
        X(i,2*j-1)=xexp(i,j)^2;
        X(i,2*j)=xexp(i,j)^1;
    end;
end;

Y=y_var;

b=X\Y;
%b=inv(X'*X)*X'*Y;

% Definition of iterations
n_iter=40;
err=0.01; % Convergence criterion

% Definition of Limit State Functions
syms x1 x2 x3 x4

a1=b(1);
a2=b(2);

```

```

a3=b(3);
a4=b(4);
a5=b(5);
a6=b(6);
a7=er;
a8=er;
a9=b(regs);

g=1-(a1*x1^2+a2*x1+a3*x2^2+a4*x2+a5*x3^2+a6*x3+a7*x4^2+a8*x4+a9);

%g=1-(a1*x1+a2*x2+a3*x2+a4*x4+a5*x1^2+a6*x2^2+a7*x3^2+a8*x4^2+a9);

gm=matlabFunction(g);

% U-dimensional space
% Definition of x1
x1_pdf=@(x1f) normpdf(x1f,x1_m, x1_s);
x1_cdf=@(x1f) normcdf(x1f,x1_m, x1_s);
x1_pdf_v=x1_pdf(x1_m);
x1_cdf_v=x1_cdf(x1_m);
x1_s=normpdf(norminv(x1_cdf_v))/x1_pdf_v;
x1_m=x1_m-(norminv(x1_cdf_v))*x1_s;

% Definition of x2
x2_pdf=@(x2f) normpdf(x2f,x2_m, x2_s);
x2_cdf=@(x2f) normcdf(x2f,x2_m, x2_s);
x2_pdf_v=x2_pdf(x2_m);
x2_cdf_v=x2_cdf(x2_m);
x2_s=normpdf(norminv(x2_cdf_v))/x2_pdf_v;
x2_m=x2_m-(norminv(x2_cdf_v))*x2_s;

% Definition of x3
x3_pdf=@(x3f) normpdf(x3f,x3_m, x3_s);
x3_cdf=@(x3f) normcdf(x3f,x3_m, x3_s);
x3_pdf_v=x3_pdf(x3_m);
x3_cdf_v=x3_cdf(x3_m);
x3_s=normpdf(norminv(x3_cdf_v))/x3_pdf_v;
x3_m=x3_m-(norminv(x3_cdf_v))*x3_s;

```

```

% Definition of x4
x4_pdf=@(x4f) normpdf(x4f,x4_m, x4_s);
x4_cdf=@(x4f) normcdf(x4f,x4_m, x4_s);
x4_pdf_v=x4_pdf(x4_m);
x4_cdf_v=x4_cdf(x4_m);
x4_s=normpdf(norminv(x4_cdf_v))/x4_pdf_v;
x4_m=x4_m-(norminv(x4_cdf_v))*x4_s;

% Calculation of Partial derivatives
dgx1=diff(g,x1);
dgx2=diff(g,x2);
dgx3=diff(g,x3);
dgx4=diff(g,x4);

% Express functions in a matlab complex form
g_m=matlabFunction(g);
dgx1_m=matlabFunction(dgx1);
dgx2_m=matlabFunction(dgx2);
dgx3_m=matlabFunction(dgx3);
dgx4_m=matlabFunction(dgx4);

% First Iteration
i=1;
x1_v(i)=x1_m;
x2_v(i)=x2_m;
x3_v(i)=x3_m;
x4_v(i)=x4_m;
g_v(i)=g_m(x1_v(i),x2_v(i),x3_v(i),x4_v(i));
dgx1_v(i)=dgx1_m(x1_v(i));
dgx2_v(i)=dgx2_m(x2_v(i));
dgx3_v(i)=dgx3_m(x3_v(i));
dgx3_v(i)=dgx4_m(x4_v(i));

b_v(i)=g_v(i)/((((dgx1_m(x1_v(i))*x1_s)^2)+((dgx2_m(x2_v(i))*x2_s)^2)+
((dgx3_m(x3_v(i))*x3_s)^2)+((dgx4_m(x4_v(i))*x4_s)^2))^0.5);

```

```

a1_v(i)=-
(dgx1_m(x1_v(i))*x1_s)/((((dgx1_m(x1_v(i))*x1_s)^2)+((dgx2_m(x2_v(i))*
x2_s)^2)+((dgx3_m(x3_v(i))*x3_s)^2)+((dgx4_m(x4_v(i))*x4_s)^2))^0.5);
a2_v(i)=-
(dgx2_m(x2_v(i))*x2_s)/((((dgx1_m(x1_v(i))*x1_s)^2)+((dgx2_m(x2_v(i))*
x2_s)^2)+((dgx3_m(x3_v(i))*x3_s)^2)+((dgx4_m(x4_v(i))*x4_s)^2))^0.5);
a3_v(i)=-
(dgx3_m(x3_v(i))*x3_s)/((((dgx1_m(x1_v(i))*x1_s)^2)+((dgx2_m(x2_v(i))*
x2_s)^2)+((dgx3_m(x3_v(i))*x3_s)^2)+((dgx4_m(x4_v(i))*x4_s)^2))^0.5);
a4_v(i)=-
(dgx4_m(x4_v(i))*x4_s)/((((dgx1_m(x1_v(i))*x1_s)^2)+((dgx2_m(x2_v(i))*
x2_s)^2)+((dgx3_m(x3_v(i))*x3_s)^2)+((dgx4_m(x4_v(i))*x4_s)^2))^0.5);

x1_v(i+1)=x1_m+b_v(i)*x1_s*a1_v(i);
x2_v(i+1)=x2_m+b_v(i)*x2_s*a2_v(i);
x3_v(i+1)=x3_m+b_v(i)*x3_s*a3_v(i);
x4_v(i+1)=x4_m+b_v(i)*x4_s*a4_v(i);

u1_v(i+1)=(x1_v(i+1)-x1_m)/x1_s;
u2_v(i+1)=(x2_v(i+1)-x2_m)/x2_s;
u3_v(i+1)=(x3_v(i+1)-x3_m)/x3_s;
u4_v(i+1)=(x4_v(i+1)-x4_m)/x4_s;

i=0 ;%%% zero counter
% (2-n_iter) Iteration
for i=2:n_iter
    g_v(i)=g_m(x1_v(i),x2_v(i),x3_v(i),x4_v(i));
    dgx1_v(i)=dgx1_m(x1_v(i));
    dgx2_v(i)=dgx2_m(x2_v(i));
    dgx3_v(i)=dgx3_m(x3_v(i));
    dgx4_v(i)=dgx4_m(x4_v(i));

    b_nom_prod(i)=
dgx1_v(i)*x1_s*u1_v(i)+dgx2_v(i)*x2_s*u2_v(i)+dgx3_v(i)*x3_s*u3_v(i)+d
gx4_v(i)*x4_s*u4_v(i);
    b_v(i)=(g_v(i)-
b_nom_prod(i))/((((dgx1_m(x1_v(i))*x1_s)^2)+((dgx2_m(x2_v(i))*x2_s)^2)
+((dgx3_m(x3_v(i))*x3_s)^2)+((dgx4_m(x4_v(i))*x4_s)^2))^0.5);
    pf_v(i)=normcdf(-b_v(i));

```

```

    a1_v(i)=-
(dgx1_m(x1_v(i))*x1_s)/((((dgx1_m(x1_v(i))*x1_s)^2)+((dgx2_m(x2_v(i))*
x2_s)^2)+((dgx3_m(x3_v(i))*x3_s)^2)+((dgx4_m(x4_v(i))*x4_s)^2))^0.5);
    a2_v(i)=-
(dgx2_m(x2_v(i))*x2_s)/((((dgx1_m(x1_v(i))*x1_s)^2)+((dgx2_m(x2_v(i))*
x2_s)^2)+((dgx3_m(x3_v(i))*x3_s)^2)+((dgx4_m(x4_v(i))*x4_s)^2))^0.5);
    a3_v(i)=-
(dgx3_m(x3_v(i))*x3_s)/((((dgx1_m(x1_v(i))*x1_s)^2)+((dgx2_m(x2_v(i))*
x2_s)^2)+((dgx3_m(x3_v(i))*x3_s)^2)+((dgx4_m(x4_v(i))*x4_s)^2))^0.5);
    a4_v(i)=-
(dgx4_m(x4_v(i))*x4_s)/((((dgx1_m(x1_v(i))*x1_s)^2)+((dgx2_m(x2_v(i))*
x2_s)^2)+((dgx3_m(x3_v(i))*x3_s)^2)+((dgx4_m(x4_v(i))*x4_s)^2))^0.5);

    x1_v(i+1)=x1_m+b_v(i)*x1_s*a1_v(i);
    x2_v(i+1)=x2_m+b_v(i)*x2_s*a2_v(i);
    x3_v(i+1)=x3_m+b_v(i)*x3_s*a3_v(i);
    x4_v(i+1)=x4_m+b_v(i)*x4_s*a4_v(i);

    u1_v(i+1)=(x1_v(i+1)-x1_m)/x1_s;
    u2_v(i+1)=(x2_v(i+1)-x2_m)/x2_s;
    u3_v(i+1)=(x3_v(i+1)-x3_m)/x3_s;
    u4_v(i+1)=(x4_v(i+1)-x4_m)/x4_s;

    e=abs(b_v(i)-b_v(i-1));
    if e<err break,
    end;
end;
b_form=b_v(i)
Pf_form=pf_v(i)
% Calculation of SORM Pf and beta
x1_MPP=x1_v(i);
x2_MPP=x2_v(i);
x3_MPP=x3_v(i);
x4_MPP=x4_v(i);
u1_MPP=u1_v(i);
u2_MPP=u2_v(i);
u3_MPP=u3_v(i);
u4_MPP=u4_v(i);

```

```

% Second order partial derivatives
d2gx1=diff(dgx1);
d2gx2=diff(dgx2);
d2gx3=diff(dgx3);
d2gx4=diff(dgx4);

d2gx1_m=matlabFunction(d2gx1);
d2gx2_m=matlabFunction(d2gx2);
d2gx3_m=matlabFunction(d2gx3);
d2gx4_m=matlabFunction(d2gx4);

% Transform to Matlab functions
% Check the variables in each Partial Derivative
d2gx1_v=d2gx1_m();
d2gx2_v=d2gx2_m();
d2gx3_v=d2gx3_m();
d2gx4_v=d2gx4_m();

% Check the variables in each Partial Derivative
dgx1_v=dgx1_m(x1_MPP);
dgx2_v=dgx2_m(x2_MPP);
dgx3_v=dgx3_m(x3_MPP);
dgx4_v=dgx4_m(x4_MPP);

% First order tensor
tens_u=((dgx1_v*(x1_s^2))^2)+((dgx2_v*(x2_s^2))^2)+((dgx3_v*(x3_s^2))^2)+((dgx4_v*(x4_s^2))^2);

% Second order tensor (table)
tens_u2=zeros(4,4);
tens_u2(1,1)=d2gx1_v;
tens_u2(2,2)=d2gx2_v;
tens_u2(3,3)=d2gx3_v;
tens_u2(4,4)=d2gx4_v;

B_mat=(1/tens_u)*tens_u2;

```

```

F_mat=[(- (dgx1_v*x1_s)/tens_u) (- (dgx2_v*x2_s)/tens_u) (-
(dgx3_v*x3_s)/tens_u) (- (dgx4_v*x4_s)/tens_u);
    0 1 0 0 ;
    0 0 1 0 ;
    0 0 0 1 ;];

F_11=-dgx1_v*x1_s;
F_22=1;
F_33=1;
F_44=1;

D1=(((F_11)^2)+((F_11)^2));
e11=1/D1;
g1=e11*F_11;

D2=((((F_22)^2)+((F_22)^2))-((abs((((F_22)^2)+(g1^2))))^2)^0.5);
e12=-((((F_22)^2)+(g1^2))^0.5)/D2;
e22=1/D2;
g2=e12*g1+e22*F_22;

D3=((((F_33)^2)+((F_33)^2))-abs((((F_33)^2)+(g1^2))^2)-
abs((((F_33)^2)+(g2^2))^2)^0.5;
e13=-((((F_33)^2)+(g1^2))^0.5)/D3;
e23=-((((F_33)^2)+(g2^2))^0.5)/D3;
e33=1/D3;
g3=e13*g1+e23*g2+e33*F_33;

D4=((((F_44)^2)+((F_44)^2))-abs((((F_44)^2)+(g1^2))^2)-
abs((((F_44)^2)+(g2^2))^2)-abs((((F_44)^2)+(g3^2))^2)^0.5;
e14=-((((F_44)^2)+(g1^2))^0.5)/D4;
e24=-((((F_44)^2)+(g2^2))^0.5)/D4;
e34=-((((F_44)^2)+(g3^2))^0.5)/D4;
e44=1/D4;
g4=e14*g1+e24*g2+e34*g3+e44*F_44;

H_mat=[g1 g2 g3 g4];
H_mat_fin=[g2 0 0 0;
    0 g3 0 0;

```

```

    0 0 g4 0;
    0 0 0 g1 ];
H_mat_fin_tr=transpose(H_mat_fin);

% Construction of f matrix
F_mat2=H_mat_fin*B_mat*H_mat_fin_tr;

k11=F_mat2(1,1);
k22=F_mat2(2,2);
k33=F_mat2(3,3);
k44=F_mat2(4,4);

k1=real(k11);
k2=real(k22);
k3=real(k33);
k4=real(k44);

b_form=b_v(i);
Pf_sorm=(normcdf(-b_form))*((1+k1*b_form)^-0.5)*((1+k2*b_form)^-
0.5)*((1+k3*b_form)^-0.5)
b_sorm= -(norminv(Pf_sorm))
%Pf_form
%end of program
toc

```